The Dispersion, Persistence, and Control of Viral Bioaerosols in Dentistry

James R. Allison

This thesis is submitted for the degree of Doctor of Philosophy

School of Dental Sciences/ Clinical & Translational Research Institute

Faculty of Medical Sciences

Newcastle University

Newcastle upon Tyne

August 2025

Abstract

Bioaerosols containing viruses and other microorganisms are dispersed from the mouth during dental procedures, posing infection risk to patients and professionals. Uncertainty over viral bioaerosols caused unprecedented worldwide disruption during the COVID-19 pandemic, and millions couldn't access dental care, impacting oral health. This project aims to determine: the extent of virus dispersion in dental bioaerosols; if dispersion can be controlled using bioaerosol control measures; and the effect of environmental parameters such as ventilation.

A model of viral dental bioaerosols was developed using two bacteriophages (MS2, phi6) infused into a mannequin's mouth during dental procedures with an air turbine handpiece. Physical aerosol was measured using optical particle counters, and bacteriophage captured in surface and air samples. Infective bacteriophage was measured using plaque assay and bacteriophage RNA quantified by reverse-transcription quantitative polymerase chain reaction. Distance of virus dispersion, persistence of virus over time, and the effect of control measures (ventilation, rubber dam, waterline disinfectants, suction, local exhaust ventilation [LEV], electric micromotor handpiece) were explored.

Without control measures, dental procedures led to dispersion of infectious virus over significant distances from the procedure (6.9 m in air, 2.8 m on surfaces), and at low ventilation rates, remained airborne for a prolonged time (46 min). Increasing ventilation rate to recommended levels reduced persistence to only a few minutes. Viral RNA recovery was greater than infectious virus, suggesting not all dispersed virus remains infectious. Control measures produced substantial reductions in physical aerosol and infective virus, particularly LEV, which often eliminated virus recovery completely.

In conclusion, viral bioaerosols in dentistry can be dispersed over substantial distances and remain airborne for considerable time. However, improved ventilation and control measures commonly used in dentistry reduce this. Infection control guidance should include when and how to employ these measures to reduce risk in everyday care and during infectious disease outbreaks.

This thesis is dedicated to Amy, Iris, and Rupert; everything I do is for you.

Acknowledgements

My first thanks must go to my family, Amy, Iris, and Rupert for always supporting me and for showing understanding when late finishes and Sundays in the lab were necessary. I hope that my work inspires them to pay attention to the details and to work hard, just as they inspire me to be kind and patient. The reminders to turn off the computer and put down the work were also immensely appreciated.

Secondly, I am indebted to the guidance and mentorship of my three supervisors, Professor Nick Jakubovics, Professor Justin Durham, and Dr Richard Holliday. They have been deeply invested in developing this work from its conception in 2020, and none of it would have been possible without their help. Their encouragement to keep going, critical suggestions, and insights from experience were invaluable and I am very grateful to have learned so much from them all.

The insights of my collaborators Dr Louise Fletcher (University of Leeds), Professor Darren Smith (Northumbria University), and Professor Thushan de Silva (University of Sheffield) were instrumental in developing my Fellowship applications which allowed me to complete this work. I am also grateful for Dr Fletcher's help in designing the experiments conducted at the University of Leeds. Similarly, Emma Tidswell and the technical team at the School of Civil Engineering, University of Leeds were incredibly welcoming and helpful.

The assistance of Dr Edgar Beltran (Universitas El Bosque, Columbia) and Dr Chris Dowson in conducting the first bacteriophage experiments was both extremely helpful to the work and also a great pleasure. I thank them both for their effort, and for the chance to work together. I am grateful to Dr Andrew Brown and Jordan Tompkins at the National Physical Laboratory (NPL) who kindly offered their insightful transdisciplinary perspectives from very early on in the work and throughout; my visit NPL was a great experience which helped me to better understand the importance of uncertainty in my work. I also acknowledge the support of NPL's Postgraduate Institute for Measurement Science who helped to facilitate this.

I am thankful for the financial support provided by my funders, and in particular the Wellcome Trust, 4ward North Clinical PhD Academy, and Faculty of Dental Surgery

of the Royal College of Surgeons of England who provided the two Fellowships that made this work possible. For supporting our early aerosol work I must thank the Faculty of Dental Surgery of the Royal College of Surgeons of Edinburgh, the British Endodontic Society, VODEX Ltd., AerosolShield Ltd., and the Newcastle upon Tyne Hospitals NHS Foundation Trust. Support from the School of Dental Sciences, Newcastle University has been unwavering since my appointment as a Clinical Fellow in 2018.

I am grateful for the encouragement and insightful suggestions of my progress panel, Professor Andrew Fisher and Dr Chris Nile. For all their help in the early aerosol work upon which this PhD builds, I thank Ekaterina (Katya) Kozhevnikova, Dr Nadia Rostami, Sarah Reay, Greta Červinskytė, Kimberley Pickering, Nicola Atkinson, Dr Chris Nile, Dr Chris Dowson, Dr Charlotte Currie, Charlotte Bowes, and David Edwards. I am extremely thankful for the help of the Newcastle Dental Clinical Research Facility Team: Nicola Atkinson, Alicia Fucile, Nichola Lansdowne, Emma Padgett, Craig Winlow – you are incredible!

The Translational Oral Biology lab is a wonderful place to work, and I am especially grateful to Philip Hardy (with apologies for the unceasing production of dirty glassware) and Katya Kozhevnikova for their constant help and support, as well as to lab members past and present for making the lab an enjoyable place to be.

An abridged version of Chapter 1 has been published in the *International Dental Journal* (Allison et al. 2024). Experiments in Chapter 3 using dental unit waterline disinfectants have been published in the *Journal of Dental Research* (Allison et al. 2022), and the work described in this section was conducted with the assistance of Dr Christopher Dowson, whose work conducting plaque assays is gratefully acknowledged. I designed and conducted the clinical experiments, and designed, analysed, and interpreted the plaque assay data generated with the assistance of Dr Dowson. Experiments in Chapter 3 using phi6 and MS2 with rubber dam were conducted with the assistance of Dr Edgar Beltran, whose contribution is gratefully acknowledged. Dr Beltran helped to conduct plaque assay analyses for this experiment. I designed all experiments, conducted the clinical simulation experiments and RT-qPCR assays, and analysed and interpreted all the data.

Table of Contents

List of Tables

List of Figures

Appendix Figures

List of Abbreviations

16s-rRNA	16S ribosomal RNA
3'	3-prime end (in relation to DNA or RNA)
5'	5-prime end (in relation to DNA or RNA)
$A_{260/280}$	Ratio of absorbance at 260 nm to absorbance at 280 nm
ACH	Air changes per hour
AGP	Aerosol-generating procedure
ANOVA	Analysis of variance
b	Bases
bp	Base pairs
C_q	Quantification cycle (equivalent to threshold cycle or C_t)
°C	Degrees Celsius
cDNA	Complementary deoxyribonucleic acid
CFU	Colony-forming units
cm	Centimetres
COVID-19	Coronavirus disease 2019
dNTP	Deoxynucleotide triphosphates
DNA	Deoxyribonucleic acid
DUWL	Dental unit waterline
EDTA	Ethylenediaminetetraacetic acid
FAM	6-carboxyfluorescein
FFP3	Filtering facepiece 3 mask
g	Gram
g	*(in italics)* Gravitational force
GC%	Percentage guanine and cytosine
h	Hours
HEPA	High-efficiency particulate air
HTM	Health technical memorandum
IPC	Infection prevention and control
kb	Kilobase
L	Litre
LEV	Local exhaust ventilation

m	Metre
M	Mole
MERS	Middle East respiratory syndrome
mg	Milligram
min	Minute
mL	Millilitre
mW	Milliwatt
MGB	Minor groove binder
mm	Millimetre
mM	Millimole
µg	Microgram
µL	Microlitre
µm	Micrometre
ng	Nanogram
NFQ	Non-fluorescent quencher
NHS	National Health Service
NIHR	National Institute of Health and Care Research
nm	Nanometre
NRT	No reverse transcriptase
NTC	No-template control
nt	Nucleotide
N95	Non-oil particulate respirator with 95% filtration efficiency
OPC	Optical particle counter
PCR	Polymerase chain reaction
PES	Polyethersulfone
PFU	Plaque-forming units
Phage	Bacteriophage
PPE	Personal protective equipment
qPCR	Quantitative polymerase chain reaction
RNA	Ribonucleic acid
RNAse	Ribonuclease
ROX	6-carboxy-X-rhodamine
rpm	Revolutions per minute

RSV	Respiratory syncytial virus
RT	Reverse transcription/ reverse transcriptase
RT-qPCR	Reverse transcription quantitative polymerase chain reaction
SARS	Severe acute respiratory syndrome
SARS-CoV-2	Severe acute respiratory syndrome coronavirus 2
spp.	Species
SD	Standard deviation
sec	Second
***Sph*I**	*Sph*I endonuclease
TAE	Tris-acetate-EDTA
Taq	*Taq* polymerase
T_m	Melting temperature
TOPO TA	Topoisomerase-based TA cloning
Tris	Tris(hydroxymethyl)aminomethane
UR1	Upper right central incisor
UV	Ultraviolet
UVC	Ultraviolet-C
V	Volt
v/v	Volume per volume
w/v	Weight per volume
WHO	World Health Organisation
∆Rn	Change (∆) in normalised reporter

Chapter 1. Literature Review

1.1 Introduction

In late March 2020, the UK entered a national lockdown due to the developing coronavirus disease 2019 (COVID-19) pandemic. Dental services were suspended in the following days due to concerns over transmission of the disease in dental surgeries (Hurley and Neligan 2020). In the UK, a series of urgent dental care networks were set up to provide emergency care (Carter et al. 2020). The main concern in dentistry during this time was the risk of dispersion of the causative agent, severe acute respiratory syndrome coronavirus 2 (SARS-CoV-2), from patients' saliva in aerosols—tiny liquid droplets suspended in the air—produced by dental instruments such as dental handpieces and scalers during dental treatment (Figure 1.1). The challenge during this period was not so much that there was a known risk, but rather that the level of risk was completely unknown, resulting in an outright halt to the provision of dental care. This meant that millions of patients missed out on dental treatment, worsening their oral health outcomes (Dickson-Swift et al. 2022; Stennett and Tsakos 2022).

This concern was also present elsewhere in healthcare, with aerosols generated during anaesthesia from endotracheal intubation and non-invasive ventilation, as well as during endoscopy and surgery with high-speed devices, posing a perceived risk to patients and health professionals (Jackson et al. 2020). These procedures, which were thought to carry the risk of aerosolising infectious fluids such as blood, saliva, or respiratory secretions in *bioaerosols* (aerosols containing biological material), are termed "aerosol generating procedures" (AGPs).

It is difficult to ascribe a single definition to the term "aerosol", and from an aerosol science perspective, this refers to any collection of liquid or solid particles of any size suspended in a gas. In the infection prevention and control (IPC) literature, however, aerosols are often defined as particles of < 5 μm which are able to mediate airborne transmission of disease (Tang et al. 2021). The same discrepancy is true for "droplets", which aerosol scientists might define as any liquid particle, and the IPC literature as particles > 5 μm which fall rapidly to the ground within 1 – 2 m and cannot mediate airborne transmission. The term "splatter" relates largely to the dental

IPC literature and is defined by some authors as droplets > 100 μm in diameter (Miller et al. 1971).

Figure 1.1. Dental Aerosols.

Aerosols produced by an air-turbine handpiece (a) adapted from Allison et al. (2021c), and (b) during a simulated procedure in a dental mannequin.

The AGP is not a new concept, becoming important during the SARS outbreak in 2002 – 2004 (Li et al. 2004; Yassi et al. 2005), and later during the influenza A (H1N1) pandemic in 2009 (Thompson et al. 2013). The World Health Organisation (WHO) defines high-risk AGPs as “medical procedures that have been reported to be aerosol-generating and consistently associated with an increased risk of pathogen transmission” (WHO 2014). It is important to note that the production of aerosols alone, without posing an increased risk of infection, is not enough to meet these criteria; this was a source of confusion in the response to COVID-19 and other outbreaks whereby simply the production of any aerosol during a procedure was conflated with carrying increased risk. The current list of AGPs according to the National Infection Prevention and Control manual for England (NHS England 2022b) is shown in table 1.1. This list was informed by a rapid review of the literature conducted by the UK IPC cell (UK IPC Cell 2022), who recommended the removal of several previously included procedures (UK Health Security Agency 2021b), including tracheal intubation and extubation (in anaesthetised patients), manual facemask ventilation, non-invasive ventilation, and high flow nasal oxygen. Much of the evidence relating to the removal of these procedures from the UK AGP list arose

from the NIHR-funded AERATOR study, which measured aerosols using particle-counting instruments and showed that increased aerosol concentrations were not observed during these procedures compared, for example, to breathing or coughing (Brown et al. 2021; Shrimpton et al. 2022; Wilson et al. 2021). Although this work was meticulously conducted, a limitation of any methodology measuring aerosol quantity alone, is that the microbiological content and therefore pathogenic potential of the aerosols cannot be measured even if the aerosols themselves are not shown to be increased. Considering all the available evidence, the IPC cell concluded that dental procedures which involve using high-speed instruments, should remain on the AGP list.

Aerosol-generating procedures (AGPs)
Awake* bronchoscopy (including awake tracheal intubation)
Awake* ear, nose, and throat (ENT) airway procedures that involve respiratory suctioning
Awake* upper gastro-intestinal endoscopy
Dental procedures (using high speed or high frequency devices, for example ultrasonic scalers/high speed drills)
Induction of sputum
Respiratory tract suctioning**
Surgery or post-mortem procedures (like high-speed cutting / drilling) likely to produce aerosol from the respiratory tract (upper or lower) or sinuses.
Tracheostomy procedures (insertion or removal).

Table 1.1. Current list of aerosol-generating procedures (AGPs) in the UK.

Taken from the National Infection and Prevention Control Manual for England (NHS England 2022b). *Awake including 'conscious' sedation (excluding anaesthetised patients with secured airway). ** The available evidence relating to respiratory tract suctioning is associated with ventilation. In line with a precautionary approach, open suctioning of the respiratory tract regardless of association with ventilation has been incorporated into the current AGP list. It is the consensus view of the UK IPC cell that only open suctioning beyond the oro-pharynx is currently considered an AGP; oral/pharyngeal suctioning is not an AGP.

Recent reviews of the evidence surrounding bioaerosols and AGPs in healthcare settings have concluded that the existing evidence is highly heterogenous and of mixed quality (ARHAI Scotland 2021; Jackson et al. 2020; Tran et al. 2012; UK IPC

Cell 2022). Furthermore, a recent report published by the National Institute for Health and Care Research (NIHR) highlighted the need for research to address gaps such as risk factors for disease transmission during AGPs, mitigation strategies, and better understanding of the relevant fundamental aerobiology (NIHR AGP Research Group 2021).

1.2 Respiratory aerosols and airborne transmission of disease

Aside from bioaerosols created during specific medical or dental AGPs (which were of great concern during SARS, H1N1 influenza, and COVID-19 outbreaks), normal respiratory activities such as breathing, talking, and coughing generate aerosols, and the amount of aerosol produced is related to the degree of respiratory effort. For example, Wilson *et al.* (2021) demonstrated a 34.6-fold increase in total aerosol particle emission during talking (95%CI: 15.2 – 79.1) and a 370.8-fold increase during coughing (95%CI: 162.3 – 847.1) compared to breathing. Another interesting study of aerosol emission rates during singing and playing wind instruments found a 28% increase in aerosol particle emission for every 1 dBA increase in sound pressure level during brass instrument playing (Volckens et al. 2022), further demonstrating the relationship between aerosol emission rates and respiratory effort.

Respiratory aerosols are thought to be generated within the respiratory tract by the interaction of turbulent airflows with the films of liquid and mucus which line the airways. During exhalation, bronchioles collapse causing fluid films to form across the small airways which burst upon subsequent inhalation, generating aerosols which are then exhaled (Asadi et al. 2019). Similar mechanisms are thought to occur as a result of laryngeal articulation during vocalisation, and in the pharynx and oral cavity during speech, producing particles of comparatively greater size than those produced in the lower airways (Johnson et al. 2011). The presence of microorganisms, including viruses, in the fluid at any of these aerosol generation sites means that microbes can be carried within respiratory aerosols.

There is now overwhelming evidence that airborne transmission of several respiratory viruses occurs by inhalation of virus-laden aerosol (Wang et al. 2021). For example, infectious SARS-CoV-2 (Lednicky et al. 2020; Santarpia et al. 2020), middle east respiratory virus (MERS) (Kim et al. 2016), influenza (Lindsley et al. 2010; Yan et al. 2018), and respiratory syncytial virus (RSV) (Kulkarni et al. 2016), as well as RNA from SARS-CoV-1 (Booth et al. 2005), rhinovirus (Myatt et al. 2004),

and measles virus (Bischoff et al. 2016) can be recovered in air samples from infected patients. Furthermore, experimental (Dick et al. 1987) and epidemiological data from humans (Azimi et al. 2021; Cowling et al. 2013; Katelaris et al. 2021; Li et al. 2021; Miller et al. 2021; Riley et al. 1978; Yu et al. 2004) and data from animal studies (Gustin et al. 2015; Hao et al. 2019; Kutter et al. 2021; Sia et al. 2020; Totura et al. 2020) confirm a substantial role for these infectious aerosols in transmitting clinical disease.

Airborne transmission is also a route of spread for some bacterial diseases, as demonstrated for *Mycobacterium tuberculosis* by elegant experiments in guinea pigs exposed to air from hospital tuberculosis wards, whereby 49% of exposed animals, but no unexposed animals, developed clinical evidence of tuberculosis (Escombe et al. 2008; Riley et al. 1962). Furthermore, viable bacterial respiratory pathogens such as *Pseudomonas aeruginosa*, *Staphylococcus aureus*, *Stenotrophomonas maltophilia*, *Achromobacter* spp., and *Burkholderia* spp. have also been isolated from air samples during coughing in patients with cystic fibrosis at distances up to 4 m and up to 45 mins after coughing (Wood et al. 2019). In this study, species isolated from air samples were identical to those in patient's matched sputum samples on sequencing. Airborne transmission of the gram-negative coccobacillus *Bordetella pertussis*, has also been demonstrated in a non-human primate model between inoculated animals and animals housed in separate cages at a distance of 7 feet (Warfel et al. 2012). There is also epidemiological evidence in rare cases of airborne transmission of pneumonic plague, caused by the gram-negative coccobacillus, *Yersinia pestis* (Kool and Weinstein 2005). Additionally, the presence of DNA from the fungal pathogen *Pneumocystis jirovecii* has also been demonstrated in the air surrounding patients with *Pneumocystis* pneumonia, and at distances of up to 8 m (Choukri et al. 2010; Fréalle et al. 2017).

Aside from human-to-human transmission via respiratory aerosols, there have been isolated reports of transmission of zoonotic bacterial pathogens such as *Francisella tularensis* (Hauri et al. 2010; Siret et al. 2006) and *Burkholderia pseudomallei* (Wu et al. 2023) via the airborne route. Indeed, due to the fact that aerosolised bacteria such as *Y. pestis*, *F. tularensis*, and *B. pseudomallei* can readily initiate respiratory disease, they have been investigated as potential biological weapons (Day and Berendt 1972; Druett et al. 1956b; Thomas et al. 2012; Thomas et al. 2009), along

with other zoonotic bacterial pathogens such as *Bacillus anthracis* (Druett et al. 1953) and *Brucella suis* (Druett et al. 1956a).

1.3 The fate of aerosols

Once in the environment, aerosols do not remain stable. For example, the momentum with which they are emitted, either during breathing, coughing, or via an instrument such as a dental handpiece, affects how long they remain in the air and how far they travel (Kwon et al. 2012). The size of aerosol particles also dictates their residence time, with larger particles settling to the ground sooner than smaller ones, under the influence of gravity. This relationship is described by Stokes' law, and whilst in still air, a spherical 100 μm-diameter particle might take 5 sec to settle to the ground from a height of 1.5 m, a 5 μm particle would remain suspended for 33 min (Wang et al. 2021). The temperature and relative humidity of the environment also influences the aerosol, as both affect the rate of evaporation (Orr et al. 1958). Smaller particles evaporate more quickly and therefore become smaller and remain suspended for longer. The ultimate size and composition of the resulting particle is also determined partly by their salt, protein, surfactant, and water content (Vejerano and Marr 2018; Xie et al. 2007).

One persisting problem in the literature relating to airborne transmission and AGPs is the conventional IPC dogma that infectious diseases are transmitted via one of three clearly defined, and mutually exclusive routes: the contact route, whereby infection is transmitted by direct contact with the patient or their surroundings; the droplet route, where transmission occurs over short distances via the patient's respiratory droplets coming into contact with an individual's mucosa; or the airborne route, which can occur over larger distances via aerosols (typically defined as particles < 5 μm diameter) from the patient's respiratory tract being inhaled or contacting an individual's mucosa (NHS England 2022b). More recently however, several authors have questioned the validity of these neat delineations and have highlighted that the literature on which they are based, dating back as far as the work of Flügge in the late 19th century, has been misinterpreted (Randall et al. 2021). For example, particles much larger than 5 μm in diameter—up to 100 μm—can remain suspended in the air and could contribute to airborne transmission. In addition to this, the concept that droplets >5 μm always settle to the ground within 2 metres of the source is erroneous, and in fact particles 50–100 μm can be carried 2 m and beyond,

particularly in indoor settings with turbulent air flows, or where droplets travel in a fast-moving plume during a cough or sneeze (Tang et al. 2021).

1.4 Deposition of bioaerosols

Once aerosolised, microbe-laden aerosols can be inhaled or deposited on exposed (e.g., oral, pharyngeal, ocular) mucous membranes, potentially initiating an infection. Aerosol particles up to 100 μm can be inhaled, and the size of these particles dictates where in the respiratory tract they are most likely to be deposited (figure 1.2). Once inhaled, aerosol particles may increase in diameter due to hygroscopic growth in the high relative humidity of the airways (Finlay et al. 1996). Larger aerosols of > 5 μm aerodynamic diameter primarily deposit in the nasopharyngeal airways, and although < 5 μm aerosols may become deposited in the upper airways, these aerosols can penetrate more deeply into the bronchial and alveolar airways. Very small aerosols < 0.1 μm are primarily deposited in bronchiolar and alveolar regions (Guha et al. 2014). The site of deposition is important, as evidence from animal models suggests that lower doses of many bacterial and viral pathogens are required to cause lethal infection when administered in small aerosols (depositing in the lower airways) compared to in large aerosols (depositing in the upper airways) with differing disease course resulting from infection at each site (Thomas 2013).

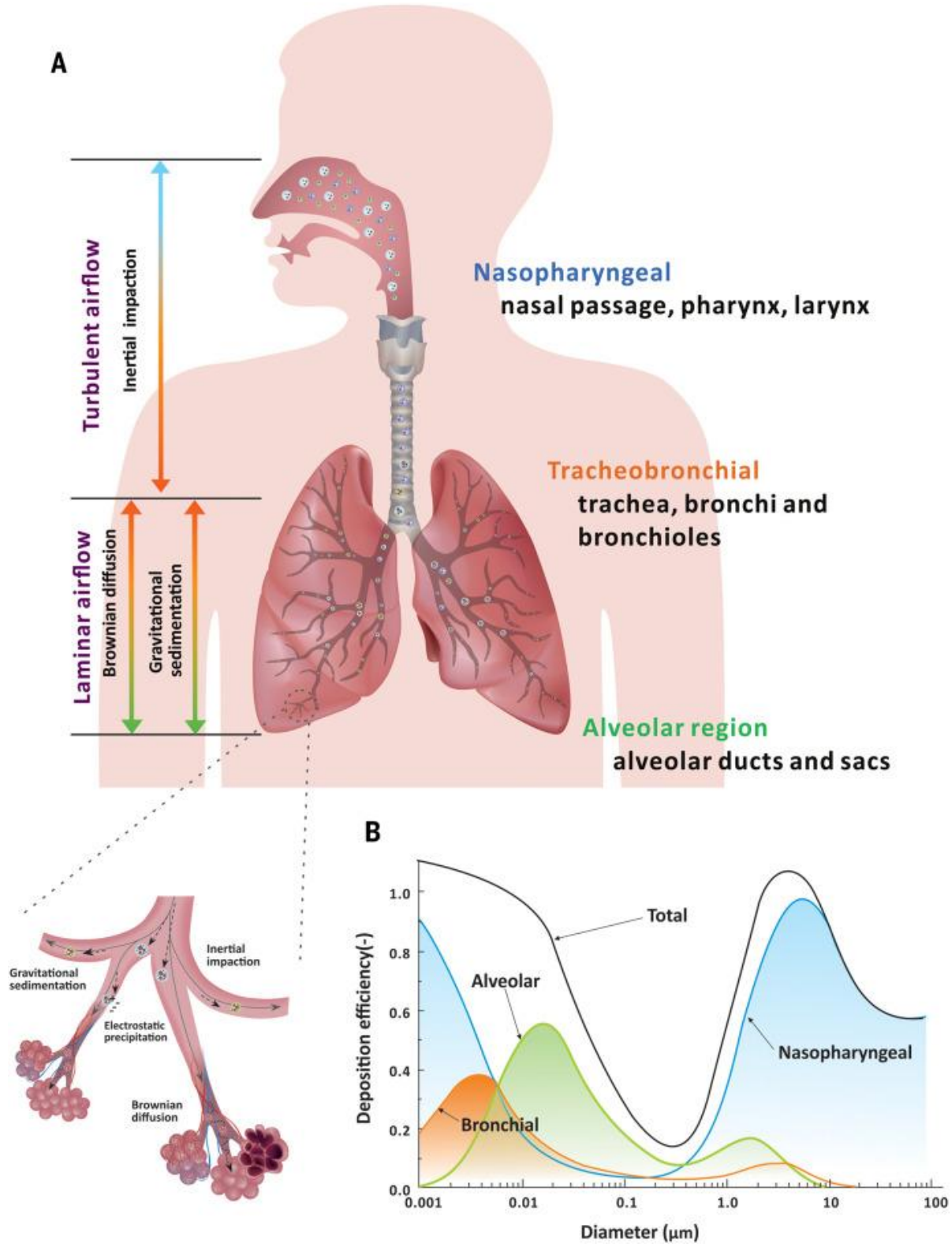

Figure 1.2. Mechanisms of aerosol deposition in the respiratory tract.

Reproduced from **(Wang et al. 2021)** CC BY 4.0 license. (A) Mechanisms of deposition in different areas of the respiratory tract, including inertial impaction (larger aerosols), gravitational sedimentation, and Brownian diffusion (smaller aerosols). (B) Deposition efficiency in different regions of the respiratory tract as a function of aerosol diameter, based on the International Committee of Radiological Protection (ICRP) lung deposition model (Hinds 1999).

1.5 Bioaerosols in dentistry

As in any setting where health professionals are in close contact with patients, dental professionals are exposed to patients' respiratory aerosols, and any microbes contained therein. In dentistry however aerosols are also generated by instruments such as air turbine handpieces and ultrasonic scalers used within the microbially-laden oral cavity. Some of the first detailed studies of bioaerosols in dentistry were conducted in the 1960s and early 1970s, following the introduction of the air turbine handpiece in the late 1950s, due to concerns surrounding aerosolised bacteria, tooth debris, and lubricating oil from these handpieces. Studies using air and surface sampling to detect oral microbes dispersed from the mouths of patients during dental procedures (Kazantzis 1961; Micik et al. 1969; Miller et al. 1971) or the presence of *Serratia marcescens* as a tracer organism (Hausler and Madden 1966; Madden and Hausler 1963) were the first to demonstrate dispersion of microorganisms from the mouth in droplets and aerosols. The authors found that the degree of dispersion was affected by the instrument used and varied by the location of sampling as well as decaying over time.

Bioaerosols were not high on the dental IPC agenda after this initial interest, although widespread adoption of the use of gloves, facemasks, and the safe use of sharps in dentistry did gradually occur during the 1980s, in part encouraged by the HIV/AIDS pandemic and prevalence of hepatitis B and C (Nield 2020). Authoritative guidance for dental IPC in the UK did not arrive until 2009 in the form of *HTM 01-05: decontamination in primary care dental practices* (Department of Health 2013), however, this included very little information on potential risks from bioaerosols. Some interest in bioaerosols by the dental profession was seen during the SARS and MERS outbreaks in the first and second decades of the 21st century (Al-Sehaibany 2017; Li et al. 2004) however it wasn't until the early stages of the COVID-19 pandemic in 2020 that the importance of bioaerosols in dentistry became fully apparent. Many of the opportunities to learn lessons on the risks posed by dental aerosols were missed prior to the COVID-19 pandemic, and it is important that we improve our understanding of effective mitigations to prevent similar widespread disruption in future outbreaks.

There is very little high-quality epidemiological evidence on the risk of infection of dental professionals via bioaerosols in the dental clinic, however one study which looked at SARS-CoV-2 seroprevalence in the north west of England during the early

COVID-19 pandemic, prior to widespread vaccination, found that previous COVID-19 infection was more likely in clinical members of the dental team (~16%), compared to both non-clinical members of the team (e.g., reception staff) and the general population at that time (~6%) (Shields et al. 2021). This may not be surprising, given that among other professions, dentistry may have one of the highest bioaerosol exposure risks due to the combination of close proximity and frequent potential exposure to pathogens (Office for National Statistics 2020).

1.6 The oral microbiota

The mouth contains many diverse microbial populations, mainly situated in highly organised biofilms located within numerous niches including mucosal, tooth, subgingival, and non-biological surfaces, as well as in saliva. The composition of these populations vary between individuals, as well as over the life course, and can change in the presence of disease states such as dental caries and periodontitis (Lamont et al. 2018). Bacterial species are numerous, and several hundred taxa have been identified. The most common species belong to genera including *Streptococcus*, *Neisseria*, *Haemophilus*, *Rothia*, *Veillonella*, and *Prevotella*, although many are unculturable and their detection relies on culture-independent methods such as sequencing (Wade 2013).

Aside from bacteria, archaea and fungi are also present within the oral cavity and contribute to microbial ecology, along with a wide diversity of viruses (Baker et al. 2017; Huynh et al. 2015). The most frequently detected viruses are bacteriophages—viruses which infect bacteria—particularly those belonging to the families *Siphoviridae*, *Podoviridae*, and *Myoviridae*. Most studies, however have used sequencing, with very few directly isolating bacteriophage (Sugai et al. 2023). It is likely that many detected sequences represent prophage genomes (bacteriophage genetic material which remains dormant in the host bacterial cell), rather than free bacteriophage virions. A variety of eukaryotic viruses are also present in health, including herpesviruses, retroviruses, and papillomaviruses (Pérez-Brocal and Moya 2018). Viruses are also present in saliva in significant quantities during active infections with viruses such as SARS-CoV-2, influenza A and B, RSV, human metapneumovirus, and parainfluenza viruses (To et al. 2017a; Yang et al. 2021b) as well as blood-borne viruses such as HIV and hepatitis B and C (Frerichs et al. 1992; Hermida et al. 2002; Kamimura et al. 2021). The diverse range of microorganisms in

the oral cavity may therefore be dispersed from the mouth into the environment due to interactions between dental instrument aerosols and oral fluids and biofilms which contain microbes.

As well as the mouth, biofilms are also present within the waterlines which supply dental instruments. The water supplied by these waterlines have been shown by sequencing to contain numerous bacterial taxa from the genera *Legionella*, *Mycobacterium*, *Serratia*, *Pseudomonas*, *Coxiella*, *Staphylococcus*, *Sphingomonas*, *Delftia, Caulobacter*, *Pedobacter*, *Stenotrophomonas, Methylobacterium*, *Novosphingobium*, and *Polaromonas*, (Hoogenkamp et al. 2021; Yoon and Lee 2019; Zemouri et al. 2020c). Dental bioaerosols are therefore highly likely to contain bacteria from these genera (Zemouri et al. 2020c) in addition to those which arise from the oral cavity.

1.7 Measurement of bioaerosols

Several methods for the measurement of aerosols in healthcare settings have been reported in the literature, for example, by detecting the microbes or microbial products arising from individual patients, quantifying the aerosols themselves by physical measurement of individual droplets, or by detection of tracers (biological or otherwise) added to aerosols to quantify them. These methods can be used in real clinical settings or in simulation models, and each approach has its own benefits and limitations.

1.7.1 Measurement of dispersed oral microbes in vivo

Some of the earliest studies of dental bioaerosols relied on detection of patients' microbiota to quantify bioaerosols produced during dental procedures. Micik (1969) used air sampling equipment to detect bacteria in aerosols during normal respiratory activities and dental procedures in a specially-designed chamber. In these experiments, the use of an air turbine handpiece produced 1,000 times as many bacterial colony forming units (CFU) as quiet breathing, and twice as many as during a sneeze; high-volume suction reduced detection of bacteria by 99.4%. The same group reported that droplets containing oral bacteria, captured using agar settle plates, were detectable 6 feet away from a procedure using an air turbine handpiece, although this was less than a sneeze (Miller et al. 1971). More contemporary applications of these methods found that the highest concentrations of droplets and

aerosols containing bacteria settled on the area of the patient's chest during dental procedures, suggesting that the zone closest to the procedure most likely carries the greatest risk of contamination (Zemouri et al. 2020c). In the same study, the authors also used 16S-rRNA gene sequencing to identify taxa dispersed into the environment and reported the presence of genera from the oral cavity (*Actinomyces*, *Corynebacterium*, *Staphylococcus*, and *Streptococcus*) as well as those present in instrument water supplies (*Acinetobacter*, *Enhydrobacter*, *Sphingomonas*), suggesting contribution of oral and dental-waterline–derived microbes. This finding is supported by Dutil *et al.* (2009) who reported the presence of dental-waterline–derived bacteria in water and air samples using bacterial culture and quantitative polymerase chain reaction (qPCR), including *Legionella* spp. and non-tuberculosis mycobacteria. Although exposure to dental-waterline–derived microbes may be hazardous, their presence makes studying patient-derived microbes in dental bioaerosols challenging. Additionally, the variability of each patient's oral microbiota, in terms of quantity and composition, makes this methodology potentially problematic. Furthermore, most studies have looked at bacteria only, and so the contribution of other infectious agents, particularly viruses, is not well understood.

A smaller number of authors have tried to detect viruses in dental bioaerosols, and this has mainly been during the COVID-19 pandemic by specific detection of SARS-CoV-2 using reverse transcription qPCR (RT-qPCR). One study reported the presence of SARS-CoV-2 RNA on settle plates in a dental surgery in five out of 24 cases where dental treatment using a scaler and air turbine handpiece was carried out on patients with known COVID-19 (Akin et al. 2021). All positive samples in this study were in patients where medium-volume suction was used during the procedure instead of high-volume suction. In a similar study, SARS-CoV-2 RNA was not detected in swabs from operators' face shields and patients' chests using RT-qPCR following dental treatment, despite the fact that 19 of the 28 patients had SARS-CoV-2 in their saliva (Meethil et al. 2021). This study did use suction, which may have eliminated viral dispersion, and patients also had a very low salivary viral load (27–912 copies/mL) which may have limited detection following dispersion. Interestingly, a study in a university dental clinic in Iran during a period of high community COVID-19 prevalence found SARS-CoV-2 RNA in 36% of air samples (Bazzazpour et al. 2022). Very little research has been done in clinical dental settings looking at viruses other than SARS-CoV-2, although one study in dental patients reported the presence of hepatitis B virus DNA using PCR, in dental aerosols from one out of three hepatitis

B carriers, during an orthodontic debonding procedure with a high-speed dental handpiece (Toroglu et al. 2003).

Whilst sampling during an infectious disease outbreak may make the recovery of any pathogen of interest more likely, most of the time patients attending the dental clinic are unlikely to have an infection, and capturing a particular pathogen becomes unlikely during periods of low community prevalence. This is the main limiting factor in studies of this kind in the dental setting, and methodological issues in sampling and detection of microbes may further complicate this approach. Additionally, if microorganisms are sampled directly from the clinic, it may be difficult to separate the contributions of different sources, such as the oral cavity, the respiratory tract, or the water supply of the dental instruments themselves.

Taken together, results from these studies suggest that the variable presence of certain viruses in the mouth compared to bacteria in general make detection challenging. Insufficient work has been done to fully characterise the oral virome, let alone the viruses present in bioaerosols in dental and other healthcare settings. The examination of RNA viruses has also largely been neglected in favour of DNA viruses. The use of metagenome sequencing approaches has not yet been applied to the study of dental bioaerosols; however, this may be a potentially useful approach. This method does not rely on amplification of specific targets, as with 16S-rRNA gene sequencing, for example, meaning that non-bacterial microbes, including viruses, can be identified. These methods may help us to better understand the diversity and potential for dispersion in bioaerosols.

1.7.2 Physical aerosol measurement

An alternative method is the physical measurement of aerosol particles, which assumes that where the absolute amount of aerosol is increased, the presence of bioaerosols and therefore infection risk is also increased. Given that microbiological methods show that microbes are indeed dispersed from the mouth during dental treatment, physical measurement of aerosols is therefore a useful approach. One issue with this method, however, is that the assumption linking aerosol quantity and pathogenic potential may not always be valid. For example, one could imagine two procedures which produce similar quantities of aerosol, but where microbial content differs widely. The main benefits of physical aerosol measurement are the rich temporal data produced, and that the relative size of the droplets within the aerosol

can be easily resolved, which as discussed, is important because size affects dispersion, persistence, and potential infectiveness (Guha et al. 2014).

Several instruments exist for measuring aerosols, as follows: optical particle counters (OPCs; figure 1.3) detect individual particles by measuring the light they scatter as they pass through a laser beam; the intensity of the light is a function of the diameter of the particle, its shape, and refractive index, and particles 0.3 – 10 μm are typically detected (although particles down to 0.1 μm can be detected with more sophisticated intracavity OPCs). OPCs can measure the diameter of aerosol particles but do so by reporting the diameter of particle of known optical density which produces the same scattered light signal, set during the instrument's calibration, as the particle being measured; this is referred to as the *optical* diameter and may differ from the detected particle's true physical diameter. To count particles smaller than is possible using an OPC, condensation particle counters (CPCs) pass a stream of particles through a chamber filled with a supersaturated vapor which condenses onto particles, thus increasing their size sufficiently to be detected and counted by the laser. These instruments can detect particles as small as 2 nm, but because their diameter is changed by the instrument, CPCs cannot measure the original diameter of particles. Aerodynamic particle sizers (APS) count particles based on how they behave in air rather than the light they scatter and measure the *aerodynamic* diameter of particles over a range of around 0.5 – 20 μm, giving a detailed particle size distribution of the aerosol. Finally, scanning mobility particle size spectrometers (SMPS) are able to generate detailed size distributions of particles over a range of 1 – 1,000 nm (TSI Inc. 2012).

Figure 1.3. An optical particle counter.
Model: Lighthouse 3016-IAQ.

Due to the convenience of physical aerosol measurement, many investigators have used these instruments to measure dental aerosols, with varying methodological rigor. One factor limiting the application of these methods is the presence of particles under normal conditions in ambient air, which are also detected by these instruments (background signal), limiting the ability to detect aerosols specifically from a dental procedure. One well-conducted study controlled the background signal using air filtration and reported increased aerosol concentrations during procedures on patients involving ultrasonic scaling, the use of an air-water syringe, and high and low speed drilling, with particles below 10 μm predominating in terms of number concentration (Dudding et al. 2022). Importantly, the authors also measured the aerosol concentrations produced by breathing and speaking, which were similar to the background signal, and coughing, which was more similar to the dental

procedures. Few other studies using physical aerosol measurement in dentistry have sought to minimise background signal or have used a patient-derived aerosol reference such as speaking or coughing; this may limit the validity of this measurement technique in other studies with patients which have not used such an approach. Particle measurement instruments have also been used in simulated clinical experiments, and are a useful way of assessing the relative reduction in aerosol concentrations during assessment of mitigation strategies such as high-volume suction (Yang et al. 2021a), local exhaust ventilation (Allison et al. 2021b; Ehtezazi et al. 2021; Shahdad et al. 2021), and electric micromotor handpieces (Allison et al. 2021c).

Although the physical measurement of aerosols is useful, and provides rich information about aerosol characteristics, the application is not without difficulties and pitfalls, which are well reviewed by Gregson *et al.* (2021). It is therefore important to interpret these studies in concert with other data from studies using complementary methods.

1.7.3 Chemical tracers

As discussed, one limitation of microbiological methods using patients' oral flora is that this varies widely between individuals, and a limitation of physical aerosol measurement is that it is difficult to determine what proportion of the aerosol's constituents come from the mouth. One approach to address this is to use a tracer, i.e., a substance that can be added to a simulated system or a clinical setting to allow certain components of the aerosol, e.g., saliva or blood, to be estimated or measured. The benefit of using a tracer, particularly in simulated settings, is that high levels of repeatability can be achieved, allowing multiple parameters to be assessed in a controlled way. An obvious limitation, however, is that sources of variation such as patient's anatomy and microbiota, or their respiratory activities, may not be accurately modelled.

A number of authors have used chemical tracers such as methylene blue (Pierre-Bez et al. 2021) and other dyes (Baldion et al. 2021; Chiramana et al. 2013; Noordien et al. 2021) or citric acid (Chiramana et al. 2013; Shahdad et al. 2020) to detect aerosols produced during simulated dental procedures. To increase detection sensitivity, other authors including our group, have used fluorescent tracers such as fluorescein (Allison et al. 2021a; Bentley et al. 1994; Dahlke et al. 2012;

Horsophonphong et al. 2021; Veena et al. 2015). In many such studies however, the tracer was added to the water used to supply the dental instruments, and so the tracer effectively shows where water from the instrument, but not necessarily saliva and potential microbes, may be transported to. Additionally, many such studies rely on visual or photographic methods of detecting the tracer which may lack sensitivity. Our research group sought to address these limitations by measuring recovered fluorescein (Figure 1.4) fluorometrically using a spectrophotometer to improve sensitivity, as well as infusing the tracer into the mouth of the mannequin to simulate saliva, rather than in dental instrument irrigant water (Allison et al. 2022; Allison et al. 2021b; Allison et al. 2021c; Holliday et al. 2021; Llandro et al. 2021). This method has proved useful for studying dental aerosols and the insights gained have informed IPC guidance in the UK (UK IPC Cell 2022).

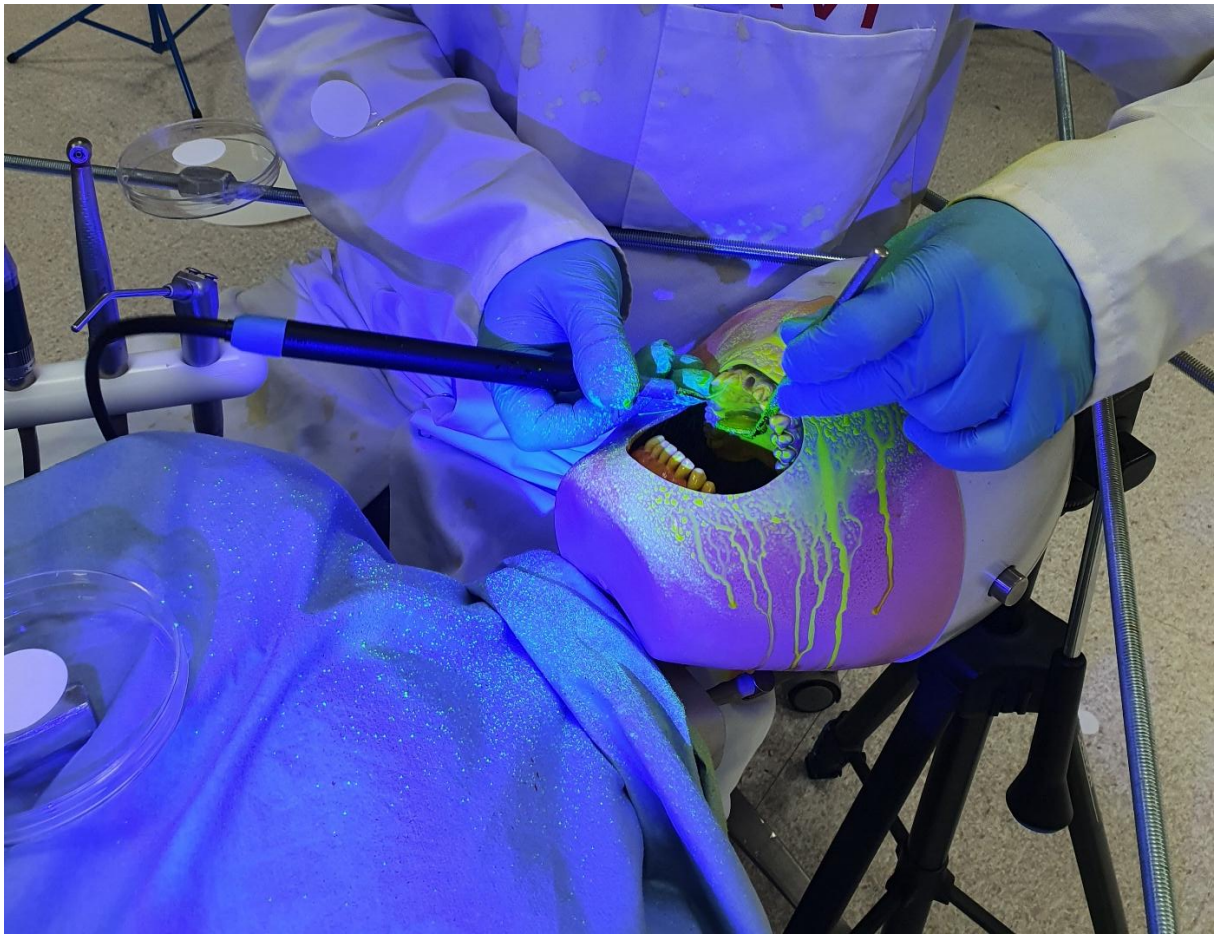

Figure 1.4. Fluorescein chemical tracer

Fluorescein added to the water supplying an ultrasonic scaler, allowing the aerosol from the procedure to be measured by quantifying dispersed fluorescein.

1.7.4 Bacterial tracers

Methods using non-biological tracers are helpful, but although these data tell us where potential pathogens in bioaerosols might go, these models do not adequately represent the biological characteristics of bioaerosols. As such, infectivity and survival of potentially dispersed microbes cannot be determined. A number of authors have sought to use bacteria as tracer organisms in simulation studies of bioaerosols, with one of the earliest studies in the field using a suspension of the gram-negative bacterium *Serratia marcescens* during simulated dental procedures with an air-turbine handpiece; this study demonstrated dispersion of the organism which decreased in quantity with increasing distance, but with smaller droplets predominating at more distant sites (Hausler and Madden 1966). Other authors have used *Streptococcus mutans* (Ionescu et al. 2020), *Lactobacillus acidophilus* (Horsophonphong et al. 2021), and *Enterococcus faecalis* (Barros et al. 2022) in a similar way. Many of the organisms used as bacterial tracers are easy to obtain, straightforward to work with, and pose little risk to human health when appropriate control measures are used. This approach is therefore very useful in demonstrating how and where bacteria are dispersed during dental procedures.

1.7.5 Viral tracers

Only a handful of studies have used viruses as tracer organisms. One study which used the RNA virus, equine arteritis virus, in the irrigant of an ultrasonic scaler operating in a steady state within a containment chamber, detected infectious virus using cell culture (RK13 cell line, *Oryctolagus cuniculus* kidney) in droplets and aerosols at up to 60 cm (Fidler et al. 2021). The inclusion of antiviral substances in the irrigant substantially reduced detection. This finding was replicated in a study using human coronavirus 229E (HCoV-229E) as a tracer during the operation of an air-turbine in a steady state inside a containment chamber (Ionescu et al. 2021). In this study, the tracer was mixed with artificial saliva and placed into the mouth of a dental mannequin during the procedure and viral RNA was detected in droplets by RT-qPCR. The authors reported detection of HCoV-229E RNA on surfaces at 25 cm, which was eliminated when hydrogen peroxide was included in the handpiece irrigant. This methodology allows controlled examination of viral dispersion during simulated procedures; however, the use of animal and human pathogens limits use

to laboratory settings only (equine arteritis virus is a notifiable equine pathogen, and HCoV-229E causes the common cold in humans).

Some authors have sought to address this by using viral tracers which do not pose a risk to human health in real clinical settings, allowing evaluation of dispersion outside of the laboratory. These studies have used bacteriophages (phages) which are viruses that infect bacteria and are harmless to humans. Whilst there are many types of phages, most possess a “tail”, which is an appendage projecting from the viral capsid allowing attachment to the host and delivery of the viral genome. The majority of phages belong to one of three families: *Myoviridae*, *Podoviridae*, and *Siphoviridae* (Harper 2021). The phage life cycle begins with the adsorption of a free virion to a host cell, resulting in delivery of the phage genome into the cell. Many phages follow a lytic life cycle, with the virus taking over the cellular machinery of the host cell in order to assemble new virions within the cell, before disrupting the cell membrane and wall, releasing progeny phage into the extracellular environment (Dennehy and Abedon 2020). Other phages follow a lysogenic life cycle, whereby once inside the host cell, the phage genome remains there (and is termed a prophage), rather than proceeding to virion production and cell lysis. Phages which follow this lifecycle are termed “temperate”, and many also retain the ability to produce lytic infection cycles (Łoś et al. 2021). First described in the early 20th century, bacteriophages have been used to treat bacterial infections, and helped researchers to elucidate many of the fundamental principles of genetics including demonstration of DNA as the primary genetic material and the function of mRNA (Mathews 2015).

In infection control studies, phages have been used as tracer organisms to simulate human viruses including studies of wastewater processing (Lin and Marr 2017), laboratory biosafety (Stern et al. 1974), and clinical IPC (Fisher et al. 2012; Reynolds et al. 2019; Tung-Thompson et al. 2015) (Figure 1.5).

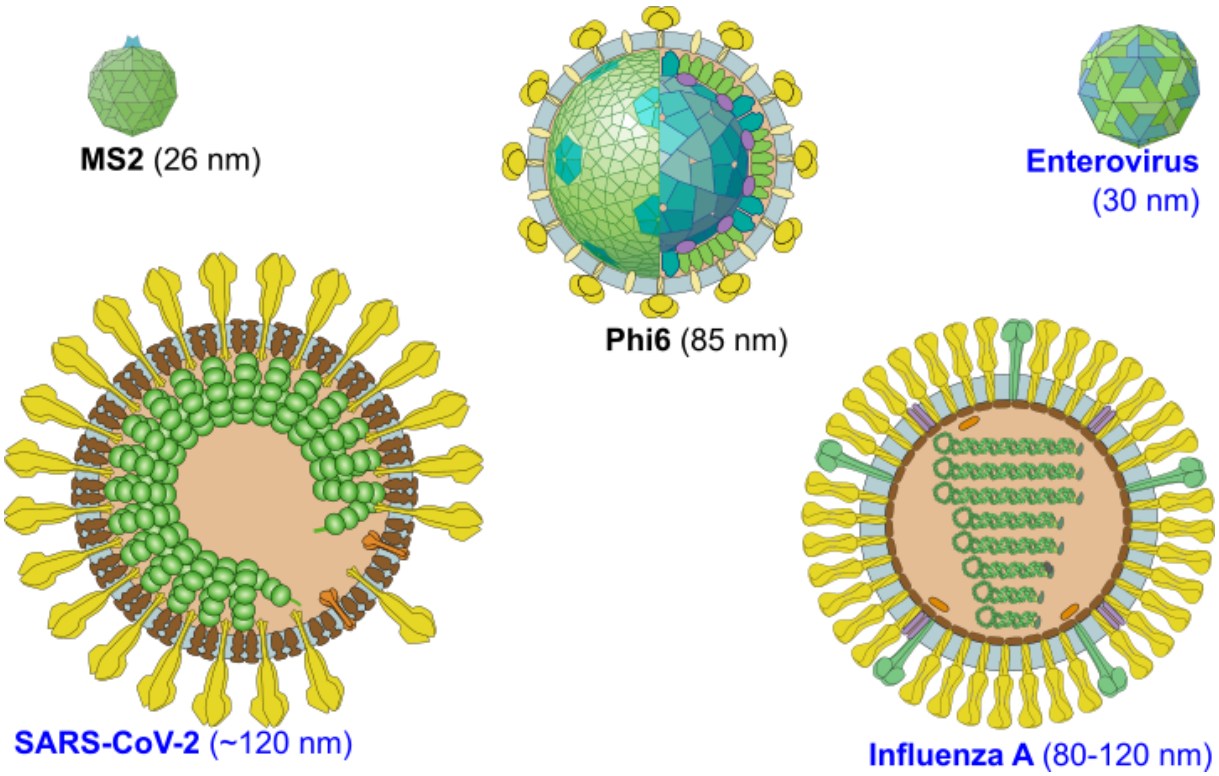

Figure 1.5 Selected virion structures

Comparison of bacteriophage MS2 and Phi6 virion structures with that of human viruses (blue text). Virion diameter is given, and virions are shown based on relative size. Virion images adapted from ViralZone, Swiss Institute of Bioinformatics. CC BY 4.0 license.

The first published study to apply phage tracers to the study of dental bioaerosols was by Vernon *et al.* (2021), using bacteriophage phi6, and demonstrated dispersion of virus from the mouth of a mannequin during a procedure using an air-turbine handpiece; this was reduced when using a non-air-turbine geared speed-increasing handpiece, high-volume suction, rubber dam, or local exhaust ventilation. A second study by our research group used a different phage (MS2) in a similar way to Vernon *et al.* and demonstrated dispersion of infectious virus during dental procedures using an air turbine handpiece at up to 3 m (Allison et al. 2022). Our study also evaluated the effects of a commonly used dental waterline disinfectant and demonstrated reduced the dispersion of virus in aerosols and droplets (data presented in Chapter 3). Additionally, we simultaneously evaluated the effect of the waterline disinfectant on a fluorescent tracer and found there was a difference between this and the results using the viral tracer, indicating that the use of a biological tracer may add additional information not obtained by chemical tracers alone. Subsequently, other authors have used the phages MS2 (Pratt et al. 2023), phi6 (Malmgren et al. 2023; Vernon et al. 2022), and phiX174 (Beltran et al. 2023; Liu et al. 2023) to investigate viral dental

bioaerosols in clinical settings. No studies using a viral tracer have yet simultaneously compared multiple virus types (e.g., enveloped/ non-enveloped) or examined the effect of environmental parameters such as ventilation, temperature, and humidity on virus dispersion and survival.

The primary method used to quantify infectious phage is the plaque assay, which was first developed by d'Herelle in 1917 (d'Herelle 2007) and was later well described by Adams in the 1950s (Adams 1959). This method uses plates of solid agar substrate overlaid with a semisolid agar medium to which the phage and host bacteria are added. The plates are incubated until discrete plaques of absent bacterial growth form in an otherwise confluent lawn of host bacteria. Each plaque, which corresponds to a three-dimensional volume of infected and lysed bacteria within the media, is assumed to have originated from a single viral particle, and on plates containing phage of an appropriate dilution, these plaques can be counted, allowing calculation of the concentration of infectious phage in the original sample. Other methods to enumerate phage include RT-qPCR or sequencing to detect phage nucleic acids, electron microscopy and epifluorescence microscopy to detect whole phage particles, and mass spectrometry (Acs et al. 2020; Clokie 2009). Many of these methods are highly sensitive, however they do not allow discrimination of infectious versus inactive phage particles as the plaque assay does.

The overall validity of the approach used may be improved by applying a combination of the above methods, as a number of authors have sought to do, particularly by adding sensitive physical aerosol measurement to a more specific approach such as recovery of microorganisms in the clinic (Choudhary et al. 2022; Rafiee et al. 2022) or the use of a biological tracer (Allison et al. 2022; Vernon et al. 2022).

1.8 Bioaerosol control measures

The dispersion of microbes in dental bioaerosols is clearly of great importance during an emerging infectious disease outbreak. During the COVID-19 pandemic, this led to the closure of dental services in many parts of the world, resulting in worsened oral health outcomes for patients unable to access care. Population measures during pandemic outbreaks such as vaccination (Beladiya et al. 2024) and face mask use (Coclite et al. 2020) may be highly effective at reducing community transmission and therefore risk to dental staff. Similarly, vaccination of healthcare workers against endemic diseases like influenza may also reduce transmission risk (Kliner et al.

2016) as this has been successfully implemented for blood borne viruses such as hepatitis B (Chen and Gluud 2005). As discussed, however, microorganisms are dispersed from the mouth in droplets and aerosols during dental treatment, along with microbes from biofilms present in dental unit waterlines (DUWLs) (Dutil et al. 2007). The existing evidence, as synthesised in several systematic reviews (Al-Yaseen et al. 2022; Gallagher et al. 2020; Innes et al. 2021; Johnson et al. 2021; UK IPC Cell 2022), suggests that procedures which use high-speed handpieces are more likely to disperse microbes during dental procedures than other instruments, and that contamination reduces with distance from, and with time after the procedure. These studies have all concluded, however, that the evidence base remains heterogenous and of low quality.

A better understanding of the risks posed by dental bioaerosols and of effective control measures may avoid the need to close services in future outbreaks. Outside of this context however, microbial dispersion is also of importance when treating patients with endemic diseases such as COVID-19, influenza, RSV, and tuberculosis. Most dental treatment in patients with active infection can be deferred, however urgent and emergency care cannot. Effective bioaerosol control measures are therefore needed to reduce exposure risk to dental professionals and other patients. A number of systematic reviews (Koletsi et al. 2020; Kumbargere Nagraj et al. 2020; Samaranayake et al. 2021) and guidance documents (National Services Scotland 2020; SDCEP 2021a; 2021b) have examined the evidence on methods of bioaerosol control, again concluding that the data are of mixed quality, with little to no data relating to dispersion of viruses in dental settings. The same is also true of the literature from other healthcare settings, with several systematic reviews of non-dental AGPs concluding that the data are highly heterogenous and often of low quality (ARHAI Scotland 2021; Chan et al. 2021; Jackson et al. 2020; Tran et al. 2012).

Dental bioaerosol control methods reported in the literature generally apply one of three approaches: 1) reducing the total amount of aerosol produced; 2) reducing the number of microbes within bioaerosol; or 3) capturing or removing bioaerosols.

1.8.1 Reducing aerosol production

Dispersion during dental procedures requires an aerosol within which to carry microbes, and control methods which reduce the total amount of aerosol are

therefore attractive. This is mainly achieved using dental instruments which produce less aerosol than the conventional air turbine handpiece. Initially introduced in the 1950s, the air turbine handpiece operates by driving compressed air through a small turbine in the head of the handpiece to spin a bur at rotational speeds up to 400,000 rpm. This air must be exhausted from the turbine, and is usually directed through the front of the handpiece, towards the tooth, along with water to cool the bur. This produces considerable aerosol (Sergis et al. 2020). An alternative design is to use an electric motor (micromotor) to drive a geared handpiece instead of an air-driven turbine, meaning that water alone can be used to cool the bur, thereby producing less aerosol (Figure 1.6). Importantly, this benefit is only present when water alone (without air) is used to cool the bur, which has not been clear in some documents recommending this approach (SDCEP 2021a).

Micromotor handpieces have been shown to produce substantially less aerosol than air turbine handpieces. For example, work by our research group using a simulation model with a fluorescent tracer measured using air-samplers, found that compared to an air turbine, which produced substantial aerosolised tracer, micromotor handpieces produced little detectable suspended aerosols at 1.7 m (Allison et al. 2021c). Another simulation study using a bacteriophage tracer found very little dispersed virus in settled (< 1 plaque-forming unit [PFU]) or suspended aerosols (< 0.08 PFU/m^3) outside of the immediate splatter zone (41 cm; defined by the authors) (Vernon et al. 2022). In another paper using the same methods, the authors also compared dispersion using micromotor handpieces to an air turbine, and found 360-fold reduction in infectious virus in settled aerosol and 195-fold reduction in suspended aerosols (Vernon et al. 2021). These findings are supported by a clinical study using aerosol particle measurement, in which measured aerosol concentration was ~100-fold lower during procedures with a surgical handpiece (electric micromotor handpiece ~40,000 rpm) compared to an air turbine handpiece (Dudding et al. 2022).

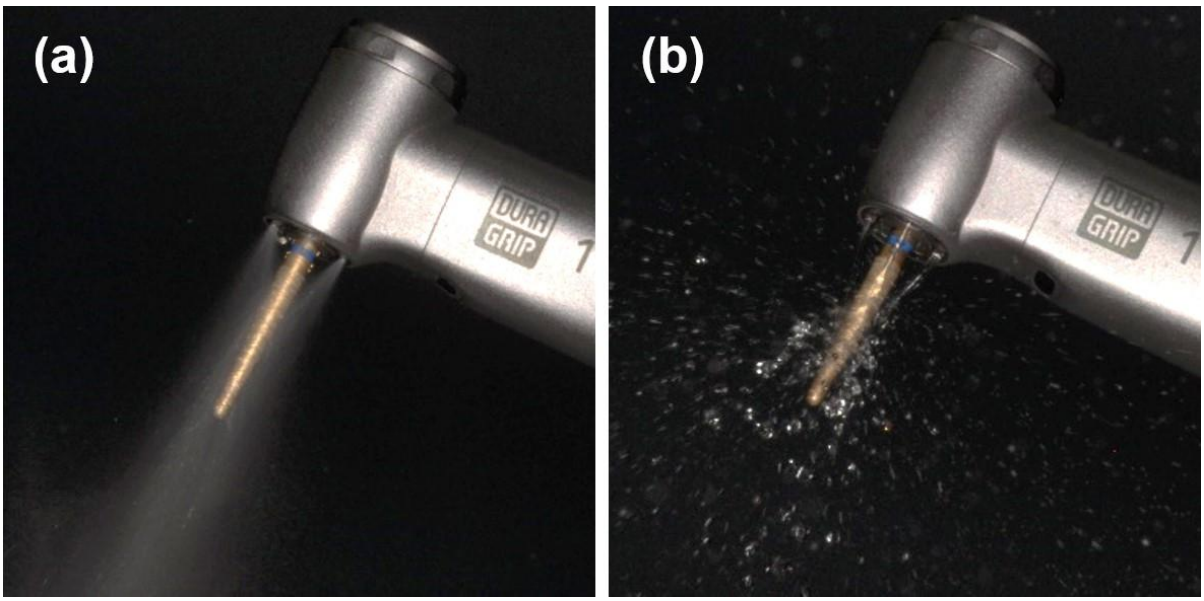

Figure 1.6. Micromotor dental handpiece

Irrigation of the micromotor handpiece with chip air activated (a) showing mist of air and water, and (b) without chip air, showing jets of water only. Originally published in the *Journal of Dentistry* (Allison et al. 2021c), the author retains the rights to the image.

1.8.2 Reducing microbial load in bioaerosols

Control measures which aim to reduce the number of microbes within bioaerosols have also been used, either by isolating the aerosol from the rest of the oral cavity, as with rubber dam, or by inactivating microbes using antiseptic mouthrinses or disinfectants in the water supplying dental instruments.

Rubber dam is a simple and inexpensive approach which has been used in dentistry for almost a century and a half (Author Unknown 1867). A sheet of rubber is placed over the mouth with holes for the teeth to be treated, effectively isolating them from the rest of the oral environment. Several systematic reviews of clinical studies have concluded that rubber dam reduces dispersion of bacteria with an estimated reduction of up to 99% at 1 m from the procedure, 70% at 2 m, and little effect at greater distances (Kumbargere Nagraj et al. 2020; Samaranayake et al. 2021; SDCEP 2021a). Conversely, one study found a 62% *increase* in recovery of bacteria from headscarves worn by operators when rubber dam was used (Al-Amad et al. 2017). However, due to the non-specific microbial analysis used, it is possible that bacteria from DUWLs were detected, and that dispersion was increased by greater deflection of the aerosol from the handpiece due to the presence of the dam. The effectiveness of rubber dam in controlling viral bioaerosols is also demonstrated by experimental data from a study using phi6 bacteriophage as a tracer, which reported

a reduction in infectious virus of 92% in settled aerosol and of 100% in air samples (Vernon et al. 2021).

A number of authors have suggested the use of antimicrobial mouthrinses such as chlorhexidine, povidone iodine, and cetylpyridinium chloride in reducing microbial load in the mouth prior to dental procedures, to thereby reduce the number of microbes dispersed in dental bioaerosols. Clinical studies have generally reported a 33 – 94% reduction in bacterial dispersion in bioaerosols when a pre-procedural mouthrinse is used (Koletsi et al. 2020; Samaranayake et al. 2021; Takenaka et al. 2022); however, not all studies have shown a reduction, with one study reporting a 59% increase in bacterial dispersion during orthodontic debonding when a chlorhexidine mouthrinse was used compared to no rinse (Dawson et al. 2016). Although several studies have demonstrated a reduction in salivary viral loads (e.g., SARS-CoV-2) following antiseptic mouthrinses use (Chaudhary et al. 2021; Hernandez-Vasquez et al. 2022), the effect on viral dispersion in dental bioaerosol remains unknown; it is reasonable, however, to assume that this is similar to the effect on bacterial bioaerosol dispersion and salivary viral load. Clinical recommendations published during the COVID-19 pandemic acknowledged this evidence base, but stopped short of recommending antimicrobial mouthrinses due to the risk of adverse effects such as allergy (SDCEP 2021a).

Disinfection of DUWLs to reduce waterline biofilm is standard practice in dentistry. Products are commercially available for periodic disinfection, which have a residual effect on biofilm accumulation, whilst other products are intended for continuous use at concentrations safe for patients (Zemouri et al. 2020a). As both types of disinfectant remain present in the water supplying dental instruments, it stands to reason that they may influence microbes present in the mouth and in bioaerosols created during dental procedures. A number of authors have suggested addition of antimicrobial agents such as chlorhexidine, sodium hypochlorite, hydrogen peroxide, and cinnamon extract to dental instrument irrigants to reduce bioaerosol dispersion, and these have been shown to reduce bacterial dispersion in clinical studies by 43 – 88% (Ashokkumar et al. 2023; Kumbargere Nagraj et al. 2020; Patil et al. 2023). No clinical studies have examined the effect of DUWL disinfectants on viral dispersion, however simulation studies with human and equine viruses in laboratory settings demonstrate elimination of infectious virus in bioaerosols using sodium hypochlorite and hydrogen peroxide in irrigants (Fidler et al. 2021; Ionescu et al. 2021). Similarly,

work by our group using MS2 bacteriophage demonstrated a 99% reduction in infectious virus at 0.5m when a commercially available agent was used (Allison et al. 2022). As with pre-procedural mouthrinses, concerns related to adverse effects of widespread antimicrobial use, including allergy, limited adoption during the COVID-19 pandemic (SDCEP 2021a).

1.8.3 Capturing bioaerosols

Suction devices are routinely used in dentistry to remove saliva and irrigants from patients' mouths during treatment, to improve access and visibility, and to maintain a dry field required during certain restorative procedures. Current standards define "high-volume suction systems" as those achieving an air flow rate of 250 L/min at the suction tip, with "medium-volume systems" achieving 90 – 250 L/min (NHS Estates 2003). Terminology used in the literature for dental suction varies, including high "speed", "velocity", or "volume" dental "suction", "evacuation", or "aspiration". Some studies have also examined systems which incorporate dental suction into devices used for oral isolation or retraction of soft tissues (Dahlke et al. 2012; Lloro et al. 2021; Suprono et al. 2021). Similarly, the effectiveness of low flowrate, small diameter suction devices referred to as "saliva ejectors" have also been measured (Graetz et al. 2022; Holloman et al. 2015; Ou et al. 2021). The term "high-volume dental suction" is used in the present thesis to refer to the intra-oral use of a large bore suction cannula designed to achieve air flow rates of ≥ 250 L/min. Clinical studies of high-volume dental suction demonstrate up to 80 – 90% reductions in bacterial dispersion during dental procedures, particularly at distances close to the dental procedure (i.e., within 30 cm) (Kumbargere Nagraj et al. 2020; Samaranayake et al. 2021; SDCEP 2021b). This is supported by data from simulation studies using droplet imaging demonstrating 92% reduction (Watanabe et al. 2023), fluorescent tracers demonstrating 75% reduction at 0.5 m and 67% 1.5 m (Allison et al. 2021a), as well as reductions in studies using a phage tracer (Malmgren et al. 2023).

To capture aerosols that escape the oral cavity, local exhaust ventilation (LEV) devices may be used. LEV, often referred to in the literature as "extra-oral suction" and aerosol "scavenging" or "extraction" systems, use an inlet positioned close to the patient's mouth which can achieve very high airflow rates (~3,000 – 5,000 L/min) to remove aerosol. The captured air is usually returned to the room after high-efficiency particulate air (HEPA) filtration. One clinical study found an 89 – 93% reduction in

bacterial dispersion when LEV was placed 10 cm from patients' mouths compared to 20 cm (Takenaka et al. 2022). Simulation studies using particle counting instruments (Ehtezazi et al. 2021) and fluorescent tracers (Allison et al. 2021b) also demonstrate reductions in detectable aerosol of up to 90% within 0.5 m from the procedure when LEV is used, reducing to 75% reduction at 2 m.

Since the COVID-19 pandemic, the importance of ventilation in dental clinics has become more widely understood. Bioaerosol can accumulate in poorly ventilated spaces, leading to increased risk of disease transmission (Li et al. 2007). There is little definitive evidence to support specific recommendations for adequate ventilation rates for dental settings, however in the UK, ventilation rates of 10 air changes per hour (ACH) are recommended for healthcare settings (NHS Estates 2003). Following a dental procedure on an infected patient, bioaerosols may persist in in the air, risking infection to others present or entering the room. Recommendations during the COVID-19 pandemic on how long after a procedure it becomes safe to enter the room without protective equipment (so called "fallow time"), were based on the limited existing evidence and expert opinion. It was suggested that larger contaminated droplets are likely to settle onto surfaces within 10 minutes after a dental procedure, with the clearance of smaller aerosols being dependant on ventilation rate: after 30 min at 10 ACH or 60 min at 5 ACH for a typical dental procedure where no other bioaerosol control method is used (National Services Scotland 2020; SDCEP 2021a; 2021b). These sources also suggest that fallow time may be reduced where other bioaerosol control methods are used. Where ventilation systems are poor or cannot be upgraded, there is evidence that air filtration using HEPA filters (also referred to in the literature as "air cleaners", "purifiers", or "scrubbers") may be effective in reducing dental bioaerosol dispersion (Kumbargere Nagraj et al. 2020; Liu et al. 2023; SDCEP 2021a).

1.8.4 Personal protective equipment

The final line of defence against infectious bioaerosols is personal protective equipment (PPE). Under normal conditions, and outside of the context of an infectious disease epidemic, the principles of standard infection control precautions apply to dental treatment (Centres for Disease Control and Prevention 2023a; NHS England 2022b). In relation to PPE, this means wearing disposable gloves, eye protection, and a fluid-resistant surgical mask where exposure to blood and saliva is

likely, in order to reduce the risk of splashing or spraying of body fluids onto the oral, pharyngeal, respiratory, or ocular mucosa. These precautions assume that the risk of inhaling infectious bioaerosols is negligible—a fair assumption during normal conditions in an asymptomatic patient. Where patients have a known or suspected infection however, then specific precautions (including PPE) appropriate to the route of transmission of that infection should be used; these are termed transmission-based precautions. For infections known to be transmitted via airborne transmission (e.g., influenza, COVID-19 and other coronaviruses, measles, tuberculosis) respiratory protective equipment such as a filtering face piece 3 (FFP3) or N95 mask, or a powered air-purifying respirator should be used when providing any care for patients to prevent inhalation of infectious respiratory bioaerosols. When performing an AGP on patients with an infection transmitted via the droplet route, respiratory protective equipment should also be worn to prevent inhalation of infectious bioaerosols (Centres for Disease Control and Prevention 2023a; NHS England 2022b). As discussed however, the classical contact/droplet/airborne transmission routes have been criticised for their over simplified approach to transmission dynamics and so risk assessment should take place for individual patients (Jimenez et al. 2022; Tang et al. 2021; Wang et al. 2021).

Outside of normal conditions, for example during an infectious disease epidemic, specific recommendations for PPE related to the causative agent may be given, as was the case in dentistry during the COVID-19 pandemic (Centres for Disease Control and Prevention 2023b; UK Health Security Agency 2021a). The evidence relating to the role of PPE in preventing infection of healthcare workers is generally of low certainty, and is largely from simulation studies assessing contamination, rather than those reporting rates of infection (Verbeek et al. 2020).

1.9 Aims and objectives

Given the current evidence base and disruption to dental services seen during the COVID-19 pandemic, there is clearly a need for better understanding of the impact of bioaerosols in dentistry and how they can be controlled. This project therefore aims to test the following hypotheses:

1. Microorganisms, including infective viruses, are dispersed from the mouth in bioaerosols during dental procedures.
2. Dispersion during dental procedures can be controlled using bioaerosol control measures.
3. Environmental parameters, such as ventilation, affect dispersion and persistence of dental bioaerosols.

These hypotheses will be tested using a clinical simulation model of dental bioaerosols with two distinct bacteriophage tracers as surrogates for human viral pathogens. The objectives of the project are to:

A. Measure the dispersion and infectivity of bacteriophage tracers in droplets and bioaerosols during simulated dental procedures.
B. Define the effectiveness (e.g., percentage reduction in bioaerosol dispersion) of bioaerosol control measures, such as high-volume dental suction, local exhaust ventilation, rubber dam, micromotor handpieces, and dental unit waterline disinfectants.
C. Demonstrate the effect of ventilation on the persistence of bioaerosols using a room-scale aerobiology chamber.

Chapter 2. Materials and Methods

2.1 Microbiological methods

2.1.1 Media and buffers

Microbiological growth media were obtained in powdered form from the suppliers in Table 2.1. The amount of powder recommended by the manufacturer was weighed using an analytical balance (PB300, Mettler Toledo, OH, USA), added to de-ionised water, and stirred using a magnetic stirrer (Stuart, UK). pH was measured using a single junction electrode (InLab Expert Pro; Mettler Toledo, OH, USA) attached to a benchtop meter (Seven Easy; Mettler Toledo, OH, USA) and corrected to pH 7.3 – 7.5 by adding sodium hydroxide using a Pasteur pipette.

Agar (Melford; Suffolk) was added at 1.4% w/v to media for agar plates before autoclaving at 121°C for 20 min (AMB430; Astell, Kent) and allowing to cool to 45 – 50°C before pouring into 90 mm polystyrene petri dishes (Fisherbrand; Fisher Scientific, USA) in a laminar-flow cabinet (TC48; Gelaire, Australia). For overlay agar used in plaque assays, agar was added at 0.7% w/v to media, which was then boiled to dissolve the agar using a stirring hotplate (Starlab, Milton Keynes) before adding 3 mL aliquots to 13 mm diameter glass screw-top tubes. The tubes containing media were then autoclave sterilised as above.

Buffers in Table 2.1 were obtained from the manufacturer shown, except for SM buffer, which was made by adding the reagents listed in table 2.1 to de-ionised water and correcting the pH to 7.5 as described. 20 mL aliquots of SM buffer were autoclave sterilised as above before storing at room temperature.

Medium or Buffer	Reagent	Amount
NZCYM	Tryptone	10 g/L
Sigma Aldrich; USA	Sodium chloride	5 g/L
	Yeast extract	5 g/L
	Magnesium sulfate heptahydrate	2 g/L
	Maltose	2 g/L
	Casamino acids	1 g/L
Tryptic Soy Broth (TSB)	Tryptone	17 g/L
Formedium; Norfolk	Sodium chloride	5 g/L
	Soya Peptone A3	3 g/L
	Dipotassium hydrogen phosphate	2.5 g/L
	Glucose	2.5 g/L
Luria-Bertani (LB) Broth	Tryptone	10 g/L
Melford; Suffolk	Sodium chloride	10 g/L
	Yeast extract	5 g/L
Super Optimal broth with Catabolite repression (S.O.C. medium)	Tryptone	20 g/L
	Yeast extract	5 g/L
	Sodium chloride	10 mM
Invitrogen; USA	Potassium chloride	2.5 mM
	Magnesium chloride	10 mM
	Magnesium sulphate	10 mM
	Glucose	20 mM
SM Buffer	Sodium chloride	100 mM
	Magnesium sulfate heptahydrate	8 mM
	Tris hydrochloride	50 mM
	Gelatin	0.01% w/v
TAE Buffer	Tris base	40 mM
Bio-Rad; USA	Acetic acid	20 mM
	EDTA, pH 8.0	1 mM
TE Buffer	Tris hydrochloride (pH 8)	10 mM
Invitrogen; USA	EDTA	0.1 mM

Table 2.1. Media and buffers.

2.1.2 Bacterial culture

Bacterial strains were obtained from the Leibniz Institut DSMZ. *Escherichia coli* W1485 (DSM 5695), an F^+ λ^- derivative of *E. coli* K-12 (Lederberg and Lederberg 1953), was obtained as a lyophilised culture, reconstituted in NZCYM liquid medium (Sigma Aldrich; Table 2.1), and inoculated onto NZCYM agar plates by streaking, before incubating overnight at 37 °C. A single colony was then picked the following day with a sterile loop and used to inoculate 5 mL NZCYM broth which was incubated overnight in a shaking incubator at 37 °C, 200 rpm.

Pseudomonas syringae pv. *phaseolicola* (HER-1102; DSM 21482) was obtained as a lyophilised culture and reconstituted in Tryptic Soy Broth (TSB; Formedium, Norfolk; Table 2.1) before inoculating onto Tryptic Soy Agar (TSA; 1.4% agar; Table 2.1) by

streaking and incubating at 25 °C for 48 h. A single colony was then picked with a sterile loop and used to inoculate 5 mL TSB which was incubated overnight in a shaking incubator at 25 °C, 200 rpm.

Expected colony morphology was confirmed before conducting phase contrast microscopy (DM750; Leica, Germany) and gram staining to confirm expected cell morphology and culture purity. Glycerol stocks were made by adding 700 µL of overnight bacterial culture to 300 µL of sterile 80% glycerol (Alfa Aesar, MA, USA) in sterile 1.5 mL cryotubes (24 % v/v final glycerol concentration) before vortexing and centrifuging for 3 – 5 s to consolidate contents. Cultures were then deposited in the laboratory's culture collection and stored at -80 °C. Working cultures were made from this master stock for subsequent use.

2.1.3 Bacteriophage culture

Bacteriophage MS2, a member of the species *Emesvirus zinderi* (DSM 13767; subsequently "MS2"), was obtained from the Leibniz Institut DSMZ GmbH as a lyophilised culture and was reconstituted in NZCYM. Bacteriophage phi6, a member of the species *Cystovirus phi6* (DSM 21518; subsequently "phi6"), was obtained from the Leibniz Institut DSMZ GmbH as an active liquid culture.

To produce isolated phage plaques, a sterile loopful of phage stock was streaked on an agar plate of the correct medium for the host (NZCYM for MS2 and *E. coli*; TSA for phi6 and *P. syringae*). 3 mL aliquots of sterilised overlay agar in 13 mm glass tubes were placed in a beaker of water and heated in a microwave oven (R-206; Sharp, Japan) at low power to melt the agar. The tubes were then placed in an electronic heating block (Techne Dri-Block™ DB100/4; Cole-Parmer, Staffordshire) set to 50 °C until use. After allowing the streaked phage to dry for a few minutes, 100 µL of overnight-grown host bacterial culture were added to 3 mL of the appropriate molten overlay medium and mixed by gentle vortexing. The mixture was then quickly poured onto the agar plate and distributed over the surface by gentle swirling. After allowing the molten agar to solidify, the plate was incubated inverted at 37 °C overnight for MS2 and at 25 °C for phi6.

After incubation, the plate was inspected to ensure confluent growth of the host bacterial lawn where phage was not streaked, and absent bacterial growth in areas of high phage concentration. Growth of individual plaques was confirmed in the

appropriate area of the plate, and a single plaque was picked by pressing the end of a sterile glass Pasteur pipette into the agar in the location of the plaque to excise the entire thickness of agar. The agar plug was then transferred to 1 mL of SM buffer in a 1.5 mL microcentrifuge tube by pressing the bulb of the Pasteur pipette. The tube was thoroughly vortexed for 1 min to disperse the phage and then centrifuged for 1 min at 15,000 x *g* (PrismR; Labnet, USA or CR-1512; CAPP, Germany) to pellet the agar debris and any bacterial cells. The supernatant was then filtered using a 0.22 µm polyether sulfone (PES) syringe filter (Fisher Scientific, USA). The purified phage lysate was stored at 4 °C and used as a working stock to seed higher volumes of phage lysate. Phage titre was then determined by plaque assay as described below.

To produce higher-volume lysates, lysis was conducted either on agar plates or in liquid media. For MS2, lysis on plates was generally found to be more reliable, whereas lysis in broth was preferable for phi6. For plate lysis, 100 µL of overnight host bacterial culture were added to a 1.5 mL microcentrifuge tube with an appropriate volume of phage lysate containing 10^4 – 10^6 Plaque-Forming Units (PFU) measured by plaque assay (e.g., 100 µL of a 10^5 – 10^7 PFU/mL phage lysate). The contents were mixed by gentle vortexing and incubated at room temperature for 5 – 10 min to allow adsorption of phage to host cells. The mixture was then added to 3 mL of the appropriate sterile molten overlay agar and mixed by gentle vortexing before pouring onto solid agar of the same medium and gently swirling the plate to distribute the overlay agar. The overlay agar was allowed to solidify before incubating the plate inverted at the appropriate temperature and duration for the host. Control plates containing only overlay agar (media control) and overlay agar with host bacteria only (host control) were included.

Following incubation, lysis of the host bacteria was confirmed by complete clearance of the plate, or by patchy growth of phage-resistant colonies of host bacteria. Confluent growth of a bacterial lawn was confirmed on the control plate. To recover phage, 3 mL of SM buffer was added to the surface of the lysed plate, and a cell scraper was used to disrupt and detach the overlay agar. The liquid and overlay agar were then recovered into a 15 mL or 50 mL centrifuge tube as appropriate for the recovered volume. Multiple plates were used to allow recovery of sufficient volumes of phage lysate. The recovered raw lysate was then vortexed at 3,000 rpm for 1 min to resuspend the phage and then centrifuged at 10,000 x *g* in a fixed-angle rotor for 10 min at 4 °C to pellet bacterial cells and agar debris (5804R; Eppendorf, Germany).

The supernatant was recovered and filtered using a 0.22 µm PES syringe filter. Where visible agar debris was present in the supernatant, the centrifugation and supernatant recovery steps were repeated, and a 0.45 µm PES filter was first used to prevent the 0.22 µm filter clogging. Titre was then determined by plaque assay, and the purified lysate was stored at 4 °C.

For lysis in liquid media, 10 mL host bacterial overnight cultures were established in 50 mL centrifuge tubes. 200 µL of phage stock (~10^8 – 10^{10} PFU/mL) were then added to the cultures which were shaken at 200 rpm at the appropriate growth temperature for the host until the culture became clear. After incubating, the lysate was centrifuged at 10,000 x *g* in a fixed-angle rotor for 10 min at 4 °C to pellet cells and debris (5804R; Eppendorf, Germany). The supernatant was then filter sterilised using a 0.2 µm sterile PES syringe filter. Titre was then determined by plaque assay, and the lysate was stored at 4 °C.

To produce purified lysates for long term storage at -80 °C, lysates were prepared as above, and host growth media was exchanged with SM buffer using a 20 mL 100 kDa molecular weight cut-off protein concentrator (Pierce; Thermo Scientific). 15 mL of phage lysate were added to the upper chamber of the protein concentrator and centrifuged at 4,000 x *g* for around 5 min at room temperature (3K10; Sigma, USA) until the volume in the upper chamber was reduced to ~ 5 mL. The flow-through was discarded, 15 mL of SM buffer were added to the upper chamber, and the centrifugation step was repeated until the volume was again reduced to ~ 5 mL. The wash and centrifugation steps were then repeated with a further 15 mL of SM buffer until the final volume was ~ 5 mL. 700 µL volumes of the purified lysate were then added to 300 µL of autoclave sterilised 80 % glycerol (24 % final glycerol concentration) in 1.2 mL cryovials. The contents were mixed by pipetting and then centrifuged for 5 sec to consolidate the liquid before placing in the -80 °C freezer for long term storage.

2.1.4 Quantification of bacteriophage by plaque assay

Ten-fold serial dilutions of the phage sample whose titre was to be determined were prepared in SM buffer covering the range expected to produce countable plaques (usually 10^{-5} – 10^{-8} dilutions for phage lysates).

To quickly determine phage titre, spot plaque assays were used, as these allow several phage dilutions to be inoculated onto a single agar plate. This is particularly useful where the expected titre is unknown as a larger range of dilutions can be plated more easily than with whole plate plaque assays. A sixteen-sector grid was drawn on the underside of an agar plate of the appropriate medium, and each sector was labelled with the appropriate dilution, including a control (Figure 2.1).

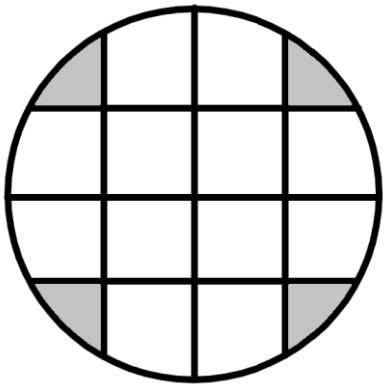

Figure 2.1. Template grid for spot plaque assays.

This grid was traced onto the underside of petri dishes for use in spot plaque assays. Shaded areas were not used.

100 µL of overnight-grown host bacteria corrected to ~ 0.6 OD_{600} (used in all plaque assays) were added to 3 mL aliquots of molten overlay agar and mixed by gentle vortexing. The mixture was poured onto the surface of an agar plate of the same medium and allowed to solidify close to a Bunsen flame. Once the overlay agar had solidified, 5 µL of SM buffer was spotted onto the control sector of the plate, and then working from more dilute to more concentrated, 5 µL of the appropriate phage dilutions were spotted onto the relevant sectors of the plate. The plate was then left with the lid slightly open, close to the Bunsen flame to allow the phage suspension to adsorb onto the agar. The plate was then incubated overnight at the appropriate temperature for the host (37 °C for *E. coli;* 25 °C for *P. syringae*).

Once sufficient host growth had occurred, the sector with 30 – 300 plaques countable plaques was identified, and equation (1) was used to calculate the titre in Plaque-Forming Units (PFU) of the original phage sample.

$$Plaque\ Forming\ Units, PFU/mL = \frac{N_{plaques}}{dilution\ factor \times volume\ of\ phage\ added(mL)} \qquad (1)$$

Whole plate plaque assays (Figure 2.2) were used where a more accurate determination of phage titre was required, and 1 – 3 replicates of each phage dilution were included depending on the required precision of the measurement. 100 µL of mid-exponential phase host bacteria were added to 100 µL of each of the phage dilutions to be tested in labelled 1.5 mL microcentrifuge tubes. The contents were mixed by gentle vortexing, and the tubes were incubated at room temperature for 5 – 10 min (long enough to allow adsorption of phage to host cells, but not so long as to produce progeny phage). The entire tube contents were then transferred to 3 mL aliquots of molten overlay agar and mixed by gentle vortexing, before the overlay agar was poured onto the bottom agar plates and distributed by gentle swirling. The overlay agar was allowed to solidify before incubating inverted at the appropriate temperature and duration to allow growth of the host bacteria (overnight at 37 °C for *E. coli;* 24 – 48 h at 25 °C for *P. syringae*). Control plates containing only overlay agar (media control) and overlay agar with host bacteria only (host control) were included.

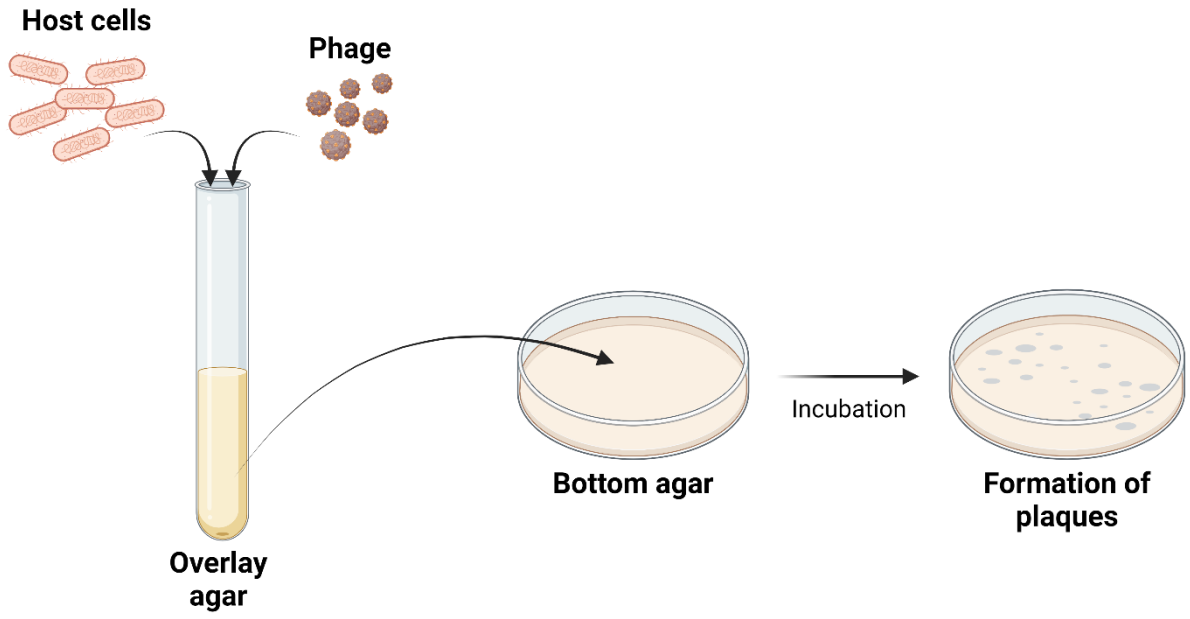

Figure 2.2. Plaque assay protocol.

Host bacterial cells and phage are added to molten overlay agar which is then layered on solid bottom agar plates and incubated to allow formation of plaques which can then be counted. Created using Biorender.com.

Plates with < 100 plaques were counted manually by marking the underside of the petri dish with a marker pen. On plates with a greater number of plaques, plates were photographed (Figure 2.3) on a black background using a petri dish digital imaging system (Don Whitley Scientific, Bingley) with side illumination and a digital camera (Samsung SM-G975F/DS; South Korea) at a distance of ~ 15 cm from the subject. Images were then transferred to a desktop computer, and plaques were counted using the multipoint tool in ImageJ v1.53k (Schneider et al. 2012). Where more than ~ 300 plaques were present, the original sample was diluted in SM buffer, and another plaque assay was conducted to produce countable plaques. Titre (plaque-forming units (PFU) /mL) was then calculated for each individual plate which contained 30 – 300 plaques using equation (1).

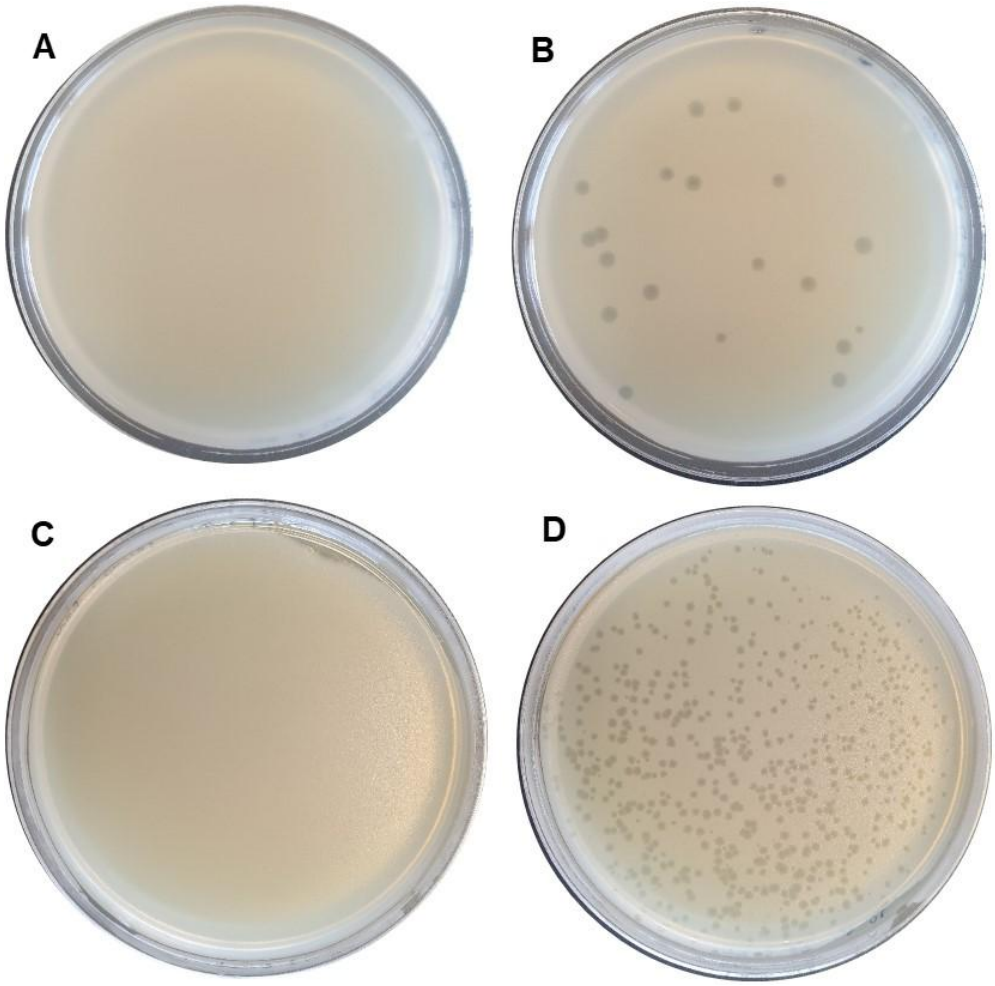

Figure 2.3. Example plaque assays.

A: control plate with only P*seudomonas syringae* added to the top agar, showing confluent bacterial lawn, and B: with phi6 also added, showing large plaques in the *P. syringae* lawn. C: control plate with *Escherichia coli* only, showing confluent bacterial lawn, and D: with MS2 also added, showing small plaques in the *E. coli* lawn.

2.2 Molecular biology methods

2.2.1 RNA extraction

Phage RNA was extracted from samples using the GeneJET viral DNA and RNA extraction kit (Thermo Scientific; USA) according to the manufacturer's instructions. When the kit was first used, the supplied lyophilised carrier RNA (polyadenylic acid) was reconstituted by adding 300 µL of the supplied eluent, and concentrated wash buffers were supplemented with 99.8% ethanol (Fisher Scientific; USA). Before each extraction, the required amount of lysis solution was supplemented with 25 µL of reconstituted carrier RNA per 1 mL of lysis solution and mixed by pipetting, and 50 µL of the supplied column preparation liquid was added to the centre of each spin column.

200 µL of each phage sample was added to a 1.5 mL nuclease-free microcentrifuge tube, to which 200 µL of lysis solution (supplemented with carrier RNA) and 50 µL of proteinase K was added. The solution was mixed by pipetting and then incubated for 15 min at 56 °C in a thermomixer set to 300 rpm (F2.0; Eppendorf, Germany). Tubes were briefly centrifuged (3 – 5 s) to collect condensate from the lid, and 200 µL of 99.8% ethanol were added before incubating for 3 min at room temperature. The tubes were briefly centrifuged, and the contents were transferred to the upper chamber of the prepared spin columns before centrifuging at room temperature for 1 min at 6,000 x *g*. The flow-through was discarded, and 700 µL of the supplied wash buffer 1 was added to the spin columns before centrifuging for 1 min at 6,000 x *g*. The flow-through was again discarded, and 500 µL of the supplied wash buffer 2 was then added to the spin columns before centrifuging for 1 min at 6,000 x *g*. The spin columns were then placed in new wash tubes and centrifuged for 1 min at 16,000 x *g*. 50 µL of eluent (preheated to 56 °C) was then added to the centre of the spin columns and incubated for 3 min at room temperature before centrifuging for 1 min at 13,000 x *g*. The eluted purified RNA was stored at -80 °C or used immediately in reverse transcription reactions.

2.2.2 Reverse transcription

Reverse transcription (RT) of extracted phage RNA was performed using the High-Capacity cDNA Reverse Transcription kit (Applied Biosystems; USA). This kit uses random primers, and whilst specific primers for MS2 and ph6 may have provided

increased RT efficiency, the use of random primers allowed both targets to be transcribed from each individual sample. Additionally, this kit had previously been optimised in our laboratory and was used consistently across all experiments. Any reduced RT efficiency resulting from random primers would therefore be consistent across samples and conditions. The kit components were thawed on ice, and the required volume of a 2X master mix was made up according to the manufacturer's instructions containing, per reaction: 2 µL reverse transcription buffer; 0.8 µL dNTPs, 2 µL random primers, 1 µL MultiScribe™ reverse transcriptase; 4.2 µL nuclease-free water (Molecular biology grade, ultrapure; Thermo Scientific, USA). The master mix was mixed on ice by pipetting, and 10 µL were transferred into 0.2 mL PCR tubes (MicroAmp™ 8-Tube strip; Applied Biosystems; USA) followed by 10 µL of purified phage RNA with mixing by pipette. A no-reverse-transcriptase (NRT) control was included by adding the appropriate volume of all reaction components to a single 0.2 mL PCR tube but substituting the 1 µL of reverse transcriptase for 1 µL of nuclease-free water. 10 µL of a representative phage RNA sample was then added to the NRT control tube. Tubes were briefly centrifuged for 3 – 5 s to consolidate contents, before reverse transcription was performed in a thermal cycler (TurboCycler Lite; Blue-Ray Biotech, Taiwan) using reaction conditions of 25 °C for 10 min, 37 °C for 2 h, 85 °C for 5 min, then hold at 4 °C. The absorbance spectra of 1 µL aliquots of each sample were measured using a spectrophotometer (ND-1000; Nanodrop Technologies Inc., USA) in triplicate. $A_{260/280}$ > 1.8 was considered acceptable. DNA concentration was disregarded as the presence of carrier RNA in the extraction step will inflate this value.

2.2.3 Quantitative polymerase chain reaction

Quantitative Polymerase Chain Reaction (qPCR) was carried out using the Premix Ex Taq™ (Probe qPCR) ROX Plus master mix (Takara Bio Europe). MS2 and phi6 primers and hydrolysis probe were obtained from Applied Biosystems (USA) according to Gendron *et al.* (2010) as shown in Table 2.2. The MS2 forward primer was located at the 1,261 – 1,283 nt position within the *mat* gene and the reverse primer was within the *cp* gene at position 1,420 – 1,401 nt which corresponds to a 160 bp PCR product. The phi6 forward primer was located on the phi6 S segment within the *phi-6S_1* gene at position 429 – 445 bp and the reverse primer was within the same gene at position 528 – 506 bp which corresponds to a 100 bp PCR product (Figure 2.4). Primers and probes were supplied at 100 µM concentration and were

diluted to 10 µM working concentration in aliquots with nuclease-free water before use, in a laminar flow cabinet (TC48; Gelaire, Australia). TaqMan (Applied Biosystems; USA) hydrolysis probes were used in qPCR assays with a 5' FAM (6-carboxyfluorescein) reporter, and a 3' nonfluorescent quencher (NFQ) and minor groove binder (MGB) moiety.

Oligonucleotide	Sequence	T_m, °C	GC%
MS2 forward primer	5'–GTC CAT ACC TTA GAT GCG TTA GC–3'	59.3	47.8
MS2 reverse primer	5'– CCG TTA GCG AAG TTG CTT GG–3'	58.6	55.0
MS2 probe	5'–FAM– ACG TCG CCA GTT CCG CCA TTG TCG–MGB/NFQ–3'	70.1	62.5
Phi6 forward primer	5'–TGG CGG CGG TCA AGA GC–3'	63.2	70.6
Phi6 reverse primer	5'–GGA TGA TTC TCC AGA AGC TGC TG–3'	62.1	52.2
Phi6 probe	5'–FAM–CGG TCG TCG CAG GTC TGA CAC TCG C–MGB/NFQ–3'	71.7	68.0
M13 forward primer (-21)	5'–TGT AAA ACG ACG GCC AGT–3'	56.5	50.0
M13 reverse primer (-29)	5'–CAG GAA ACA GCT ATG ACC–3'	52.1	50.0

Table 2.2. Oligonucleotides used in RT-qPCR and Sanger sequencing.

MS2 and phi6 primers and probes were taken from Gendron *et al.* (2010). FAM: 6-carboxyfluorescein; MGB: minor groove binder; NFQ: nonfluorescent quencher.

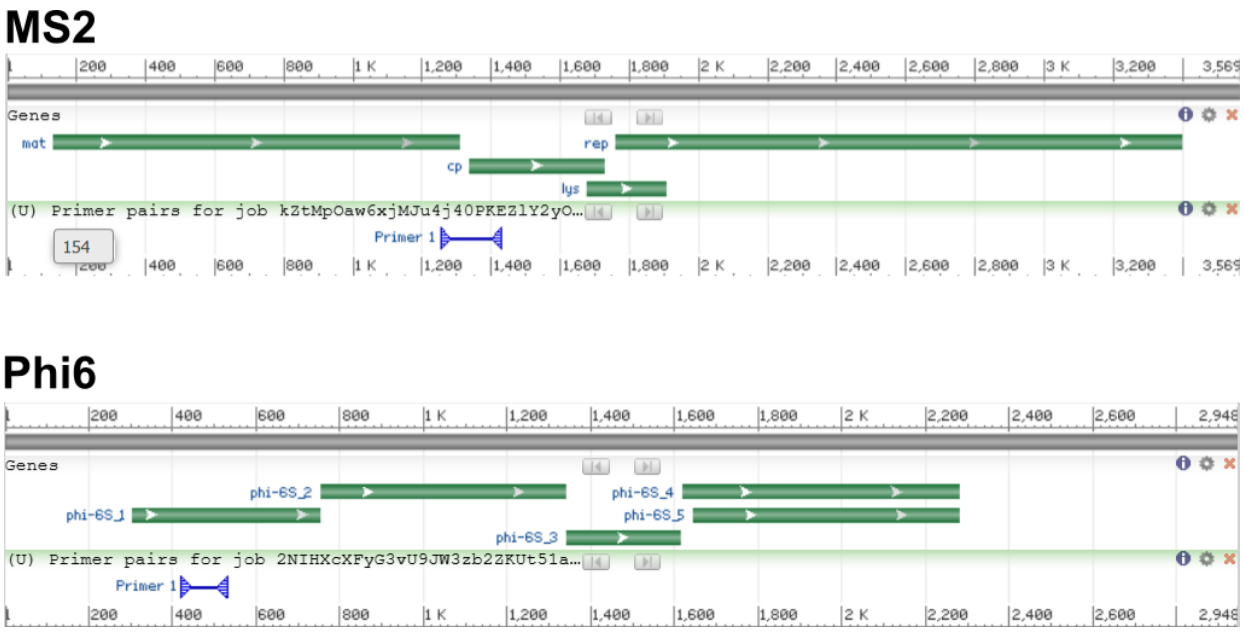

Figure 2.4 MS2 and Phi6 primer binding sites

Alignment of primers to reference sequences for MS2 (NC_001417.2) and Phi6 (NC_003714.1). Genes are annotated, and the PCR product with forward and reverse primers (arrows) are displayed in blue labelled “primer 1”.

To prevent contamination of qPCR, all steps were performed using dedicated pipettes, plasticware, and lab coat in a laminar flow cabinet (TC48; Gelaire, Australia). Reagents and cDNA were thawed before briefly pulse-vortexing and centrifuging (3 – 5 s) to resuspend contents. A master mix was made up according to the manufacturer’s instructions with the following volumes per reaction: 10 µL Premix Ex Taq (2X) (Probe qPCR) ROX Plus; 0.4 µL forward primer (0.2 µM final concentration); 0.4 µL reverse primer (0.2 µM final concentration); 0.8 µL probe (0.4 µM final concentration); 6.4 µL nuclease-free water. The master mix was then mixed on ice by pipetting. 18 µL of master mix were added to the bottom of the wells of a 96-well PCR plate (MicroAmp™ Optical 96-Well; Applied Biosystems, USA) and 2 µL of nuclease free water (Molecular biology grade, ultrapure; Thermo Scientific, USA) was added to the walls of No Template Control (NTC) wells. Once all wells were complete, reagents were put away before opening any cDNA samples. cDNA was centrifuged before opening to consolidate contents of the tubes. 2 µL of cDNA template (including the no reverse transcriptase control) were added to the walls of the wells in the 96-well plate. All reactions were conducted in triplicate. Wells were sealed with optical film (MicroAmp™ Optical Adhesive Film; Applied Biosystems, USA) and the plate was centrifuged for 10 – 15 s to eliminate bubbles and consolidate well contents. The plate was loaded into a QuantStudio 3 qPCR machine

(Applied Biosystems; USA) and the reaction was started with the following conditions: 30 s initial denaturation at 95 °C; 40 cycles of 95 °C for 5 s then 60 °C for 34 s. After completion, the sealed plate was stored at -20 °C.

qPCR analysis was performed using the Thermo Fisher Connect cloud-based platform (Thermo Fisher Scientific, USA) using the "Design and Analysis" and "Standard Curve" software modules. An automatic baseline was determined by the software, and a defined ΔRn threshold of 0.04 was used for all analyses. Quantification cycle (C_q) was determined for each well when its fluorescence signal crossed this threshold. Mean C_q and standard deviation were reported for each group of replicates.

To determine efficiency of the RT-qPCR, ten-fold serial dilutions of phage lysate were made up in SM buffer covering a 6 Log_{10} range. RNA was extracted and cDNA synthesised for each individual sample as above. qPCR was then conducted in triplicate, and efficiency of the RT-qPCR was calculated using the Design and Analysis software module within the Thermo Fisher Connect platform by plotting C_q versus Log_{10}(template quantity) and calculating the slope of a linear regression curve fitting these points. The slope was then used in equation (2) to calculate efficiency of the reaction, and efficiency 0.9 – 1.1 was deemed acceptable (Svec et al. 2015).

$$Efficiency = -1 + 10^{\left(\frac{-1}{Slope}\right)} \quad (2)$$

2.2.4 Agarose gel electrophoresis

DNA was visualised using agarose gel electrophoresis. Agarose powder (Melford, Suffolk) was dissolved at 0.8 – 1.2 % w/v in 50 mL of tris-acetate-EDTA (TAE) buffer by heating in a microwave oven (R-206; Sharp, Japan) at medium power until dissolved. 3 µL of ethidium bromide (Sigma Aldrich; USA) were added to the agarose before pouring into a gel tray with comb and allowing the gel to solidify after removing bubbles using a pipette tip. 7 µL of DNA was mixed with 3 µL of loading buffer (HyperLadder; Meridian Bioscience, USA) in a 0.2 mL tube by pipetting before adding the contents to the wells of the gel. 5 µL HyperLadder 100 bp (100 – 1013 bp) or HyperLadder 1kb (250 – 12,007 bp) DNA molecular size markers (Meridian

Bioscience, USA) were also included on the gel depending on the expected size of the DNA to be visualised. Electrophoresis was conducted in a horizontal tank with a direct current power supply (Power Pac basic; Bio-Rad, USA) at 80 v for ~ 45 min with TAE as the running buffer. Following electrophoresis, the gel was removed and imaged by UV transillumination (G:Box; Syngene, Cambridge).

2.2.5 Plasmid DNA standards

Plasmids containing MS2 and phi6 sequence extracts were made by cloning phage PCR products into plasmids using TOPO TA cloning. This allowed use of plasmid DNA for absolute quantification in qPCR. MS2 and phi6 RNA was extracted using the GeneJET viral DNA and RNA extraction kit (Thermo Scientific; USA), and reverse transcribed using the High-Capacity cDNA Reverse Transcription kit (Applied Biosystems; USA) as described above. A spectrophotometer (ND-1000; Nanodrop Technologies Inc., USA) was used to take triplicate measurements of 1 µL aliquots of each sample to measure DNA concentration and absorbance spectra. $A_{260/280} > 1.8$ was considered acceptable.

Basic PCR was then performed using reagents supplied in the TOPO TA Cloning Kit for Sequencing (Invitrogen, USA). The MS2 and phi6 primers in Table 2.2 and recombinant *Taq* polymerase (Invitrogen, USA) were used in the PCR, by adding the following to each 50 µL reaction in 0.2 mL PCR tubes (MicroAmp™ 8-Tube strip; Applied Biosystems; USA): 5 µL 10x PCR buffer; 0.5 µL dNTPs (50 mM); 2 µL of each primer (10 µM); 0.2 µL *Taq* polymerase (5 units/µL); 1 µL cDNA template. Negative controls were included using nuclease-free water instead of template for both primer sets. PCR was conducted using a QuantStudio™ 3 real-time PCR system (Applied Biosystems, USA) with reaction conditions as follows: initial denaturation at 95 °C for 1 min, then 35 cycles of: 95 °C for 15 sec; 60 °C for 15 sec; and 72 °C for 10 sec; followed by a final extension for 7 min at 72 °C. PCR products and negative controls were visualised using a 1.2 % agarose gel to confirm single product amplification.

Cloning reactions using the pCR™4-TOPO® vector (Figure 2.5) were set up with MS2 and phi6 PCR products. The TOPO TA Cloning Kit for Sequencing (Invitrogen, USA) was used by adding the following volumes of the supplied reagents to 2 µL of PCR product in a 0.2 mL PCR tube: 1 µL pCR™4-TOPO® vector; 2 µL nuclease-free water;

1 µL supplied salt solution. Contents were mixed gently by pipetting and incubated at room temperature for 5 min before immediately placing on ice.

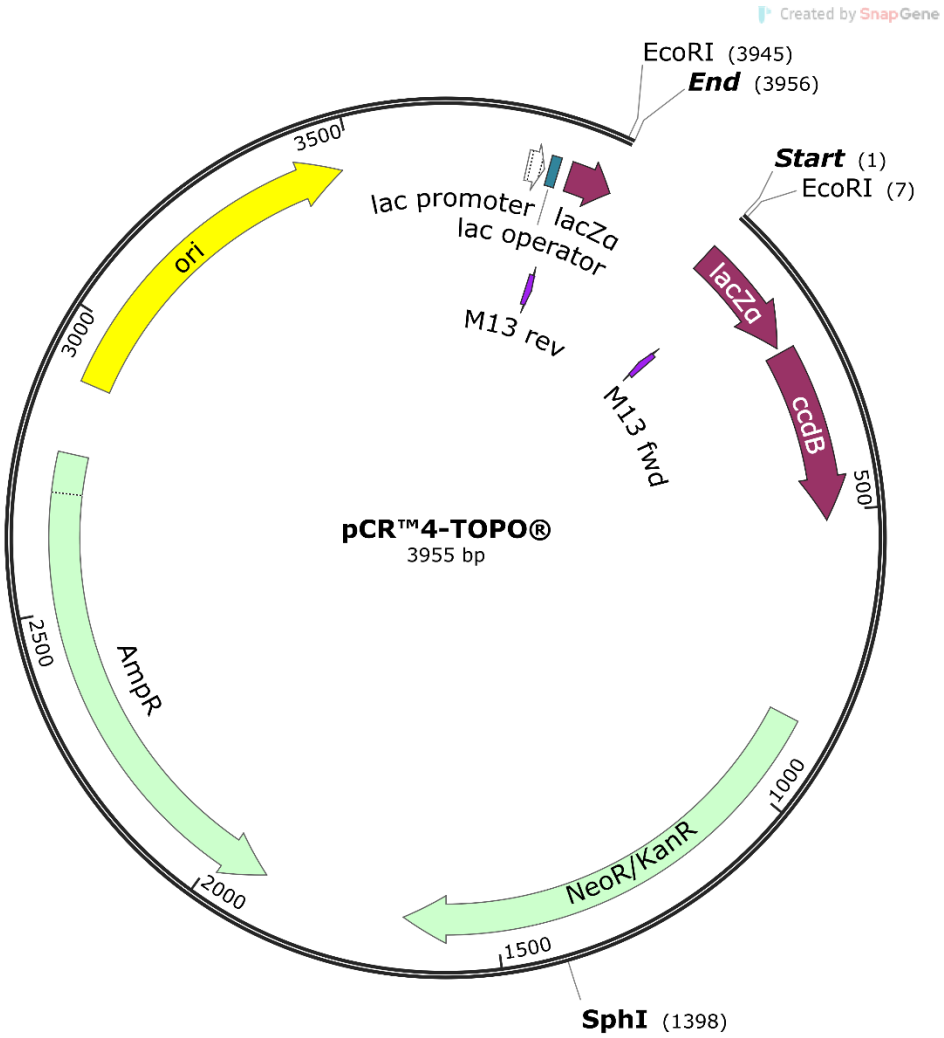

Figure 2.5. pCR™4-TOPO® vector map.

Locations of *Eco*RI and *Sph*I restriction sites, ampicillin (Amp^R) and neomycin/kanamycin (Neo^R/Kan^R) resistance genes, origin of replication (ori), M13 sequencing primer sites, and the *lacZα-ccdB* gene fusion are shown.

2 µL of the cloning reaction were added to One Shot™ Chemically Competent *E. coli* TOP10 cells (Invitrogen, USA) and mixed gently by pipetting before incubating on ice for 5 min. Heat shock was performed by incubating at 42 °C in a water bath (JB1; Grant, Cambridgeshire) for 30 s before immediately placing on ice. 250 µL of S.O.C. medium (Table 2.1) were then added before shaking horizontally in a shaking incubator (KS 4000 i control; IKA, Oxford) at 37 °C, 180 rpm for 1 h.

25 µL and 50 µL aliquots of the transformation mixture were spread on separate LB agar plates containing 50 µg/mL ampicillin and incubated overnight at 37 °C.

Following incubation, numerous white colonies were formed. The pCR™4-TOPO® vector allows positive selection as it contains the lethal *ccdB* gene (Bernard 1996) which is expressed fused to the C-terminus of the *LacZα* fragment. Ligation of a PCR product disrupts the *ccdB-LacZα* gene fusion and so only cells which have taken up a recombinant plasmid containing the insert can survive. Inclusion of *bla* confers ampicillin resistance, such that when grown on media with ampicillin, cells which have not taken up the plasmid cannot grow. 4 colonies from each transformation were picked and inoculated into separate 50 mL centrifuge tubes containing 5 mL LB with 50 mg/mL ampicillin and grown overnight at 37 °C, 200 rpm.

2.2.6 Plasmid DNA extraction

Plasmid DNA was extracted from *E. coli* TOP10 cells (Invitrogen, USA) using the PureLink Quick Plasmid Miniprep Kit (Invitrogen; USA). Wash buffers were supplemented with 99.8% ethanol (Fisher Scientific; USA) before first use, and RNAse A was added to the supplied resuspension buffer as recommended by the manufacturer before storing at 4 °C. 1 – 5 mL of overnight bacterial culture was centrifuged in a 1.5 mL microcentrifuge tube or 15 mL centrifuge tube for 10 min, 4,000 x *g* at 4 °C (CR-1512; CAPP, Germany/ 3K10; Sigma, USA) to pellet the cells. All centrifugation steps were performed at room temperature. The pellet was then resuspended in 250 µL of the supplied resuspension buffer supplemented with RNAse A. 250 µL of lysis buffer were then added and mixed by inverting the tube which was then incubated at room temperature for 5 min. 350 µL of precipitation buffer was added, and the tube was shaken to homogenise before centrifuging for 10 min, 12,000 x *g*. The supernatant was transferred to a spin column and centrifuged for 1 min, 12,000 x *g*. The flow through was discarded and 500 µL of wash buffer (W10) was added to the column and incubated for 1 min before centrifuging for 1 min, 12,000 x *g*. The flow through was then discarded and 700 µL of wash buffer (W9) was added to the spin column and incubated for 1 min before centrifuging for 1 min, 12,000 x *g*. The flowthrough was again discarded, and the column centrifuged again for 1 min, 12,000 x *g.* The column was then placed into a 1.5 mL microcentrifuge tube and a 75 µL aliquot of preheated (65 – 70 °C) TE buffer was added to the centre of the column and incubated for 1 min. Where downstream sequencing was planned, nuclease-free water was used instead of TE buffer. The column was then centrifuged for 2 min, 12,000 x *g* to elute the plasmid DNA. A spectrophotometer (ND-1000; Nanodrop Technologies Inc., USA) was used to take

triplicate measurements of 1 µL aliquots of each sample to measure absorbance spectra. $A_{260/280}$ > 1.8 was considered acceptable.

2.2.7 Plasmid standard verification

Plasmids containing MS2 and phi6 PCR products were linearised by digestion for 1 h with *Sph*I restriction enzyme in rCutSmart™ buffer (New England Biolabs; MA, USA) at 37 °C according to the manufacturer's instruction. 5 µL buffer was added to ~1 µg DNA and 1 µL *Sph*I, made up to a total volume of 50 µL with nuclease-free water. DNA was then visualised on a 1% agarose gel to confirm that the linearised plasmid was of the expected molecular weight.

20 µL aliquots of purified plasmids (50 – 100 ng/µL) were sent to a commercial sequencing provider (TubeSeq service; Eurofins Genomics Europe GmbH) for dideoxy chain termination (Sanger) sequencing using an Applied Biosystems 3730XL instrument. Plasmids were sequenced in the forward and reverse direction using M13 forward and reverse primers (Table 2.2) supplied by the sequencing provider, which straddle the insert region of the pCR™4-TOPO® plasmid. Plasmids isolated from two colonies were sent for sequencing for each construct. Glycerol stocks were made from each isolated colony and stored at -80 °C.

Alignment to NCBI reference sequences for MS2 (accession: NC_001417.2) and phi6 (NC_003714.1) was assessed using SnapGene v6.2 (GSL Biotech, LLC) and Benchling Molecular Biology (https://benchling.com/). Plasmids verified by sequencing were allocated the names pCR4-MS2 and pCR4-phi6 respectively and were deposited in the laboratory's culture collection in *E. coli* TOP10 cells at -80°C. All other transformants and isolated plasmids were discarded.

2.2.8 Plasmid DNA qPCR standard curves

Dilutions of pCR4-MS2 and pCR4-phi6 plasmid DNA were made in nuclease-free water to approximately 1.5 ng/µL, and DNA concentration was measured with a Qubit™ 4 fluorometer using the Qubit™ 1x dsDNA HS assay (Invitrogen; MA, USA). Individual measurements were made in triplicate and averaged, and three biological replicates were conducted on consecutive days. An online calculator, which uses the calculation in equation (3) (New England Biolabs NEBioCalculator, available at: https://nebiocalculator.neb.com/#!/dsdnaamt) was used to derive copy number/µL

based on the mean measured DNA concentration of plasmid standards and the size of the plasmids (pCR4-MS2 = 4,116 bp; pCR4-phi6 = 4,056 bp).

$$DNA, molecules = \frac{DNA\ mass,\ \ g \times (6.022 \times 10^{23},\ \ molecules/mol)}{((DNA\ length,\ \ bp) \times (617.96,\ \ g/mol/bp)) + 36.04,\ \ g/mol} \quad (3)$$

10-fold serial dilutions of the plasmid standards were made up in nuclease-free water covering the range 3.38 x 10^{-1} – 3.38 x 10^{6} copies / µL for MS2 and 2.90 x 10^{-1} – 2.90 x 10^{6} copies / µL for phi6. 2 µL of each standard (approximately 6 x 10^{-1} – 6 x 10^{6} copies per reaction) were used in qPCR as described above. No-template controls were included using nuclease-free water. Three independent qPCRs were conducted using the standards, each with three technical replicates per experiment. A fixed ∆Rn threshold of 0.04 and auto-baseline was used. Standard curves were derived by fitting a linear regression equation to C_q and Log_{10}(copy number) replicate values for each standard. R^2 was calculated, and the efficiency of the qPCR was calculated using equation (2).

The limit of detection (LoD) of qPCR assays for MS2 and phi6 were determined using the discrete threshold method according to Klymus *et al.* (2020), defined as the lowest concentration standard that amplified in ≥ 95% of replicates. Samples with quantities below the LoD were assigned a value of 0 in subsequent analyses.

2.3 Clinical simulation experiments using a mannequin model

2.3.1 Environment

Clinical simulation experiments were conducted in various dental treatment rooms and open plan clinics at Newcastle Dental Hospital, Newcastle upon Tyne Hospitals NHS Foundation Trust. Individual dental treatment rooms of 45.0 – 51.5 m^3, located in the Dental Clinical Research Facility were used in experiments in Chapters 3 and 5. These rooms were ventilated via a supply-extract, centrally supplied mechanical ventilation system using ceiling vents, providing 3.30 – 4.96 Air Changes per Hour (ACH). The open plan Clinical Simulation Unit (CSU), an 825 m^3 open plan teaching laboratory containing dental simulators, was used in experiments described in Chapter 4. The CSU was also ventilated by central mechanical ventilation, providing

6.46 ACH. Ventilation rates were measured on behalf of Newcastle upon Tyne Hospitals Foundation Trust by an external contractor as part of a commissioned building ventilation survey.

Experiments described in Chapter 4 were conducted in the Bioaerosol Chamber facility at the School of Civil Engineering, University of Leeds (Hiwar et al. 2025; King et al. 2013). This is a 32.25 m^3 sealed biosafety level 2 chamber supplied with HEPA-filtered air with variable ventilation rate, temperature, and relative humidity. Experiments were conducted in this facility at two ventilation rates: 1.5 ACH and 11.7 ACH. Ventilation rate was confirmed as part of routine calibration of the facility by the School of Civil Engineering using a balometer (Model PH721, TSI Incorporated, Shoreview, MN). The ventilation configuration in the facility uses a clean airflow path with a high, wall-mounted inlet vent and a low wall-mounted outlet vent diagonally opposite. The chamber was ventilated at the maximum airflow rate (11.7 ACH) between those experiments which used a lower air exchange rate.

For all experiments, where possible, temperature of 20 - 25°C and relative humidity <70 %RH was maintained, corresponding to levels deemed acceptable for healthcare settings according HTM 03-01 (NHS England and NHS Improvement 2021). Parameters measured during experiments are given in the relevant results chapters.

2.3.2 Mannequin model

In experiments in individual dental treatment rooms at Newcastle Dental Hospital, a dental mannequin (P-6/3 TSE, Frasaco GmbH; Germany) with model teeth (Frasaco GmbH, Germany) was attached to a dental chair (A-dec Inc.; USA) positioned ~80 cm above the floor. In experiments in the Bioaerosol Chamber, the same mannequin was attached to a platform in the centre of the chamber with the upper incisor teeth positioned 80 cm from the ground. In experiments in open plan clinics, a free-standing dental simulator (Model 4820; A-dec, OR, USA) was used and was positioned with the same tooth 80 cm from the ground.
A two-channel syringe pump (Legato 101, KD Scientific; USA) was used to introduce a suspension of MS2 and phi6 phage into the mouth of the mannequin at a titre of ~ 10^7 – 10^{11} PFU/mL, which is in the observed range of salivary viral load for human pathogens including SARS-CoV-2 (To et al. 2017b; Yang et al. 2021b). Titres used for each experiment are given in the relevant results chapters. Phage suspension was delivered through two, 1-mm internal diameter tubes which passed through the

rubber “cheeks” of the mannequin and opened adjacent to the tooth undergoing a dental procedure in each experiment. The suspension was delivered at a flow rate of 1.0 – 1.5 mL/min which represents the upper range of normal human total stimulated saliva flow (Ship et al. 1991). Prior to starting the procedure, 1 mL of the same phage inoculum was added to the labial surfaces of the upper teeth using a 1 mL syringe. The dental mannequin was cleaned between experiments using disinfectant wipes (Clinell Universal Wipes; GAMA Healthcare, UK), followed by 70% ethanol.

2.3.3 Dental procedures

Dental procedures were conducted in clinical simulation experiments using a range of dental instruments as shown in Table 2.3. The instrument flow rate was measured by dispensing the irrigant into a 50 mL volumetric flask for 1 min and calculating the mean of three replicates. Measurements of instrument flow rate were obtained at least on each day of experimentation. Procedures were conducted according to standard clinical practice by a single dentally trained operator with over 10-years’ experience.

The crown preparation procedure on the mannequin’s upper right central incisor tooth was conducted in the same manner for all experiments. The order was as follows: depth cuts in the incisal and labial surfaces (~1 mm) were first made with a coarse tapered crown bur; a 1mm chamfer margin was then cut around the entire tooth; reductions were made to the labial, incisal, mesial, and distal surfaces to the final desired contour; the palatal reduction was made with a coarse rugby ball bur; finally, the entire preparation was refined with a fine tapered crown bur. This procedure took precisely 10 minutes, with palatal reduction occurring at approximately 5 mins, and refinement of the tooth surface continuing until the end of the 10 mins.

2.3.4 Bioaerosol control measures

Several bioaerosol control measures (Figure 2.6) were tested in experiments described in Chapter 3 and 5, as shown in Table 2.4. These mitigations were applied according to standard clinical practice unless otherwise stated by a single, dentally trained operator with over 10-years’ experience. High-volume dental suction flow rate was measured using an airflow meter designed for dental suction units (Ramvac Flowcheck; DentalEZ) by calculating the mean of three measurement replicates.

Measurements of suction flow rate were obtained at least on each day of experimentation. Airflow rate of the LEV device in Table 2.4 was taken from the manufacturer's product literature.

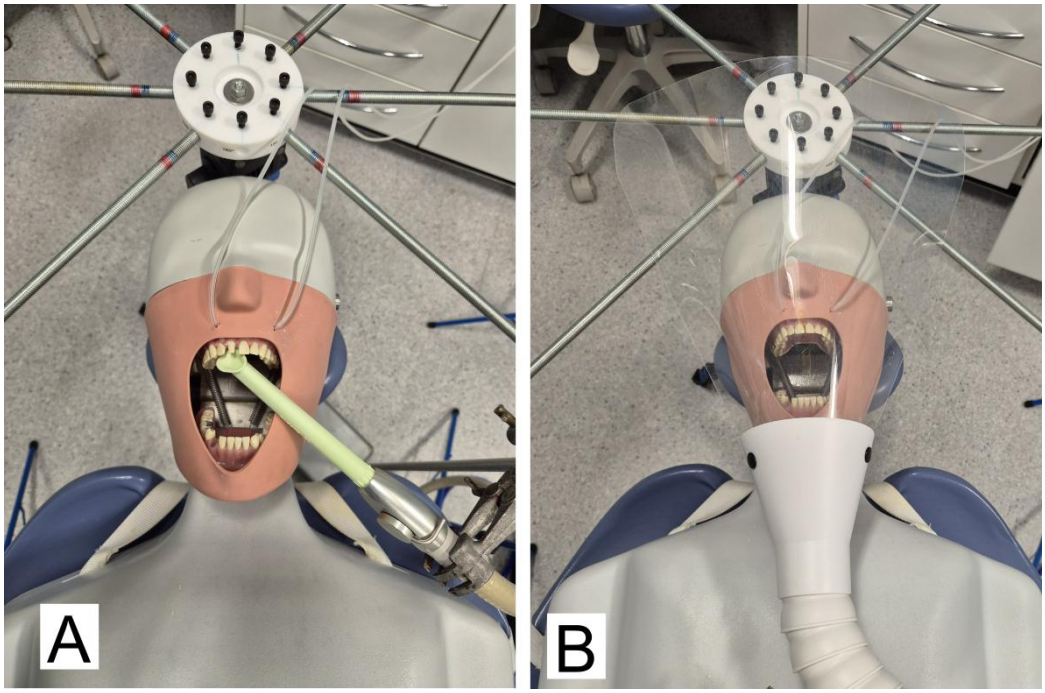

Figure 2.6. Dental suction and LEV control measures

(A) dental suction and (B) local exhaust ventilation (LEV) used in bioaerosol control measure experiments (Chapter 5).

Instrument	Irrigant and flow rate	Procedure	Duration
High-speed air-turbine handpiece (Synea TA-98, W&H (UK) Ltd.; St Albans, UK *or* EXPERTtorque LUX E6680L, Kavo; Germany) with diamond burs (Rugby Ball 379, Shoulder 856SG & 856G; Drendel and Zweiling, Germany)	Tap water, 29.3 – 45.1 mL/min (actual rates given in results chapters), chip air activated	Crown preparation on the upper right central incisor tooth.	10 min
1:5 speed increasing electric micromotor handpiece (Ti-Max Z95L; NSK, Japan) with diamond burs (Rugby Ball 379, Shoulder 856SG & 856G; Drendel and Zweiling, Germany) driven by an electric motor (NLX Nano; NSK, Japan) at 200,000 rpm.	Tap water, 44.8 mL/min (SD: 1.3), chip air not activated	Crown preparation on the upper right central incisor tooth	10 min

Table 2.3. Dental instruments and procedures used during clinical simulation experiments.

Mitigation	Details
High-volume dental suction	Dental suction using an 8.2 mm aspirator tip at an air flow rate of 238.8 L/min (SD:3.3). This was fixed in position 1 cm from the tooth undergoing the procedure with a retort stand. The suction tip was connected to Newcastle Dental Hospital's centrally supplied dental suction.
Rubber dam	Rubber dam (Henry Schein, UK) was applied to maxillary teeth from first premolar to opposite first premolar. A ~15 mm diameter hole was cut in the centre of the dam to prevent pooling of water from the handpiece as suction was not used. Winged molar rubber dam clamps (Henry Schein, UK) were placed on the dam at the first premolar positions, and the dam was affixed to a rubber dam frame (Henry Schein, UK). The assembled construct was then applied to the mannequin at the beginning of each experiment (after phage solution had been added to the tooth surfaces) using rubber dam clamp pliers, and floss to seat the dam between the teeth. Finally, the rubber dam was released from the wings of the clamps to seat the dam around the cervical areas of the clamped teeth.
Local Exhaust Ventilation (LEV)	A DentalAIR UVC AGP Filtration system (DA-UVC1001; VODEX Ltd.) was used as the LEV device. This device uses a HEPA filter compliant with EN1822 standards at a nominal airflow rate of 5,000 L/min of air and includes a 254-nm, 27-mW/cm^2 UVC source in the airflow before filtration. The centre of the device's inlet nozzle was positioned 10 cm inferior to the chin of the mannequin and 3 cm above the plane of the mannequin's mouth. The device was operated at the maximum airflow setting.
Dental unit waterline (DUWL) disinfectant	ICX (A-dec; OR, USA), a commercially available dental waterline disinfectant intended for continuous use, containing active ingredients sodium percarbonate and silver nitrate, was added the water supplying the dental instrument at the manufacturer's recommended concentration of 106.2 mg/L.

Table 2.4. Bioaerosol control measures used during clinical simulation experiments.

2.4 Aerosol and droplet sampling methods

2.4.1 Sampling rig construction

A sampling rig was constructed consisting of a central hub made from a circular polytetrafluoroethylene billet with 10 mm holes drilled at 45° intervals around the circumference to supported eight, 10 mm diameter threaded steel bars which were secured centrally by threaded thumbscrews secured into the hub and supported distally by tripod stands. The bars could be extended from 1 – 4 m, allowing a maximum coverage area of 8 m in diameter. 90 mm aluminium disks were attached to bars at intervals of 0.5 m using spring clips bonded to the underside of the disks with epoxy resin (90 mm polystyrene Petri dishes were used instead of aluminium disks in initial experiments in Chapter 3). Filter papers were placed on platforms to capture settled aerosols and droplets (Figure 2.7), along with surrounding benches in experiments in enclosed surgeries. Sampling locations were measured relative to the centre of the rig, which was positioned as close to the head of the mannequin as possible and on a plane ~84 cm above the floor; this was also the height of the benches used for other sampling locations. Free-standing retort stands, or those attached to the rig, were used to support air sampling equipment described below.

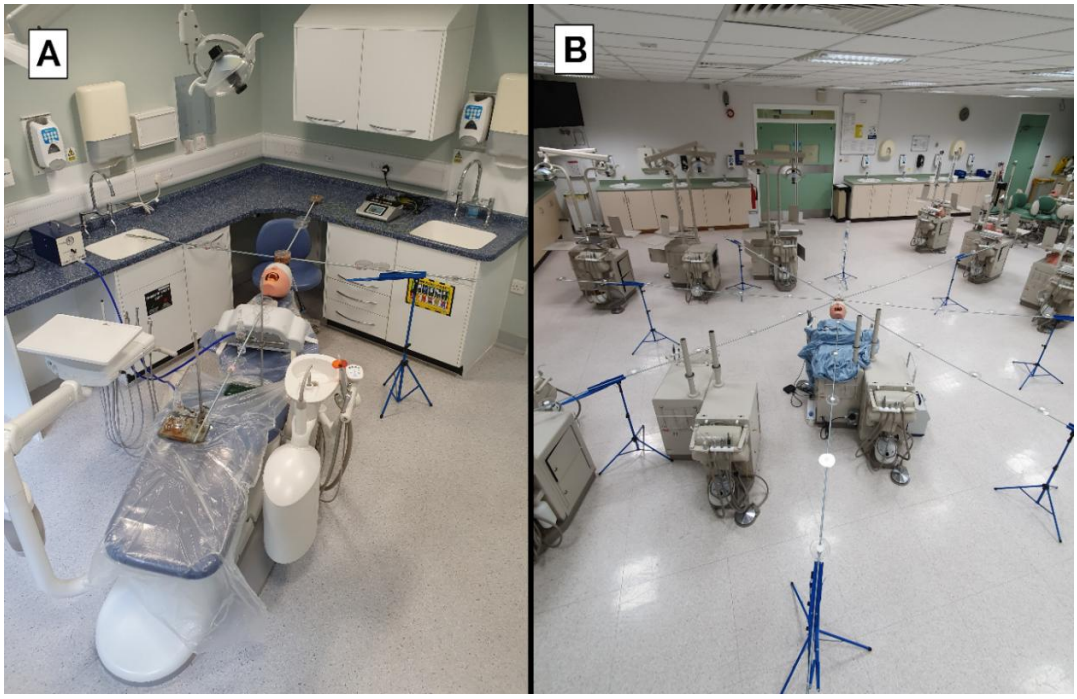

Figure 2.7. Aerosol sampling rig.
Rig constructed from 10 mm threaded steel bar supported by tripod stands as used in A) enclosed dental treatment rooms and B) open plan clinics.

2.4.2 Droplet and settled bioaerosol sampling

To capture droplets and settled aerosols, autoclave-sterilised, 30 mm diameter cotton-cellulose filter papers (Whatman, Cytiva; USA) were positioned in appropriate sampling locations and pre-wet with 100 µL of SM buffer immediately before the experiment. In initial experiments (Chapter 3), samples were collected using tweezers, which were cleaned with 70% ethanol between samples, and placed into sterile tubes for transport to the laboratory. In subsequent experiments, samples were placed in open sterile 50 mm petri dishes (Cytiva; USA), which were sealed with lids before transport to the laboratory to minimise handling. In the lab, filter papers were folded with tweezers using aseptic technique and transferred into 1 mL spin columns with a 30 µm pore size polyethylene membrane (Pierce; Thermo Fisher Scientific, USA) and a silicone end cap. 500 µL of SM buffer were then added (350 µL deionised water was used during initial experiments in Chapter 3) and samples were incubated at room temperature for 20 min before shaking in a horizontal orientation for 20 min using an orbital shaker at 300 rpm. Column end caps were then removed, and the columns were placed into new 2 mL microcentrifuge tubes before centrifuging at 15,000 x *g* for 3 min to elute phage for use in plaque assays and RT-qPCR. The area of the filter papers (7.07 cm^2) was used to calculate PFU/cm^2 and copies/cm^2.

To determine the efficiency of recovery of phage from filter papers, a 10 µL inoculum containing 5.8 x 10^5 PFU/mL of MS2 and 4.5 x 10^7 PFU/mL of phi6 was spiked onto individual filter papers in triplicate. Filter papers were pre-wet before inoculation with 100 µL of SM buffer to prevent drying of phage, except one sample which was left dry. After being left for 30 min on the bench in covered, sterile 90 mm petri dishes, filter papers were processed as above. Separate samples were also processed by incubating only (no shaking) or by vortexing at 3,000 rpm for 1 min instead of shaking. Negative control filter papers were included by inoculating with 10 µL SM buffer instead of phage. Positive control samples were included by spiking 10 µL of the same inoculum into 500 µL of SM buffer in a spin column but with no filter paper, and processing by shaking as above. Positive control samples with the spin column membrane removed were also included to test if the presence of the spin column membrane had any effect on phage recovery. Eluted samples were then measured using plaque assays and RT-qPCR and recovery efficiency was calculated by comparing to positive controls (with the column membrane intact).

To compare recovery on filter papers during clinical simulation experiments to alternative methods reported in the literature (Beltran et al. 2023; Vernon et al. 2021; Vernon et al. 2022), 90 mm diameter petri dishes were also placed in appropriate positions in initial experiments (Chapter 3) to capture droplets and settled aerosols. Plates of the appropriate medium (TSA for *P. syringae* and NZCYM for *E. coli*) were overlain with 3 mL of molten overlay agar seeded with 100 µL of overnight-grown host bacterial cells. Plates were prepared immediately before experiments, uncovered at the start of experiments, and closed at the end, before transporting to the laboratory and incubating for 24 h at the appropriate temperature for the host bacteria (37 °C for *E. coli*, 25 °C for *P. syringae*). Plaques were then counted, and the surface area of the plates (63.62 cm^2) was used to calculate PFU/cm^2. Negative controls were obtained by placing samples in an adjacent, enclosed surgery for the duration of each experiment and collecting and processing these in the same way at the end of the experiment.

2.4.3 Air sampling for suspended bioaerosol

Suspended aerosols were captured using all glass, cyclone air samplers (BioSampler; SKC Inc., USA; Figure 2.8). BioSamplers were filled with 20 mL of SM buffer (distilled water during initial experiments with MS2 only in Chapter 3) and operated at 12 – 12.5 L/min using a sampling pump (BioLite+; SKC Inc., USA). Flow rate was calibrated using a rotameter (SKC Inc., USA). At the end of the experiment, buffer was manually swirled in the sampler in the opposite direction to the vortex created during operation, in order to resuspend any phage adsorbed to the vessel walls. The buffer was then poured into a sterile 50 mL centrifuge tube and transported to the laboratory. Samplers were cleaned with laboratory detergent/disinfectant (1:20 Chemgene HLD_4L, Byotrol; UK), rinsed with 70% ethanol and then deionised water, before sterilising by autoclaving. Negative control samples were obtained by running an air sampler in an adjacent, enclosed surgery for the duration of each experiment, or in the location of the experiment before the experiment began.

Figure 2.8. BioSampler air sampling equipment

BioSampler all glass air samplers used in experiments. Left image: custom designed sampling rig allowing individual samplers to be run consecutively in the same location (used in experiments in Chapter 4). Right image: samplers run simultaneously in different locations.

2.4.4 Physical aerosol measurement with an optical particle counter

A laser diode optical particle counter (OPC; 3016-IAQ, Lighthouse, USA) was used to measure particle number concentration of all suspended aerosol and was calibrated to ISO 21501-4 by the manufacturer. The OPC had six particle-size channels (0.3, 0.5, 1.0, 2.5, 5.0, and 10.0 µm), a sampling flow rate of 2.83 L/min, and concentration limit of 282.5 particles/cm^3 at 10% coincidence loss. The sampling frequency was set to 1 – 0.2 Hz (one sample every 1 – 5 sec). The device also measured temperature and relative humidity at the same frequency.

2.5 Statistical Methods

SPSS Statistics 27 (SPSS Inc.; USA) and GraphPad Prism 9 (GraphPad Software, LLC; USA) were used for data analysis. $\alpha = .05$ with appropriate correction for multiple comparisons was used for all analyses.

The assumption of normal (Gaussian) distribution was assessed using quantile-quantile plots and the Shapiro-Wilk test. Comparison of normally distributed interval data between two groups was achieved using the student's *t* test, and where the assumption of normality was violated, the Mann-Whitney *U* test (Wilcoxon rank-sum test) was used instead. Corresponding paired tests were used for paired data.

One-way ANOVA was used to compare interval data between multiple groups on a single nominal or ordinal variable, with *post-hoc* Tukey's honestly significant difference (HSD) test for multiple comparison of groups, or Dunnett's test where groups were compared to a single control group. Homogeneity of variances was assessed using Bartlett's test, and where the assumptions of one-way ANOVA were violated, the Kruskal-Wallace test was used. For comparison of interval data between multiple groups on two variables, two-way ANOVA was used, and the Šidák correction was used for multiple comparisons between groups.

Pearson's *r* and Spearman's ρ with associated *p* were used to assess linear and monotonic correlations between variables. Relationships between two variables were assessed using linear regression or nonlinear regression using a one phase decay exponential model as appropriate. The most appropriate model was selected by visual assessment of curve fit, residual plots, and R^2. 95% confidence bands, and/or 95% prediction bands were reported. To assess the recovery of phage at different distances in dispersion experiments and at different times after the procedure in persistence experiments (Chapter 4), the intercept of regression curves with $y = 0$ (plaque assay data) or $y = limit\ of\ detection$ (RT-qPCR data) was calculated to determine at what distance from the source, or time from the procedure, recovery of infectious phage or phage RNA would be expected to be zero, based on the regression models. Bland-Altman plots were used to compare agreement between two measures, including average bias and 95% limits of agreement.

For time-series data (e.g., OPC data), Area Under the Curve (AUC) was calculated with associated standard error from replicate curves, and then a *t*-test or ANOVA was used to compare groups.

Where appropriate, $Log10$ transformation of raw data was used to allow visualisation. The function: $Log_{10}(x + 0.01)$ was used to allow correction of zero values.

Chapter 3. Optimising a Clinical Simulation Model of Dental Bioaerosols

3.1 Introduction

Bioaerosols are emitted from multiple sources in the dental clinic (e.g., dental procedures, dental instrument irrigants, patients' and dental professionals' respiratory activities, environmental sources) and variation between individuals in emission rates and microbial composition makes studying the bioaerosols produced during dental procedures challenging *in vivo*. Simulation models allow standardisation of parameters such as the dental procedure and the ability to exclude patient variation such as respiratory activities and oral microbiota. These models are therefore attractive for studying dental bioaerosols. The use of a specific tracer which can be put into the mouth of a dental mannequin during a simulated dental procedure allows the aerosols specifically produced by the dental procedure to be more reliably studied. Although our group has previously published work using simulation models with a fluorescent tracer (Allison et al. 2021a; Allison et al. 2021b; Allison et al. 2021c; Holliday et al. 2021; Llandro et al. 2021), these models are limited by the fact that such tracers offer no biological information, for example, the survival and infectivity of any microorganisms dispersed within bioaerosols.

The use of viruses relevant to human health (e.g., influenza, SARS-CoV-2, RSV) as tracers in a simulation model would be an ideal approach, however the need for appropriate biosafety measures mean that this is not practical in real clinical settings. Indeed, several authors have used mammalian viruses to model dental bioaerosols (Fidler et al. 2021; Ionescu et al. 2021), however this has been limited to the laboratory environment only. Bacteriophages (phages) are ideal candidate viruses to use as viral tracers in the clinic as they pose no risk to human health, and measurement of infectious virus using bacterial plaque assays is much easier than viruses of eukaryotes where cell or tissue culture methods are required.

The experiments described in this chapter using bacteriophage MS2 to study the effect of a dental unit waterline (DUWL) disinfectant have been published in the *Journal of Dental Research* (Allison et al. 2022), but prior to this, only one other study had used a bacteriophage (phi6) in clinical simulation experiments in dental settings

(Vernon et al. 2021). Other authors have subsequently published data using bacteriophage models with MS2 (Pratt et al. 2023), phi6 (Vernon et al. 2022), and the ssDNA *E. coli* phage, PhiX174, which is a member of the *Microviridae* family (Beltran et al. 2023; Liu et al. 2023). Our group, however, remains the only group which has not relied upon the direct settlement of phage onto growth media seeded with host bacteria in Petri dishes for the detection of phage, but rather eluting phage captured on filter papers. Importantly, the relative recovery efficiency of phage from Petri dishes and filter papers has not yet been reported in the literature. The additional potential advantages of using filter papers are that: 1) dilution of concentrated samples is possible where there are too many plaques to accurately count, and 2) by eluting phage from filters, subsequent analysis using molecular methods such as RT-qPCR is possible. The ability to quantify recovered phage nucleic acids by RT-qPCR and compare this to the amount of infectious phage by plaque assay is necessary to determine what proportion of dispersed phage remains infective following dispersion. This is important because the measurement of human viruses (e.g., SARS-CoV-2, influenza) in clinical studies has often relied on RT-qPCR, and infectious virus is often not recoverable from samples which are PCR positive (Moore et al. 2021; Thompson et al. 2013; Winslow et al. 2022).

As little prior work has been done to optimise phage sampling using filter papers or for the absolute quantification of phage tracers by RT-qPCR, initial experiments were conducted to determine how the phage tracers and assays performed in the clinical setting and laboratory; this was initially conducted using a single phage (MS2). Bacteriophage MS2 is a member of the species *Emesvirus zinderi* in the family *Fiersviridae*, with non-enveloped, non-tailed, 26 nm diameter virions (figure 3.1) and a 3,569 nt single-stranded positive-sense RNA genome encoding four proteins. MS2 adsorbs to the F pilus of its host *Escherichia coli* via the single maturation protein present on the surface of its capsid (Meng et al. 2019).

All previous studies of dental bioaerosols using viral tracers have used a single virus, however different viruses are known to have different survival characteristics depending on the presence of a viral envelope, features of their environment such as relative humidity, and the presence of other solutes such as salt, proteins, and surfactants (Fedorenko et al. 2020; Firquet et al. 2015; Lin et al. 2020; Zargar et al. 2022). For this reason, in subsequent experiments, a second phage—phi6—was used simultaneously to assess how survival of phage in dental bioaerosols differs

between viruses which differ in the possession of a viral envelope. Bacteriophage phi6, a member of the species *Cystovirus phi6* in the family *Cystoviridae*, is an enveloped, non-tailed virus with 85 nm diameter virions and a 13,385 bp double-stranded RNA genome, which is divided into three linear segments (S, M, L segments). Phi6 virions adsorb to retractile pili of its gram-negative host *Pseudomonas syringae*, which brings the virions into contact with the bacterium's outer membrane. The viral envelope then undergoes fusion with the bacterial membrane which is mediated by the viral surface receptor protein P3 (Roine et al. 1998). Local digestion of the host cell's peptidoglycan layer occurs via protein P5 on the nucleocapsid, allowing the nucleocapsid to enter the bacterial cytoplasm by invagination of the plasma membrane (Poranen et al. 1999). Expression by *E. coli* and *P. syringae* of the pili required for phage to adsorb to the host cells is known to vary based on environmental factors (Goldlust et al. 2023; Sistrom et al. 2015). As described in Chapter 2, preparation of host bacterial cultures was therefore carried out according to the same protocol in each experiment to minimise variation and ensure consistent host infection efficiency by phage in samples during plaque assays.

The two phages used in this project (enveloped phi6 and non-enveloped MS2) were chosen as surrogates for human viruses due to their broad structural similarity to several enveloped (e.g., coronaviruses, influenza, respiratory syncytial virus), and non-enveloped (e.g., norovirus, adenovirus, rhinovirus) human pathogens. MS2 and phi6 have also been used as surrogates for clinically relevant viruses in previous non-dental studies (Anderson et al. 2023; Fedorenko et al. 2020; Fisher et al. 2012; Tung-Thompson et al. 2015; Zargar et al. 2022).

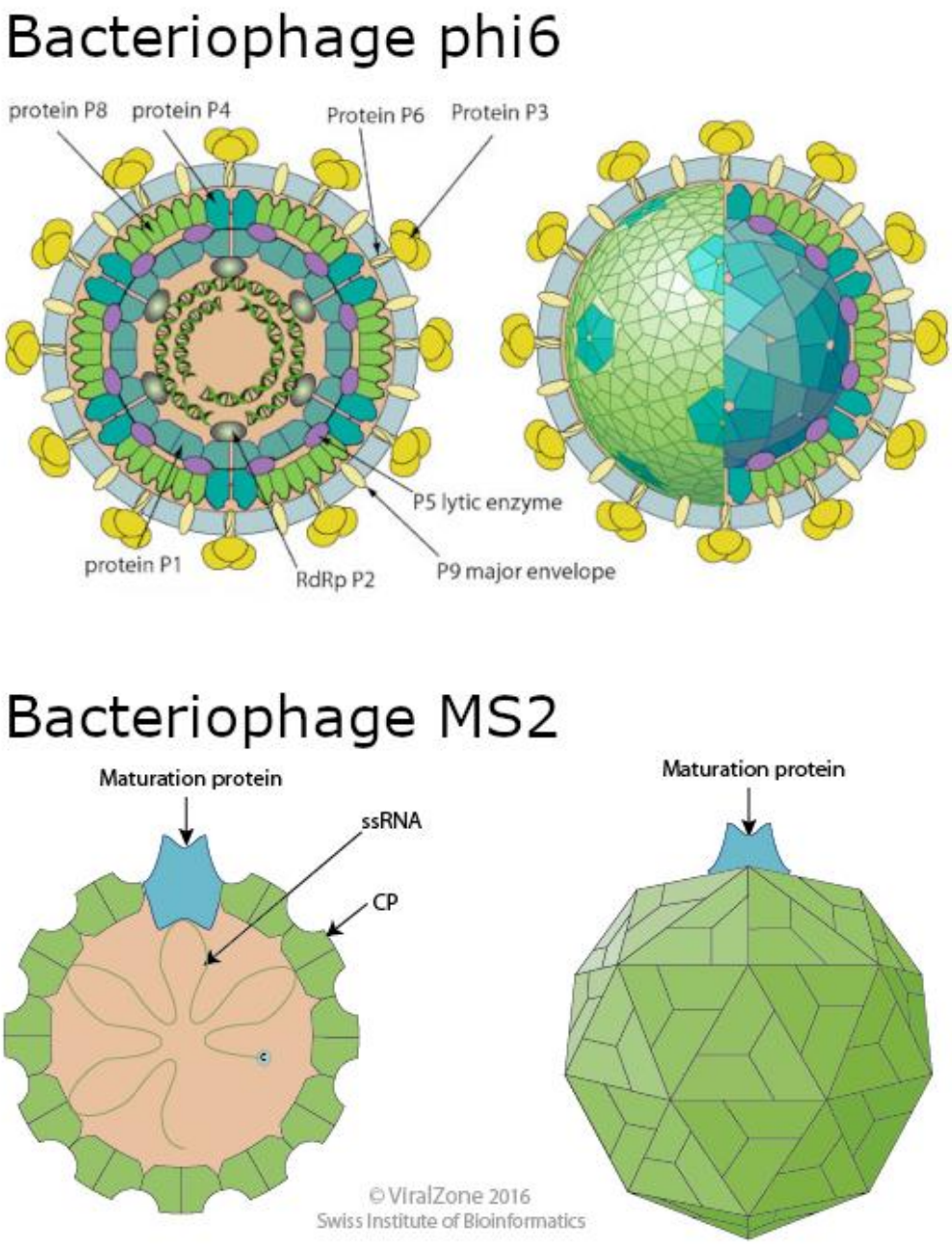

Figure 3.1. Bacteriophage phi6 and MS2 virions.
Source: ViralZone, Swiss Institute of Bioinformatics. CC BY 4.0.

The primary aim of the initial experiments described in this chapter was to optimise the use of MS2 and phi6 as viral tracers to study dental bioaerosols in the clinic; however, the experiments also provided an opportunity to begin to test the efficacy of dental bioaerosol control measures and to demonstrate the ability of the simulation model to detect differences in dispersion of phage when such measures were employed.

Initially, the effect of a dental unit waterline (DUWL) disinfectant on virus recovery was explored. These agents are widely used in dental settings to control biofilms in the waterlines supplying dental instruments. Although much work has been done examining the effect of DUWL disinfectants on microbial biofilms, very few authors had considered the effect of these disinfectants on microbes dispersed from the mouth in bioaerosols (Dutil et al. 2007; Sethi et al. 2019). This was an attractive first bioaerosol control measure to address because it is not possible to measure its effect using a non-biological method of measurement, such as particle counting instruments or chemical tracers. Whilst these approaches have been well described in the literature, they have primarily been used to assess physical measures of aerosol control (such as capturing aerosol with dental suction or removing it from the air by increasing ventilation rate) rather than affecting the viability of viruses within the aerosol. This is because the mechanism of DUWL disinfectants is not to reduce aerosols *per se* but to reduce the viability of any microorganisms contained within them. The DUWL disinfectant, ICX® (A-dec Inc.; USA) which contains sodium percarbonate and silver nitrate, was chosen due to its existing use in the author's institution and extensive use in dentistry generally. ICX® is intended for continuous use in DUWLs at a concentration of 106.2 mg/L; the manufacturer does not give a detailed breakdown of the proportions of the product's constituent parts.

Secondly, the effectiveness of rubber dam was explored. Rubber dam has been used in dentistry for well over a century (Author Unknown 1867), and is routinely used during restorative dental treatment to isolate the teeth being treated from the rest of the mouth. No studies have assessed the efficacy of rubber dam on the dispersion of human viruses in clinical studies, however, one study used a viral tracer (phi6) in a simulation model to assess rubber dam (Vernon et al. 2021). The authors of this study demonstrated substantially reduced detection when rubber dam was used. Importantly the model used by the authors only incorporated a single viral tracer, and so it is not clear whether rubber dam is effective in controlling dispersion of different viruses, such as MS2. We therefore chose to assess the effect of rubber dam during the first experiments using both MS2 and phi6 together.

3.2 Aims and objectives

The aim of this chapter is to develop and characterise a simulation model of dental bioaerosols and bioaerosol control measures using multiple bacteriophage tracers. The specific objectives are to:

- Develop a reliable RT-qPCR assay for absolute quantification of MS2 and phi6.
- Optimise a simulation model of dental bioaerosols in a clinical environment using plaque assays and RT-qPCR to detect bacteriophage tracers.
- Demonstrate the ability of the clinical simulation model to detect differences in bioaerosol dispersion when dental bioaerosols control measures are used.
- Test the effect of DUWL disinfectants and rubber dam on the dispersion of viable and non-viable viral particles in dental bioaerosols.

3.3 RT-qPCR assay optimisation

3.3.1 RT-qPCR efficiency with phage cDNA

Plaque assays allow detection of infectious phage; however, they do not give any indication of the dispersion of inactive phage particles. RT-qPCR assays, based on previously reported primers and probe (Gendron et al. 2010), were therefore optimised to allow absolute quantification of MS2 and phi6 RNA. Efficiency of the assay was first determined using cDNA synthesised from RNA extracted from 10-fold dilutions of MS2 and phi6 phage lysates.

The efficiency of the assay covering the range 2.32 x 10^1 – 2.32 x 10^7 PFU/reaction, was 98.37% for MS2 (R^2 = 0.999), and for phi6, covering the range 7.20 x 10^1 – 7.20 x 10^7 PFU/reaction, this was 98.91% (R^2 = 0.995; figure 3.2). Agarose gel electrophoresis of PCR products showed specific amplification of a single band of the expected size (160 bp for MS2 and 100 bp for phi6; figure 3.3). Representative qPCR amplification plots are shown in appendix figure A.1.

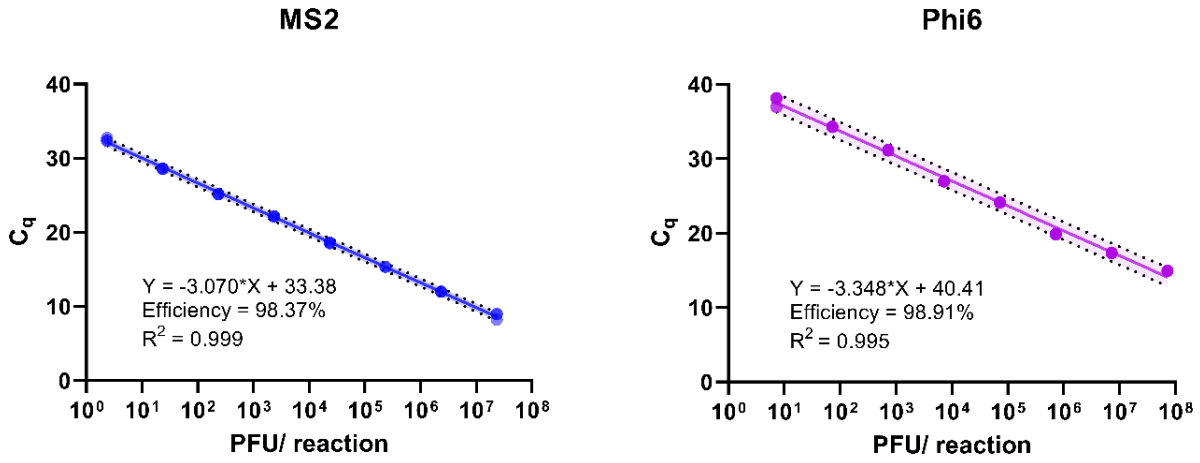

Figure 3.2. RT-qPCR standard curves for MS2 and phi6 primer and probe sets.

Produced using cDNA synthesised from MS2 and phi6 lysates (*n* = 3 independent replicates per standard). PFU/ reaction = plaque forming units per 2 µL reaction, calculated by plaque assay of the original purified phage lysate. Coloured shaded area surrounding linear regression curves represent 95% prediction intervals (95% of observations are expected to fall within this). Linear regression equation, corresponding R^2, and calculated efficiency of the qPCR are shown.

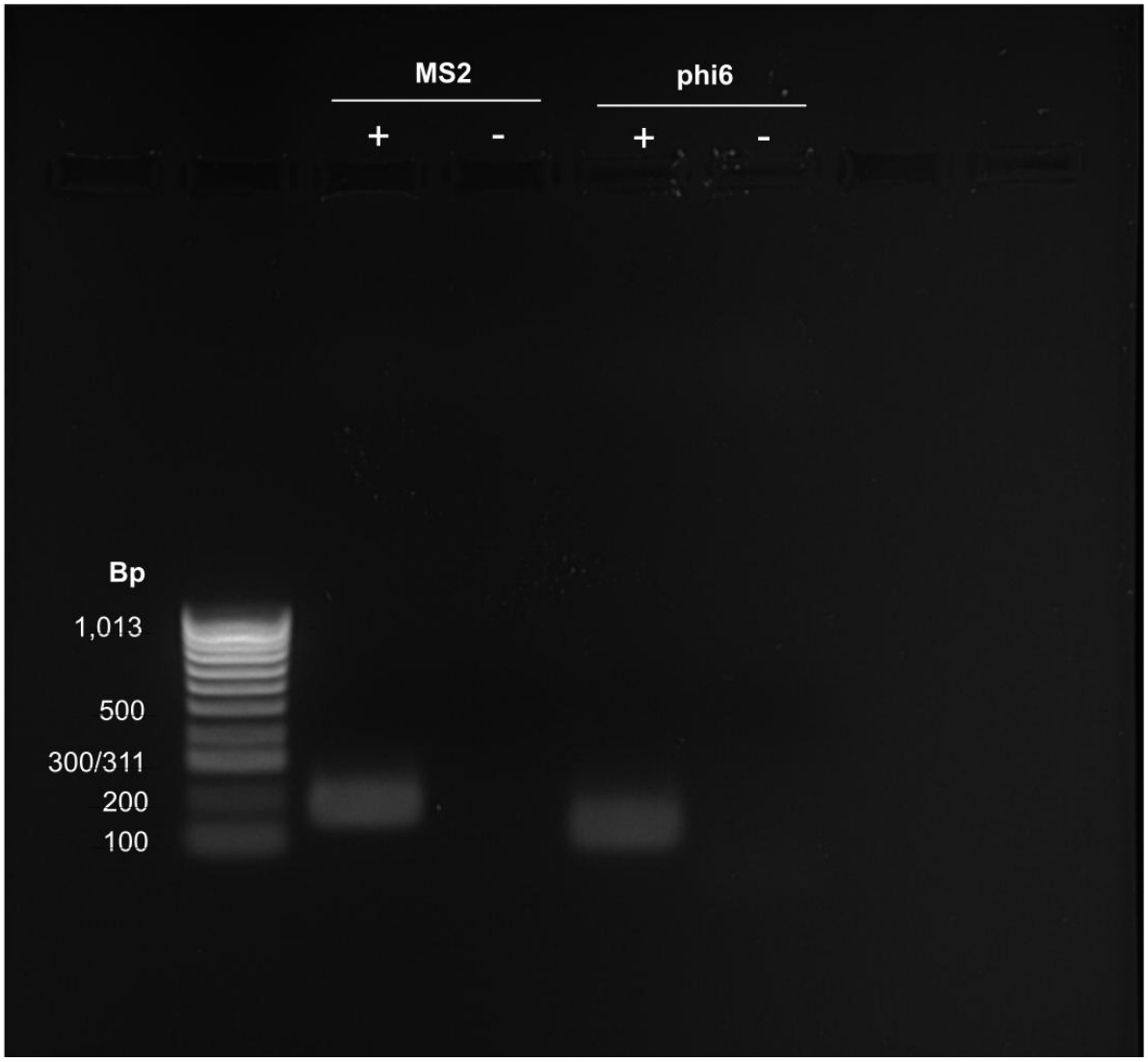

Figure 3.3. Agarose gel electrophoresis of MS2 and phi6 RT-qPCR product.

1% agarose electrophoresis gel (80 v, 50 min). 100 bp – 1,013 bp DNA molecular weight marker (HyperLadder; Meridian Bioscience, USA) included in the left most lane. Single amplification products are seen at expected sizes (MS2: 160 bp; phi6: 100 bp).

3.3.2 Verification of plasmid DNA standards

To allow absolute quantification of phage, plasmid DNA standards containing MS2 and phi6 PCR product inserts were constructed using TOPO TA cloning. Basic PCR of cDNA synthesised from MS2 and phi6 RNA extracted from phage lysates produced adequate quantity and quality DNA for cloning (MS2 = 149.7 ng/µL, $A_{260/280}$ = 2.06; phi6 = 244.2 ng/µL, $A_{260/280}$ = 2.14). Agarose gel electrophoresis confirmed a single product at the expected molecular weight (figure 3.4).

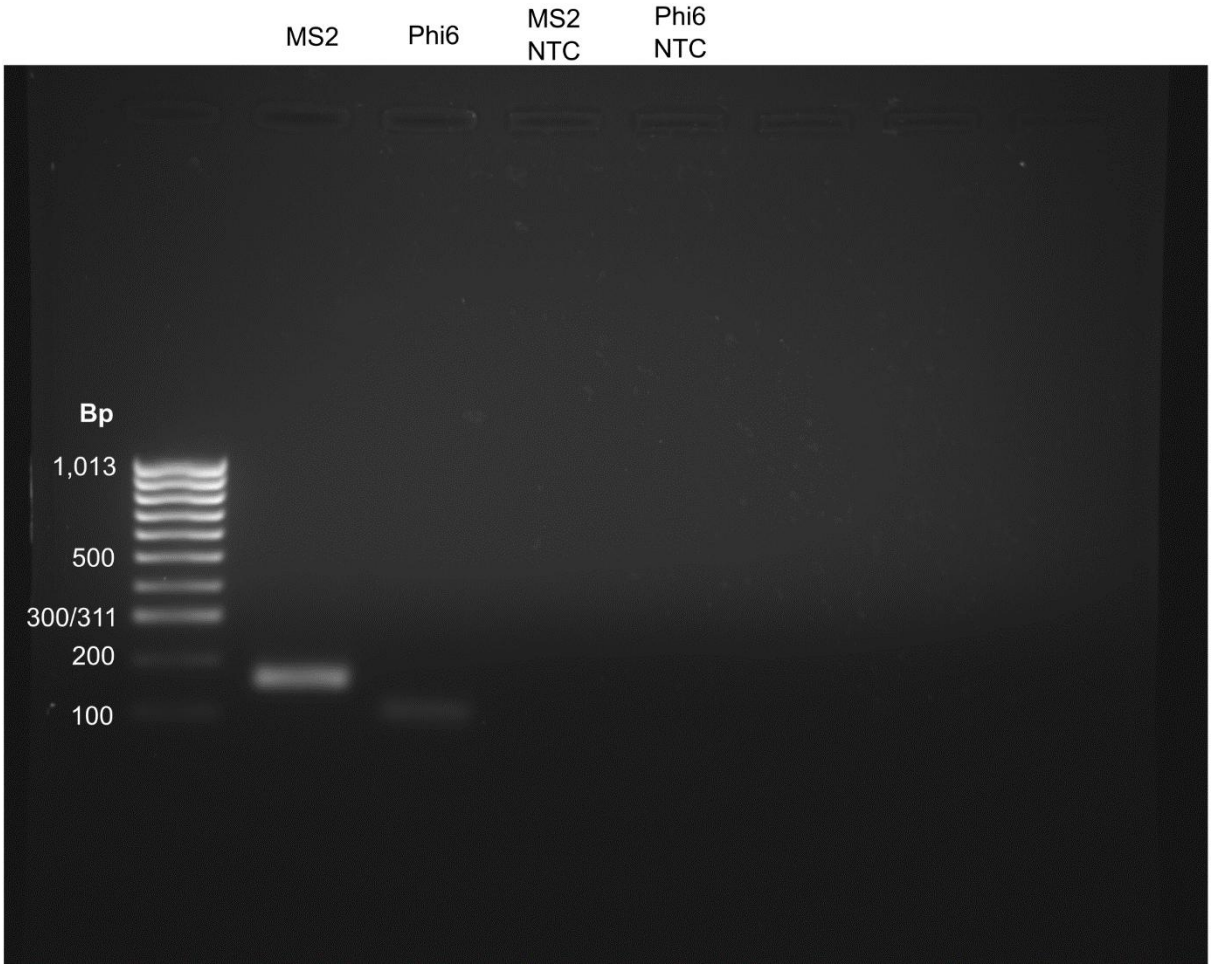

Figure 3.4. Agarose gel electrophoresis of MS2 and phi6 basic PCR products.

1.2 % agarose electrophoresis gel (80 v, 45 min). 100 bp – 1,013 bp DNA molecular weight marker (HyperLadder; Meridian Bioscience, USA) included in lane 1. NTC: no-template control.

TOPO TA cloning of phage PCR products was then conducted using the pCR™4-TOPO® vector in *E. coli* TOP10 cells (Invitrogen, USA). Purified plasmids were linearised with *Sph*I and separated on a 1 % agarose gel (figure 3.5). Undigested plasmids showed bands at ~2.5 kb, corresponding to covalently closed circular plasmid DNA, and at > 10 kb corresponding to open circular (nicked) plasmid DNA. For plasmids digested with *Sph*I, bands corresponding to linearised plasmid DNA were observed at the expected size of ~4kb for plasmids containing MS2 (4,116 bp) and phi6 (4,056 bp) inserts. Some residual open circular plasmid DNA was observed in digested plasmid lanes (> 10kb) suggesting some incomplete digestion. The digestion protocol could have been further optimised, however, the result provided sufficient initial verification of the plasmids prior to sequencing.

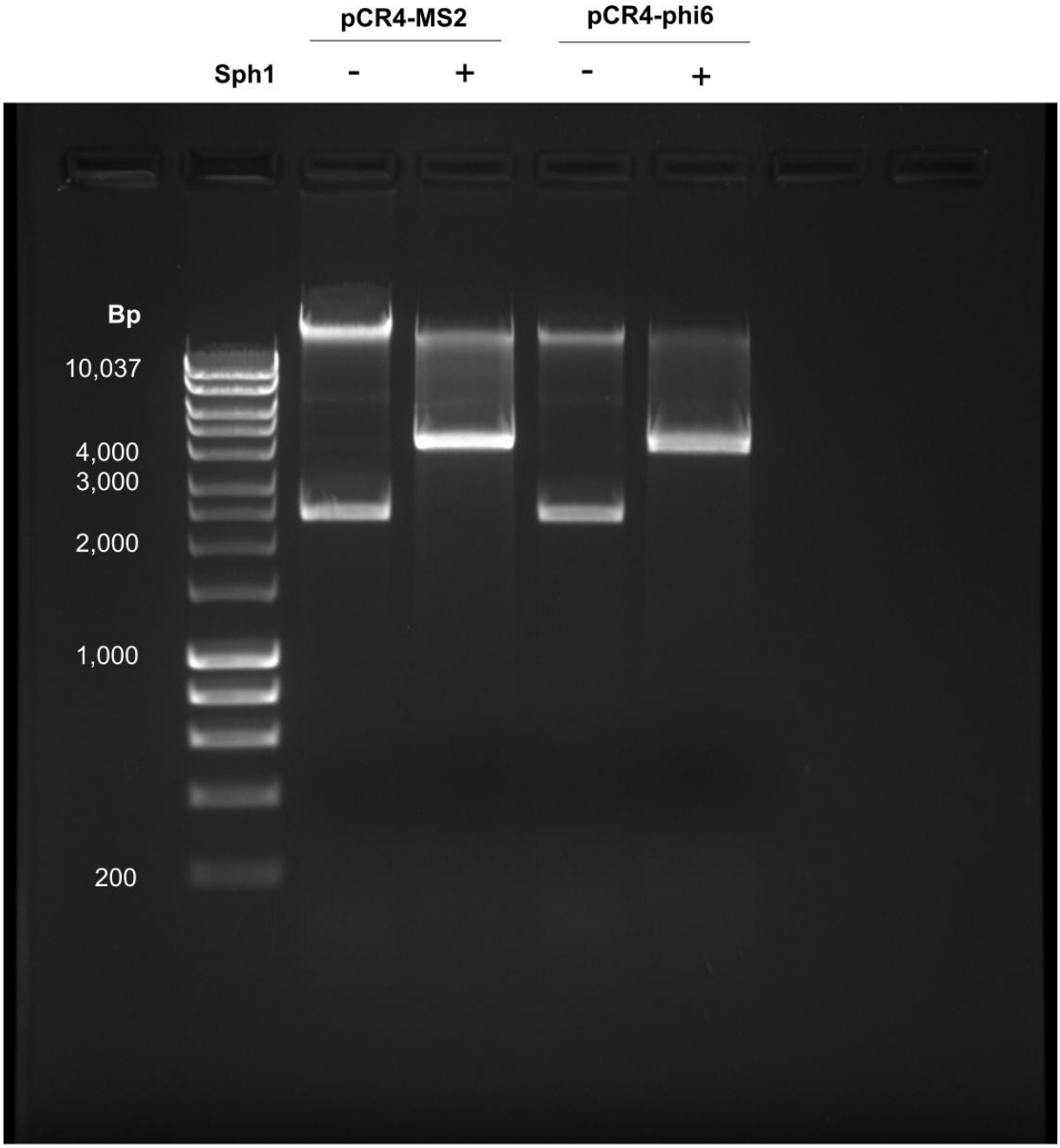

Figure 3.5. Agarose gel electrophoresis of pCR4-MS2 and pCR4-phi6 plasmid constructs.

Plasmids separated on 1% agarose gel (80 v, 55 min) with and without prior linearisation using *Sph*I. 1 kbp DNA ladder included in lane 1. pCR4-MS2 and pCR4-phi6 plasmids have an expected size of 4,116 bp and 4,056 bp, respectively.

Sanger sequencing of the pCR4-MS2 and pCR4-phi6 constructs using M13 forward and reverse primers, which straddle the vector's insert region, confirmed alignment of the constructs to MS2 and phi6 PCR products expected from NCBI reference sequences (NC_001417.2 and NC_003714.1 respectively; figure 3.6).

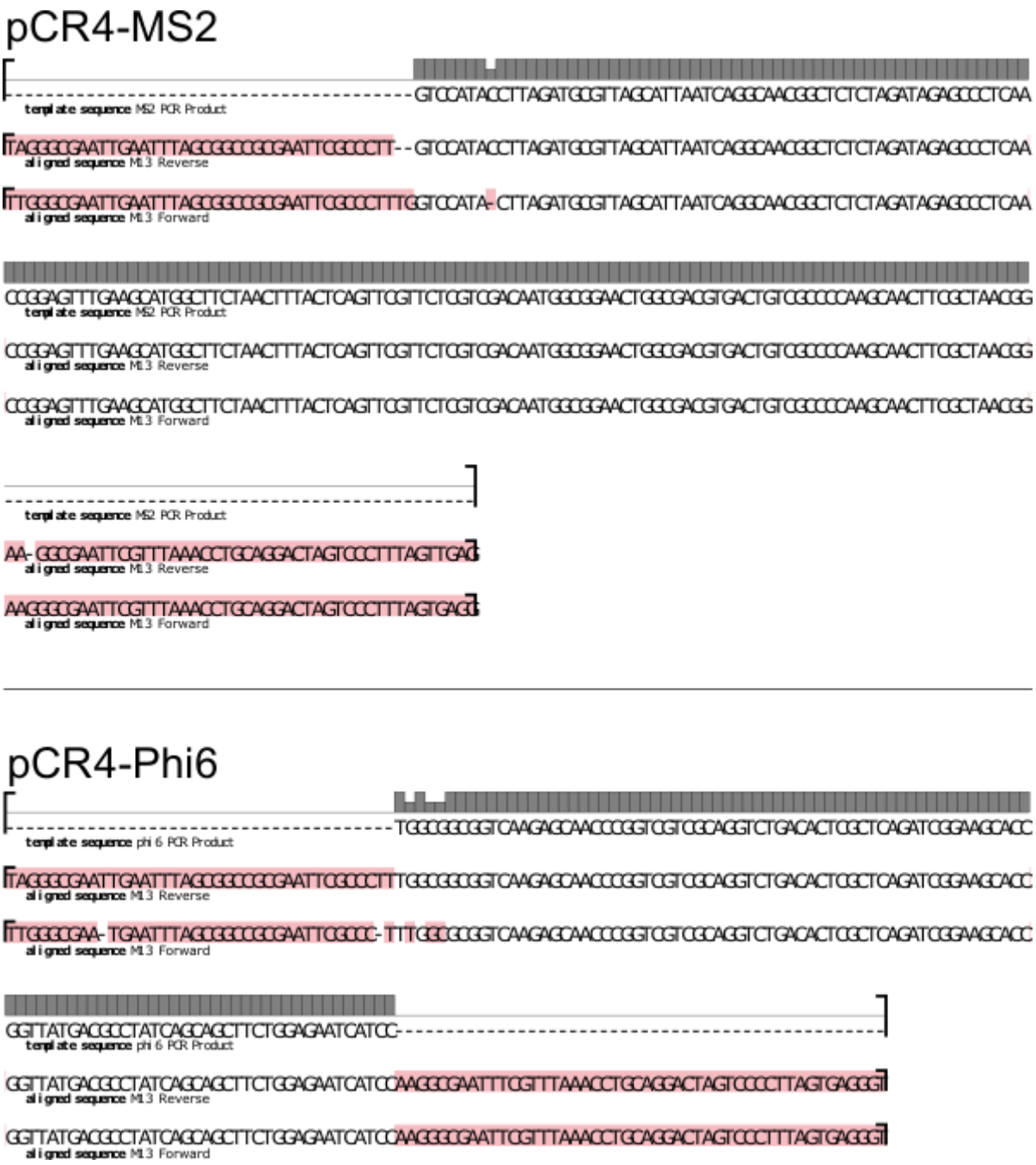

Figure 3.6. Sequences of pCR4-MS2 and pCR4-phi6 plasmid constructs.

Alignments of expected MS2 and phi6 PCR products taken from NCBI reference sequences (NC_001417.2 and NC_003714.1 respectively; template sequence) to sequencing reads of the insert region of pCR4-MS2 and pCR4-phi6 plasmids (aligned sequences). Sanger sequencing was performed using M13 forward and reverse primers which straddle the insert site of the original pCR™4-TOPO® vector. Misalignments of sequence reads shown in red correspond to the vector sequence.

3.3.3 Plasmid DNA standard curves

Following verification of pCR4-MS2 and pCR4-phi6 plasmids, standard curves were constructed using qPCR to allow absolute quantification of phage RNA recovered during clinical simulation experiments. Plasmid DNA was isolated using a column-

based extraction kit as described in Chapter 2 (section 2.2.6), and DNA concentration was measured using a spectrophotometer (ND-1000; Nanodrop Technologies Inc., USA; Figure 3.7) before diluting samples to approximately 1.5 ng/µL in nuclease-free water. DNA concentration of the diluted plasmid standards was then measured accurately using a Qubit spectrofluorometer, by taking the average of 9 replicate measurements. Measured DNA concentration was then used to calculate copy number per µL for each standard (see section 2.2.8). Standards were then 10-fold serially diluted, covering the ranges 3.38×10^{-1} – 3.38×10^{6} copies/µL for MS2 and 2.90×10^{-1} – 2.90×10^{6} copies/µL for phi6, before conducting qPCR. Derived standard curves (figure 3.8) demonstrated good efficiency across a 7-Log_{10} range of input DNA (MS2: 111.7%; phi6: 106.8%) and excellent curve fit (R^2_{MS2} = 0.991; R^2_{phi6} = 0.987). For MS2, the limit of detection was calculated at 33.8 copies/µL, and for phi6, this was 2.9 copies/µL.

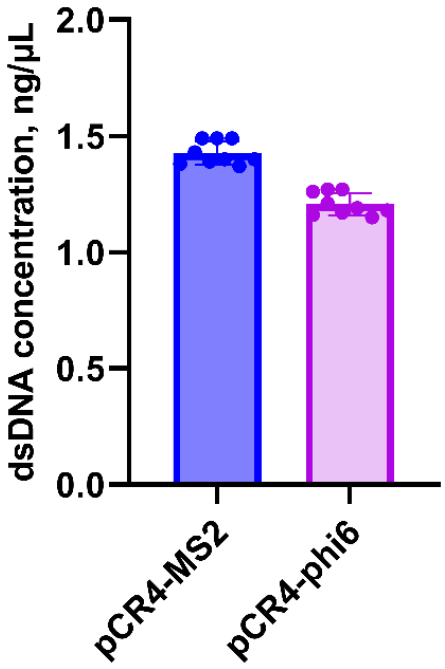

Figure 3.7. pCR4-MS2 and pCR4-phi6 plasmid DNA concentration.

Determined by fluorometric measurement using a Qubit™ 4 fluorometer. *n* = 9 measurement replicates.

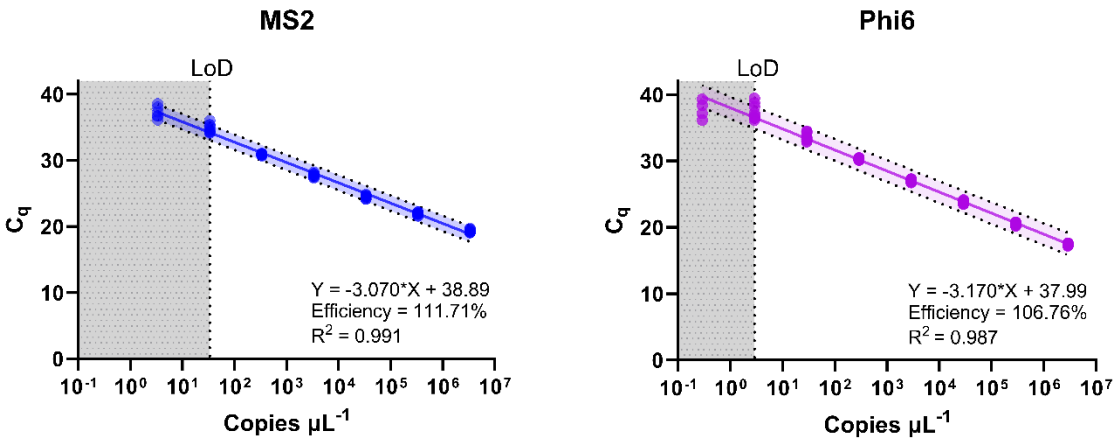

Figure 3.8. qPCR standard curves derived using pCR4-MS2 and pCR4-phi6 plasmid DNA standards.

n = 3 independent replicates per standard. Coloured shaded area surrounding linear regression curves represent 95% prediction intervals (95% of observations are expected to fall within this). Linear regression equation, corresponding R^2, and efficiency of qPCR are shown. Limit of detection (LoD) is shown by the grey shaded areas.

3.4 Recovery of phage from filter papers

The recovery efficiency of phage from filter paper samples was determined by spiking a 10 µL inoculum of 5.8 x 10^5 PFU/mL MS2 and 4.5 x 10^7 PFU/mL phi6 (confirmed by plaque assays immediately prior to the experiment) onto pre-wet filter papers, and a non–pre-wet control in triplicate, and comparing this to samples where the inoculum was spiked directly into buffer. Two positive controls were tested, either with or without the presence of the polyethylene membrane which comes supplied in the spin columns used for phage elution.

Recovery of infectious phage measured by plaque assay was not significantly different with or without the presence of the spin column membrane in positive controls for MS2 (unpaired *t* test, $t(4) = 0.727$, $p = 0.508$) or phi6 ($t(6) = 1.514$, $p = 0.181$), although recovery appeared to be more variable for phi6 without the column membrane in place (figure 3.9). Columns with the original membranes were therefore selected for further use.

Compared to positive control samples (with column membranes), recovery of MS2 in plaque assays from filter paper samples processed by shaking, incubation only, and vortexing was 66.4%, 49.1%, and 71.3%, respectively. Recovery was lower for phi6 at 3.5%, 4.4%, and 3.8%, respectively. No phage was recovered in plaque assays from non–pre-wet filter papers for either phage.

There was a significant difference in plaque assay recovery for different sample processing methods (positive control samples not included in comparison) for MS2 (one-way ANOVA, $F(3, 8) = 8.152$, $p = 0.008$), with the mean recovery of infectious phage from non–pre-wet samples being significantly lower than from vortexed samples (Tukey's HSD, $p = 0.010$) and shaken samples ($p = 0.014$) which had been pre-wet. No significant differences were observed for phi6 ($F(3, 8) = 1.101$, $p = 0.403$).

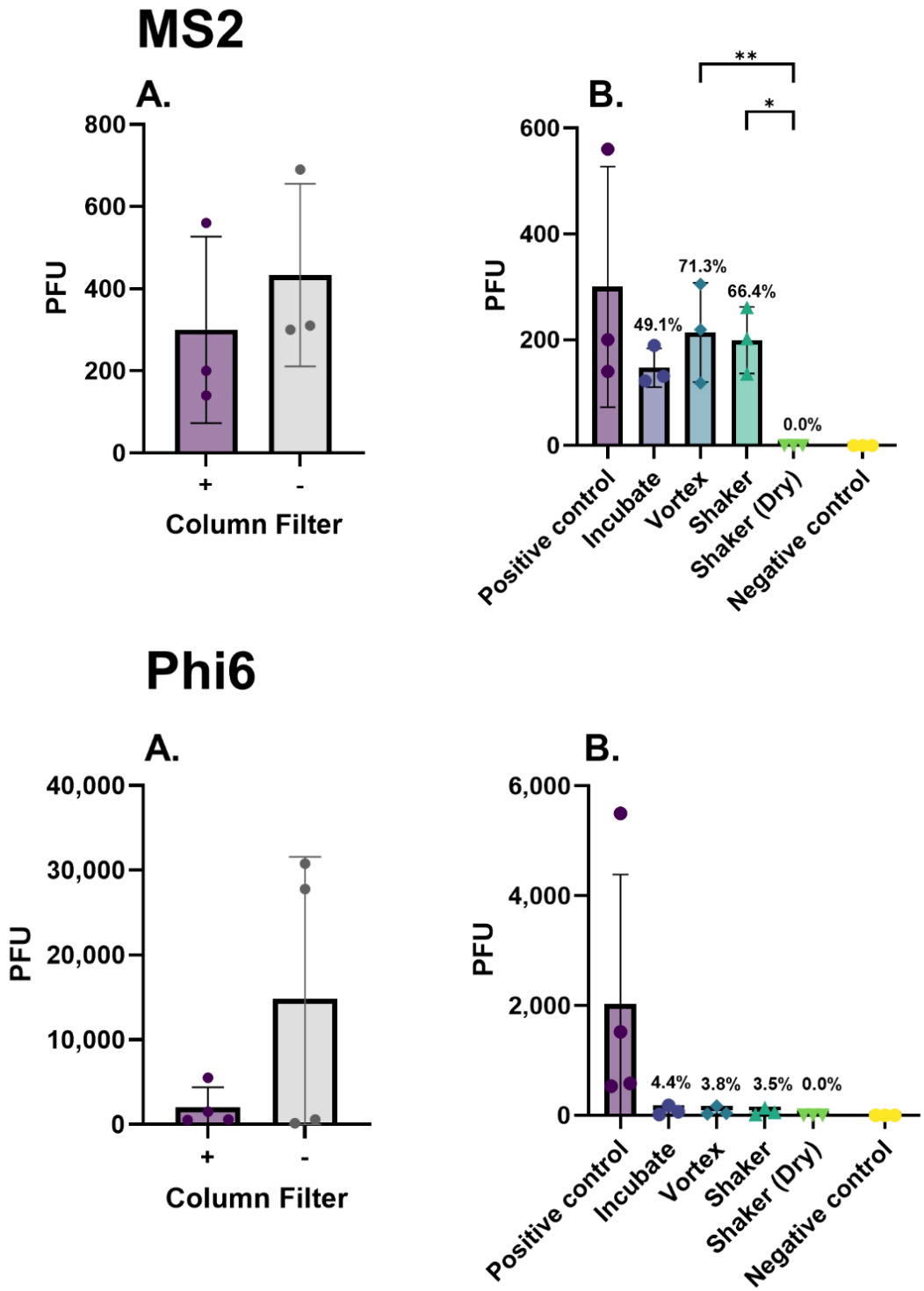

Figure 3.9. Recovery of infectious phage from filter papers following various processing methods.

n = 3 independent replicates (4 for phi6 positive controls). A. recovery from positive control samples with or without the originally supplied spin column membrane filters. B. recovery following different sample processing methods, * = $p < 0.05$; ** = $p < 0.01$ (one-way ANOVA with post hoc Tukey's HSD test).

A similar pattern was seen with recovery of phage RNA from filter papers using RT-qPCR. This was not significantly different with or without the presence of the spin column membrane for MS2 (unpaired *t* test, $t(6) = 0.272$, $p = 0.795$) or phi6 ($t(6) = 0.552$, $p = 0.601$) (figure 3.10).

Compared to positive control samples, recovery of MS2 RNA from filter paper samples processed by shaking, incubation, and vortexing was 53.8%, 57.1%, and 55.4%, respectively. Recovery of phi6 RNA was lower at 5.6%, 15.6%, and 6.4%, respectively. Unlike in plaque assays, recovery from non–pre-wet filter papers using RT-qPCR was 4.9% for MS2 and 15.4% for phi6.

Comparison of the effect of different processing methods on the recovery of phage RNA between processing methods, showed a significant difference for MS2 (one-way ANOVA, $F(3, 8) = 21.69$, $p < 0.001$), with the mean recovery of infectious phage from non–pre-wet samples being significantly lower than from vortexed samples (Tukey's HSD, $p < 0.001$), shaken samples ($p = 0.001$), and incubated samples ($p < 0.001$) which had been pre-wet. No significant differences were observed for phi6 ($F(3, 8) = 1.048$, $p = 0.423$).

As recovery was poor from non–pre-wet filter papers for both phages using plaque assays and RT-qPCR, filter papers were pre-wet with SM buffer in subsequent experiments. As recovery was not significantly different between other methods, shaking (300 rpm, 20 min) was selected as the preferred protocol, as multiple samples could be processed simultaneously more easily than with vortexing. Incubation alone was not chosen, as recovery of infectious MS2 was lower, even if this did not reach significance (figure 3.10)

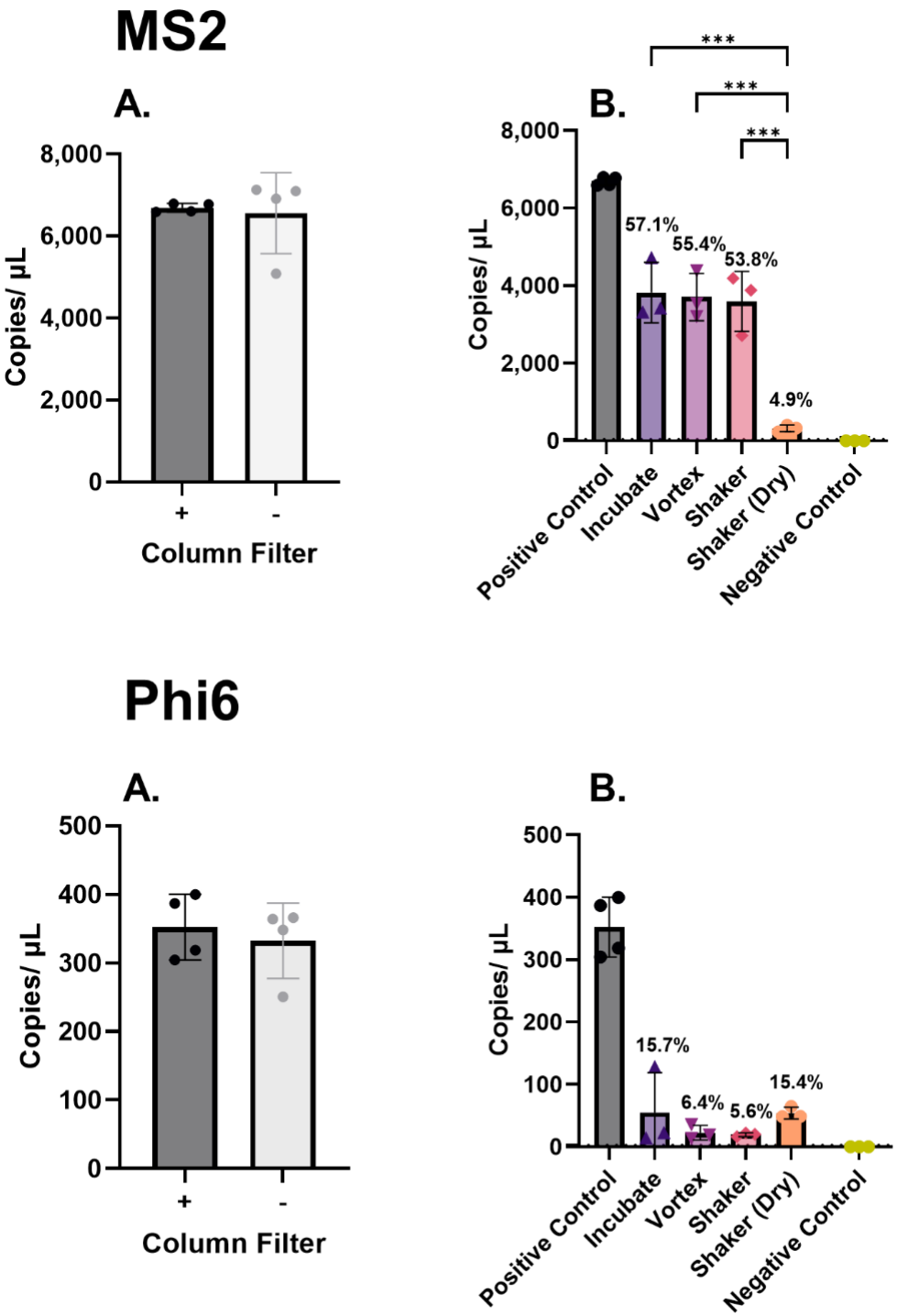

Figure 3.10. Recovery of phage RNA from filter papers quantified by RT-qPCR.

n = 3 independent replicates (4 for positive controls). A: recovery from positive control samples with or without the supplied spin column membrane filters. B: recovery following different sample processing methods; *** = $p < 0.001$ (one-way ANOVA with *post hoc* Tukey's HSD test). Dotted horizontal lines show limit of detection of the RT-qPCR assay.

3.5 The effect of a DUWL disinfectant on phage viability

As the first experiments in the clinic would use MS2 as the initial phage tracer and aimed to test the effect of the dental unit waterline (DUWL) disinfectant ICX®, it was necessary to first test the effect of ICX® on MS2 in the laboratory. Two-fold serial dilutions of ICX® in de-ionised water were made, covering the range 6.25 – 100 % of the manufacturers' concentrations (6.64 – 106.2 mg/L final ICX® concentration), and these were added to in triplicate to MS2 (2 x 10^7 PFU/mL final concentration) along with a negative control containing no ICX®. Samples were incubated for 10 min at room temperature before quantifying infectious phage by plaque assay.

ICX® had a statistically significant effect on MS2 plaque counts (one-way ANOVA, $F(5, 12) = 16.29$, $p < 0.001$; figure 3.11) and compared to the control condition (0% ICX®), all concentrations above 6.25% had significantly lower mean plaque counts (Dunnett's test; 12.5% $p = 0.013$; 25%, 50%, 100% $p < 0.001$). Plaque counts were highly negatively correlated with disinfectant concentration ($\rho = -.848$, $p < .001$).

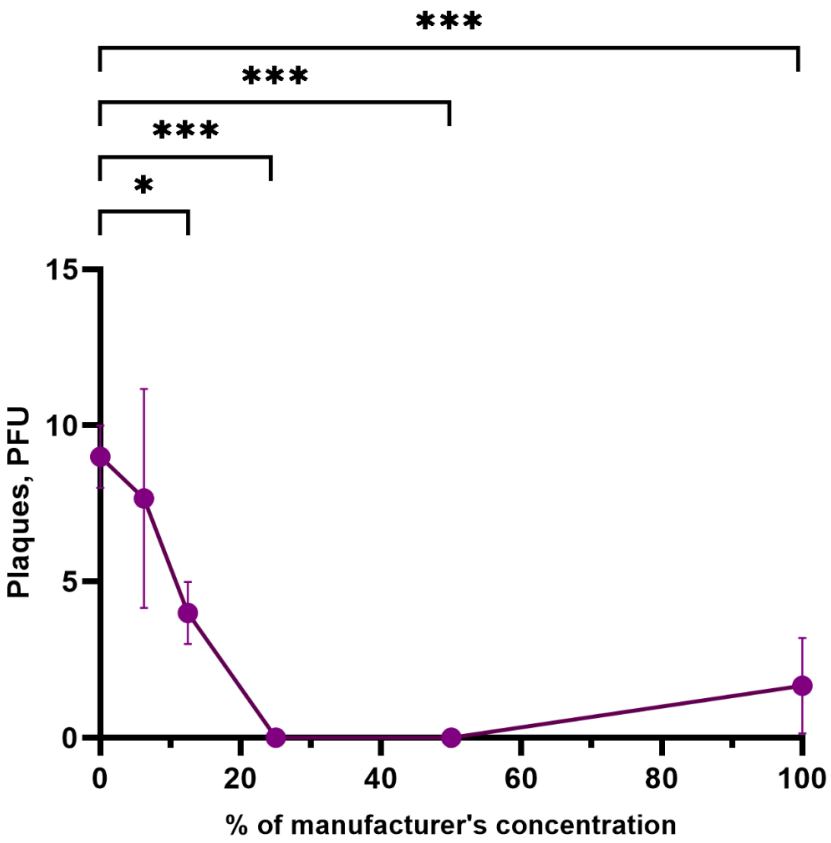

Figure 3.11. Effect of ICX® on MS2 viability.

n = 3 per data point, error bars show standard deviation. PFU: Plaque-Forming Units. * = $p < 0.05$, *** = $p < 0.001$, one-way ANOVA with *post hoc* Dunnett's test compared to 0%.

3.6 Effect of ICX® on infectious MS2 in a clinical simulation model

Having determined the effect of ICX® on MS2 viability in the laboratory, initial clinical simulation experiments were performed using MS2 as a tracer. The primary aim was to characterise the simulation model with MS2; however, these experiments were an ideal opportunity to measure the effect of the presence of a DUWL disinfectant in the dental instrument irrigant on dispersion of infective virus during a dental procedure. Experiments were conducted in a 44.96 m^3 dental surgery with a ventilation rate of 4.96 ACH. Sampling locations are shown in figure 3.12.

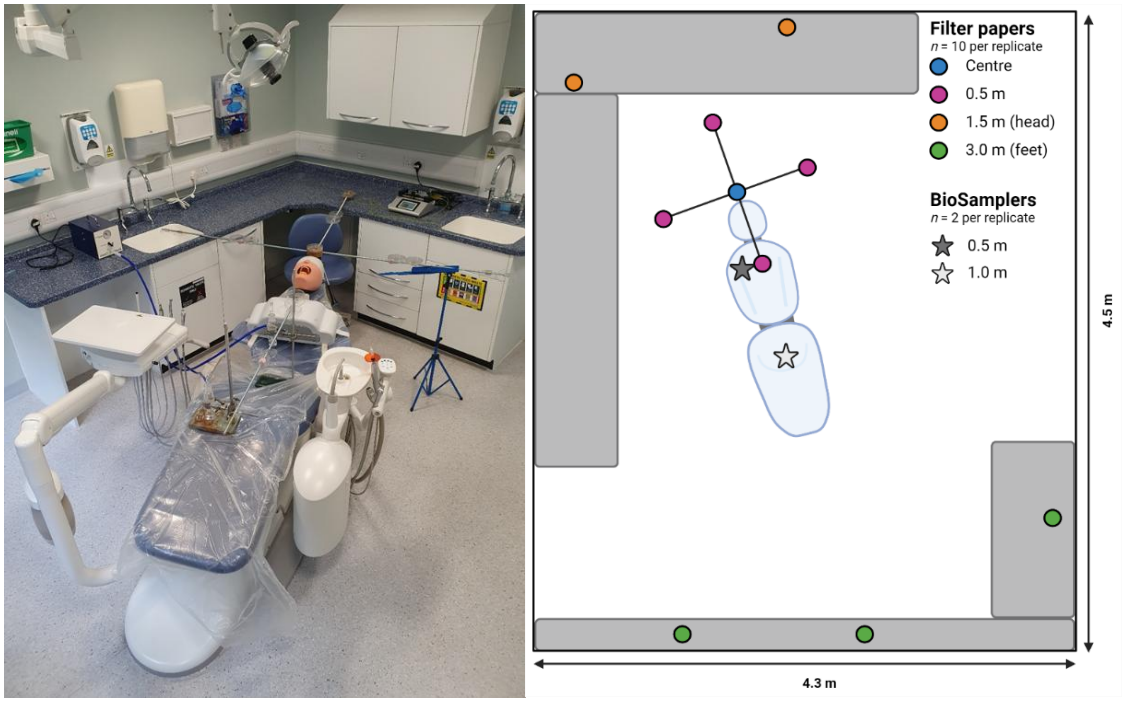

Figure 3.12. Sampling locations in clinical simulation experiments with ICX® and MS2. Created using BioRender.com.

10-min crown preparations were performed on the mannequin's upper right central incisor tooth using an air turbine handpiece with an irrigant flow rate of 38.3 mL/min. No dental suction or other aerosol control method was used. Two conditions were investigated: 1) tap water as the handpiece irrigant; 2) ICX® in tap water at the manufacturer's recommended concentration (106.2 mg/L). Three replicates were conducted per experimental condition. Dental unit water lines were flushed with at least 10 L of tap water before experiments to remove any residual DUWL disinfectant and experiments with tap water were conducted first. MS2 suspension (2 x 10^7 PFU/mL) was infused into the mannequin's mouth at 1.5 mL/min; the suspension

also contained 1 g/L fluorescein to compare results to this previously used tracer. Details of this are reported elsewhere (Allison et al. 2022).

Overall, a substantial reduction was seen in the detection of infectious MS2 in settled aerosols and droplets from filter paper samples when ICX® was used (two-way ANOVA, main effect for ICX®, $F(1, 56) = 25.99$, $p < .0001$), and detection reduced with increasing distance from the procedure (main effect for distance, $F(4, 56) = 11.85$, $p < .0001$), with a significant interaction of the two factors ($F(4, 56) = 10.53$, $p < .0001$; Figure 3.13). Considering specific distances from the procedure, the difference between ICX® and water was statistically significant at the centre of the sampling rig (Šídák's multiple comparisons test, mean difference 11.22 PFU/cm^2 [95%CI: 6.14 – 16.30]; $p < 0.0001$,) and at 0.5 m (mean difference 5.85 PFU/cm^2 [95%CI: 3.01 – 8.39]; $p < 0.0001$). Highest plaque counts were obtained from central filter papers (water mean [SD]= 11.88 [0.85] PFU/cm^2; ICX® = 0.66 [0.16] PFU/cm^2) with little detected at 1.5 m or 3.0 m (figure 3.14). When considering the average amount of phage dispersed per cm^2 across all sampling locations during each replicate, ICX® reduced dispersion of MS2 from an average of 3.59 PFU/cm^2 (SD:0.06) with water by 96.5% to 0.13 PFU/cm^2 (SD:0.03; $t(4) = 93.98$, $p < 0.0001$).

Infectious phage was recovered from 0.5 and 1.0 m BioSamplers during ICX® replicates (mean [SD] = 456.87 [152.29] and 101.53 [87.92] PFU/m^3 respectively) but not during experiments with water or in any negative control samples.

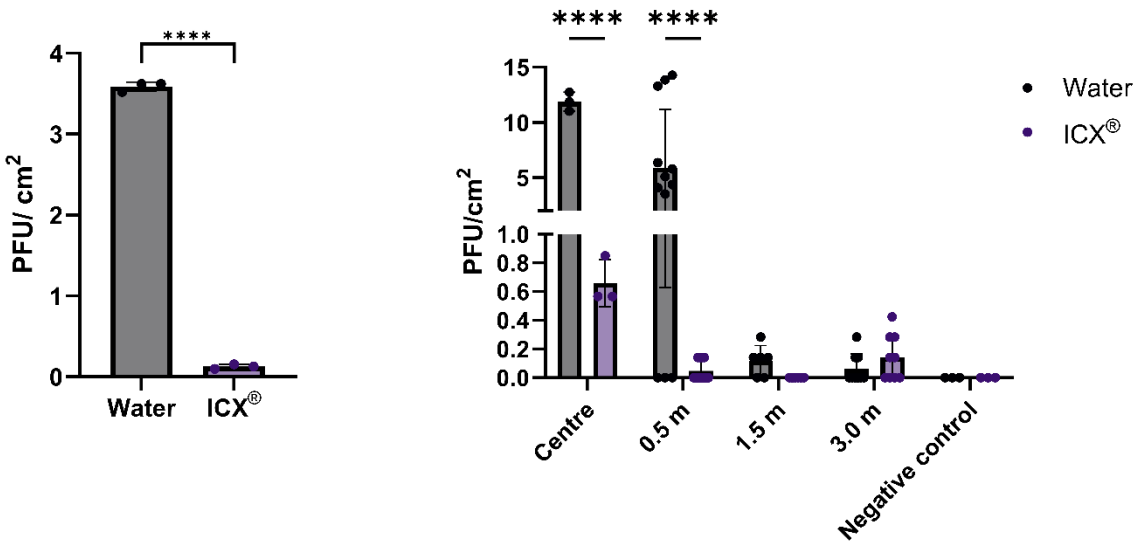

Figure 3.13. Effect of ICX® on detection of infectious MS2 on surfaces following crown preparation of an upper incisor with an air turbine handpiece.

Left panel shows the average PFU/cm^2 across all samples in each replicate; **** = $p \leq 0.0001$ (unpaired *t* test). Right panel shows each individual sample grouped by distance from the procedure from all 3 replicates: **** = $p \leq 0.0001$ (two-way ANOVA with Šidák correction; factors: distance and presence of ICX). PFU = Plaque Forming Units

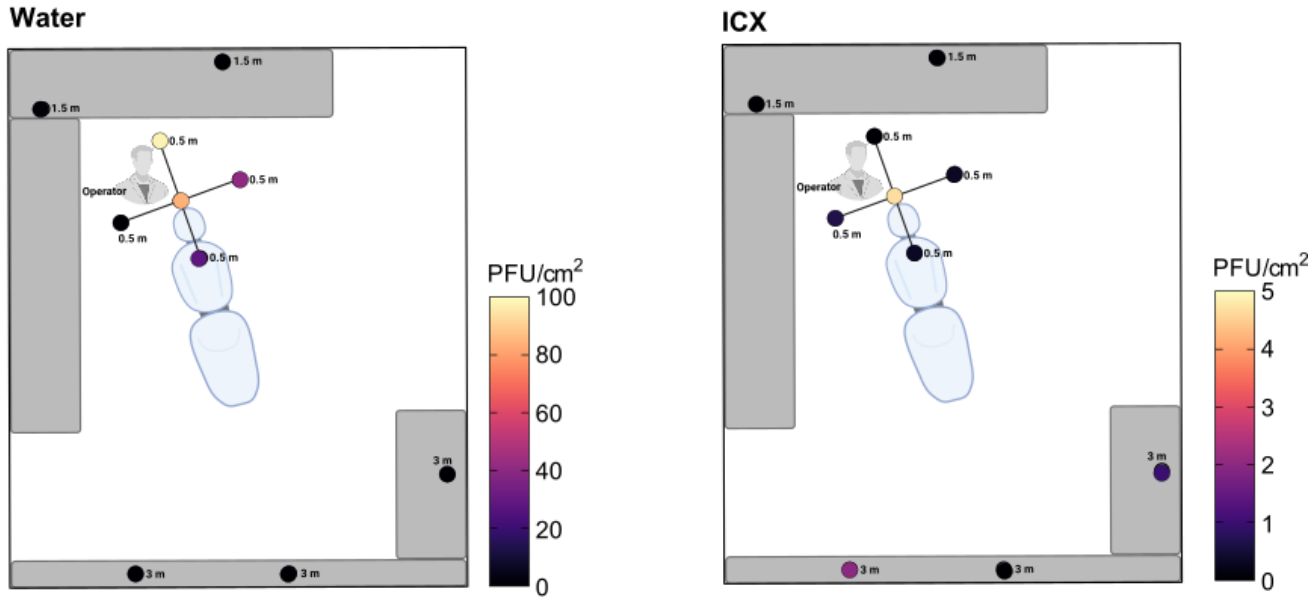

Figure 3.14 Spatial dispersion of MS2 with a dental unit waterline disinfectant

Dispersion of the MS2 tracer in surface samples at each sample location with and without ICX dental unit waterline disinfectant. Each sample location shows the average of three replicates. The heatmap scale is different for water and ICX figures and equates to the maximum MS2 recovered during each condition.

3.7 Effect of ICX® on physical aerosol concentration

To test whether the reduction in the recovery of infectious MS2 with ICX® was due to inactivation of phage in dental bioaerosols by the DUWL disinfectant, rather than by a reduction in the total amount of physical aerosol produced, the effect of ICX® on aerosol particle number concentration from the air turbine handpiece was also tested in separate experiments using an OPC. The same air turbine handpiece was operated in a steady state for 30 min with coolant flow rate of 22 mL/min in a 51.45 m^3 enclosed dental surgery with a ventilation rate of 3.30 ACH. To minimise background particle number concentration and improve signal-to-noise ratio, central mechanical ventilation was supplemented by placing two High-Efficiency Particulate Air (HEPA) filtration units (DA-UVC1001; VODEX Ltd., UK) in the room at the foot and head of the dental chair. Each device provided a nominal clean-air delivery rate of 5,000 L/min, together contributing an equivalent air exchange/filtration rate of 11.66 ACH. This equates to a total equivalent rate of 14.96 ACH assuming homogenous airflow. Background particle number concentration with supplementary HEPA filtration was measured at 1.48 particles/cm^3 (SD: 0.73) from 40 min of data.

An air turbine handpiece with a tapered diamond bur was fixed in position with the tip of the bur 1 cm below the incisal edge of the upper right central incisor tooth (figure 3.14), and three experimental conditions were tested: 1) water as the irrigant; 2) ICX® at the manufacturer's recommended concentration of 106.2 mg/L (1x ICX®); 3) ICX® at ten times the manufacturer's recommended concentration (1.062 g/L; 10x ICX®). A single replicate of each condition was performed; however, the total sampling time (30 mins) was equivalent to three repetitions of the 10-min procedure in the prior clinical simulation experiments with MS2. This was because disturbance of the room air by starting and stopping the experiment introduces air currents and therefore variation in particle number concentration; 30 min of continuous OPC data were therefore obtained for each condition instead of three 10-min replicates to avoid this.

The OPC was positioned 30 cm above the plane of the handpiece, and 30 cm inferior to the mouth of the mannequin (figure 3.15). Sampling began at 10 min before the handpiece was operated and for 30 min of handpiece operation (40 min sampling total), with a sampling frequency of 0.2 Hz (1 sample every 5 seconds). HEPA filtration units were run for at least 20 min before the first experiment, and for at least 1 hour between experiments to ensure particle counts returned to baseline.

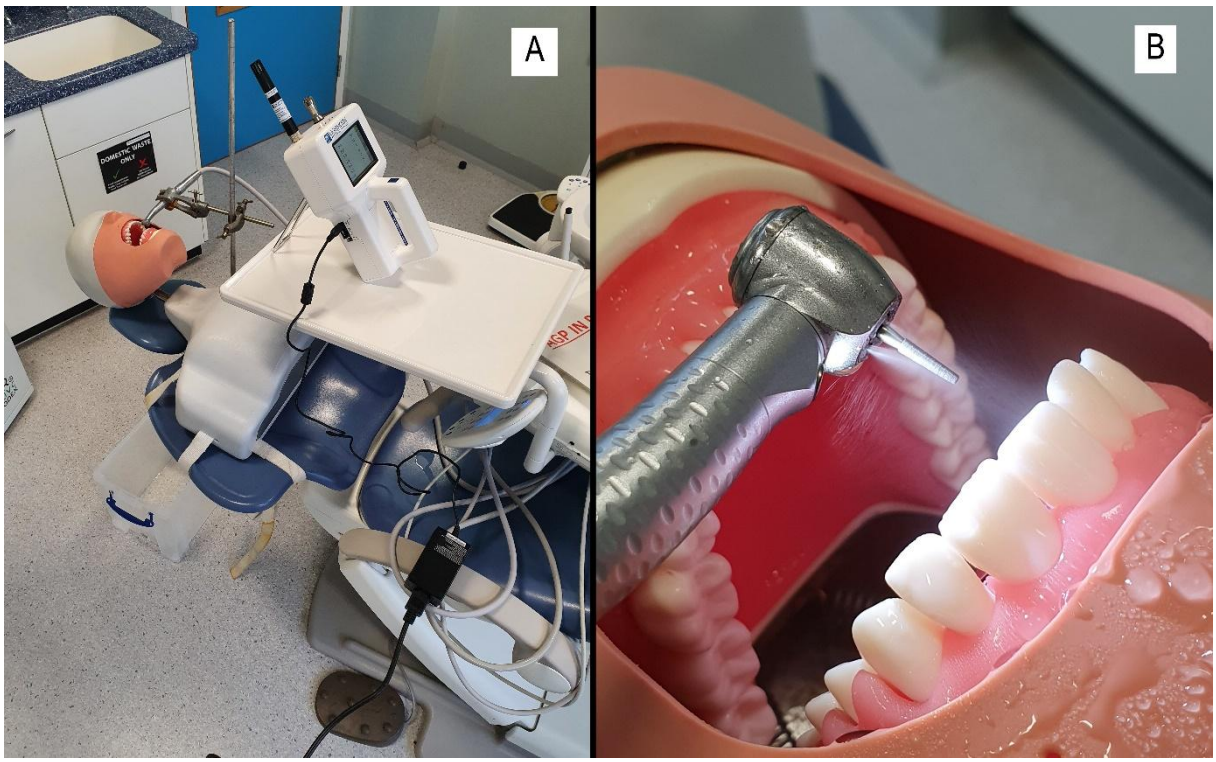

Figure 3.15. Positioning of (A) OPC and (B) air turbine handpiece during aerosol concentration measurements with ICX®.

Mean particle number concentration during min 20 – 40 (i.e., after 10 mins of handpiece operation, when particle number concentration had stabilised) was statistically significantly lower for 1x ICX® than for water, with a mean difference of 7.68 [95%CI: 5.49 – 9.88] particles/cm^3 (One-way ANOVA with *post hoc* Dunnett's = <0.0001; figure 3.16), however the time series data for these groups overlap substantially (figure 3.17), suggesting that there is no clinically meaningful difference in the amount of aerosol produced by the air turbine with these two irrigants. Mean particle number concentration was substantially higher for 10x ICX® than for water with a mean difference of 67.26 [95%CI: 65.05 – 69.48] particles/cm^3 (p < 0.0001). The time series data for the 10x ICX® was markedly separated from the other two groups, suggesting a clinically meaningful increase in aerosol production for the 10x ICX® group. The 10x ICX® group produced a greater proportion of the smallest particles measured by the instrument (0.3 µm) at 79.2% of particles measured, compared to 73.0% for water and 75.4% for 1x ICX® (figure 3.18). This may be due to the effects of the detergent in ICX on surface tension, thereby producing smaller aerosol droplets.

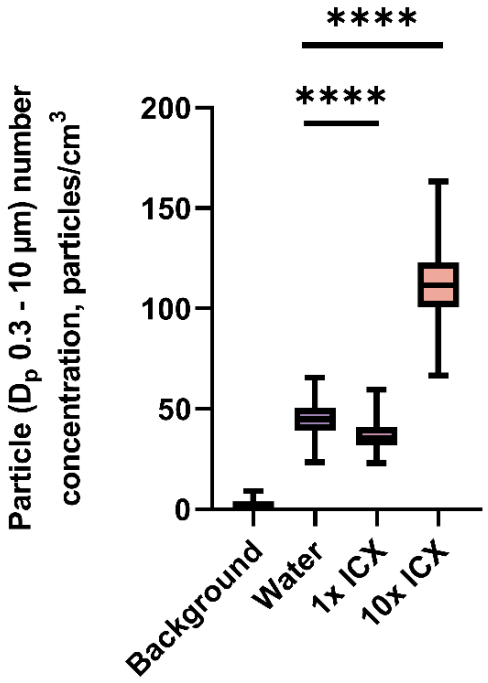

Figure 3.16. Aerosol particle number concentration from an air turbine handpiece.

Handpiece operated continuously, 20 mins of measurements with a 5 sec sampling interval taken once concentration stabilised after 10 mins of handpiece operation. Background data taken from 40 min of data in total from 4 separate measurements (not included in ANOVA). Handpiece irrigant was either tap water, ICX® at the manufacturer's concentration (1x), or ICX® at ten times manufacturer's concentration (10x); D_p = particle diameter. **** = $p \leq 0.0001$ (one-way ANOVA with *post hoc* Dunnett's test).

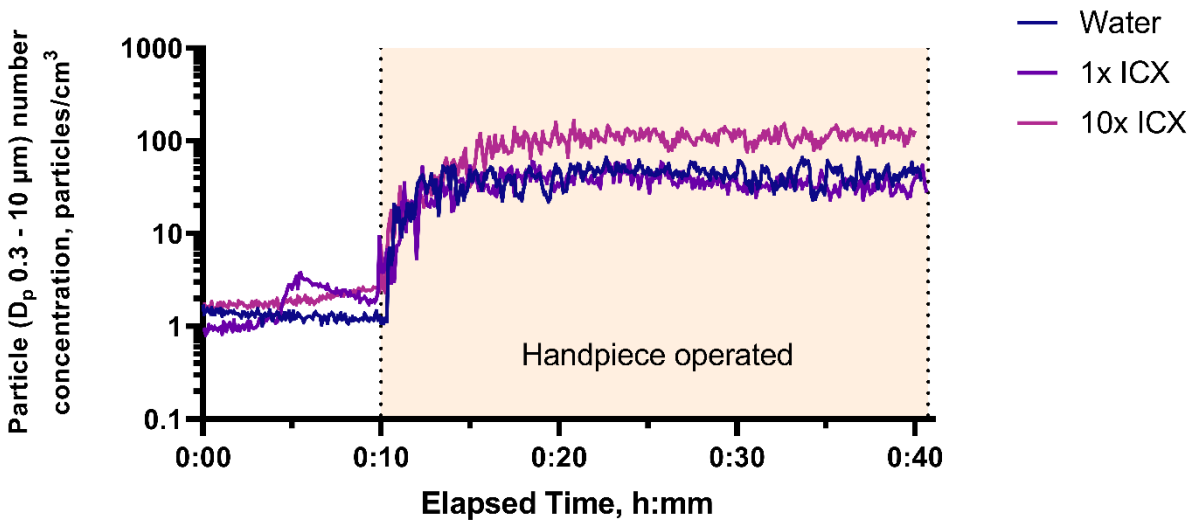

Figure 3.17. Aerosol particle number concentration over time for an air turbine handpiece.

Handpiece operated continuously during the time bounded by the orange shaded area. Handpiece irrigant was either tap water, ICX® at the manufacturer's concentration (1x), or ICX® at ten times manufacturer's concentration (10x); D_p = particle diameter. Sampling interval = 5 sec.

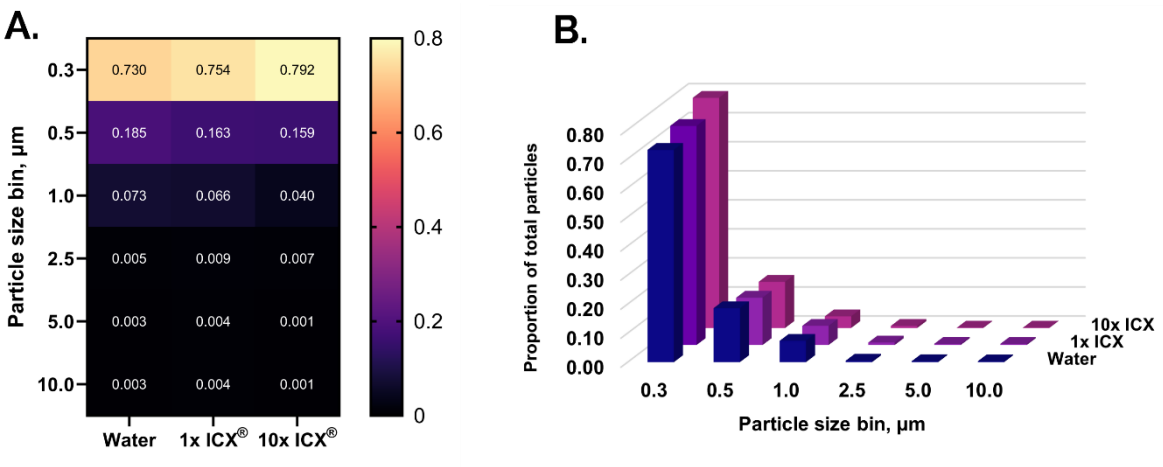

Figure 3.18. Particle size distribution from a continuously operated air turbine handpiece.

Proportion of total particles detected for each particle size bin with different irrigants shown as (A) heatmap (numbers in cells show proportion of total for that particle size) and (B) grouped bar chart. 1x ICX® = ICX® at manufacturer's concentration; 10x ICX® = ICX® at ten times manufacturer's concentration. 20 mins of measurements with a 5 sec sampling interval taken once concentration stabilised after 10 mins of handpiece operation.

3.8 Comparing sampling methods in a multi-phage tracer model

Having demonstrated the ability of the clinical simulation model to detect differences in dispersion with a single phage, two phages with differing virion structure (enveloped phi6 and non-enveloped MS2) were next used to explore differences in dispersion. Filter papers were placed in the environment in the same way as experiments with MS2 alone, however, Petri dishes lawned with host bacteria (*E. coli* and *P. syringae*) were also placed in key locations alongside filter papers to compare this previously reported method of phage recovery (Beltran et al. 2023; Liu et al. 2023; Vernon et al. 2021; Vernon et al. 2022) to elution from filter papers. These experiments were also used as an opportunity to measure the effectiveness of rubber dam, and so replicates were conducted both with and without rubber dam.

Experiments were conducted in a 51.45 m^3 enclosed single dental surgery with 3.30 ACH. 1mL of phage suspension (MS2: 5.30 x 10^{10} PFU/mL; phi6: 8.05 x 10^{12} PFU/mL) was added to the surfaces of the teeth of the mannequin immediately before beginning experiments. In experiments using rubber dam, this was done before the rubber dam was placed. Phage tracer at the same titre was infused into the mouth of the mannequin (beneath the rubber dam where this was used) at a total flow rate of 1 mL/min.

10-min crown preparations were performed on the upper right central incisor using an air turbine dental handpiece with irrigant flow rate of 27 mL/min. No dental suction or other bioaerosol control measure was used. Two conditions were investigated: 1) no rubber dam; 2) rubber dam. Two replicates were conducted per experimental condition. Dental unit water lines were flushed with at least 10 L of tap water before experiments to remove any residual DUWL disinfectant.

For experiments using rubber dam, the dam was perforated in locations corresponding to the maxillary teeth mesial to and including the first premolars. A ~15 mm diameter hole was cut in the centre of the dam to prevent pooling of water from the handpiece, as no dental suction was used during experiments. Winged molar rubber dam clamps were placed on the dam at the first premolar positions, and the dam was affixed to a rubber dam frame. The assembled construct was then applied to the mannequin at the beginning of each experiment (after phage had been added to the tooth surfaces) using rubber dam clamp pliers, and dental floss to seat the dam between the teeth. Finally, the rubber dam was released from the wings of the clamps to seat the dam around the cervical areas of the clamped teeth (figure 3.19).

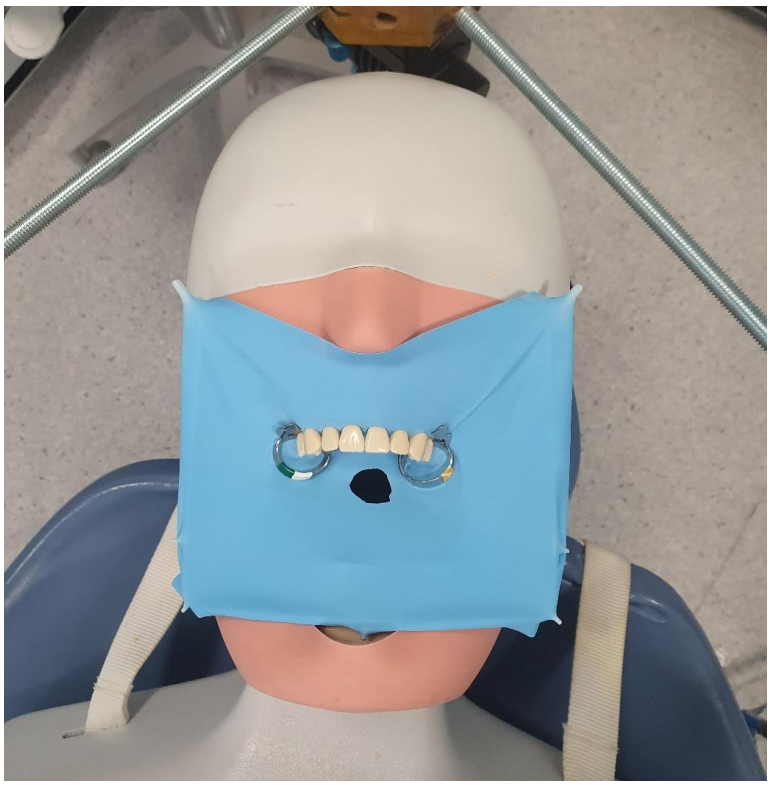

Figure 3.19. Rubber dam.

Premolar clamps and dam used to isolate the maxillary teeth of the dental mannequin from right first premolar to left first premolar. A hole was cut in the dam to allow drainage of handpiece irrigant, as suction was not used.

To compare sampling efficiency of filter papers to that of Petri dishes, both sample types were placed in sampling locations shown in Figure 3.20. Distances were measured relative to the centre of the rig, which was positioned 22 cm superior to the UR1 tooth and on a plane 84 cm above the floor; this was also the height of the benches used for other sampling locations. Positive control samples of the phage solution and aspirates from the mannequin's mouth were collected after each experiment.

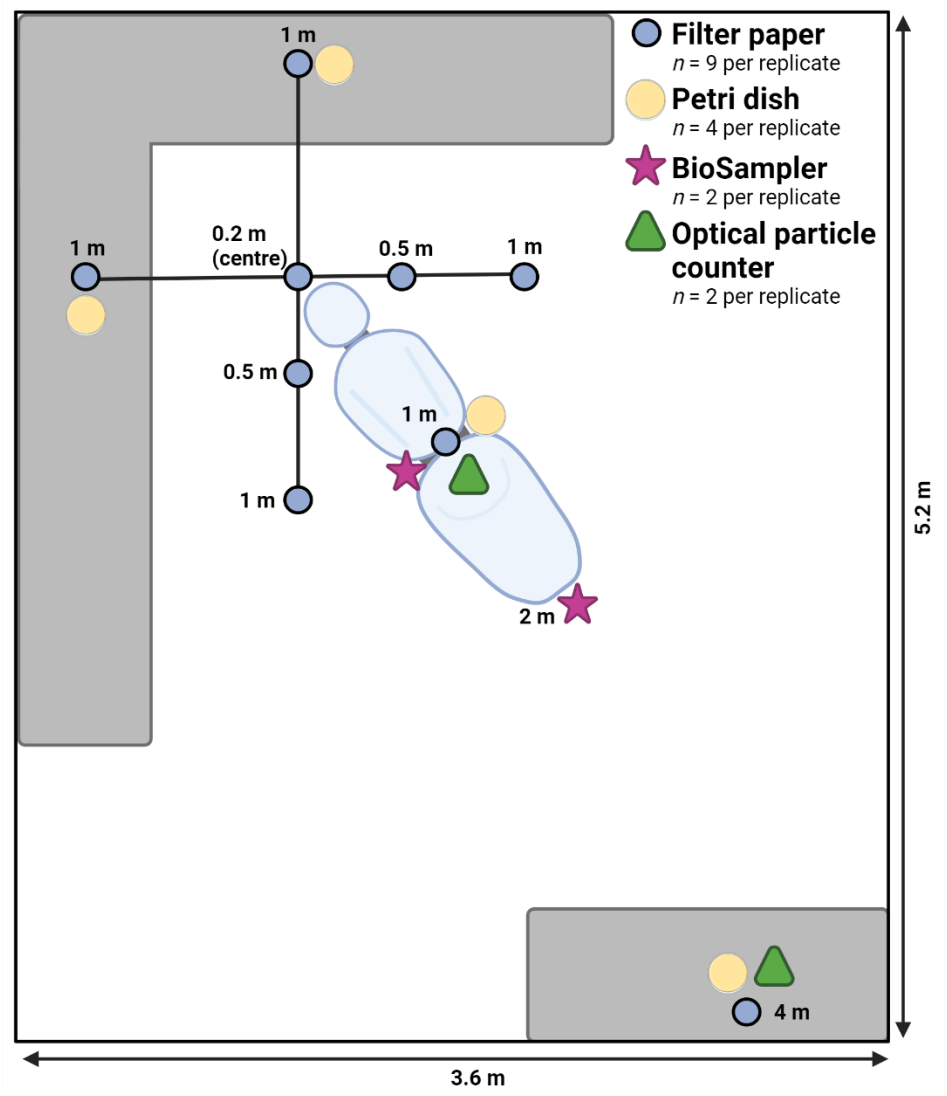

Figure 3.20. Sampling locations in clinical simulation experiments with MS2 and phi6. Created using BioRender.com.

Recovery of infectious phage (MS2 or phi6) from locations where both sample types were present was significantly greater ($p < 0.0004$, Wilcoxon matched pairs signed rank test) for filter papers (Mean [SD] = 3.13 [9.11] plaques/cm^2) compared to Petri dishes (Mean [SD] = 0.14 [0.33] plaques/cm^2). The equation describing the

relationship between the two, derived by linear regression, was $y = 30.08\,x - 0.1485$, where y = filters and x = plates (R^2:0.952). This curve was heavily influenced by a single phi6 sample from the centre location; Curves including and excluding this data point are shown in Figure 3.21, and a breakdown for each individual phage is shown in Figure 3.22.

In 6 of 32 samples, phage was recovered from plates (0.06 plaques/cm^2; SD=0.05) where none was recovered from filter papers. On no other occasion was the recovery of phage from plates greater than from filter papers (figure 3.21).

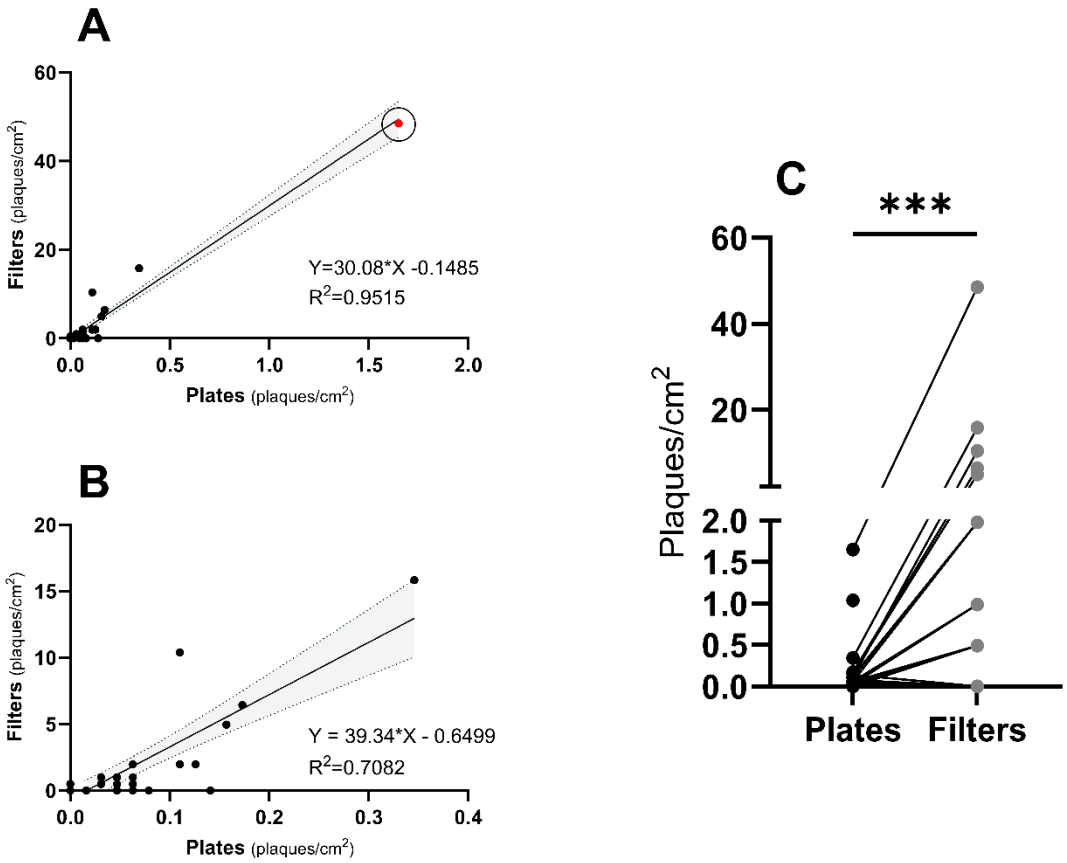

Figure 3.21. Relative recovery of infectious phage.

Recovery of either phage (MS2/phi6) from filter papers and agar in Petri dishes (plates), corrected for surface area. Two replicates from experiments with rubber dam and two without were included with four locations, each sampling two phages (32 data points in total). A: scatter plot showing linear equation, R^2 and 95% confidence bands of the equation. B: as for A, but with the circled datapoint in red excluded. C: Recovered phage from each sample type, solid lines connect samples from the same location collected during the same experiment. *** = p ≤ 0.001 (Wilcoxon matched pairs signed rank test).

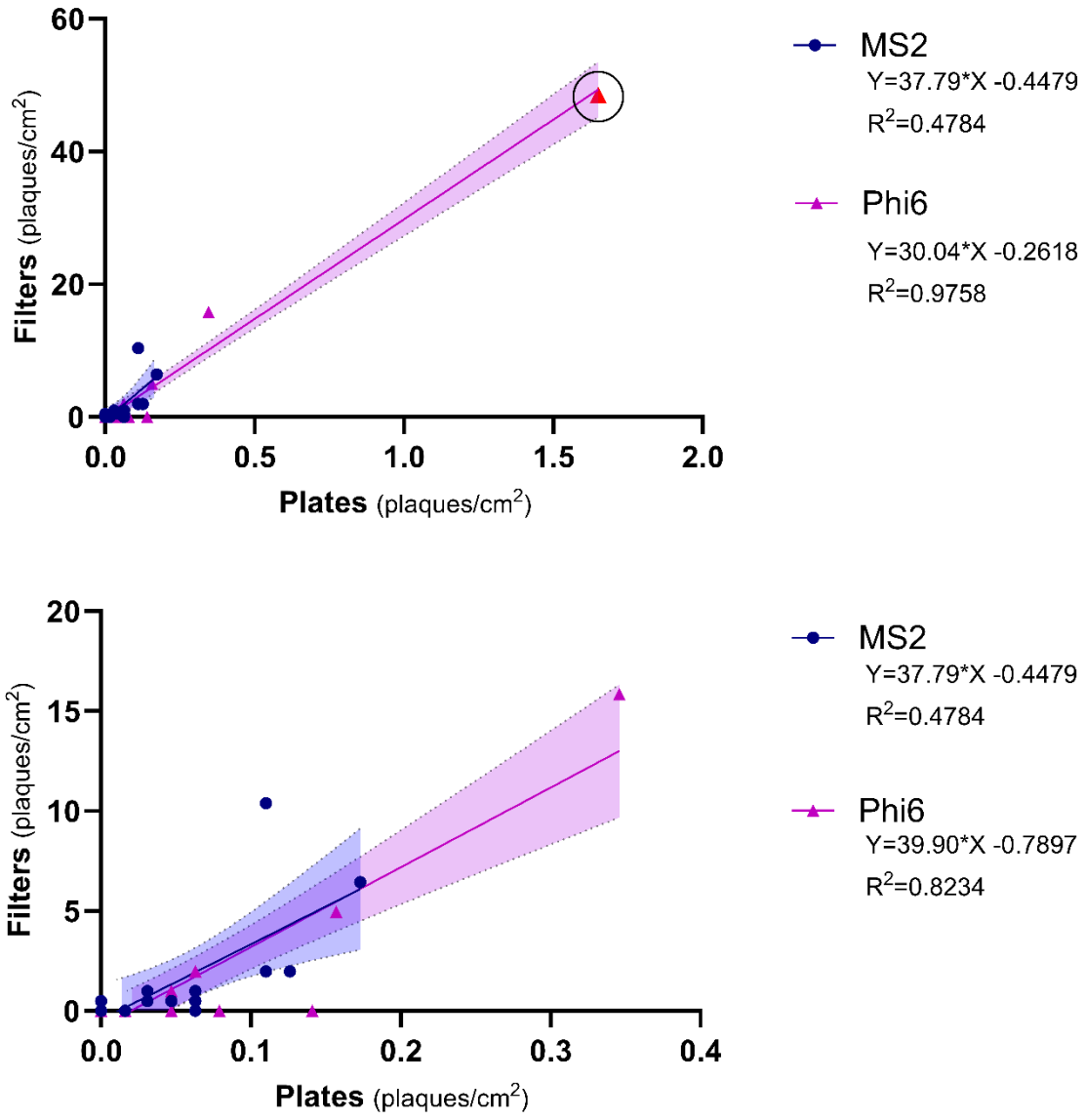

Figure 3.22. Relative recovery of infectious phage per phage.

Recovery from filter papers and agar in Petri dishes (plates), corrected for surface area for both MS2 and phi6. Two replicates from experiments with rubber dam and two without were included with four locations, each sampling two phages (32 data points in total). Upper panel: recovery on plates versus filters, showing linear equation, R^2 and 95% confidence bands for each individual phage (MS2 and phi6). Lower panel: as for upper panel, but with the datapoint in red excluded.

3.9 Effect of rubber dam on aerosol concentration

To determine whether the use of rubber dam results in a difference in aerosol concentration, particle number concentration was measured using an OPC during rubber dam experiments at 1 and 4 m from the procedure. At 1 m, substantial elevations in aerosol particle number concentration were seen during the 10-min

dental procedure (up to one hundred-fold) and decayed towards baseline following the procedure (figure 3.23). At 4 m, steady but modest increased aerosol concentration was seen during the dental procedure (up to 20-fold) but without the extreme spikes observed at 1 m.

Significant differences in Area Under the Curve (AUC) were seen for the main effects of rubber dam (two-way ANOVA $F(1, 4) = 41.35$, $p \leq 0.003$) and distance ($F(1, 4) = 475.7$, $p \leq 0.0001$). At 1 m, AUC was 6.4% higher with rubber dam but was not statistically significant (*post hoc* Šídák's, $p = 0.253$) and at 4 m this was 23.6% higher with rubber dam ($p < 0.020$). This suggests that rubber dam causes a small increase in the total amount aerosol detected at 4m, but not at 1m.

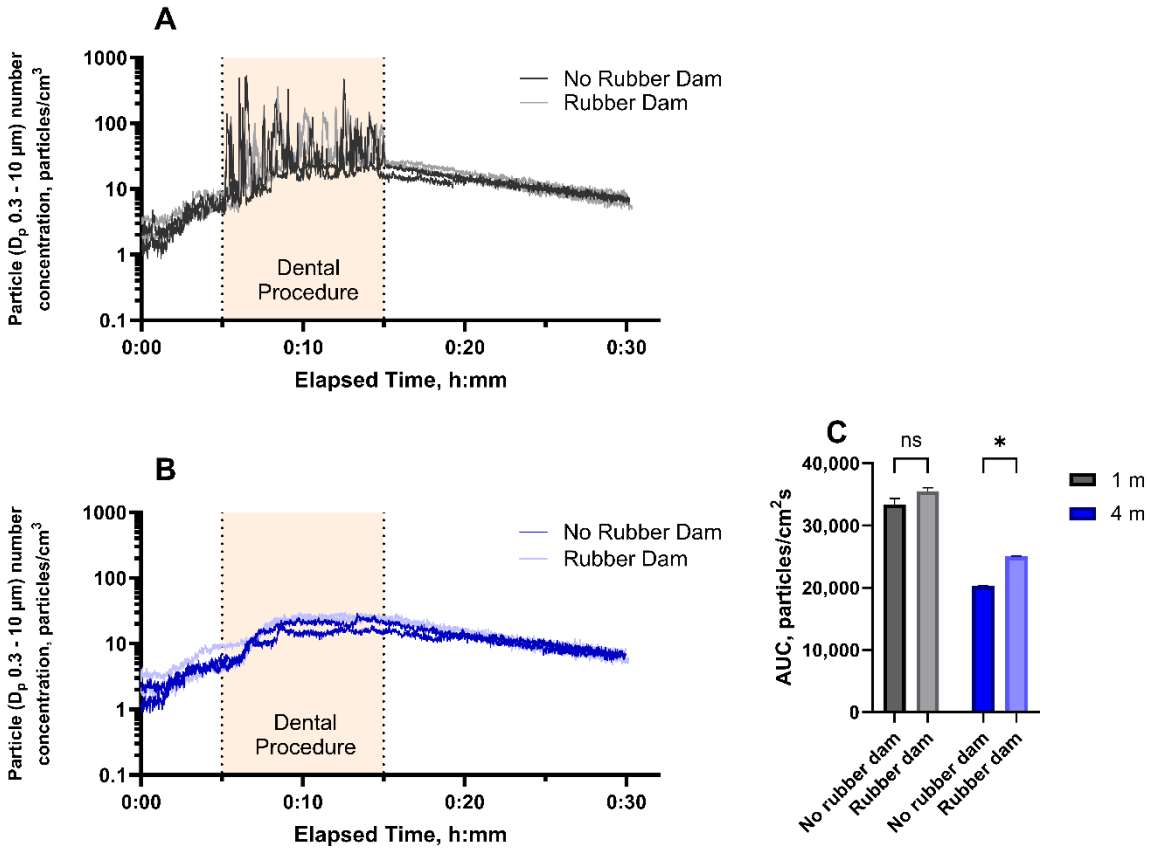

Figure 3.23. Aerosol particle number concentration over time during a 10-min clinical procedure using an air turbine handpiece with and without rubber dam.

Sampling was at 1 m (A) or 4 m (B) from the dental procedure with a 1 sec sampling interval. Dp = particle diameter. C: Area Under the Curve (AUC) of time series OPC data (2 replicates per bar). ns= not statistically significant, * = $p \leq 0.05$ (two-way ANOVA with post hoc Šídák correction).

3.10 Effect of rubber dam on recovery of infectious phage

3.10.1 Settled aerosols and droplets on surfaces

Without rubber dam, recovery of infectious MS2 and phi6 in settled aerosol and droplets from filter papers samples was highest at 0.22 m with reduced recovery at greater distances from the procedure (figure 3.24, figure 3.25). No MS2 or phi6 was recovered in negative control samples.

For MS2, rubber dam reduced the recovery of infectious phage overall (two-way ANOVA rubber dam main effect, $F(1, 27) = 6.692$, $p = 0.015$), although the main effect of distance was not significant ($F(3, 27) = 1.966$, $p = 0.143$) and rubber dam was not a significant factor at any individual distance in *post hoc* comparisons (Šídák's, $p > 0.05$). Considering the average recovery of phage across all samples at all distances for each replicate, rubber dam reduced dispersion of MS2 overall by 86.3% ($t(2) = 6.052$, $p = 0.026$).

For phi6, rubber dam also reduced the recovery of infectious phage overall (two-way ANOVA rubber dam main effect, $F(1, 28) = 7.866$, $p = 0.009$), with distance being a non-significant factor in the ANOVA model ($F(3, 28) = 2.111$, $p = 0.121$). Rubber dam eliminated detection of infectious phi6. The reduction was statistically significant at the 0.2 m distance in *post hoc* comparisons (Šídák's, $p = 0.013$). Considering the average recovery of phage across all samples at all distances for each replicate, rubber dam reduced dispersion of phi6 overall by 100.0% ($t(2) = 9.543$, $p = 0.0108$).

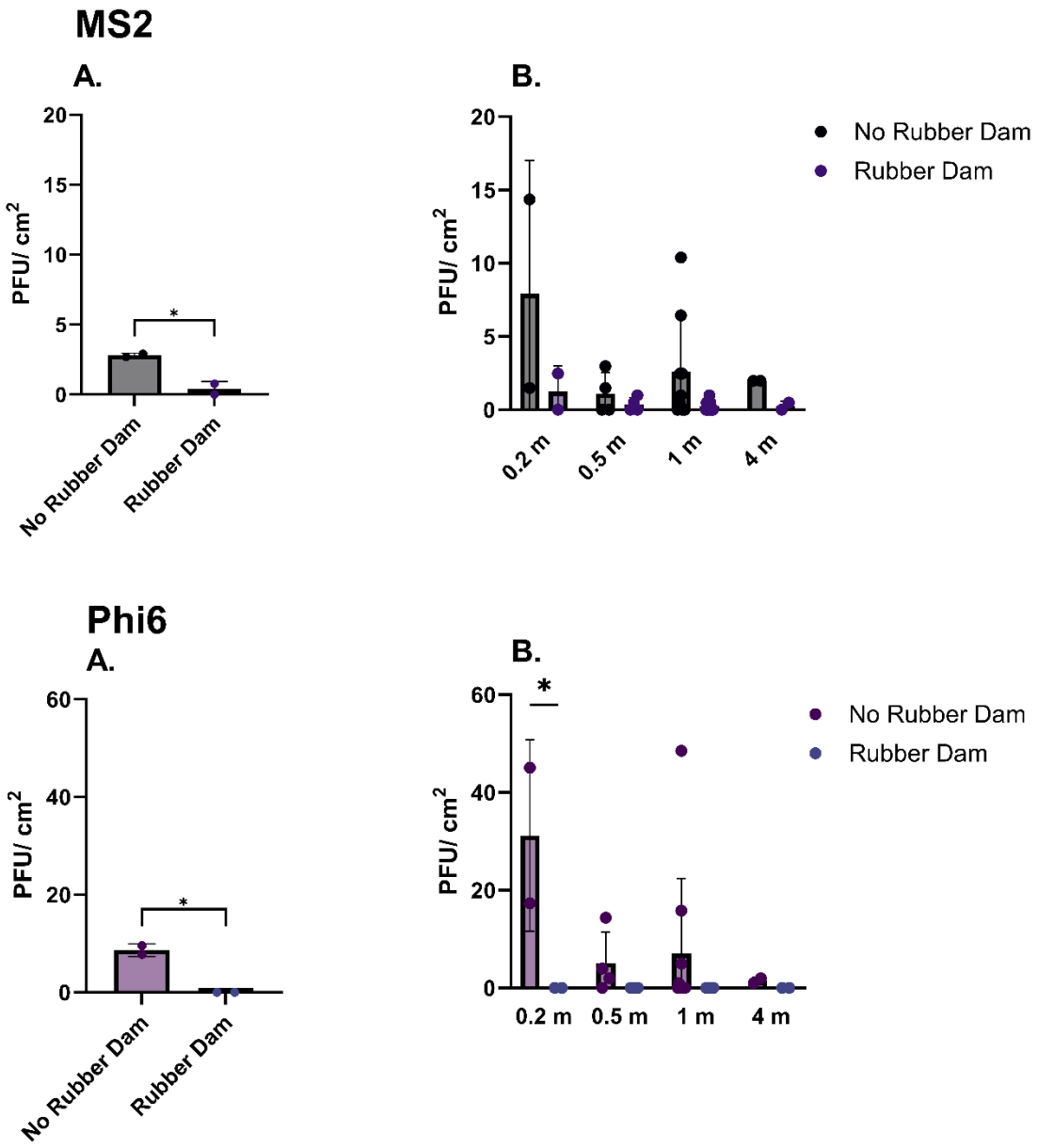

Figure 3.24. MS2 and phi6 recovered from surface samples with and without rubber dam.

A: Each data point represents the average of all samples in each replicate (*n* = 2 replicates); * = p<0.05, unpaired t test. B: Data show each individual filter paper sample across all replicates by distance from the procedure; * = $p < 0.05$, two-way ANOVA with post hoc Šídák's test.

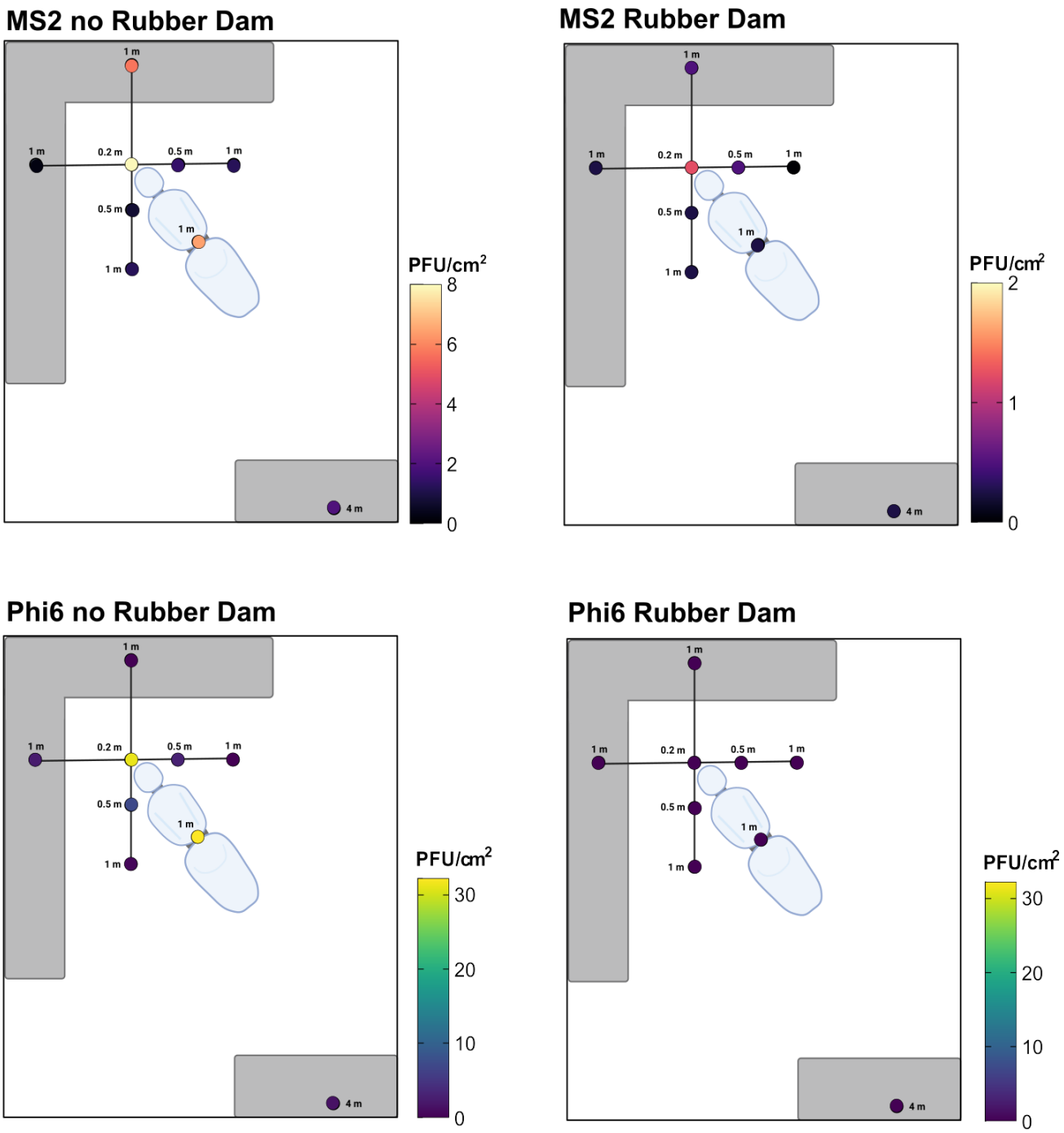

Figure 3.25 Spatial dispersion of MS2 and phi6 with and without rubber dam

Dispersion of MS2 and phi6 in surface samples at each sample location with and without rubber dam. Each sample location shows the average of two replicates. The heatmap scale is different for the two MS2 figures and equates to the maximum MS2 recovered during each condition.

3.10.2 Suspended aerosols in air samples

For both MS2 and phi6, recovery of infectious phage in suspended aerosols in BioSamplers was similar at 1 m and 2 m without rubber dam (figure 3.26), and no MS2 or phi6 was recovered in negative control samples.

Considering the average recovery in BioSamplers across both distances for each replicate, rubber dam reduced recovery in air samples by 85.7% for MS2 and by 100% for phi6, however, differences were not statistically significant (MS2: $t(2) = 2.683$, $p = 0.115$; phi6: $t(2) = 3.667$, $p = 0.067$).

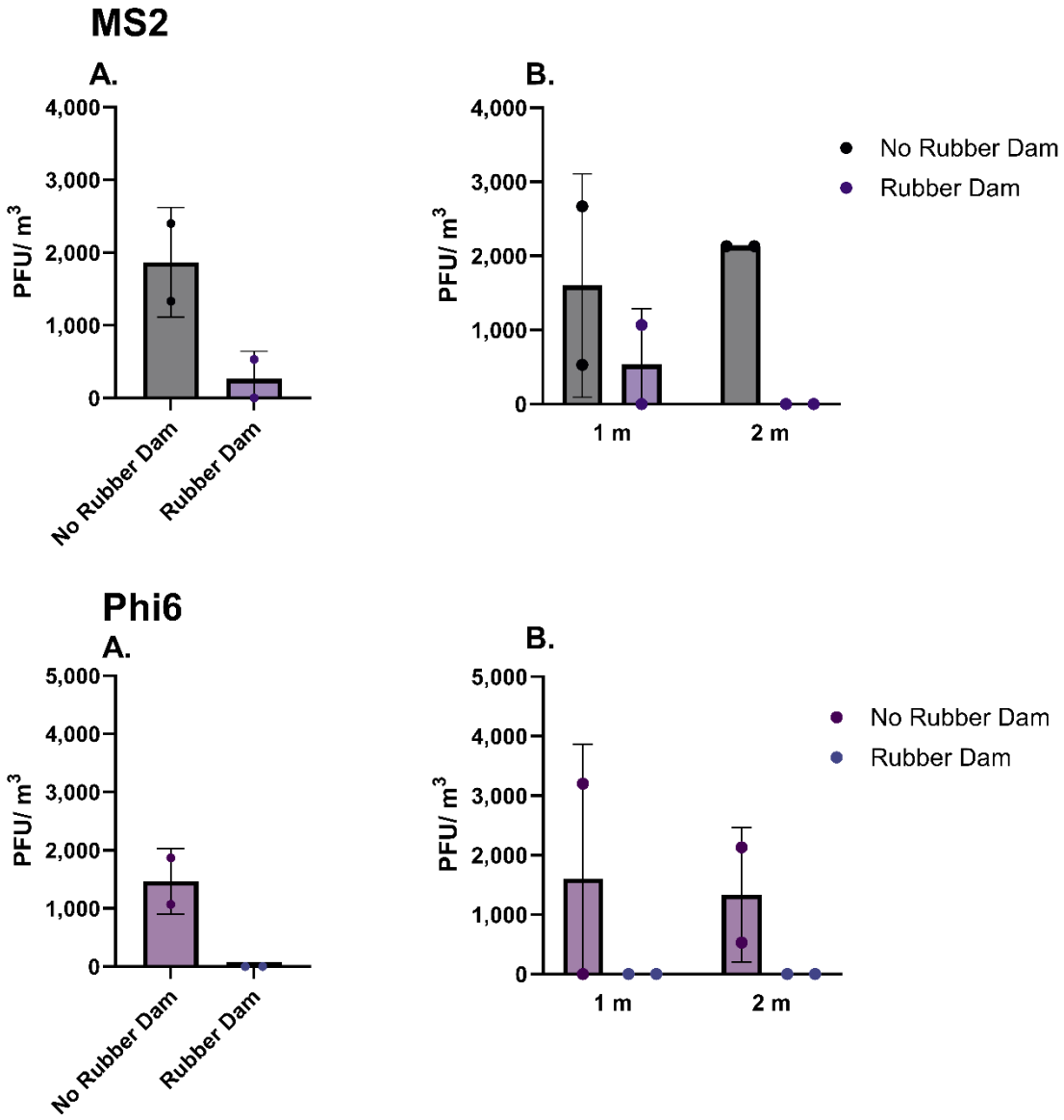

Figure 3.26. MS2 and phi6 recovered from air samples with and without rubber dam.

A: Each data point represents the average of all samples in each replicate (n = 2 replicates).
B: Data show each individual samples across all replicates by distance from the procedure.

3.11 Phage detection by RT-qPCR

Eluted phage from filter paper samples was stored at -80 °C for six months prior to RNA extraction and reverse transcription whilst the RT-qPCR assay was optimised. Positive control samples taken from the phage tracer, and aspirates from the mannequin's mouth following the procedure contained high levels of both MS2 and phi6 RNA (~10^{10} copies/mL). For both phages, negative control samples during the RNA extraction step (H_2O), reverse transcription step (no-RT), and qPCR step (no-template) were below the LoD of the RT-qPCR assay, except one H_2O sample and one no-RT sample (figure 3.27). Negative control samples taken during the clinical simulation experiment (filter paper and BioSampler) were below the LoD, except one filter paper sample (MS2: 6.9 x 10^5 copies/cm^2; phi6 3.0 x 10^5 copies/cm^2) and one BioSampler sample (MS2: 67.4 x 10^5 copies/m^3; phi6 3.9 x 10^5 copies/m^3); these samples did not contain any infective phage in plaque assays.

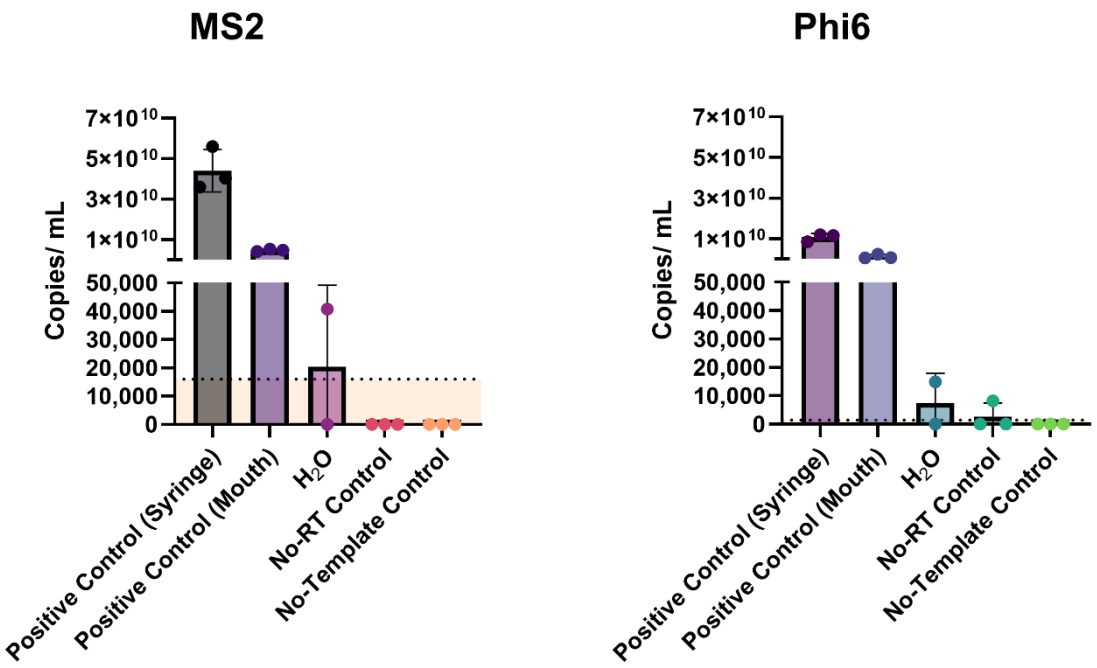

Figure 3.27. MS2 and phi6 RNA in control samples from rubber dam experiments detected by RT-qPCR.

Dotted line defining the orange shaded area denotes limit of detection. Positive controls taken from the phage tracer used in experiments (syringe) and aspirated from the mouth of the mannequin following experiments (mouth). Negative controls from RNA extraction (H_2O), reverse transcription (no-RT), and qPCR (no-template) steps. *n* = 3 except for H_2O (*n* = 2).

Detection of MS2 and phi6 RNA in settled aerosols and droplets from filter papers samples was greater when no rubber dam was used; there was little detection

beyond 1 m without rubber dam, or beyond 0.2 m with rubber dam (figure 3.28). When considering the average recovery in samples across all distances for each replicate, rubber dam reduced the amount of MS2 RNA detectable by 92.9%, and by 92.4% for phi6, although neither reached statistical significance (MS2: $t(2) = 0.927$, $p = 0.452$; phi6: $t(2) = 1.077$, $p = 0.394$).

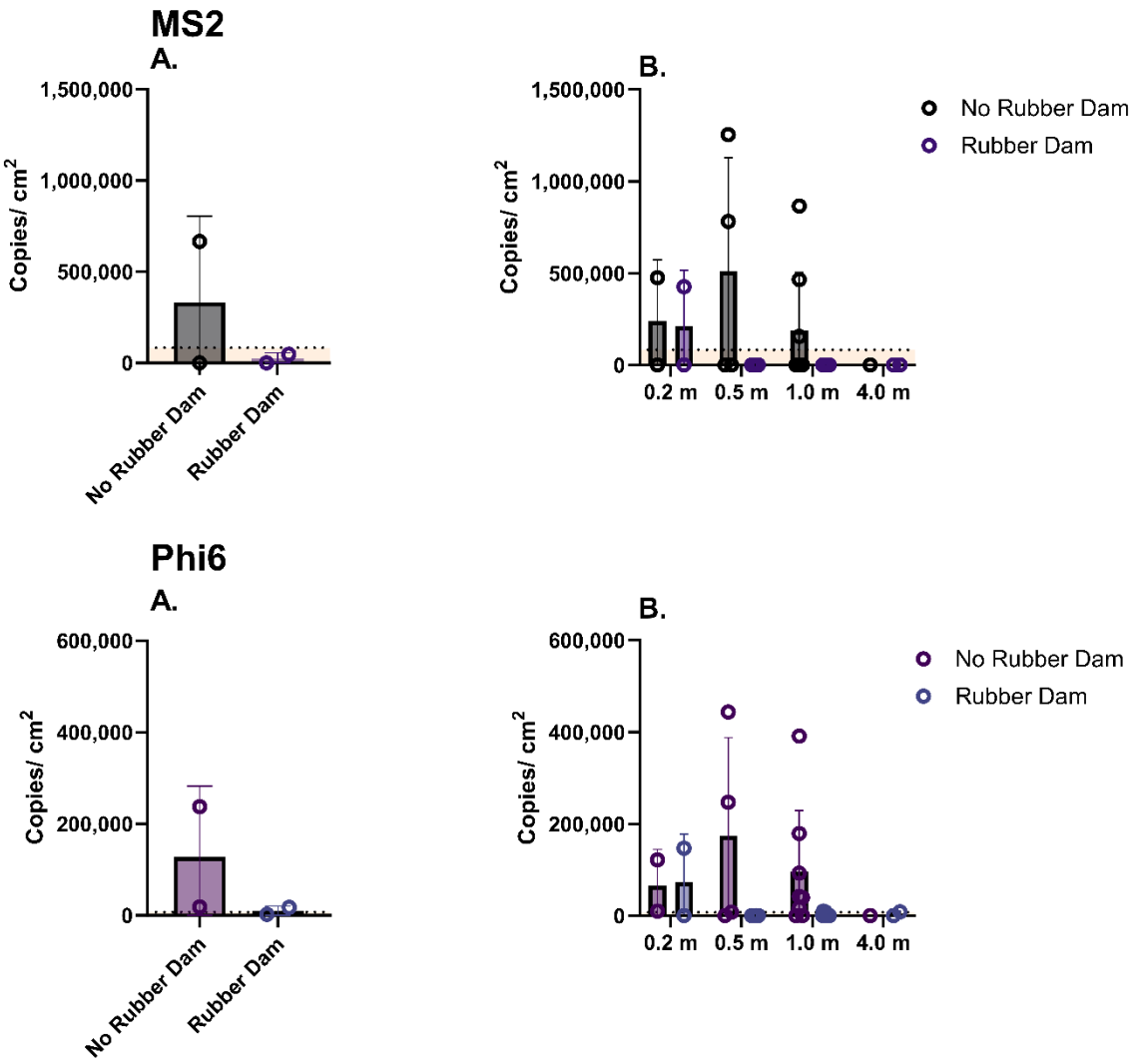

Figure 3.28. MS2 and phi6 RNA detected in droplets and settled aerosols by RT-qPCR with and without rubber dam.

Dotted line defining the orange shaded area denotes limit of detection. A: Each data point represents the average of all samples in each replicate ($n = 2$ replicates); B: Data show each individual filter paper sample across all replicates by distance from the procedure.

Due to sample loss (sample accidentally discarded), only one replicate worth of BioSampler RT-qPCR data was available for the no rubber dam condition ($n = 1$ available). Therefore, no statistical tests were performed due to the single data point

for this condition. As with plaque assays, recovery was similar at 1 m and 2 m distances. Considering the average recovery in all air samples (1 m and 2 m), rubber dam reduced recovery of MS2 RNA by 100%, and of phi6 RNA by 97.8% (figure 3.28).

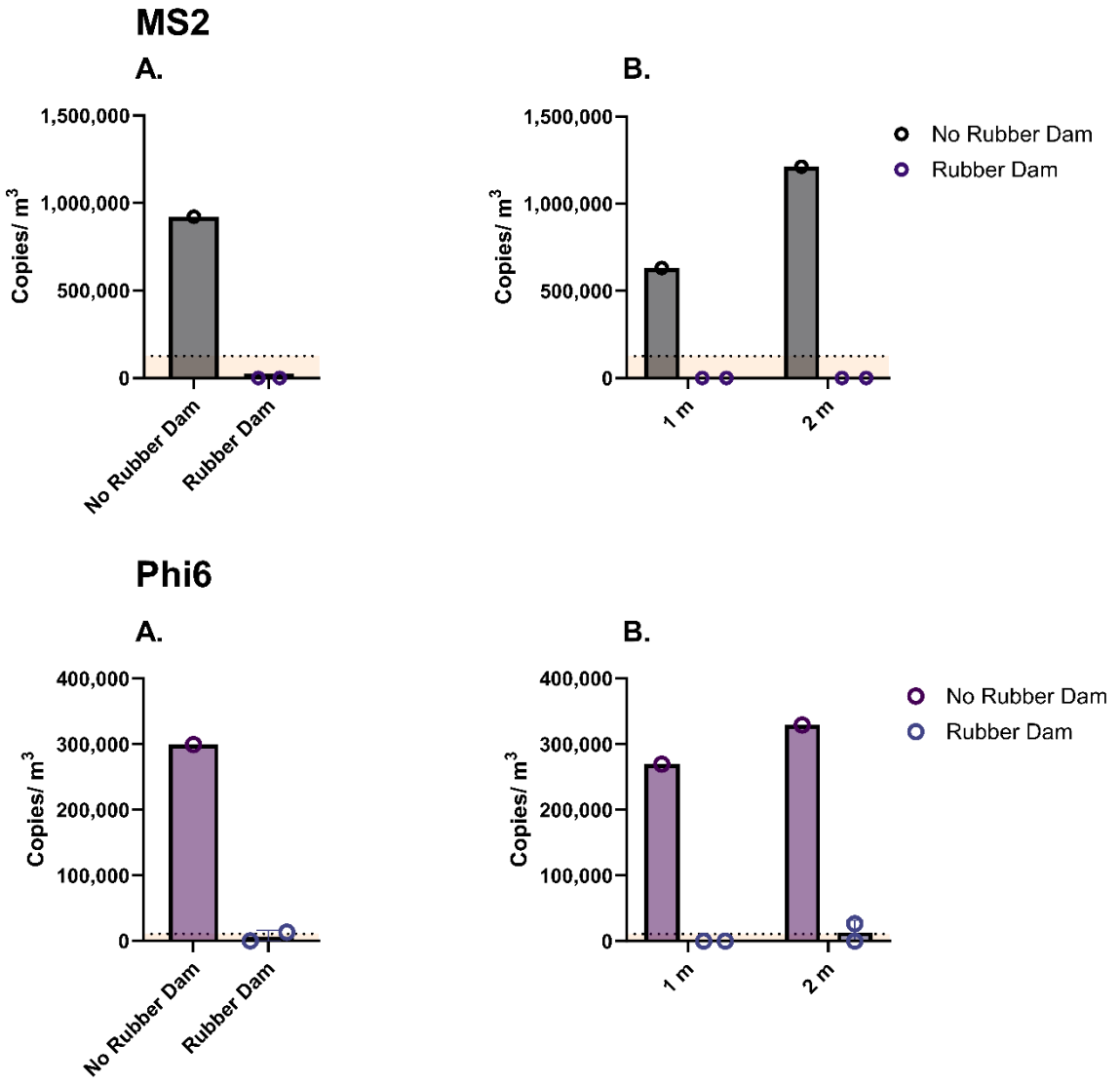

Figure 3.29. MS2 and phi6 RNA detected in air samples by RT-qPCR with and without rubber dam.

A: Each data point represents the average of all samples in each replicate (*n* = 2 replicates, however only one replicate's data is available for the no rubber dam condition). B: Data show each individual sample across all replicates by distance from the procedure.

3.12 Relationship of infectious phage to phage RNA

Comparison of the amount of infectious phage recovered from filter papers to the amount of phage RNA shows no correlation between plaques and copies for MS2 (Spearman's ρ = 0.299 [95%CI: -0.043 – 0.578], p = 0.076) and a weak correlation for phi6 (ρ = 0.421 [95%CI: 0.098 – 0.664], p = 0.011). A linear regression curve fitted to the data showed poor curve fit for both MS2 (R^2 = 0.006) and phi6 (R^2 = 0.025). There was no correlation between plaques and copies for BioSampler samples for MS2 (ρ = 0.523, exact p = 0.095) or phi6 (ρ = 0.550, exact p = 0.097). The linear regression curve also had poor fit to the data for MS2 (R^2 = 0.462) and phi6 (R^2 = 0.193; figure 3.30).

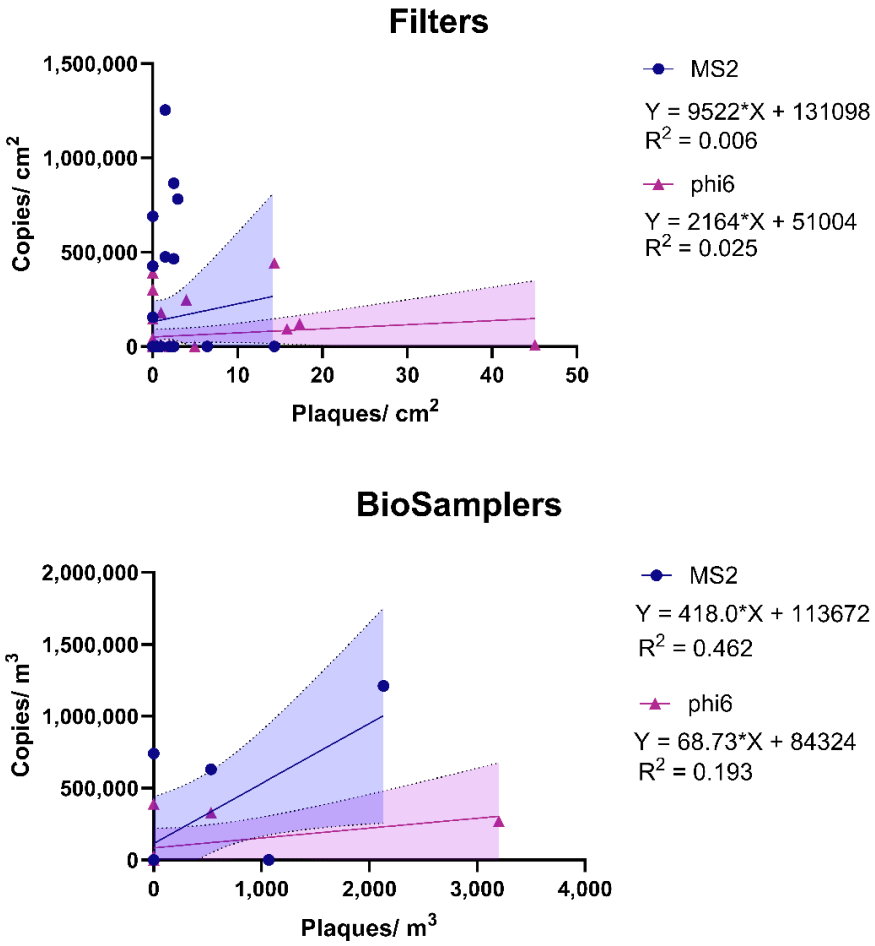

Figure 3.30. Relationship of infectious phage and phage RNA recovered from dental bioaerosols.

Scatter plot of infectious MS2 or phi6 phage (plaques) and phage RNA (copies) recovered in settled aerosols and droplets from filter papers (n = 36 per phage) and in suspended aerosols from BioSamplers (n =9 per phage) following a 10-min dental procedure with or without rubber dam. Coloured shaded area surrounding linear regression curves represent 95% confidence intervals of curves. Curve equations and corresponding R^2 values are shown.

3.13 Discussion

The aim of initial experiments was to characterise the mannequin simulation model and demonstrate its ability to represent infective virus dispersion during dental procedures using multiple phage tracers. The dispersion of infectious MS2 and phi6 was demonstrated, recapitulating what is seen with oral microorganisms in dental bioaerosols *in vivo*. No human studies have yet assessed the dispersion of infective viruses in dental aerosols, however one study reported the detection by enzyme-linked immunosorbent assay and PCR of Hepatitis B Virus (HBV) in aerosols during orthodontic debonding on HBV carriers (Toroglu et al. 2003), and two studies have demonstrated dispersion of SARS-CoV-2 in dental settings using RT-qPCR. Akin *et al.* (2021) recovered SARS-CoV-2 RNA from settled aerosols and droplets at distances of 0.9 – 3.1 m in 5 of 24 patients with COVID-19 following use of an air turbine and ultrasonic scaler, and Bazzazpour *et al.* (2022) recovered RNA from 36% of environmental air samples in dental clinics during the first wave of the COVID-19 pandemic in Tehran, Iran. Another study using RT-qPCR failed to detect SARS-CoV-2 RNA on surface samples taken from around a dental procedure in individuals with asymptomatic COVID-19 and low salivary copy numbers (Meethil et al. 2021). One recent study attempted to detect respiratory viruses using an end-point PCR panel in air samples taken during various dental treatments in 12 patients (Choudhary et al. 2022). The authors were able to isolate bacteria in aerosols but not viruses, highlighting the difficulties of studying viruses in dental bioaerosols from individuals without an acute infection or where infection/carrier status is unknown. This demonstrates the utility of a simulation model for studying viral dispersion.

Because oral bacteria are easier to detect and work with than the viruses present in the oral cavity, there are comparatively more robust data from human studies on the dispersion of bacteria in dental bioaerosols; for example, Zemouri *et al.* (2020c) demonstrated increased bacterial dispersion compared to background levels in settled aerosols and droplets on agar plates during dental procedures at 30 cm from the patient's mouth and on the instrument tray close to the procedure, but not at 1.5 m. This study also demonstrated increased airborne bacterial concentrations using a BioSampler at 0.5 m from dental procedures compared to baseline. Taken together, the present data therefore replicate the dispersion of microorganisms in dental bioaerosols seen in human studies.

Much of the previous literature has used Petri dishes with microbial growth media to capture dispersed bacteria in human and simulation studies (Barros et al. 2022; Boccia et al. 2023; Rayyan et al. 2022; Zemouri et al. 2020c). Relying on bacterial culture allows detection of viable bacteria, however many bacterial species cannot be cultured easily in the laboratory, and other microbes (e.g., fungi, archaea, protozoa) are not usually detected. Culture-independent methods which rely on molecular detection (e.g., PCR, sequencing) allow detection of unculturable microbes, however this method is unable to distinguish viable form non-viable organisms. Approaches which combine both types of methodology are therefore useful.

Studies with bacteriophage tracers have generally also used growth media seeded with host bacteria to capture a phage tracer (Beltran et al. 2023; Vernon et al. 2021; Vernon et al. 2022). Whilst this is an effective methodology, there are a number of potential limitations: 1) nucleic acid extraction and downstream analysis using PCR or sequencing is not possible; 2) it is more difficult to accurately quantify microbial numbers at heavily contaminated sites (>300 CFU or PFU) as further sample dilution is not possible; 3) where numerous microbes contained within a single droplet fall onto an agar plate, a single colony or plaque may be formed, leading to underestimation of microbial quantity. This is not the case with elution from filter papers, whereby microbes can be fully dispersed before enumeration. For these reasons, capture on filter papers and subsequent elution was used.

The results suggest that recovery of phage is around 30 – 40 times greater on filter papers in the same site compared to using host-seeded media. This is most likely because complete dispersion of phage is achieved prior to plaque assays when using filter papers, or because the porous filter paper matrix captures and retains the phage better than direct deposition on growth media. It is also possible that on plates, there is less opportunity for the phage to fully adsorb to its host (which is suspended in the agar matrix) compared to with filter papers, whereby eluted phage and host are incubated together in suspension before enumeration, potentially allowing more complete adsorption of phage to host. Sampling directly onto growth media may mimic aerosol deposition onto mucosal surfaces, as infection can proceed directly. However, sampling onto filter papers is more comparable to deposition onto inert surfaces, particularly porous surfaces like fabric and clothing. Given that mucosal surfaces (ocular, oropharyngeal) are usually protected from

larger droplets by PPE, simulation of surface deposition using filter papers may be a more valid approach.

Despite this, the total recovery efficiency of infectious phage from cotton-cellulose filter papers appears to be moderate at 66.4% for MS2, but much lower at 3.5% for phi6. This may perhaps be because phi6 virions are more easily disrupted due to the presence of a lipid membrane, compared to those of the non-enveloped MS2; this is consistent with the findings of other studies comparing recovery of the two phages from surfaces (Anderson et al. 2023). The presence of the filter membrane which is supplied in the spin column appears to have little effect on recovery and leaving this in place has the added benefit of retaining the filter paper sample and buffer in the upper part of the chamber prior to centrifugation. Zero recovery was seen in dry filter papers which had not been pre-wet, confirming that this is a necessary step, likely due to the sensitivity of phage virions to desiccation; this again reproduces previous data on recovery from wet and dry surfaces for both MS2 and phi6 (Anderson et al. 2023). Although no significant differences in recovery were observed between processing methods of pre-wet filter papers, shaking is preferable for practical reasons, as it is easier to shake multiple samples simultaneously in a rack than having to repeat a vortexing step for individual samples. A similar pattern was seen in the recovery of phage RNA from filter papers, at 53.8% for MS2 and 6.5% for phi6, which suggests that losses in phage recovery are likely predominantly due to the retention of phage particles on filters rather than loss of infectivity, however it may be that disruption of phage particles (and therefore loss of infectivity) and degradation of free RNA occur simultaneously. Recovery of these phages after spiking onto less porous polycarbonate or polytetrafluoroethylene (PTFE) filters with elution in larger volumes (5 mL) of TSB has been shown to approximate 100% (Gendron et al. 2010). Polycarbonate filters, however, are not flexible enough to allow manipulation into tubes for analysis, and the high hydrophobicity of PTFE makes them inappropriate for sampling during dental procedures, where they are likely to become quite wet at locations close to the procedure. Relative recovery of approximately 1% has been reported for MS2 and phi6 sampled directly from aerosols onto gelatin filters (Tseng and Li 2005), however comparable data for relative recovery from phage spiked onto gelatin filters are not available. Moreover, gelatin filters are very fragile and require higher elution volumes (~5 mL), thereby diluting the sample. The protocol used therefore balances an acceptable recovery rate with low elution volume and good practicality.

Without bioaerosol control measures, the highest levels of infectious MS2 and phi6 recovered in settled aerosols and droplets from surfaces were seen within the first 0.5 – 1 m from the dental procedure, which coincides with the highest aerosol particle concentration measured by OPC. The probability of aerosols and droplets settling onto surfaces is likely to be greatest closest to the source as larger droplets will settle out quickly under the influence of gravity, and so this finding is not surprising, but is reassuringly consistent with much of the existing literature. Other studies using a single phage tracer (Vernon et al. 2021; Vernon et al. 2022) as well as those using particle counting instruments (Yang et al. 2021a), fluorescent tracers (Allison et al. 2021a; Holliday et al. 2021), and clinical studies sampling bacteria (Ashokkumar et al. 2023; Suprono et al. 2021; Zemouri et al. 2020c) have all reported the highest aerosol concentrations closest to the source.

In experiments with rubber dam using MS2 and phi6 together, infectious phage was detected in suspended aerosols using BioSamplers, and this was greatest when no bioaerosol control measures were used, which is consistent with the dispersion of bacteria in dental bioaerosols in human studies (Bennett et al. 2000; Choudhary et al. 2022; Dutil et al. 2007; Zemouri et al. 2020c). Interestingly, detection in experiments with MS2 and phi6 was similar in BioSamplers at 1 m and 2 m for both phages when no rubber dam was used. This may be because small aerosols (< 5 μm) have a much longer residence time in the air and can therefore travel greater distances from the source than larger aerosols (< 100 μm) and droplets (Wang et al. 2021) which are more likely to settle on surfaces, as seen closest to the dental procedure. During experiments with ICX® using MS2 alone, low levels of infectious MS2 were recovered from BioSamplers at 0.5 and 1.0 m, but not during experiments with water. Given the reduction in detection on surfaces when ICX® was used, the reason for this is unclear, but it may that the unavoidably variable nature of a real dental procedure means that phage is dispersed from the mouth stochastically and is detected in unexpected places. This is particularly the case in suspended aerosols captured by BioSamplers which are more able to disperse larger distances.

Recovery of phage RNA was much greater than recovery of infective phage. The amount of phage determined by qPCR is usually higher than by plaque assay, as the former does not require phage particles to be intact or infectious for quantification. However, in previous reports, the differences between qPCR and plaque assay have been modest when performed on laboratory-cultured phage lysates (Anderson et al.

2011; Peng et al. 2018). The large discrepancy in the present data suggests that a proportion of the phage dispersed in dental bioaerosols loses its infectivity in the process. This is reflected in the poor correlation between plaque assay and RT-qPCR in aerosol samples from rubber dam experiments, since many samples had high levels of phage RNA but no infective phage. This phenomenon is seen in human studies which sample respiratory viruses from aerosols in hospital settings, whereby viral nucleic acids are readily detected, but infectious virus is less commonly recovered (Binder et al. 2020; Lednicky et al. 2020; Moore et al. 2021; Winslow et al. 2022). Similarly, data from a SARS-CoV-2 human challenge study suggests that viral load in nose and throat swabs based on viral RNA is greater by several orders of magnitude than from culture of infectious virus throughout the course of infection (Killingley et al. 2022). These data support the validity of the simulation model.

These data demonstrate that our model can detect differences in phage dispersion when bioaerosol control measures are used. This is particularly useful for bioaerosol control measures which affect viability of microorganisms, such as DUWL disinfectants, rather than those affecting overall aerosol dispersion. The active agents in ICX®, sodium percarbonate and silver nitrate, disrupt viral proteins and nucleic acids (McDonnell and Russell 1999), and measurement of the effect of DUWLs on bioaerosols dispersion has not been possible hitherto with chemical tracers such as fluorescein or methods which measure aerosol concentration alone. MS2 was compared to fluorescein as a tracer in the experiments with ICX® described in this chapter, and the phage tracer performed better in its ability to detect differences in dispersion when ICX® was used; these data have been published elsewhere and are not discussed further in the present thesis (Allison et al. 2022).

ICX® contains the active ingredients sodium percarbonate and silver nitrate, which produce viral inactivation by disrupting viral proteins and nucleic acids (McDonnell and Russell 1999). ICX® reduced MS2 viability in solution in laboratory experiments, consistent with its effect on bacteria in DUWL biofilms (Zemouri et al. 2020a). In clinical experiments, ICX® in instrument irrigation solutions reduced dispersion of infectious MS2 in aerosols and droplets by 96.5%. OPC data confirmed that at the manufacturer's concentration, total aerosol concentration is not decreased by a clinically relevant amount, and that at 10-times normal concentration, aerosol concentration was actually increased; the mechanism behind this is unclear, but it may that the presence of concentrated surfactants reduces particle size and

therefore increases particle number concentration. Indeed, a trend of an increasing proportion of particles in the 0.3 µm diameter channel was seen with increasing ICX® concentration in OPC experiments with ICX®. This finding is of clinical importance and means that disinfectants commonly used to control DUWL biofilms, which are designed to be used continuously in irrigant solutions, have the potential to reduce dispersion of pathogens from the mouth within aerosols and droplets, and this measure is likely already in place in many dental settings.

No other studies have yet tested the impact of DUWL disinfectants on viral dispersion in the clinic; however, two studies have assessed this in laboratory environments. Ionescu *et al* (2021) found reduced dispersion of aerosolised human coronavirus HCoV-229E RNA following the use of an air turbine handpiece when hydrogen peroxide was included in the irrigant, and Fidler *et al.* (2021) demonstrated reduced dispersion of Equine Arteritis Virus aerosolised by an ultrasonic scaler when 0.5% sodium hypochlorite or electrolysed water were used as irrigants. These laboratory findings support the present data, and similar observations have been reported with dispersed bacteria in human studies. For example, Ashokkumar *et al.* (2023) reported large differences in dispersed bacteria in settled aerosols and droplets collected on Petri dishes following ultrasonic scaling, and Rayyan *et al.* (Rayyan et al. 2022) found reduced dispersed bacteria on Petri dishes following endodontic procedures when 0.1% sodium hypochlorite was used in dental waterlines. One difficulty in these clinical studies is understanding how much of the dispersed bacteria are from the mouth, and how much are from the waterlines themselves, as it is well known that dental waterlines contain an abundant and complex microbiota (Hoogenkamp et al. 2021; Yoon and Lee 2019) which is influenced by the presence of DUWL disinfectants (Zemouri et al. 2020b). Indeed, data from sequencing studies suggest that only a small proportion of the dental bioaerosol microbiota appears to be attributable to the mouth (Meethil et al. 2021; Rafiee et al. 2022). This again highlights the usefulness of the viral tracer model, as it is possible to study the dispersion of oral microbes in isolation separate from the contribution of the waterline microbiota.

In experiments using rubber dam, total aerosol concentration measured by OPC was increased by 23.6% at 4 m, but not at 1 m when the dam was used. Given that increased dental aerosol concentrations are seen when instruments are used at the front of the mouth compared to on posterior teeth (Watanabe et al. 2023), it is

perhaps unsurprising that the presence of a rubber dam means that greater concentrations of aerosol particles escape from the mouth. The increased aerosol seen in the present experiments with rubber dam was therefore likely due to handpiece aerosol being deflected into the room by the dam rather than being directed back into the oral cavity. Importantly, this aerosol did not contain phage, as the dam separated the handpiece aerosol from virus in the mouth.

Interestingly, one clinical study reported increased dispersion of bacteria when rubber dam was used (Al-Amad et al. 2017), however this may be due to increased dispersion of DUWL-derived bacteria as a result of the dam deflecting the handpiece aerosol out into the environment. Other clinical bacterial (Tag El Din and Ghoname 1997) and simulation studies using phage (Vernon et al. 2021) and fluorescent tracers (Dahlke et al. 2012) have reported 20 – 100% reductions in dispersion when rubber dam was used. This is similar to the present data, where rubber dam reduced the detection of infectious MS2 by 86.3% and phi6 by 100.0%, and phage RNA detection was reduced by 92.9% for MS2 and 92.4% for phi6. Furthermore, adding phage tracer to the surfaces of the teeth before placement of the rubber dam, as in the present study, to simulate residual saliva may be more realistic than other similar studies which have not done so (Vernon et al. 2021).

The flow rate of the phage tracer (simulating saliva) used in experiments was 1.0 – 1.5 mL/min which is a conservative approximation of human stimulated whole saliva flow rates. Data pooled from three studies with 262 participants suggests a stimulated whole saliva flow rate in healthy individuals of 2.18 mL/min (SD: 0.74) (Nederfors et al. 2004; Ono et al. 2007; Yamamoto et al. 2009). Given that dental instruments are present in the mouth during a dental procedure, it is reasonable to assume a stimulated rather than unstimulated saliva flow rate. Similarly, the phage titre used in these experiments ($2 \times 10^7 – 8 \times 10^{12}$ PFU/mL) was reasonable compared to reported respiratory virus salivary viral loads of 1.1×10^6 virions/mL (range: $8 \times 10^0 – 6.1 \times 10^{12}$) for SARS-CoV-2 in asymptomatic individuals (Yang et al. 2021b) and 2.0×10^6 copies/mL (range: $1.8 \times 10^3 – 1.6 \times 10^9$) for influenza A in hospitalised patients (To et al. 2017b).

Plasmid DNA was used as a standard for absolute quantification as this is a robust and reliable method which allows standards to be easily stored in *E. coli* and isolated when needed. One disadvantage of this method, however, is that any variation introduced during the reverse transcription of phage samples is not accounted for

using the plasmid DNA standards. An alternative method would be to use *in vitro* transcribed RNA, which is then subsequently reverse transcribed and included in qPCR to derive a standard curve (Gregorova et al. 2022).

These data have several important limitations, not least that the *in vitro* simulation model does not represent the inherent variability of human anatomy, salivary flow rates, viral load, operator variability, and dental instrument design and irrigation flow rates seen in clinical practice. However, the use of realistic parameters (e.g., salivary viral load and flow rate), standardisation of the model across replicates and use of a single operator offers the ability to test parameters in a much more controlled manner than is possible in clinical studies. Additionally, the inherent antimicrobial properties of saliva (Vila et al. 2019) were not accounted for, and saliva may therefore further reduce dispersion of pathogens in bioaerosols *in vivo* compared to the present model. These findings may not necessarily be representative of the behaviour of other viruses, in particular human pathogens, in the oral environment and dental bioaerosols. Finally, the development and optimisation of the RT-qPCR assay meant that the RT-qPCR analysis did not take place until several months after the experiments, and eluted phage samples were stored at -80 °C before RNA extraction; this delay may have caused a reduction in the amount of RNA available for extraction, reducing the amount detected in RT-qPCR assays. This demonstrates the importance of timely analysis which is ensured in subsequent experiments. Considering these limitations and comparing to the existing literature, these data support the validity of the present dental bioaerosol simulation model and provide confidence in the ability to use it in subsequent experiments.

In the following chapters, this model will be used to further explore the spatial dispersion of viruses during a dental procedure, and for how long after a dental procedure they remain in the air. Whilst understanding the risk from dental bioaerosols is important, we also need to know how to manage this risk. The efficacy of methods to control dental bioaerosols, for example increasing ventilation or the use of other bioaerosol control measures like dental suction, will therefore also be explored.

Chapter 4. Dispersion and Persistence of Dental Bioaerosols

4.1 Introduction

One key question in our understanding of the risk posed by dental bioaerosols is where and how far microbes contained in aerosols are dispersed. This is vital as unless we understand where at-risk areas are around a dental procedure, it is impossible to implement effective infection control measures. Several authors have sought to understand this using different approaches, however one setting in which there is a real need to understand dispersion distance is the open plan dental clinic. These clinics with multiple dental units in open or partially enclosed treatment bays are often found in dental teaching hospitals where students or trainees treat patients under the supervision of one or more clinical supervisors. Being open-plan, supervisors can manage several students or trainees more easily than if treatment took place in enclosed surgeries or operatories. During the COVID-19 pandemic, uncertainty over the distance of dental bioaerosol dispersion in open-plan clinics caused much concern and disruption in dental teaching institutions in the UK and across the world (Dental Schools Council and Association of Dental Hospitals 2020). Early work to understand the dispersion distance of dental bioaerosols focused on the detection of viable bacteria in the environment following a dental procedure, with the author of one study reporting increased detection of viable bacteria above baseline at 11 m from active treatment areas (Grenier 1995). More recent applications of these methods suggest that the distance of dispersion of bacteria is not always consistent, and the room configuration is important, as even at 1.5 m from the procedure, viable bacteria are not always detected during dental treatment in an enclosed dental surgery (Zemouri et al. 2020c). Complementary methods using a fluorescent tracer during simulated dental procedures confirm the potential for dispersion of dental aerosols over large distances in open plan clinics (Allison et al. 2021a; Holliday et al. 2021), but with the direction of dispersion also being an important factor, with higher levels of dispersion seen opposite the operator and over the patient (Allison et al. 2021a; Allison et al. 2021c). Comparatively less research has looked at the dispersion distance of viruses in dental bioaerosols. One study conducted during the COVID-19 pandemic reported SARS-CoV-2 RNA in 36% of air

samples during dental treatment in clinics in Iran of various sizes. Samples which contained viral RNA, were on average 1.31 m from the procedure (Bazzazpour et al. 2022). Other studies looking at viral dispersion have generally used a viral tracer model (bacteriophage Phi6, PhiX174), being conducted only in enclosed surgeries at sampling distances up to 2 m, and have found that detection of the viral tracer decreases with increasing distance from the procedure (Beltran et al. 2023; Vernon et al. 2021). Experiments in the previous chapter also used an enclosed dental surgery, with sampling at up to 3 m, and found that viral recovery reduced with increasing distance (Allison et al. 2022). The dispersion distance of viruses during dental procedures has not yet been explored in an open plan clinic and nor has the dispersion of multiple viruses in the same experiment. This is important because the behaviour of viruses with different survival in aerosols or on surfaces cannot be easily compared where only a single viral tracer is used. Similarly, recovery of infectious virus has been relied upon in previous studies, unlike in studies of viral aerosols in real clinical settings which have generally relied on molecular detection, for example, using RT-qPCR (Akin et al. 2021; Bazzazpour et al. 2022; Meethil et al. 2021).

As well as the distance of dispersion, the persistence of infectious bioaerosol over time is also an important consideration. This dictates when it may be safe for individuals to enter a potentially infectious environment without personal protective equipment such as respiratory protective equipment. This was another key consideration in dentistry during the COVID-19 pandemic, and in the UK, national guidance was issued on how long it was necessary to allow potentially-infectious bioaerosol to disperse before allowing another patient into the dental surgery (SDCEP 2021a; 2021b). This was termed the post-operative fallow time and ranged between 10 – 60 min depending on the ventilation rate of the room and any aerosol control measures used (e.g., high volume suction). A number of authors have used particle counting methods to measure the persistence of aerosols after a dental procedure, either using simulated procedures (Allison et al. 2021b; Allison et al. 2021c; Ehtezazi et al. 2021; Shahdad et al. 2021) or measurements taken during patient treatment (Graziani et al. 2021). The time taken for aerosol concentration to reach baseline levels varies between studies, with elevations above baseline observed even at 90 min post procedure in an unventilated space (Shahdad et al. 2021). A simulation study by Ren *et al.* demonstrated the dependence of aerosol clearance rate on room ventilation, with removal of 95% of the aerosol taking longer

than 30 min in a room with 3 air changes per hour (ACH) but taking only 7 min in a room with 35 ACH (Ren et al. 2021). Fewer studies have looked at aerosol persistence using methods other than particle detection, for example, one study using a fluorescent tracer during simulated procedures in an open plan clinic ventilated at 6.5 ACH found little additional settled tracer in surface samples after 10 min following the end of the procedure (Holliday et al. 2021). A study using bacteriophage PhiX174 as a viral tracer and *Serratia marcescens* as a bacterial tracer, combined with numerical modelling in an enclosed surgery (5 ACH) showed 99% reduction in detection of released tracer at 90 min, but detectable amounts still present even at 120 min (Liu et al. 2023). Ventilation is clearly an important factor, both for the total amount of bioaerosol dispersed, and the persistence of the aerosol over time. Current UK guidance for ventilation in healthcare settings stipulates that new dental facilities should be ventilated to provide a clean airflow path (supply at high level, extract at low level) with an air exchange rate of 10 ACH, temperature range of 20 - 25°C, and maximum 70% relative humidity (RH) (NHS England and NHS Improvement 2021). Because dental clinics are found in many different settings ranging from purpose-built hospitals to converted residential properties, the ventilation configuration in these clinics are highly variable. No good cross-sectional data exist however it is likely that many dental practices fall short of the recommended 10 ACH, with some surgeries lacking any natural or mechanical ventilation.

4.2 Aims and objectives

The aim of the experiments described in this chapter is to understand the spatial dispersion and temporal persistence of viral bioaerosols generated during dental procedures. The specific objectives are to measure the:

- Spatial dispersion of dental bioaerosols and the infective potential of these using a bacteriophage tracer model during simulated dental procedures in an open-plan dental clinical setting.
- Persistence over time of dental bioaerosols at high and low ventilation rates using a room-scale aerobiology chamber.

4.3 Spatial dispersion of dental bioaerosols – specific methods

To explore the spatial dispersion of viral bioaerosols, experiments were conducted in an 825 m^3 open plan clinical teaching laboratory to allow sampling over an 8 m diameter area. The room was ventilated by supply-extract central mechanical ventilation providing 6.46 ACH via ceiling vents. The sampling rig was set at 84 cm above the floor, with its central hub positioned 22 cm superior to the upper right central incisor of the mannequin. Eight, 4 m sampling arms were spaced at 45° intervals, with filter paper samples placed on platforms along each arm at 0.5 m intervals. One sample was placed on the centre of the rig. BioSamplers were spaced along the 90° arm at 0.5 m, 1 m, 2 m, and 4 m. Two optical particle counters (OPCs) were placed on the 180° arm at 1 m and 4 m. This equates to 64 surface samples per replicate (256 total across 4 replicates), and 4 air samples per replicate (16 total). Sampling locations are shown in figure 4.1. Four replicates of the experiment were conducted.

A 10-min crown preparation was conducted on the upper right central incisor tooth with an air turbine handpiece (Synea TA-98, W&H (UK) Ltd.; St Albans, UK) with diamond burs (Rugby Ball 379, Shoulder 856SG & 856G; Drendel and Zweiling, Germany), and a coolant flow rate of 31.8 mL/min (SD: 0.5) with chip air activated. OPC sampling began 5 min before the procedure started, and BioSamplers were started 2 min before the procedure. All sampling continued until 5 min after the end of the 10-min procedure (total sample time: 20 min OPC; 17 min BioSampler). A suspension of MS2 (mean titre 1.28 x 10^{10} PFU/mL, SD: 4.50 x 10^9) and phi6 (mean titre 3.13 x 10^{10} PFU/mL, SD: 8.49 x 10^9) was infused into the mouth of the mannequin at 1.5 mL/min.

For surface samples, where at any given distance from the procedure, multiple samples were present across different sampling arms (e.g., eight 1 m samples per replicate across 0 – 315° arms), the mean recovery of all samples within a replicate was calculated for each distance (0 – 4 m) and this was plotted and averaged for all replicates (n = 4) during subsequent analyses. Recovery was plotted by distance, and nonlinear regression was used to describe the relationship before calculating the intercept of the curve with the x axis (limit of detection [LoD] was used for RT-qPCR analyses).

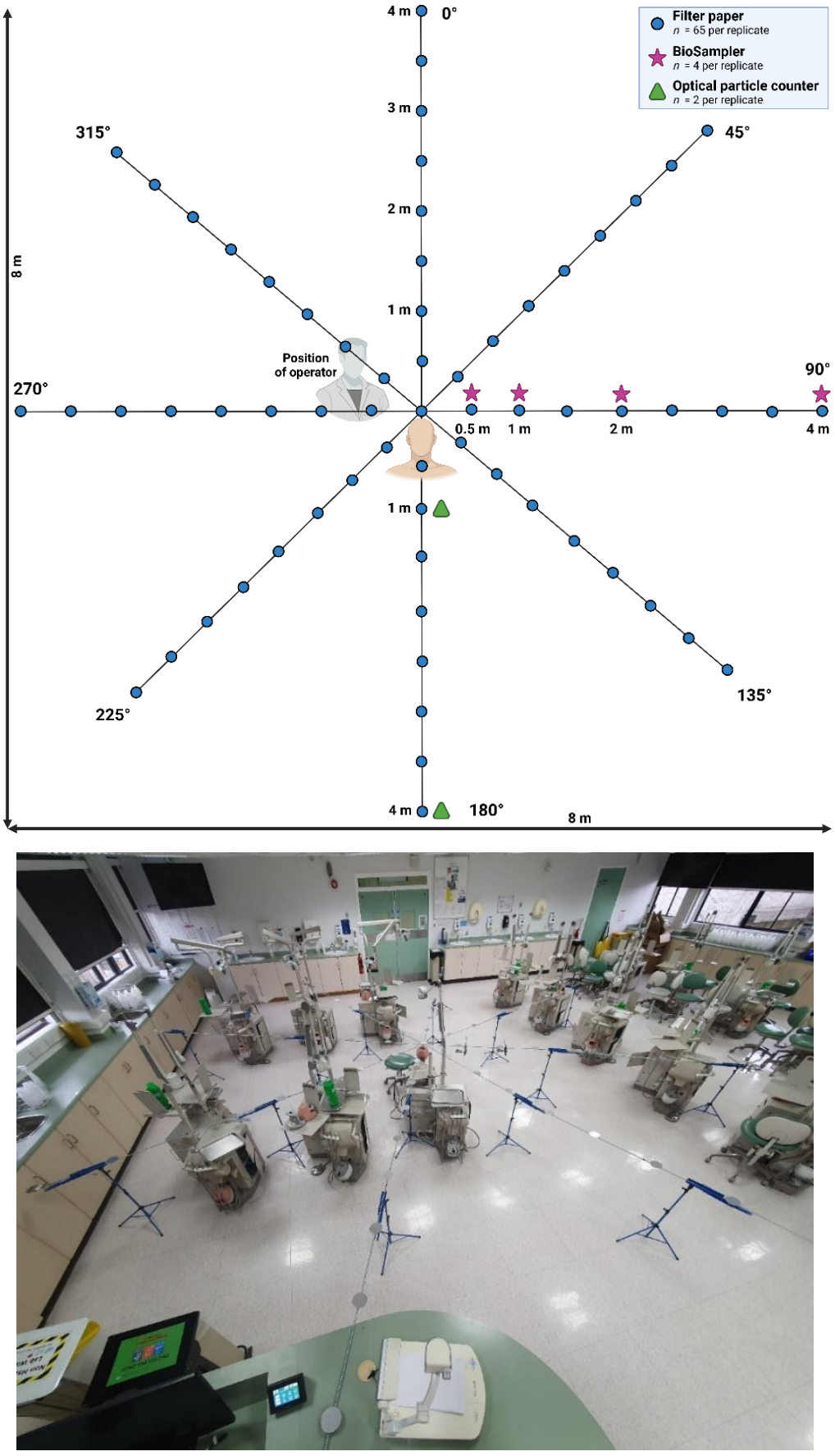

Figure 4.1. Overview of bioaerosol spatial dispersion experiments.

Upper panel: schematic diagram of sampling locations; lower panel: photograph of open plan setting and sampling rig around the mannequin.

4.4 Aerosol particle concentration at 1 m and 4 m

Experiments in the open plan dental clinic aimed to explore the distance of dispersion of bioaerosols from a dental procedure. Mean temperature during experiments was 22.18 °C (SD: 0.90) and mean humidity was 31.36 %RH (SD: 3.29). Mean background particle number concentration in the 5 min before the procedure (baseline) was 4.46 (SD: 1.17) particles/cm^3 at 1 m and 3.87 (SD: 0.21) particles/cm^3 at 4 m. During the 10-min dental procedure, at 1 m mean aerosol concentration increased to 37.8 (SD: 26.3) particles/cm^3, showing sharp spikes in aerosol concentration of 10 – 100-fold above baseline (figure 4.2). At 4 m from the procedure, a modest increase in aerosol concentration was seen, with mean 7.08 (SD: 0.97) particles/cm^3, but without the distinct spikes in concentration seen at 1 m. After the end of the end of the procedure particle concentration reduced to the baseline within 5 min at both locations.

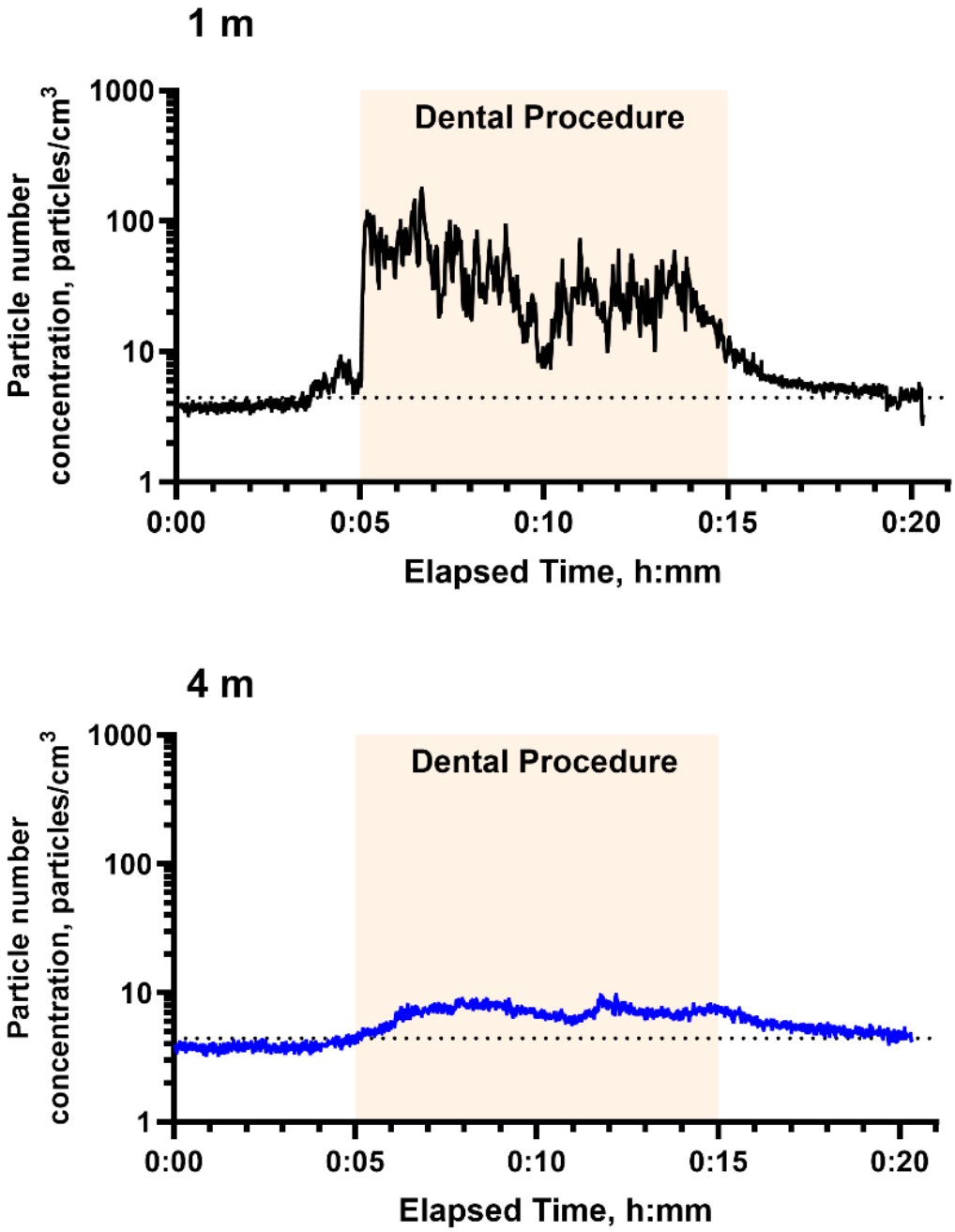

Figure 4.2. Aerosol concentration measured at 1m and 4m.

Particle number concentration was summed across all optical particle counter size channels (0.3, 0.5, 1.0, 2.5, 5.0, 10.0 µm). Average of 4 replicates shown with sampling rate of 1 Hz. The orange shaded area denotes the period of the dental procedure (10 min) and the dotted line denotes the mean aerosol concentration in the 5 min preceding the procedure at that location (baseline; *n* = 4). Individual replicate data are shown in appendix figure A.2.

4.5 Dispersion of infectious phage

Positive control samples taken from the inoculum infused into the mouth of the mannequin confirmed MS2 mean titre of 1.28×10^{10} PFU/mL (SD: 4.50×10^{9}) and phi6 mean titre of 3.13×10^{10} PFU/mL (SD: 8.49×10^{9}). No growth of phage was

seen in plaque assays for any of the assay negative controls (host and media controls), or in any of the experiment negative controls for surface samples (filters). One out of four experimental negative control BioSamplers had 3.9 PFU/L MS2 (just above the LoD of the assay of 0.98 PFU/L, and well below 52.1 PFU/L mean recovery in non-control samples).

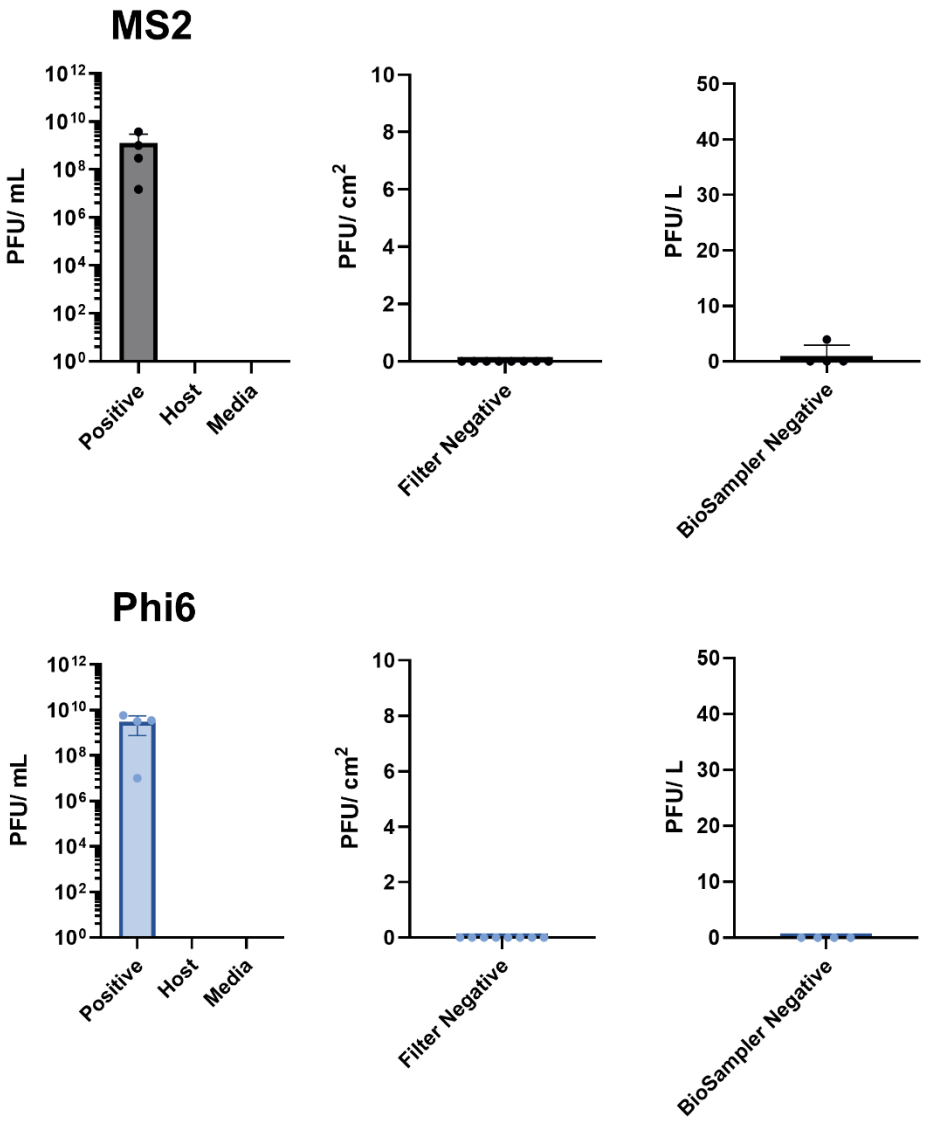

Figure 4.3. Infectious phage in control samples.

Infectious MS2 and phi6 measured by plaque assay in positive and negative control samples (positive, host, media, BioSampler *n* = 4; filter *n* = 8). Individual data points, mean, and standard deviation are shown. PFU: Plaque-Forming Units.

During the dental procedure, recovery of both phages was greatest in surface samples at the centre of the sampling rig and at 0.5 m locations, with recovery reducing sharply beyond this distance for phi6, and beyond 1 m for MS2. Overall recovery of MS2 in surface samples was 419-fold higher than the recovery of phi6

despite a similar starting inoculum. Recovery in air samples was highest at 0.5 m and 1 m locations, however there was a more gradual reduction in recovery at distances beyond this compared to in surface samples, and the recovery of MS2 and phi6 in air samples was similar (table 4.1).

Surface Samples				
Distance	**MS2**		**Phi6**	
	Mean (PFU/cm²)	*SD*	***Mean (PFU/cm²)***	*SD*
0 m	**922.4**	1,524.7	**5.3**	10.1
0.5 m	**2,147.2**	3,855.4	**1.9**	2.3
1 m	**117.6**	214.3	**0.4**	0.8
1.5 m	**0.3**	0.5	**0**	0
2 m	**0.2**	0.3	**0**	0
2.5 m	**0.1**	0.2	**0**	0
3 m	**0.4**	0.5	**0**	0
3.5 m	**0.4**	0.5	**0**	0
4 m	**0.2**	0.3	**0**	0
Air samples				
	MS2		**Phi6**	
	Mean (PFU/L)	*SD*	***Mean (PFU/L)***	*SD*
0.5 m	**120.6**	134.1	**103.2**	79.4
1 m	**101.2**	116.9	**112.5**	148.5
2 m	**55.6**	66.2	**64.0**	72.2
4 m	**20.3**	36.3	**16.4**	29.1

Table 4.1. Recovery of infectious phage in surface and air samples by distance from the procedure.

Each value shows mean recovery across 4 experimental replicates at that distance. PFU: plaque-forming units. SD: standard deviation.

Dispersion of phage was seen in a directional pattern and was not evenly distributed across all sampling arms surrounding the procedure. The greatest dispersion was seen was seen on 135°, 180°, and 270° sampling arms, corresponding to locations opposite the operator and over the mannequin, which a real clinical scenario would be over the patient's body and dental chair. Mean recovery shown by sampling arm is presented in table 4.2 and heatmaps showing spatial distribution across the entire sampling rig are shown in figure 4.4.

Angle	MS2		Phi6	
	Mean (PFU/cm²)	*SD*	***Mean (PFU/cm²)***	*SD*
0°	**2.4**	4.4	**0.0**	0.0
45°	**9.2**	25.5	**0.0**	0.0
90°	**6.2**	17.4	**0.0**	0.0
135°	**388.7**	819.7	**1.4**	3.0
180°	**282.0**	749.4	**1.3**	2.5
225°	**9.0**	24.1	**0.0**	0.0
270°	**1,570.0**	4,439.0	**0.0**	0.0
315°	**0.1**	0.2	**0.0**	0.0
(Centre)	*(922.4)*	*(1524.7)*	*(5.3)*	*(10.1)*

Table 4.2. Recovery of infectious phage in surface samples by sampling location.

Mean recovery at all distances excluding the centre of the rig (0.5 – 4 m) for each sampling arm (0° - 315°) across 4 experimental replicates. Recovery from the centre of the rig shown separately in brackets for comparison. PFU: plaque-forming units. SD: standard deviation.

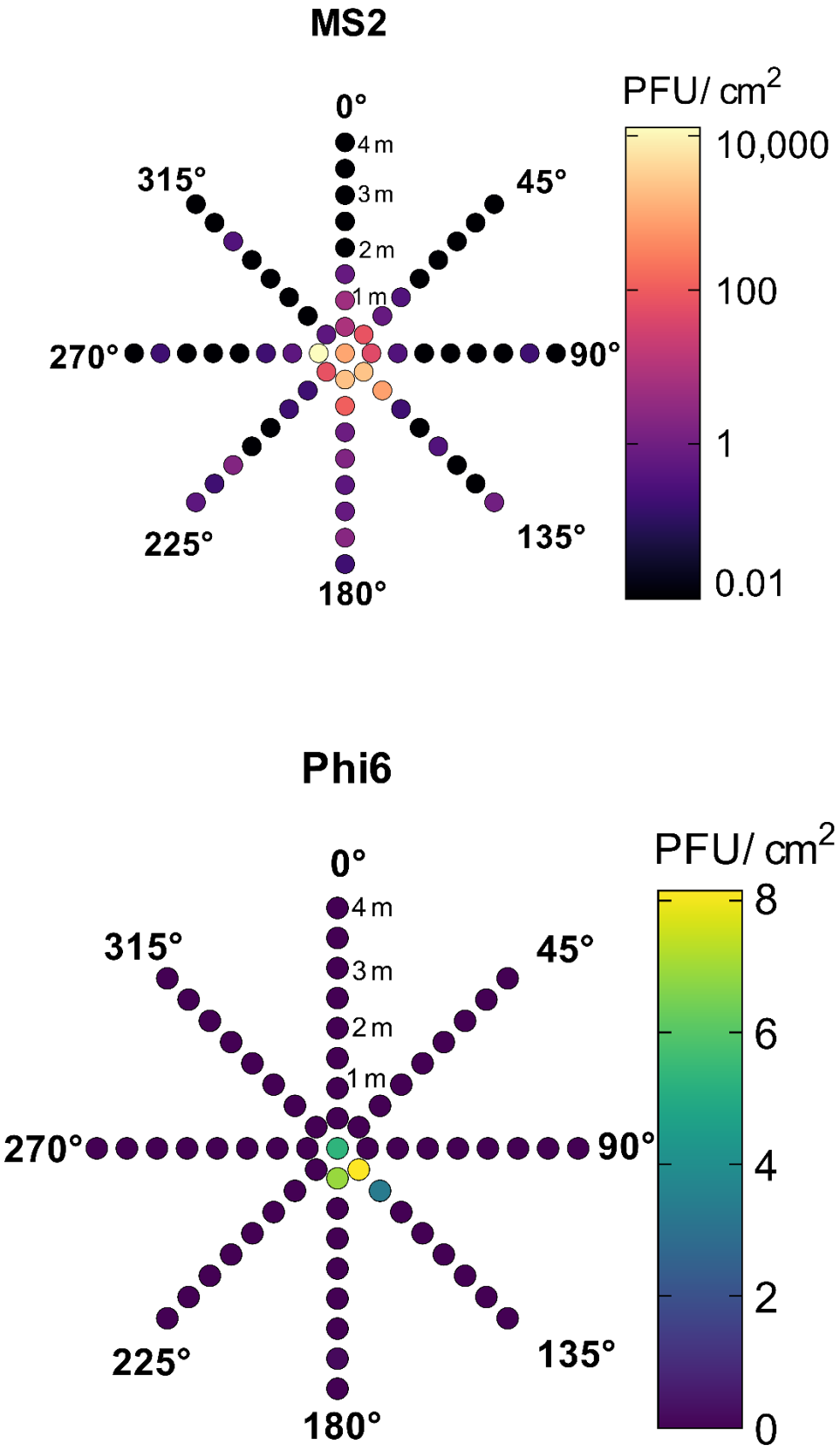

Figure 4.4 Dispersion of infectious phage in surface samples.

Heatmaps showing raw values for phi6 and on a logarithmic scale for MS2 using the function $Log_{10}(raw\ value\ +\ 0.01)$ to correct for zero values. Sample location is equivalent to the schematic in figure 4.1. Each location is the mean of four replicates at that location. PFU: Plaque-Forming Units.

Nonlinear regression curves and equations describing the relationship between recovery of phage and distance from the procedure can be seen in figure 4.5. Regression curves for each individual sampling arm are shown in appendix figure A.3 and A.4. Intercepts of the regression curves with the *x* axis (indicating the distance where recovery of infectious phage is expected to be zero) were calculated and are show in table 4.3.

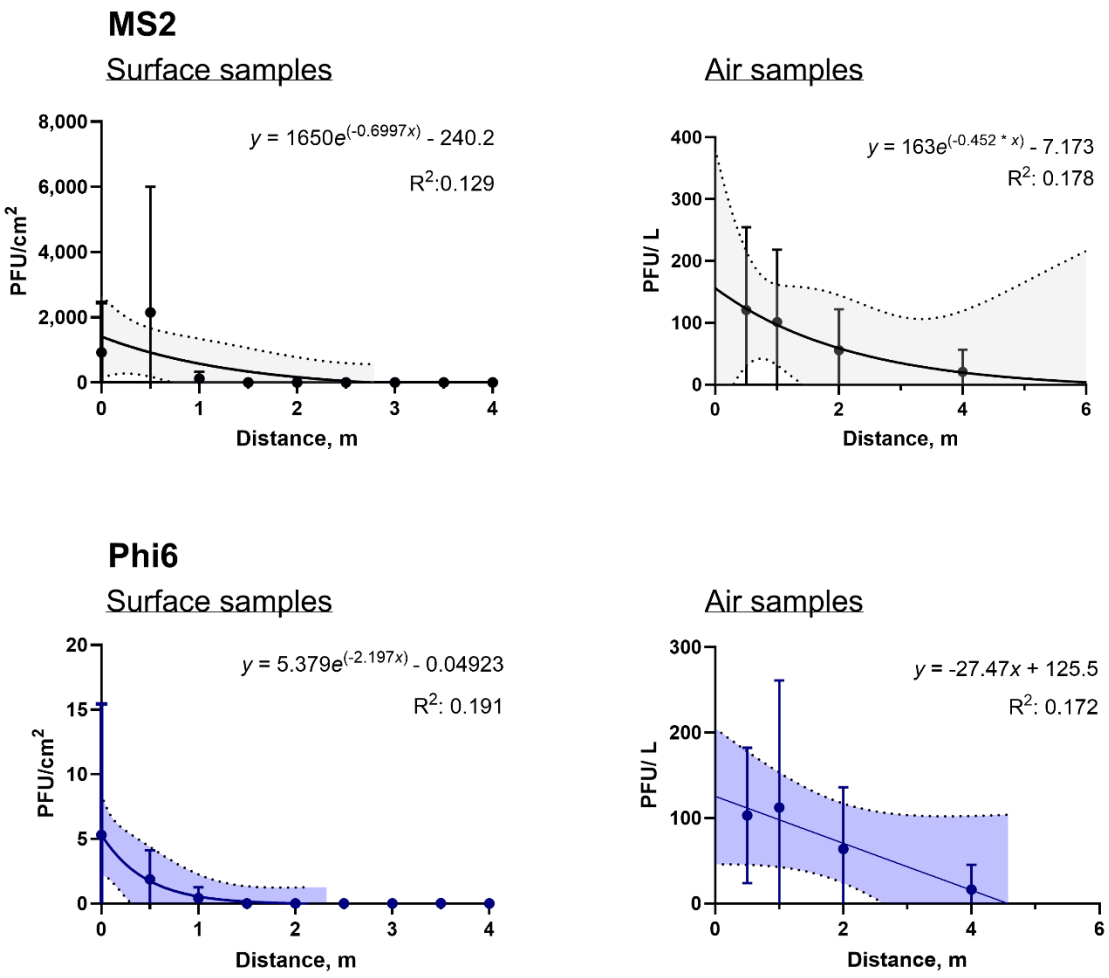

Figure 4.5. Dispersion of infectious phage over distance.

Recovery of MS2 and phi6 in surface samples from filter papers or air samples using BioSamplers from four experimental replicates. Each data point shows the mean amount of phage recovered in plaque assays at that distance averaged across four replicates of the experiment. Error bars show standard deviation. Non-linear regression curves (one-phase decay model, except for Phi6 air samples which uses straight line), curve equations, and R^2 are shown. Surrounding shaded areas represent 95% confidence intervals of the curve. PFU: Plaque-Forming Units.

	Surface samples	Air samples
MS2	2.75 m	6.91 m
Phi6	2.14 m	4.57 m

Table 4.3. Distance of infectious phage dispersion.

Distances from the dental procedure that recovery of infectious phage would be expected to reach zero. Determined by calculating intercept of the regression curve describing recovery over distance, with the x axis. Regression curves and equations are shown in figure 4.5.

4.6 Dispersion of phage RNA

Positive control samples from the phage inoculum showed this to contain 1.55 x 10^{12} (SD: 8.63 x 10^{11}) copies/mL MS2, and 6.92 x 10^{9} (SD: 6.24 x 10^{9}) copies/mL phi6, as measured using RT-qPCR. Plasmid DNA standards also amplified as expected, showing 1.50 x 10^{12} (SD: 2.60 x 10^{12}) copies/mL for MS2 plasmid standards and 1.18 x 10^{10} (SD: 1.81 x 10^{9}) copies/mL for phi6 standards (figure 4.6).

One of three MS2 assay negative controls for the RNA extraction step amplified (1.38 x 10^{5} copies/mL; limit of detection [LoD] 1.69 x 10^{4} copies/mL), however, all other assay negative controls (RNA extraction, reverse transcription, and qPCR steps), were negative.

Two of eight MS2 negative control filter papers amplified (mean 7.06 x 10^{3} copies/cm^{2} in these samples; LoD: 1.19 x 10^{3} copies/cm^{2}), and three of four negative BioSamplers (mean 5.79 x 10^{5} copies/L; LoD: 1.66 x 10^{3} copies/L). Two of eight phi6 negative filters amplified (2.58 x 10^{3} copies/cm^{2}; LoD: 1.03 x 10^{2} copies/cm^{2}), and one of four negative BioSamplers (2.50 x 10^{3} copies/L; LoD: 1.42 x 10^{2} copies/L). All other experiment negative controls were negative.

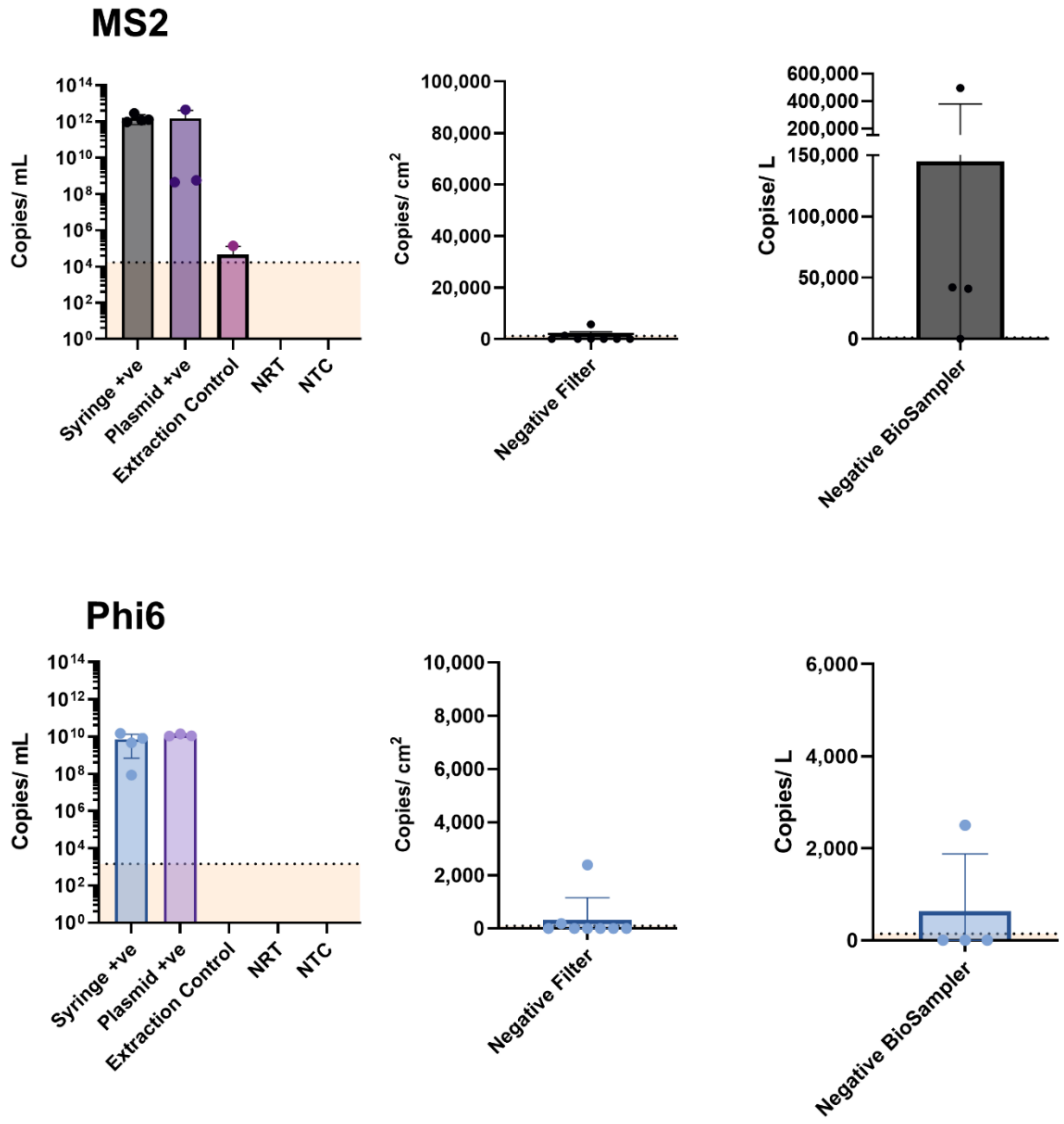

Figure 4.6. Phage RNA in control samples.

Individual values, mean, and standard deviation shown. NRT: no-reverse–transcriptase control; NTC: no-template control. Dashed line defining orange shaded area denotes limit of detection of the RT-qPCR assay. *n* = 8 for filters; *n* = 4 for BioSamplers & syringe +ve (inoculum from experiments); *n* = 3 for others.

As with recovery of infectious phage, RNA recovery for both phages was greatest in surface samples at the centre of the sampling rig and at 0.5 m locations, with recovery reducing sharply beyond this distance for phi6, and beyond 1 m for MS2. Overall recovery of MS2 RNA in surface samples was 181-fold higher than recovery of phi6 RNA. Recovery in air samples was highest at 0.5 m and 1 m locations, however there was a more gradual reduction in recovery at distances beyond this compared to surface samples. Overall recovery of MS2 RNA in air samples was 43-fold greater than for phi6 RNA (table 4.4).

Surface Samples				
	MS2		**Phi6**	
	Mean (Copies/cm²)	*SD*	***Mean (Copies/cm²)***	*SD*
0 m	**3.5×10^6**	4.3×10^6	**1.9×10^4**	2.7×10^4
0.5 m	**9.7×10^6**	1.6×10^7	**5.4×10^4**	7.2×10^4
1 m	**2.3×10^5**	4.3×10^5	**9.8×10^2**	1.6×10^3
1.5 m	**7.4×10^2**	5.5×10^2	**0.0×10^0**	0.0×10^0
2 m	**8.8×10^2**	7.6×10^2	**8.7×10^0**	1.7×10^1
2.5 m	**4.4×10^3**	4.9×10^3	**2.3×10^1**	4.7×10^1
3 m	**1.4×10^3**	2.5×10^3	**7.4×10^0**	1.5×10^1
3.5 m	**7.3×10^3**	1.2×10^4	**1.0×10^1**	2.1×10^1
4 m	**3.3×10^3**	6.1×10^3	**9.4×10^0**	1.9×10^1
Air samples				
	MS2		**Phi6**	
	Mean (Copies/L)	*SD*	***Mean (Copies/L)***	*SD*
0.5 m	**4.5×10^4**	3.1×10^4	**1.1×10^3**	9.1×10^2
1 m	**2.9×10^4**	3.3×10^4	**6.9×10^2**	9.5×10^2
2 m	**3.0×10^4**	3.0×10^4	**5.1×10^2**	6.8×10^2
4 m	**9.4×10^3**	1.0×10^4	**3.1×10^2**	3.6×10^2

Table 4.4. Recovery of phage RNA in surface and air samples by distance from the procedure.

Each value is an average across 4 experimental replicates of all samples at that distance. SD: standard deviation.

Dispersion of phage RNA was seen in a directional pattern and was not evenly distributed across all sampling arms surrounding the procedure. As with infectious phage, the greatest dispersion was seen was seen on 135°, 180°, and 270° sampling arms, corresponding to locations opposite the operator and over the mannequin. Heatmaps showing spatial distribution across the entire sampling rig are shown in Figure 4.7.

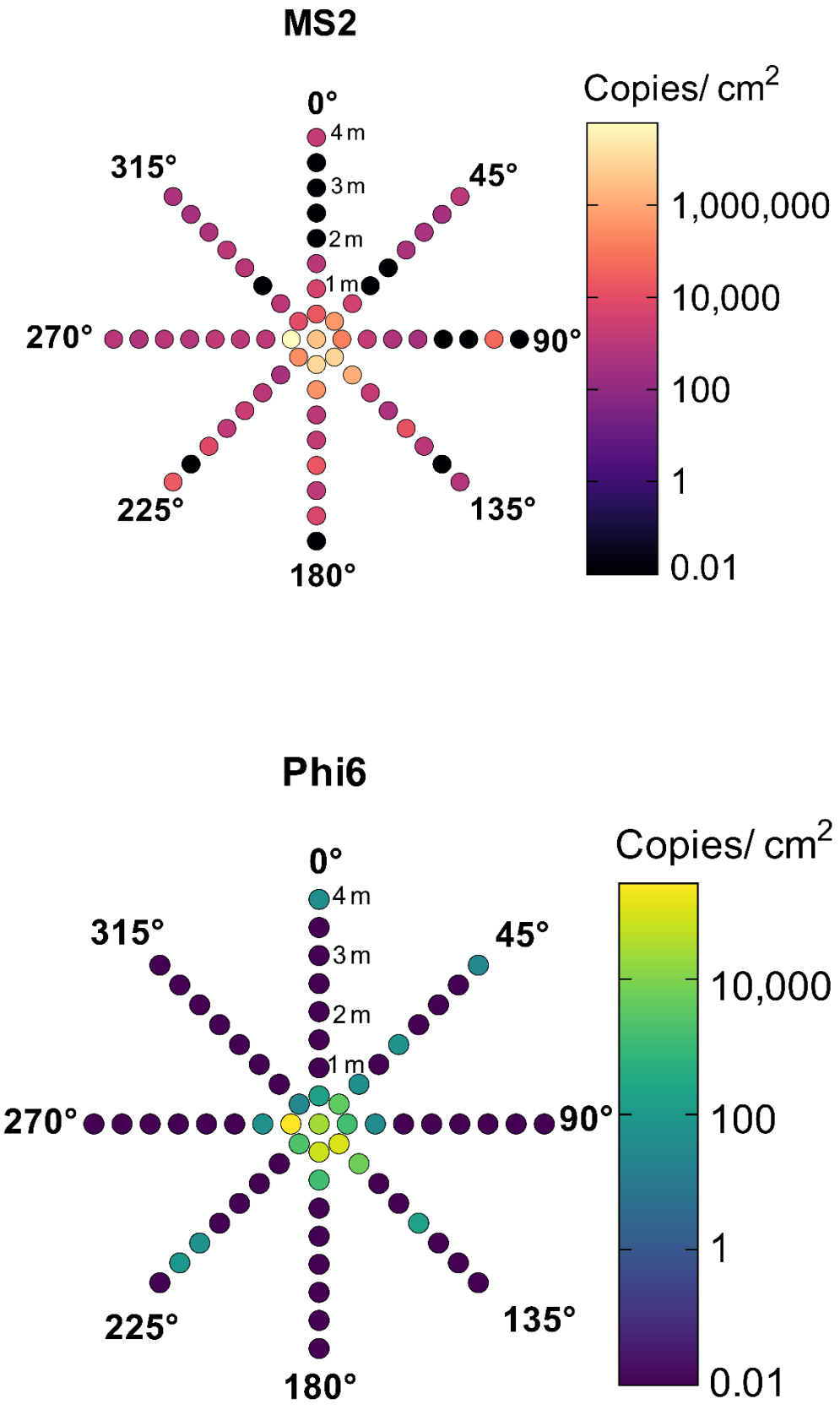

Figure 4.7. Dispersion of phage RNA in surface samples.

Heatmaps showing recovery of phage RNA on a logarithmic scale using the function $Log_{10}(raw\ value\ +\ 0.01)$ to correct for zero values. Sample location is equivalent to the schematic in figure 4.1. Each location is the mean of four replicates at that location. PFU: Plaque-Forming Units.

Nonlinear regression curves and equations describing the relationship between recovery of phage RNA and distance from the procedure can be seen in figure 4.8. Intercepts of the regression curves with the LoD of the RT-qPCR assay (indicating the distance where recovery is expected to fall below the LoD) were calculated and are show in table 4.5.

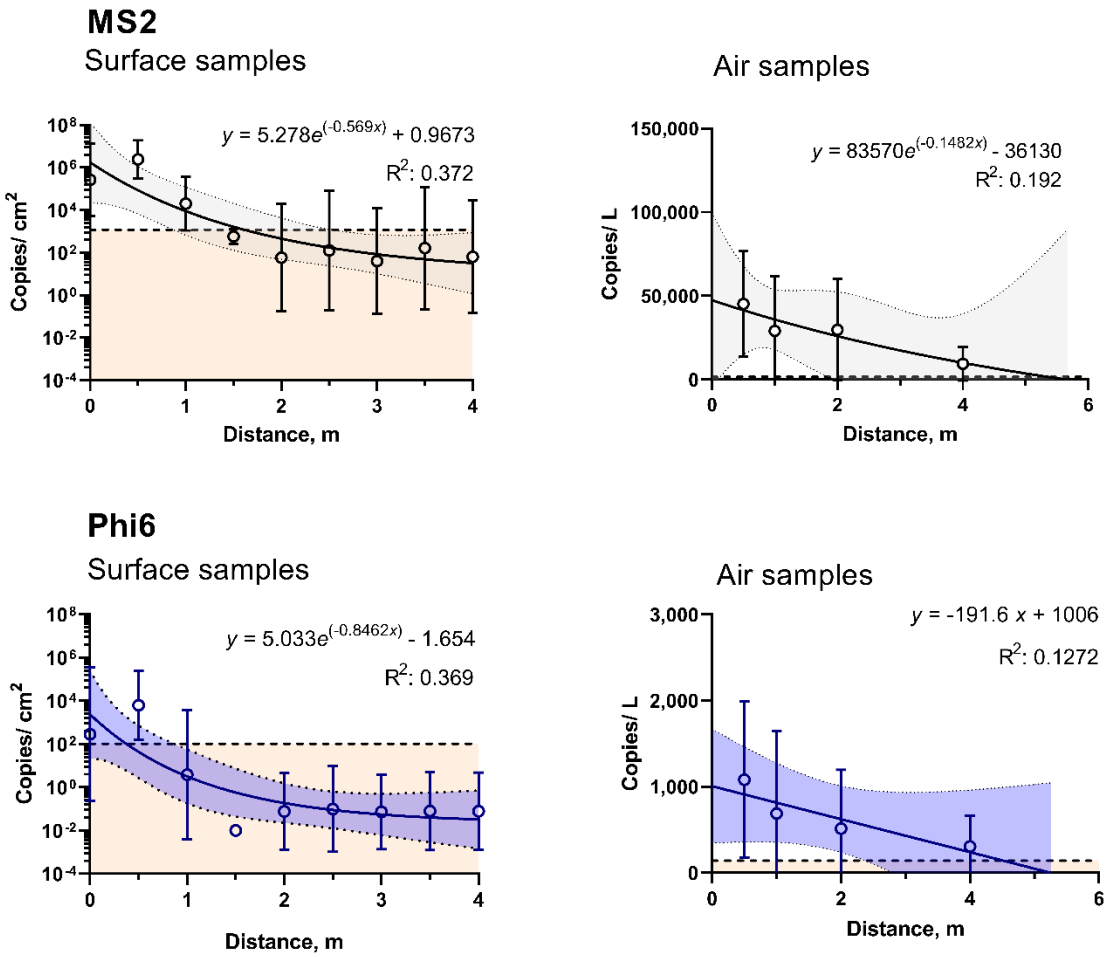

Figure 4.8. Dispersion of phage RNA over distance.

Recovery of phage RNA in surface samples from filter papers or air samples using BioSamplers from four experiment replicates. Each data point shows the mean amount of phage RNA in samples at that distance averaged across four replicates of the experiment. Geometric mean and SD shown for surface samples, arithmetic mean and SD shown for air samples. Non-linear regression curves, R^2, and equations (one-phase decay model, except straight line for phi6 air samples) are shown, with surrounding shaded areas representing 95% confidence intervals of the curve. Dashed line defining orange shaded area denotes RT-qPCR assay limit of detection.

	Surface samples	Air samples
MS2	1.61 m	5.36 m
Phi6	0.37 m	4.51 m

Table 4.5. Distance of phage RNA dispersion.

Distances from the dental procedure that recovery of phage RNA would be expected to fall below the RT-qPCR assay limit of detection. Determined by calculating intercept of regression curve describing recovery over distance, with $y = \text{limit of detection}$. Regression curves and equations are shown in figure 4.8.

4.7 Relationship of infectious phage to phage RNA

For all samples from dispersion experiments, linear regression was used to describe the relationship between infectious phage and phage RNA recovered from the same samples. Examination of curves revealed outlying values (n = 3) which were skewing regression curves, these were (plaques, copies): MS2 surface samples (5.02 x 10^4, 2.33 x 10^8), MS2 air samples (0, 4.96 x10^5), and phi6 surface samples (0, 1.01 x 10^6). No outlying values were identified for phi6 air samples, and regression curves and equations with all values included are shown in appendix figure A.5. Outlying values were excluded and resulting regression curves and equations are shown in Figure 4.9. This demonstrated that recovery of phage RNA was consistently greater than that of infectious phage, with linear regression coefficients ranging from 5.9 – 3,166 depending on the phage and sample type (surface or air sample). Goodness of fit ranged from R^2: 0.04 – 0.81 depending on the phage and sample type. There were several samples in which no infectious phage was recovered but where phage RNA was recovered, however, there were very few samples in which infectious phage, but no phage RNA was recovered.

Bland-Altman plots in figure 4.10 show the ratio (plaques/ copies) between the two measures plotted against their average. Biases (mean ratio) from Bland-Altman analyses were consistently above zero (shown for each sample type in figure 4.10), confirming that recovered phage RNA was consistently higher than infectious phage in the same samples.

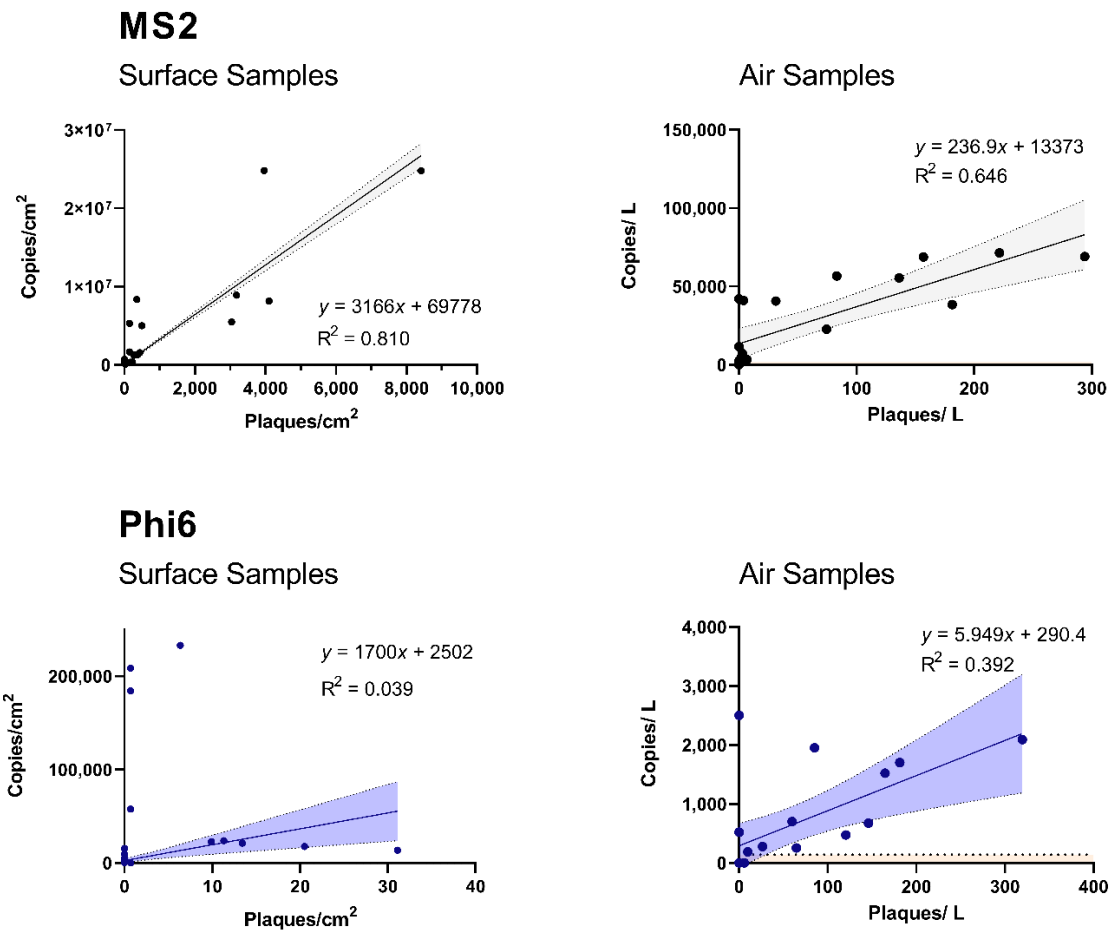

Figure 4.9. Relationship between infectious phage and phage RNA.

Linear regression with outliers removed, of infectious MS2 and phi6 phage (plaques) versus phage RNA (copies) recovered from surface samples and air samples. Linear regression curves and 95% confidence intervals (shaded areas) are shown, along with curve equations and associated R^2. The dashed line enclosing the orange shaded area denotes the limit of detection of the RT-qPCR assay.

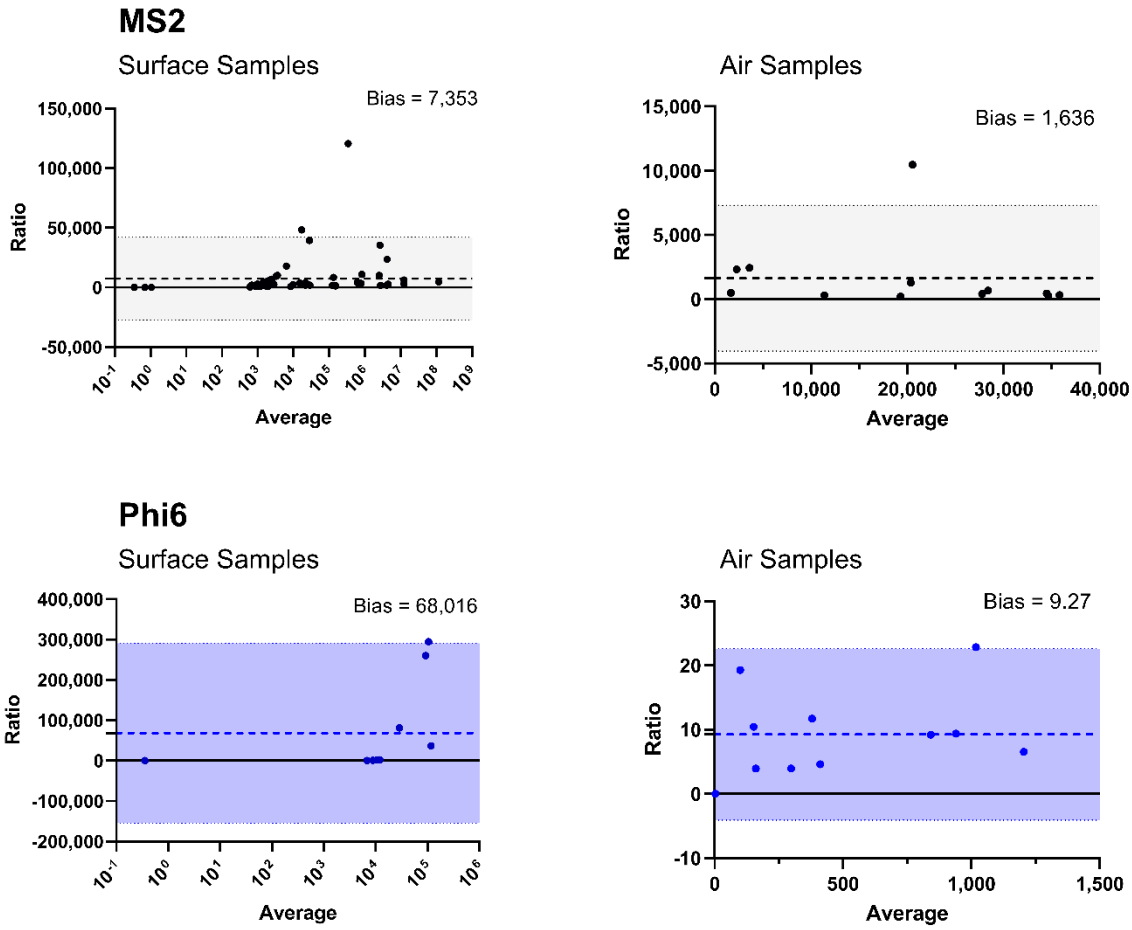

Figure 4.10. Bland-Altman plots of RT-qPCR versus plaque assay.

Plots show the ratio (copies/plaques) of infectious phage plaques (measured by plaque assay) to phage copies (measured by RT-qPCR) for MS2 and phi6 in surface and air samples plotted against the average of the two measures. Solid black horizontal line represents a ratio of 0 (no difference). The thick, central dashed line represents the average ratio (bias) and the shaded areas defined by fine dotted lines indicate 95% limits of agreement (bias +/- 1.96 × standard deviation).

4.8 Temporal persistence of dental bioaerosols – specific methods

Experiments exploring the persistence of infectious phage and phage RNA in the air after dental procedures were conducted in a 32.25 m^3 aerobiology chamber at Leeds University School of Civil Engineering (Figure 4.11) at two ventilation rates: 1.5 and 11.7 ACH. These ventilation rates were chosen as they were the maximum and minimum rates the facility could operate at, allowing a maximal difference in conditions. These parameters also translate well to a typical dental treatment room without mechanical ventilation (1.5 ACH), and just above the 10 ACH recommended for new dental facilities (NHS England and NHS Improvement 2021). 10-min crown preparations were conducted on the upper right central incisor tooth with an air

turbine handpiece (EXPERTtorque LUX E6680L, Kavo; Germany) driven by a portable dental unit (Celesta II, Belmont; Japan) connected to a compressed air cylinder providing 4.5 bar supply pressure controlled via a regulator (series 8500, BOC; Woking, UK). The handpiece coolant flowrate was 33.8 (SD:1.4) mL/min and chip air was activated. MS2 and phi6 inoculum was infused into the mannequin's mouth at 1.5 mL/min, and 1 mL of inoculum was used to cover the labial surfaces of the teeth immediately before the procedure.

A bank of eight BioSamplers was positioned in an arc around the mannequin (Figure 4.11), with each inlet located 40 cm from the mannequin's mouth. Each BioSampler was connected to a custom-made vacuum manifold which allowed each sampler to be switched on or off in sequence for the desired length of time. The vacuum pump was positioned outside of the chamber and was switched on remotely using a remote-controlled power supply (RA-103, AEI Security; UK). Samplers were operated at 12.5 L/min for 2 min each and the operator remained seated in the chamber until the end of sampling. For each replicate, one negative control sample was taken prior to starting the experiment. One sample was collected in the final 2 min of the dental procedure (minute 8 – 10 of the procedure) and was plotted as time zero in subsequent analyses, corresponding to the bioaerosol concentration at the end of the procedure. Six two-min air samples were then taken following the end of the procedure. For the first replicate, which was at 1.5 ACH, samples were conducted consecutively, with no gap between each one (i.e., 0–2, 2–4, 4–6, 6–8, 8–10, 10–11, 11–12 min). Because phage was recovered in these samples at up to 10–12 min, the decision was taken to leave a 2 min gap between each sample to extend the period of sampling in subsequent replicates (n = 3 for each ventilation rate). Samples were therefore taken after the procedure in these replicates at 2–4, 6–8, 10–12, 14–16, 18–20, 22–24 min. The OPC was positioned immediately next to the samplers and began sampling 5 min before the start of the procedure, and at ended after the last BioSampler sample was taken.

Buffer was removed from the samplers and transported in 50 mL centrifuge tubes to the Leeds School of Civil Engineering Microbiology laboratory, which is housed in the same facility as the bioaerosol chamber. Plaque assays were conducted immediately and 200 µL aliquots were stored at -80°C for subsequent RT-qPCR analyses, which were completed within 4 weeks of experiments at the Newcastle Translational Oral Biosciences laboratory.

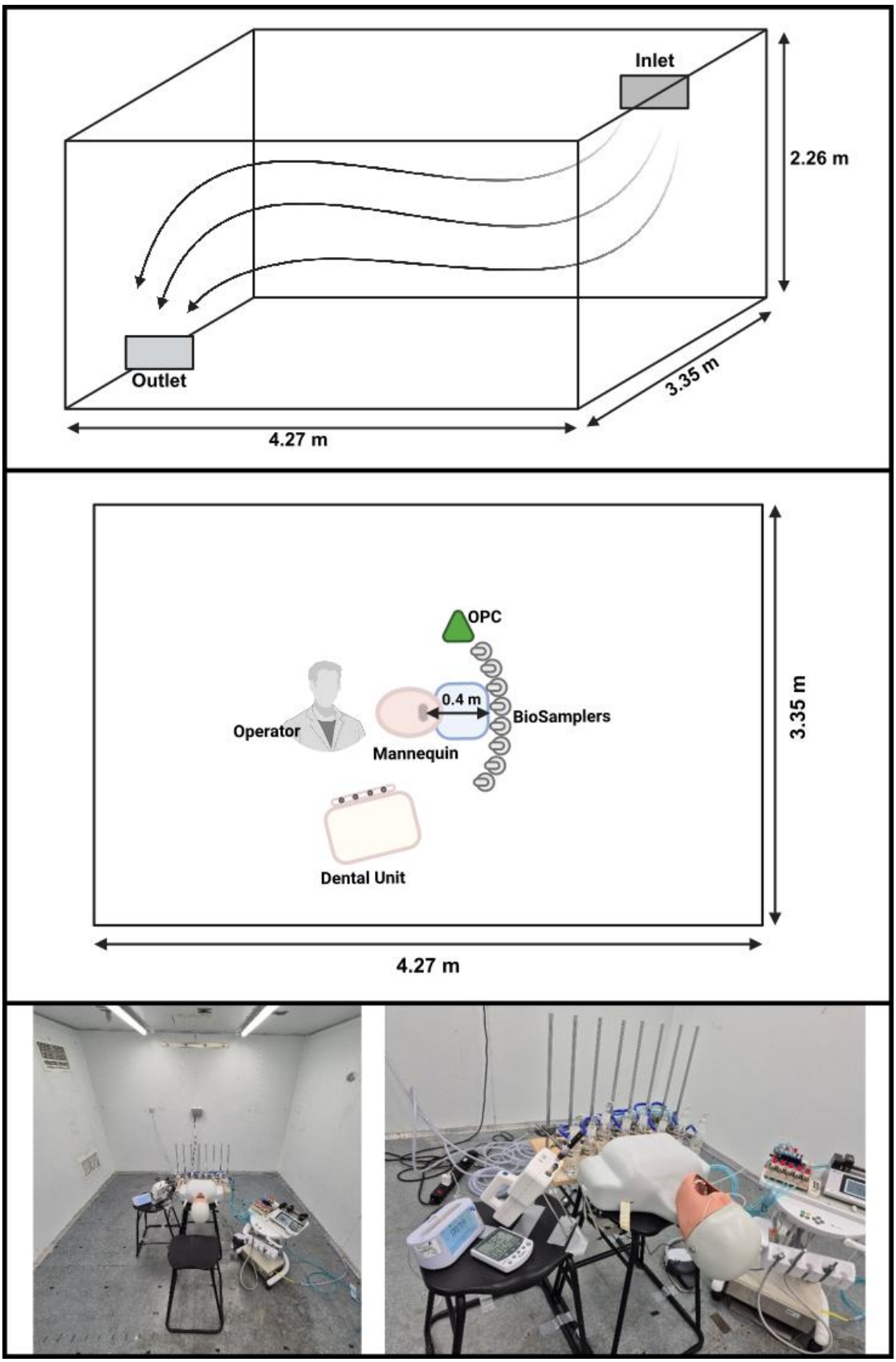

Figure 4.11. Aerobiology chamber used in bioaerosol persistence experiments.

Upper panel: overview of the chamber and ventilation configuration; Middle panel: plan view of the experimental setup; Lower panel: photographs of experimental setup. OPC: optical particle counter.

4.9 Aerosol particle concentration over time and effect of ventilation rate

During experiments, mean temperature at 1.5 ACH was 27.08 °C (SD: 0.60), and at 11.7 ACH was 25.45°C (SD: 0.45). Mean humidity was at 1.5 ACH was 31.27%RH (SD: 1.90), and at 11.7 ACH was 39.78 %RH (SD: 2.46). At 1.5 ACH, mean background particle number concentration in the 5 min before the procedure (baseline) was 18.87 (SD: 0.41) particles/cm^3 and at 11.7 ACH this was 3.46 (SD: 0.23) particles/cm^3.

During the 10-min dental procedure, at 1.5 ACH, the mean aerosol concentration increased to 113.4 (SD: 51.19) particles/cm^3, showing sharp spikes in aerosol concentration of 10 – 100-fold above baseline (Figure 4.12). At 11.7 ACH there was a smaller increase in aerosol concentration, with mean 69.79 (SD: 34.78) particles/cm^3, with similar spikes in aerosol concentration. At 1.5 ACH aerosol concentration did not return to baseline during the 24 minutes of sampling after the end the procedure. At 11.7 ACH, aerosol concentration reduced steadily after the procedure, approaching baseline within the period of sampling.

There was an 80.9% reduction ($t(5) = 6.12$, $p = 0.002$) in mean area under the curve (AUC) following the procedure at 11.7 ACH compared to at 1.5 ACH (417.4 vs 2190.0 [particle/cm^3]·min; Figure 4.13).

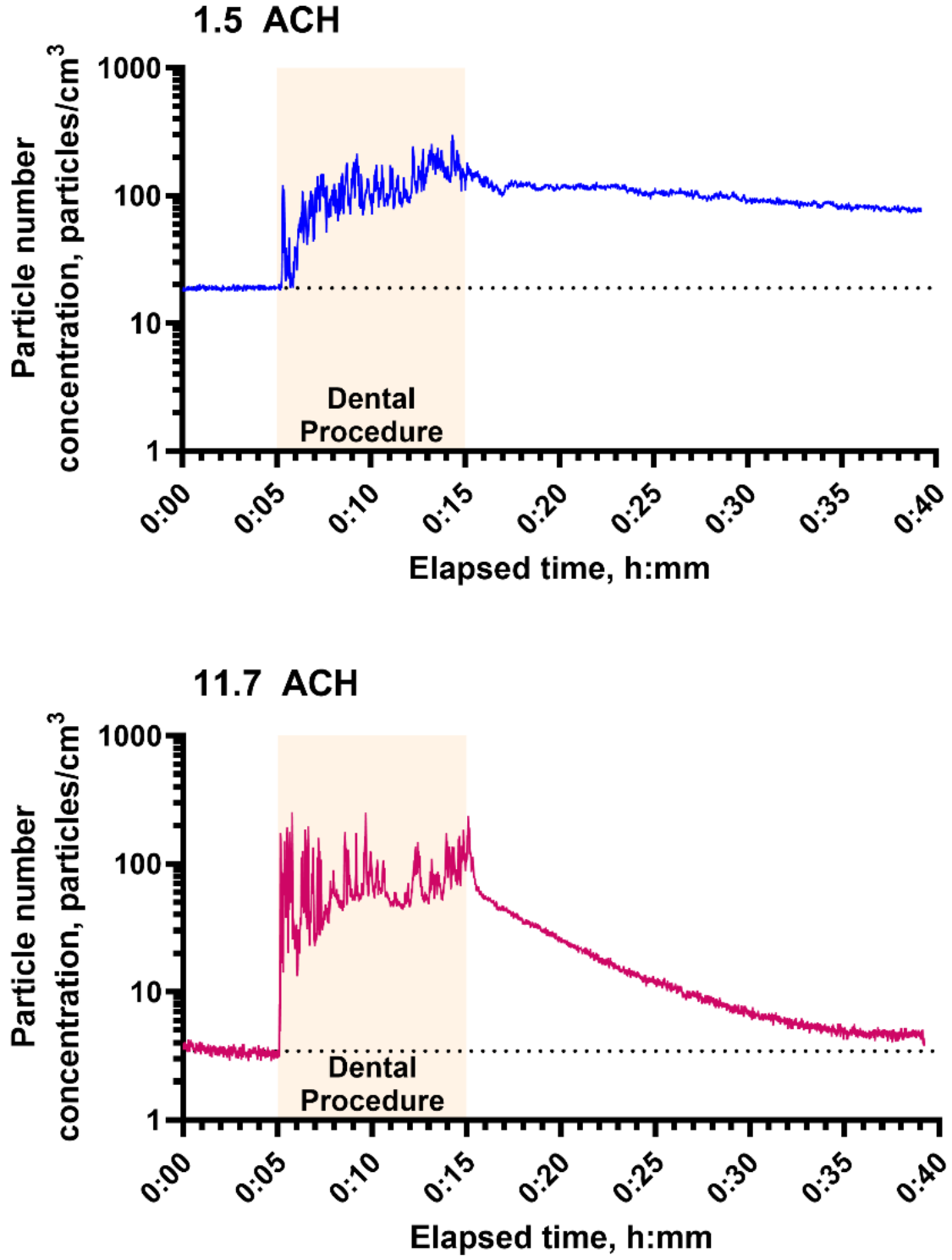

Figure 4.12. Aerosol concentration over time at 1.5 and 11.7 air changes per hour (ACH).

Aerosol particle number concentration during bioaerosol persistence experiments measured by optical particle counter during a 10-min dental procedure (denoted by orange shaded area). Particle concentration was summed across all particle size channels (0.3, 0.5, 1.0, 2.5, 5.0, 10.0 µm). Average of data from three, 39-min replicates (one additional replicate [n = 4] included of 27-min duration for 1.5 ACH only). Sampling rate 1 Hz. Dotted line denotes the mean aerosol concentration in the 5 min preceding the procedure at that ventilation rate. Individual replicate data are shown in appendix figure A.6.

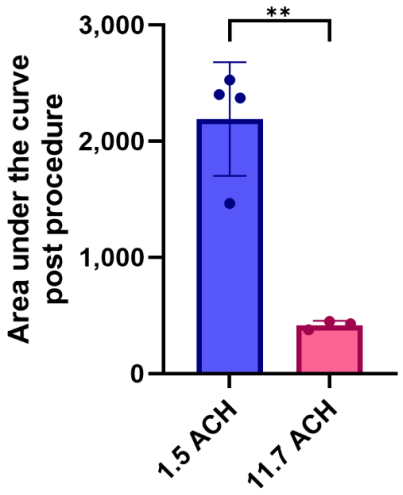

Figure 4.13. Aerosol concentration at 1.5 and 11.7 air changes per hour (ACH). Area under the curve after the dental procedure (from 15 min onwards). Data from three replicates for 11.7ACH and four replicates for 1.5ACH. **: $p < 0.01$, unpaired *t* test.

4.10 Persistence of infectious phage

Plaque assays confirmed the titre of the phi6 inoculum to be 3.14 x 10^{10} (SD: 8.06 x 10^{9}) PFU/mL, however, MS2 titre was lower than expected at 9.71 x 10^{7} (SD: 5.88 x 10^{7}) PFU/mL. As limited time had been allocated to experiments in the Leeds Aerobiology Chamber, it was not possible to repeat experiments with MS2 at higher titre. Neither phage was seen in experiment or assay negative control samples (Figure 4.14).

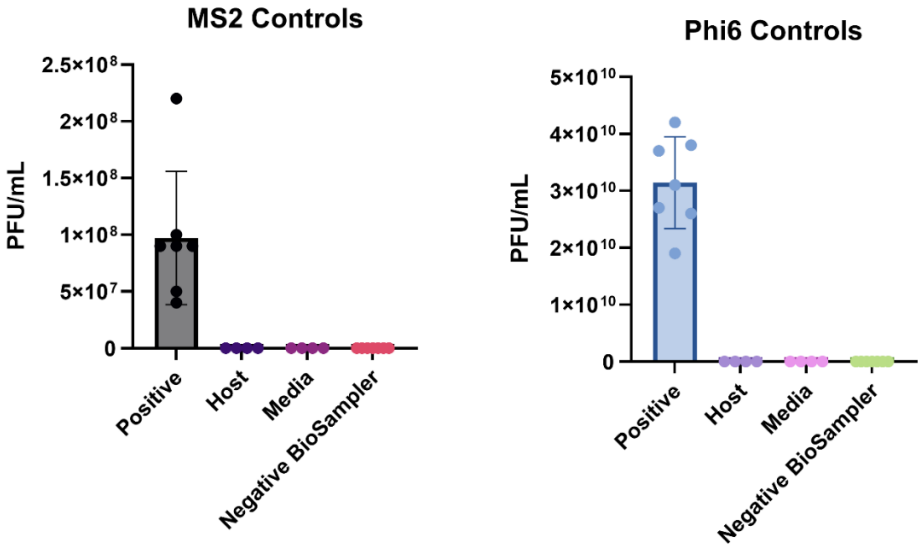

Figure 4.14. Infectious phage in control samples. Infectious phage in positive and negative control samples (*n* =7). Individual values, mean, and standard deviation shown. PFU: Plaque-Forming Units.

Due to the low starting inoculum of MS2, recovery of infectious MS2 was also low compared to that of Phi6, however, MS2 was recovered in air samples even at 19 min following the procedure at 1.5 ACH. No MS2 was recovered after the procedure at 11.7 ACH (table 4.6). Recovery of phi6 was much greater, and at 1.5 ACH, continued to be high even at 23 min after the procedure. No recovery of phi6 was seen after 3 min at 11.7 ACH.

Nonlinear regression curves describing the relationship of phage recovery over time following the procedure are shown in figure 4.15, and the maximum expected time after the procedure that infectious phage would be expected to be recovered, calculated by determining the intercept of regression curves with the x axis, are shown in table 4.7.

MS2						
Time, min	**1.5 ACH**			**11.7 ACH**		
	Mean (PFU/L)	*SD*	*n*	***Mean (PFU/L)***	*SD*	*n*
0	**2.0**	4.0	4	**2.7**	4.6	3
1	**0.0**	-	1	**-**	-	-
3	**6.0**	7.7	4	**0.0**	0.0	3
5	**0.0**	-	1	**-**	-	-
7	**8.0**	9.2	4	**0.0**	0.0	3
9	**0.0**	-	1	**-**	-	-
11	**0.0**	0.0	4	**0.0**	0.0	3
15	**2.7**	4.6	3	**0.0**	0.0	3
19	**2.7**	4.6	3	**0.0**	0.0	3
23	**0.0**	0.0	3	**0.0**	0.0	3
Phi6						
Time, min	**1.5 ACH**			**11.7 ACH**		
	Mean (PFU/L)	*SD*	*n*	***Mean (PFU/L)***	*SD*	*n*
0	**166.0**	179.6	4	**101.3**	80.9	3
1	**248.0**	-	1	**-**	-	-
3	**156.0**	142.6	4	**8.0**	8.0	3
5	**480.0**	-	1	**-**	-	-
7	**174.0**	118.7	4	**0.0**	0.0	3
9	**360.0**	-	1	**-**	-	-
11	**148.0**	100.9	4	**0.0**	0.0	3
15	**74.7**	20.1	3	**0.0**	0.0	3
19	**77.3**	99.4	3	**0.0**	0.0	3
23	**146.7**	146.7	3	**0.0**	0.0	3

Table 4.6. Infectious phage in air samples after a dental procedure.

Recovery of infectious phage following a dental procedure at 1.5 air-changes per hour (ACH) and 11.7 ACH. The midpoint of each 2-min sampling period is given as the time of the sample (i.e., 1 min represents a sample taken from 0 – 2 min after the procedure). Time 0 represents a sample taken for the final 2 min of the 10-min dental procedure. One replicate at 1.5 ACH was conducted with consecutive sampling 1 – 11 min after the procedure, subsequent 1.5 ACH replicates (n = 3) and all 11.7 ACH replicates (n = 3) collected samples from 0 – 23 min with 2 min spacing between each sample. n for each timepoint is therefore between 1 – 4 as shown.

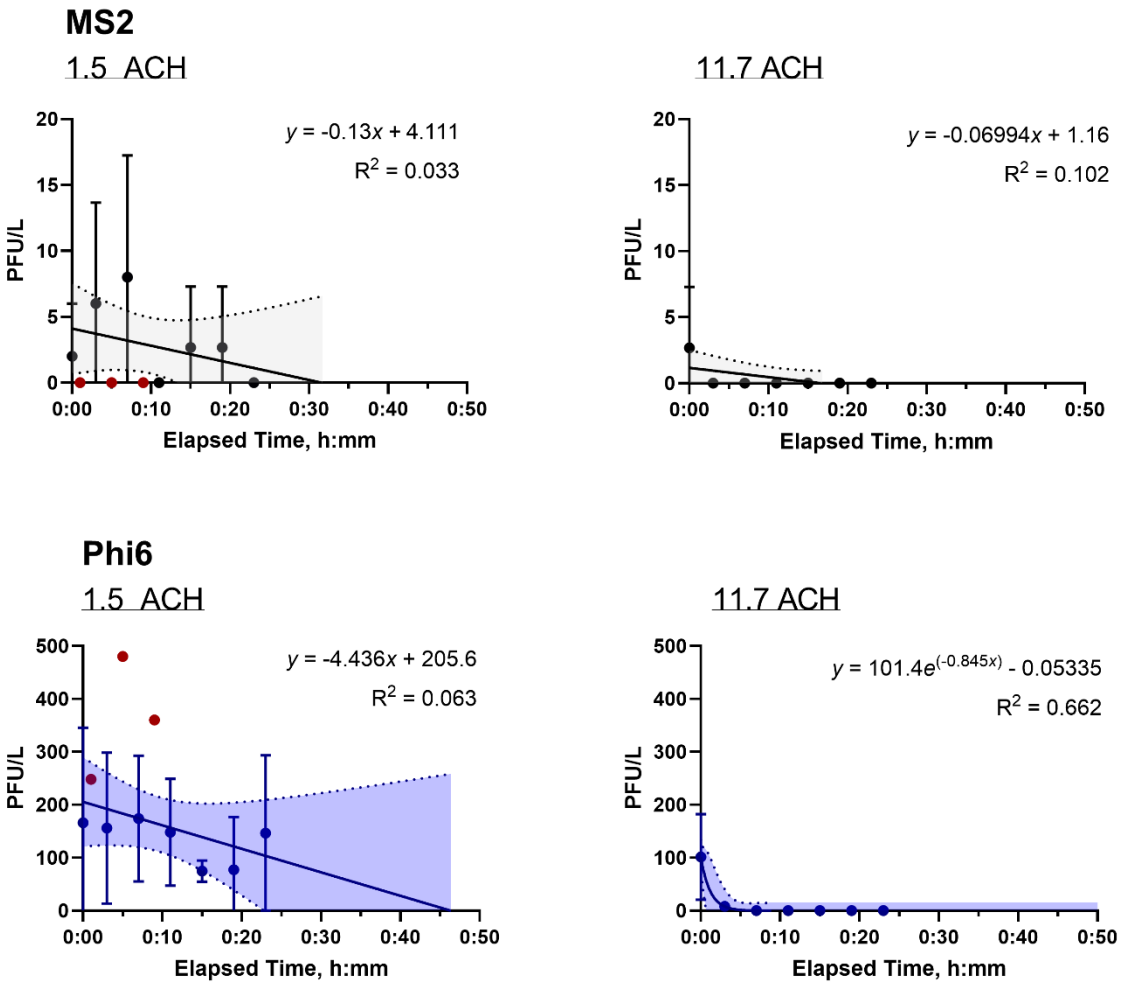

Figure 4.15. Infectious phage in air samples after a dental procedure.

Recovery of infectious phage following a 10-min simulated dental procedure in an enclosed chamber at 1.5 and 11.7 air changes per hour (ACH). One sample was taken in the last 2 min of the procedure (plotted as time 0:00) and 6 further 2-min samples were taken with 2 min between the end of one sample and beginning of the next (24 min sampling period in total). The midpoint of each 2-min air sample is plotted as the mean and standard deviation of at least 3 replicates. For a single replicate at 1.5 ACH only, sampling was conducted for 6 *consecutive* 2-min periods after the end of the procedure (i.e., no spacing between samples; 12 min sampling total). Red datapoints denote samples taken during this replicate only (1, 5, 9 min; n = 1) and other timepoints for 1.5 ACH up to 12 min (3, 7, 11 min) therefore include 4 replicates in total. Regression curves (straight line, except one phase decay for phi6 11.7 ACH) are plotted, with 95% confidence intervals as dotted line around curve where it was possible to calculate these. The x axis is extended beyond the period of sampling (23 min) this to show entire regression curves.

	1.5 ACH	11.7 ACH
MS2	31.62 min	16.58 min
Phi6	46.35 min	8.93 min

Table 4.7. Duration of infectious phage persistence in air samples.

Time after the dental procedure that recovery of infectious phage would be expected to fall below zero. Determined by calculating intercept of regression curve describing recovery over time, with the *x* axis. Regression curves and equations are shown in figure 4.15.

4.11 Persistence of phage RNA

Positive control samples from the phage inoculum showed this to contain 6.26 x 10^{11} (SD: 8.35 x 10^{10}) copies/mL MS2, and 1.46 x 10^{10} (SD: 5.84 x 10^{9}) copies/mL phi6. Plasmid DNA standards also amplified as expected, showing 2.84 x 10^{8} (SD: 6.36 x 10^{6}) copies/mL for MS2 and 1.69 x 10^{10} (SD: 2.65 x 10^{8}) copies/mL for phi6 standards.

One of seven phi6 experiment negative controls (negative BioSampler) amplified (2.33 x 10^{3} copies/ L; LoD 1.16 x 10^{3} copies/ L), however, all other negative controls were negative (figure 4.16).

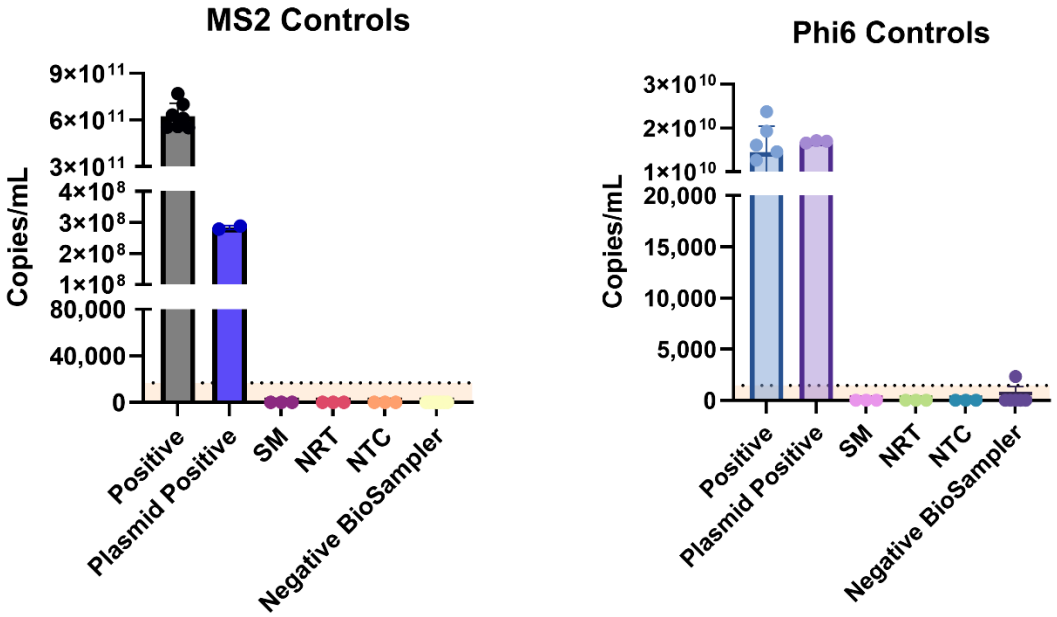

Figure 4.16. Phage RNA in control samples.

Recovery of Phage RNA in positive and negative control samples (positive, negative BioSampler *n* =7; phi6 plasmid positive *n* =2; all others *n* =3). Individual values, mean, and standard deviation shown. Dashed line delineating orange shaded area denotes RT-qPCR assay limit of detection. SM: extraction control; NRT: no-reverse–transcriptase control; NTC: no-template control.

As with infectious phage, recovery of MS2 RNA was less consistent than for Phi6. MS2 RNA was recovered in individual air samples even at 11 min following the procedure at 1.5 ACH, however the mean recovery for each timepoint remained below the RT-qPCR assay LoD for this target (1.35×10^4 copies/L). No MS2 RNA was recovered at 11.7 ACH (table 4.8). Recovery of phi6 was more consistent, and at 1.5 ACH, continued to be high even at 23 min after the procedure, although a relative reduction was observed after around 15 min. No recovery of phi6 was seen after 3 min at 11.7 ACH.

Nonlinear regression curves describing the relationship of phage RNA recovery over time following the procedure are shown in figure 4.17, and the maximum expected time after the procedure that phage RNA would be expected to be recovered, calculated by determining the intercept of regression curves with the LoD are shown in table 4.9. This was not calculated for MS2 as mean recovery at each timepoint remained below the LoD for this target.

MS2						
Time, min	**1.5 ACH**			**11.7 ACH**		
	Mean (copies/L)	*SD*	*n*	***Mean (copies/L)***	*SD*	*n*
0	**3,897.0**	7,794.0	4	**0.0**	0.0	3
1	**0.0**	-	1	**-**	-	-
3	**11,298.9**	22,597.9	4	**0.0**	0.0	3
5	**0.0**	-	1	**-**	-	-
7	**0.0**	0.0	4	**0.0**	0.0	3
9	**0.0**	-	1	**-**	-	-
11	**3,456.8**	6,913.6	4	**0.0**	0.0	3
15	**0.0**	0.0	3	**0.0**	0.0	3
19	**0.0**	0.0	3	**0.0**	0.0	3
23	**0.0**	0.0	3	**0.0**	0.0	3
Phi6						
Time, min	**1.5 ACH**			**11.7 ACH**		
	Mean (copies/L)	*SD*	*n*	***Mean (copies/L)***	*SD*	*n*
0	**1,836.9**	2,173.1	4	**0.0**	0.0	3
1	**4,225.5**	-	1	**-**	-	-
3	**17,623.9**	33,817.5	4	**3,663.4**	6,345.3	3
5	**3,778.1**	-	1	**-**	-	-
7	**1,838.0**	1,790.9	4	**0.0**	0.0	3
9	**4,147.7**	-	1	**-**	-	-
11	**1,468.8**	2,198.4	4	**0.0**	0.0	3
15	**614.9**	1,065.1	3	**0.0**	0.0	3
19	**842.7**	729.9	3	**0.0**	0.0	3
23	**616.3**	1,067.5	3	**0.0**	0.0	3

Table 4.8. Phage RNA in air samples after a dental procedure.

Recovery of phage RNA in air samples over time following a dental procedure at 1.5 air-changes per hour (ACH) and 11.7 ACH. The midpoint of each 2-min sampling period is given as the time of the sample (i.e., 1 min represents a sample taken from 0 – 2 min after the procedure). Time 0 represents a sample taken for the final 2 min of the 10-min dental procedure. One replicate at 1.5 ACH was conducted with consecutive sampling 1 – 11 min after the procedure, subsequent 1.5 ACH replicates (n = 3) and all 11.7 ACH replicates (n = 3) collected samples from 0 – 23 min with 2 min spacing between each sample. n for each timepoint is therefore between 1 – 4 as shown.

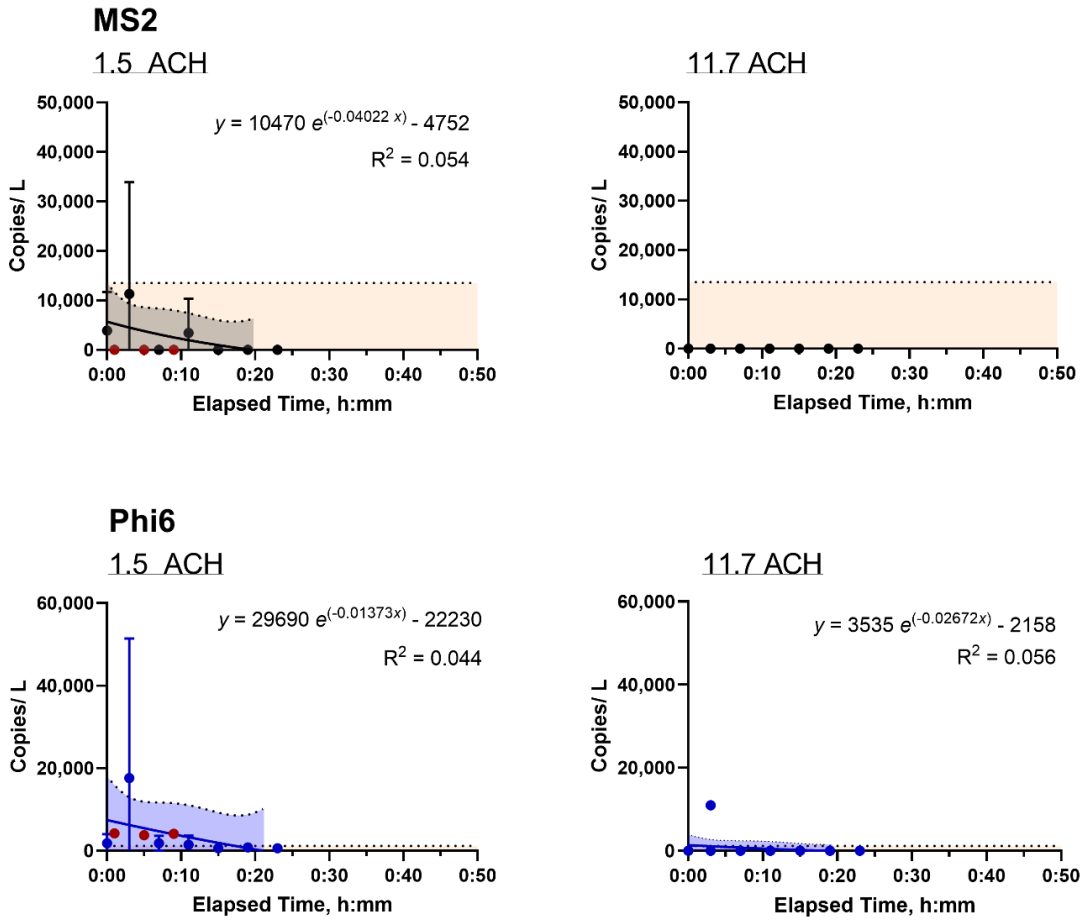

Figure 4.17. Phage RNA in air samples after a dental procedure.
Recovery of phage RNA (MS2 and phi6) in air samples following a 10-min simulated dental procedure in an enclosed aerobiology chamber at 1.5 and 11.7 air changes per hour (ACH). One sample was taken in the last 2 min of the procedure (plotted as time 0:00) and 6 further 2-min samples were taken with 2 min between the end of one sample and beginning of the next (24 min sampling period in total). The midpoint of each 2-min air sample is plotted as the mean and standard deviation of at least 3 replicates. For a single replicate at 1.5 ACH only, sampling was conducted for 6 *consecutive* 2-min periods after the end of the procedure (i.e., no spacing between samples; 12 min sampling total). Red datapoints denote samples taken during this replicate only (1, 5, 9 min; $n = 1$) and other timepoints for 1.5 ACH up to 12 min (3, 7, 11 min) therefore include 4 replicates in total. Nonlinear regression curves (one phase decay) are plotted, with 95% confidence intervals as dotted line around curve where it was possible to calculate these. Dashed line delineating orange shaded area denotes RT-qPCR assay limit of detection.

	1.5 ACH	11.7 ACH
MS2	Not calculated	Not calculated
Phi6	17.37 min	2.37 min

Table 4.9. Duration of phage RNA persistence in air samples.

Time after the dental procedure that recovery of phage RNA would be expected to fall below the RT-qPCR assay limit of detection. Determined by calculating intercept of regression curve describing recovery over time, with $y = \text{limit of detection}$. Regression curves and equations are shown in figure 4.17.

4.12 Discussion

In dispersion experiments, large increases in aerosol concentration measured by OPC were seen during the dental procedure, and this was greatest at 1 m. More modest increases were seen at 4 m. As well as increased physical aerosol during the procedure, infectious MS2 and phi6 was also dispersed, reaching highest levels within the first 1m around the procedure. Phage RNA was highest in the same location but was recovered in consistently higher amounts than that of infectious phage. Persistence experiments demonstrated high levels of infectious virus in air samples after a dental procedure which remained elevated for a prolonged period at low ventilation rates (1.5 ACH). At increased ventilation rates (11.7 ACH), infectious MS2 was not detected after the end of the dental procedure, and phi6 was not detected after 3 min following the procedure.

These results are consistent with published data using particle counting methods to look at dental aerosols from various dental instruments. For example Dudding *et al.* (2022) demonstrated considerable (~200-fold) increases in aerosol concentration during treatment in patients using an air turbine handpiece, which was much greater than other instruments such as an ultrasonic scaler. Because the air turbine is consistently reported to produce more aerosol than other instruments, this instrument was chosen for use in the present experiments, representing a worst-case scenario. Other authors have demonstrated much variation in the time taken for aerosol concentration to reduce to baseline after a dental procedure, with times ranging from 10 – 60 min (Allison et al. 2021b; Ehtezazi et al. 2021; Shahdad et al. 2021). More important than how much aerosol is produced, however, is what is contained within the aerosol. The literature is clear that bacteria from the mouth and from dental unit waterlines are dispersed over considerable distances (Rafiee et al. 2022; Zemouri et al. 2020c), however much less is known about the dispersion of viruses.

The present experiments, which studied an unmitigated 10-min dental procedure with an air turbine handpiece in an open-plan clinical setting with modest ventilation rate (6.46 ACH), demonstrate that infectious virus is indeed dispersed over distances which may pose infection risk to staff and other patients. Based on regression analyses, infectious MS2 and phi6 would be expected to be detectable on surfaces within 2.75 m and 2.14 m of the procedure, respectively. This means that in an unmitigated scenario, and when virus is present within a patient's mouth, the operator, assistant, and patient will likely be contaminated with infectious virus via

droplets and larger aerosols settling onto surfaces. This dispersion distance also suggests that most surfaces in a single enclosed dental surgery could potentially become contaminated during such a procedure; this would be the case in a dental surgery such as the 4.3 m x 4.5 m room used in experiments described in Chapter 3. Additionally, in an open-plan clinic, bays separated by less than this distance would be expected to receive surface contamination if a procedure were conducted in an adjacent bay. Within these distances, the use of personal protective equipment such as a fluid resistant mask and eye protection as a universal precaution would be needed to prevent contamination by large droplets and aerosols (likely > 100 μm)(Tang et al. 2021), as well as a fluid resistant bib or gown dependant on the infection risk and local policies.

In air samples, the expected distance of dispersion from regression analyses was greater than in surface samples, equating to 6.91 m and 4.57 m for MS2 and phi6, respectively. Compared to surface samples, aerosols recovered from air samples will likely contain smaller particles with longer residence times, which can penetrate the airways more deeply, potentially leading to more severe infection (Thomas 2013). These data suggest that in a typical enclosed dental surgery, without any other aerosol mitigation, anyone within the room would be exposed to potentially infectious aerosol via inhalation. Similarly, without any mitigation, spacing of > 6.91 m would be required between bays on an open-plan clinic with a similar ventilation configuration to prevent inhalation of potentially infectious aerosol. Where the potential for infection is high (known infectious patient or during an infectious disease outbreak), the use of respiratory protective equipment will be necessary within these distances. These experiments represent a worst-case scenario, with no mitigation of bioaerosol and high salivary viral load, and so it is likely that aerosol control measures used in routine clinical practice will reduce this dispersion distance substantially. The effect of such control measures is explored in the following chapter.

At each location much higher quantities of RNA were recovered than that of infectious phage. This is not surprising given the sensitivity of the RT-qPCR assay, and is consistent with recovery of infectious virus versus detection by RT-qPCR in human viral infections such as with SARS-CoV-2 (Killingley et al. 2022). Interestingly though, the distance over which RNA recovery would be expected to reach zero from regression analyses was lower in surface samples than was the case for infectious phage, particularly for phi6 (Infectious phi6: 2.14 m, phi6 RNA: 0.37 m). For air

samples, the expected maximum RNA recovery distance was more similar to that of infectious phage. This is an unexpected finding, as greater sensitivity would be expected for RT-qPCR than for plaque assays. It is possible that the difference is related to stability of phi6 RNA on filter papers, particularly at greater distances where lower amounts of phage RNA were present. Efforts were made however to prevent desiccation of filters (prewetting, sealing vessels after the experiment, same day elution), and eluates were stored immediately at -80°C prior to RNA extraction. As described in Chapter 3, recovery of phage RNA from filter papers (MS2: 53.8% recovery; phi6: 5.6%) was similar to the recovery of infectious phage (MS2: 66.4%; phi6: 3.5%) and so this would not account for the difference seen in regression analyses.

Furthermore, the RT-qPCR assay LoD for phi6 was lower (2.9 copies/µl) than for MS2 (33.8 copies/µL), and so this is unlikely to account for the lower dispersion distance for phi6. Despite low limits of detection at the level of the assay however, only a proportion of the starting sample is taken at each step of the RT-qPCR protocol (e.g., sample elution, RNA extraction, reverse transcription, qPCR). Only a small proportion of the original RNA in the sample will therefore end up in the final assay. As a result, limits of detection are higher when accounting for this, and when correcting for surface area in surface samples and air volume for air samples (MS2 LoD: 1,194.8 copies/cm^2, 1,656.1 copies/L; phi6 LoD: 102.6 copies/cm^2, 142.2 copies/L). It is likely that this may account for the difference in regression results between infectious phage and phage RNA, and in future work, optimising the protocol to use a greater proportion of the starting material (e.g., by sample concentration and higher volume qPCR reactions) may help to lower the corrected LoD. The difference between recovery of infectious phage and phage RNA has implications for studies which rely on molecular detection methods alone such as those using qPCR (Bazzazpour et al. 2022; Meethil et al. 2021) or sequencing (Poolkerd et al. 2024; Rafiee et al. 2022) as these may not provide the full picture on the impact of potentially-infectious aerosols. For instance, in the present experiments there were samples where phage RNA, but no infectious phage was recovered.

As observed in other studies (Allison et al. 2021a; Holliday et al. 2021), dispersion was not equally distributed around the procedure, with greater dispersion seen opposite the operator and over the “patient”. This is a useful observation as it allows the identification of “hot spots” where surface contamination is more likely, and where

surface disinfection can be particularly focussed. It should be noted however, that this pattern of dispersion may be affected by factors such as the position of the operator and their handedness, as well as the presence of an assistant (Figure 4.18); the latter has been shown to influence airflow and surface contamination patterns in fluorescent tracer studies (Allison et al. 2021a).

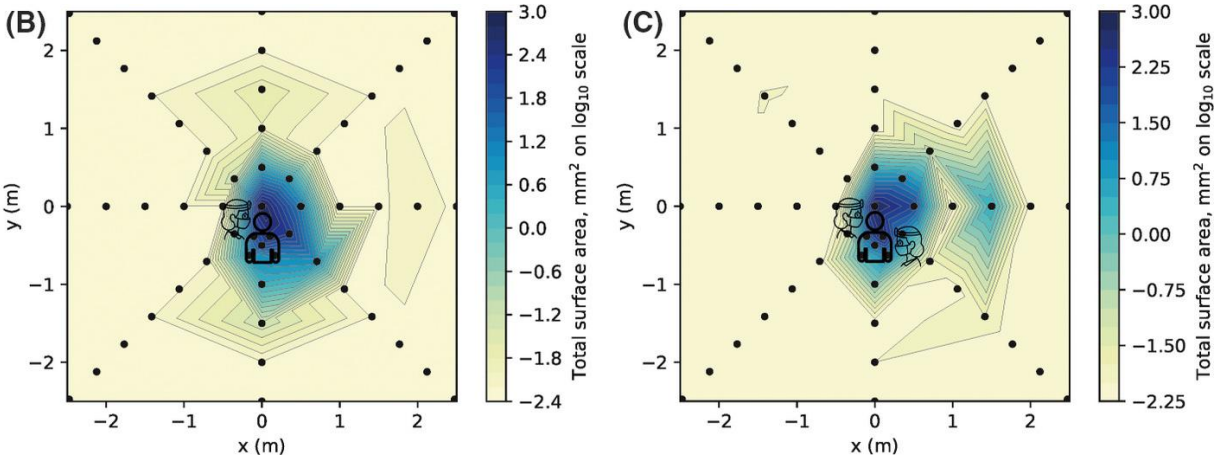

Figure 4.18 Spatial dispersion of a fluorescent tracer

Heatmap showing dispersion of a fluorescent tracer around a simulated dental procedure (anterior crown preparation using an air turbine handpiece, with dental suction), (B) without the presence of a dental assistant and (C) with the presence of a dental assistant. Tracer deposition is increase in locations behind the assistant when the assistant is present. Figure adapted from (Allison et al. 2021a), published under CC BY 4.0 license.

The amount of virus recovered during dispersion experiments would be likely to initiate infection if similar amounts of pathogenic virus were dispersed *in vivo*. Taking an example viral air concentration of 100 PFU/L, which was seen at < 1 m for MS2 and phi6, a respiratory rate of 14 breaths per minute, and a tidal volume of 0.5 L, then an individual would likely inhale 7,000 PFU during a 10-min dental procedure. This is much greater than the minimum infectious dose of many human respiratory pathogens such as SARS-CoV-2 (55 focus-forming units (Killingley et al. 2022)), influenza H2N2 (0.42 – 2.1 PFU (Alford et al. 1966)), and respiratory syncytial virus (70 PFU (Bischoff 2010)), and provides strong evidence that dental treatment without any other mitigating factor in an infectious individual is able to deliver sufficient dose to initiate an infection.

In persistence experiments in the aerobiology chamber, at the low ventilation rate of 1.5 ACH, aerosol particle concentration measured by OPC remained high after the procedure and did not return to baseline within the period of sampling (24 min post

procedure). The aerosol also contained infectious phage, which was recovered up to the end of the sampling period and remained high throughout. Regression analyses suggested that MS2 would be expected to reach zero after 31.63 min and phi6 after 46.35 min at this air exchange rate. The estimate for MS2 however should be regarded with caution, as the titre of phage used was lower than intended. This will have reduced the amount of MS2 in air samples and may impact the ability to detect this phage compared to if a higher titre inoculum was used. 9.71×10^7 PFU/mL MS2 was used, compared to 3.14×10^{10} PFU/mL for phi6, which equates to a 323-fold lower than intended titre. Correction of the results obtained with MS2 by this factor should however give an indication of what quantity of MS2 might be expected to be recovered if the intended titre were used. As with dispersion experiments, despite substantially greater amounts of recovered phage RNA compared to infectious phage, regression analyses suggest a shorter time to expected zero detection of phi6 RNA at 1.5 ACH (17.37 min) compared to infectious phage (46.35 min). Regression was not performed for MS2 RNA, as despite recovery above the LoD in some replicates, mean recovery for each timepoint remained below the LoD of the assay.

At the higher ventilation rate of 11.7 ACH, which is comparable to the 10 ACH recommended in current guidance for new dental facilities in England (NHS England and NHS Improvement 2021), aerosol particle concentration measured by OPC reduced to baseline levels within the sampling period (24 min). There was a sharp decrease after the procedure, initially in a linear fashion, with some slowing of the rate as aerosol concentration approached baseline. This was accompanied by a sharp reduction in recovery of infectious phage, with no MS2 detected after the procedure, and no phi6 from 3 min after the procedure. Regression analyses suggest an expected zero recovery time at 11.7 ACH of 16.58 min for MS2 and 8.93 min for phi6. Again, the MS2 data should be interpreted cautiously due to the low titre of the inoculum. Phi6 concentration immediately after finishing the procedure (time 0:00) was also lower at 11.7 ACH (101.3 PFU/L) compared to at 1.5 ACH (166.0 PFU/L). These results suggest that ventilation rate is a key factor in the rate of clearance of potentially-infective bioaerosols both *during* and *following* a dental procedure, which is consistent with the results of other studies using particle counting methodologies (Longo et al. 2023; Shahdad et al. 2021). The present approach is highly novel however, as such experiments using a dental procedure in a highly controlled bioaerosol chamber have not previously been described. No other bioaerosol control measures or mitigations were used in these experiments. Such measures would be

expected to supplement the beneficial effect demonstrated here of increased ventilation; this has previously been shown by supplementing mechanical ventilation with HEPA air purifiers to remove aerosol (Ren et al. 2021).

These data support the guidance for dental settings issued during the COVID-19 pandemic (SDCEP 2021a; UK Health Security Agency 2021a) on appropriate fallow times during an infectious disease outbreak where community transmission is high. Such an approach would also be appropriate when treating a patient with a known infection spread by droplet (when conducting an AGP) or airborne routes. This guidance suggests a fallow time of 60 min in settings with poor ventilation (1 – 2 ACH) where other mitigations such as dental suction are not used, and a minimum fallow time of 10 min at ventilation rates > 10 ACH where dental suction is used or 15 min without suction at this ventilation rate. Given the substantial effectiveness of aerosol removal at 11.7 ACH, it is possible that a lower rate, between 1.5 and 11.7 ACH, would still provide an acceptable aerosol clearance time but be easier for dental service providers to achieve. Future work should therefore seek to assess a wider range of air exchange rates to better understand minimum safe parameters.

Studies using viral tracers are useful in infection control research as they allow various parameters to be tested in a controlled manner which may be difficult in clinical studies, however, choosing the right surrogate is important. For example, in dispersion experiment surface samples, detection of phi6 was 419-fold less than for MS2 despite a similar starting inoculum and similar recovery in air samples. This would suggest that MS2 is more robust on surfaces and may be a suitable surrogate for other non-enveloped viruses such as norovirus (Kimmitt and Redway 2016; Tung-Thompson et al. 2015). Any viral pathogen with similar stability on surfaces to MS2 may pose a risk of fomite-mediated transmission from contaminated surfaces. Both MS2 and phi6 had similar recovery in air samples, suggesting similar stability in aerosols and therefore both are likely to be useful surrogates for viral pathogens where airborne transmission is a feature. Choosing the wrong surrogate (i.e., phi6 as a surrogate for a virus that behaves more like MS2 on surfaces) may lead to drawing the wrong conclusions about risk. In future, were an outbreak of a new pathogen to occur as was seen during the COVID-19 pandemic, it would be important for future studies to select viral surrogates with similar physical and virological properties to the pathogen of interest.

Apart from a single negative control BioSampler in dispersion experiments, no plaque assay negative controls contained phage, however there were a few RT-qPCR negative control samples which amplified above the LoD. These were largely experiment negative controls (filter papers or BioSamplers) rather than assay controls and were mostly only slightly above the LoD. Three BioSampler negative controls in dispersion experiments for MS2 amplified at lower C_q values, however. This demonstrates that despite meticulous processes to prevent contamination of samples during experiments, the highly sensitive nature of the RT-qPCR assay can be problematic, as infectious phage was not seen in these samples during plaque assays.

Dental procedures then, have the potential to produce bioaerosols which when treating an infective patient, contain enough virus to cause infect dental professionals and other patients. Without further control measures, dental professionals who work close to the patient's mouth may be exposed to these infective aerosols. Small aerosols travel much further (> 4 m) than larger aerosols and droplets which are more concentrated close to the patient (< 1 m). These infective bioaerosols remain in the air for a long time (30 – 40 min) after a procedure where ventilation is poor, however increasing ventilation to above 10 ACH reduces this persistence to 10 – 15 min. Given this, there is a need for further measures to control infective dental bioaerosols to reduce the risk they pose to acceptable levels. The efficacy of several bioaerosol control measures is explored in the following chapter.

Chapter 5. Dental Bioaerosol Control Measures

5.1 Introduction

The previous chapter demonstrated that bioaerosols created during dental procedures can travel significant distances from the source and remain in the air for some time after the procedure, particularly at low ventilation rates. The data suggest that in a real-world setting without bioaerosol control measures, dental professionals are likely to be exposed to well above the infectious dose of a range of human viral pathogens when treating a patient with an acute viral infection. There are few epidemiological data on the risk of healthcare associated infection via dental bioaerosols, however one study of 1,507 individuals looking at SARS-CoV-2 seroprevalence in dental professionals during the early COVID-19 pandemic found higher rates of prior infection in clinical members of the dental team (16.7%) compared to non-clinical staff in dental practices (6.3%) and the local population at the time (6 – 7%) (Shields et al. 2021). This suggests that there may be an increased risk of infection in dental professionals, supporting the present experimental data and that of other authors.

If there is a risk of transmitting infection to dental professionals and other patients, then control measures are needed to reduce this risk to an acceptable level. This may be during an infectious disease outbreak, as seen during the COVID-19 pandemic, or when treating a patient with an endemic infection. In Chapter 3, two dental bioaerosol control measures were shown to be effective. In these experiments, the use of a dental unit waterline (DUWL) disinfectant reduced the recovery of infectious MS2 by 96.5%, and the use of a rubber dam reduced infectious MS2 by 86.3% and phi6 by 100%. Both measures aim to reduce the amount of viable virus escaping the mouth within bioaerosols. DUWL disinfectants inactivate the virus and rubber dam isolates the tooth being treated from the virus-containing saliva. Two further approaches to bioaerosol control have also been described: 1) reducing the total amount of aerosol produced by dental instruments; 2) capturing the aerosol after it is produced to reduce exposure to those in the vicinity.

Many bioaerosol control measures were included in guidance published during the COVID-19 pandemic to reduce the risk of infection when community transmission was high (SDCEP 2021a; UK Health Security Agency 2021b). This guidance is now

withdrawn, however, and the current National Infection Prevention Manual for England mentions only the use of personal protective equipment and ventilation, but not other specific control measures. Whilst Chapter 4 showed the effectiveness of ventilation in reducing the total amount and residence time of virus in dental bioaerosols, there are further opportunities to reduce bioaerosol risks with specific control measures used during dental treatment.

One of the most frequently used instruments in dentistry is the air-turbine handpiece. It produces a fine mist of pressurised air and water to cool the bur and tooth and operates at speeds of up to 400,000 rpm. As a result, the air-turbine handpiece produces significant aerosol (Sergis et al. 2020). This fast-moving aerosol, containing very small droplets, therefore has the potential to carry microorganisms from the mouth. One method of reducing the total amount of aerosol produced is by using a handpiece driven by an electric motor instead of an air-driven turbine, which can operate at up to 200,000 rpm. The electric-motor–driven (micromotor) handpiece does not need to vent air from the front of the handpiece as is necessary with an air-turbine handpiece, and jets of water alone can be used to cool the bur without pressurised air. This produces less aerosol overall and droplets are of a larger size, travelling shorter distances and remaining airborne for a shorter time (Allison et al. 2021c; Sergis et al. 2020).

Only one group has previously explored the effect of using an electric micromotor handpiece on the dispersion of viruses following a dental procedure. Vernon *et al.* (2021), using a mannequin simulation model, demonstrated reductions of bacteriophage phi6 in surface and air samples of over 99% when the micromotor handpiece was used compared to an air-turbine handpiece. Importantly however, whilst similar reductions have been shown in aerosol particle concentration and the dispersion of a fluorescent tracer (Allison et al. 2021c), the effect of a micromotor handpiece has only been studied using a single virus (enveloped bacteriophage phi6). It is therefore important to reproduce this using other viral tracers, ideally with multiple viruses in the same experiments, to compare the effect between organisms within the same model and under the same conditions.

Whilst reducing the total amount of aerosol produced by dental instruments is a useful approach, any high speed instrument will produce some aerosol, as even without an irrigant, oral fluids become aerosolised when they contact a spinning bur (Sergis et al. 2020). Additionally, patients themselves produce respiratory aerosols

when breathing, speaking, and coughing (Wilson et al. 2021) which in an infected individual contain significant quantities of virus, correlating with the risk of transmission (Alsved et al. 2022). There is therefore a benefit to bioaerosol control methods which capture aerosols at source, preventing further dissemination and reducing risk to those providing care. One such measure, which is widely used in routine dental care, is high-volume dental suction. Dental suction is delivered by a suction cannula connected to a central vacuum supply, and is used to evacuate saliva, dental instrument irrigants, blood, and debris from the mouth. This improves patient comfort, protects the airway, and allows improved visibility for the operator. An additional benefit however is that dental aerosols are also captured. For example, studies using particle counters demonstrate reductions in physical aerosol escaping the mouth when dental suction is used (Ehtezazi et al. 2021; Shahdad et al. 2021). Suction also addresses the dispersion of microorganisms within dental bioaerosols, with a 98% reduction in adenosine triphosphate bioluminescence (marker of bacterial contamination) reported with suction during treatment in patients (Lloro et al. 2021). Reduction in viral dispersion of up to 56% has also been reported using a mannequin simulation model with bacteriophage phi6 (Malmgren et al. 2023; Vernon et al. 2021).

Finally, local exhaust ventilation (LEV) devices may be used to capture dental bioaerosols. Dental LEV devices use high air flow rates to extract air from around the procedure before filtering it using high-efficiency particulate air (HEPA) filters and recirculating the air back into the room. LEV is also often described as extraoral suction/ extraction/ evacuation/ scavenging and has been shown to reduce physical dental aerosol concentration (Barrett et al. 2022) and dispersion of a fluorescent tracer by 74 – 100 % (Allison et al. 2021b). Reductions of 74% in bacterial dispersion at 50 cm with a *Lactobacillus acidophilus* tracer have also been reported (Horsophonphong et al. 2021), and in a mannequin model using bacteriophage phi6, viral dispersion was 60% lower with LEV (Vernon et al. 2021). Again, the effect of both suction and LEV on the dispersion of viruses in dental bioaerosols has only been studied using a single enveloped virus (bacteriophage phi6), and so further work is needed to compare effectiveness of these measures on both enveloped and non-enveloped viruses.

The present model, using the non-enveloped bacteriophage MS2 and enveloped bacteriophage phi6, therefore provides an ideal opportunity to test the efficacy of a micromotor handpiece, dental suction, and LEV in reducing viral dispersion

compared to using an air turbine handpiece with no other bioaerosol control measure.

5.2 Aims and objectives

The aim of the experiments described in this chapter was to determine the effectiveness of three dental bioaerosol control measures (dental suction, LEV, micromotor handpiece) in reducing the dispersion of enveloped and non-enveloped viruses. The specific objectives were to:

- Define the relative effectiveness of bioaerosol control measures in reducing total aerosol concentration.
- Compare the particle size distribution of aerosol produced using different control measures.
- Assess the effectiveness of control measures in reducing the dispersion of infectious virus and viral RNA.

5.3 Dental bioaerosol control measures – specific methods

Experiments were conducted to test the efficacy of bioaerosol control measures in a 44.96 m^3 dental surgery with a ventilation rate of 4.96 ACH. Sampling locations (Figure 5.1) were chosen based on areas shown in Chapter 4 as most likely to be contaminated during the dental procedure. This corresponds to 1 m around the procedure, which is where the operator and assistant are situated during a real procedure and is therefore most clinically relevant. 10-min crown preparations were performed on the upper right central incisor tooth of the dental mannequin, and an inoculum containing 1.22 x 10^{10} (SD:1.41 x 10^{10}) PFU/mL MS2 and 3.17 x 10^{10} (SD:8.52 x 10^9) PFU/mL phi6 was infused into the mannequin's mouth at 1.5 mL/min with 1 mL of inoculum added to all surfaces of the mannequin's teeth immediately before beginning the experiment.

Filter paper samples were pre-wet with 100 µL of SM buffer immediately before the experiment. Sampling began 3 min before the procedure to allow a short period of measurement of the baseline aerosol concentration and then continued for 5 min after the 10-min dental procedure (18 min total). A short, 5-min, post-procedure sampling period was chosen to minimise drying of filter papers and evaporation of BioSampler buffer. Also, because persistence experiments in Chapter 4 showed high concentrations of aerosolised phage are produced immediately after the procedure decaying quickly at higher ventilation rates, prolonged sampling was unnecessary. The ventilation rate in this setting (4.96 ACH) was between the two rates used in the experiments in Chapter 4 (1.5 ACH and 11.7 ACH).

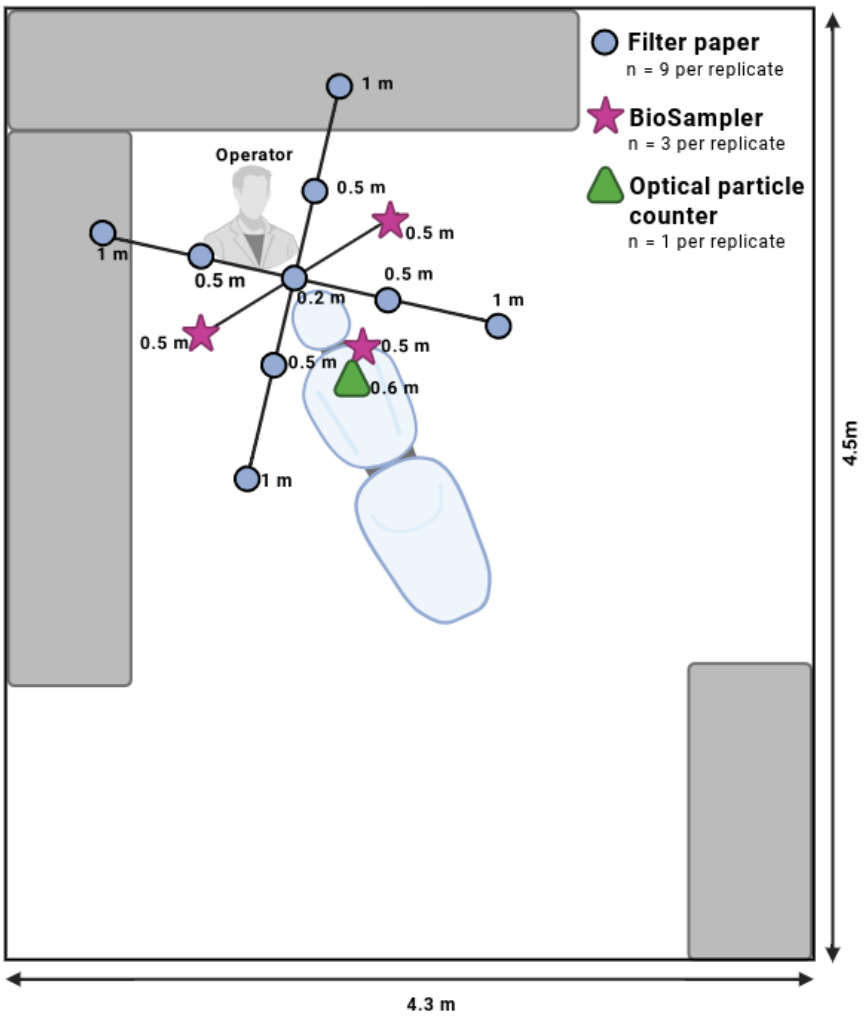

Figure 5.1. Sampling locations in bioaerosol control experiments.
Schematic diagram showing experimental setup and sampling locations.

Experiments were performed under the following conditions (*n* = 3 per condition):

- **Control:** crown preparation with an air turbine handpiece (Synea TA-98; W&H Ltd., UK). Coolant flow rate: 45.1 mL/min (SD: 1.6), chip air activated.
- **Suction:** as for control, but with high-volume dental suction (238.8 L/min air flow rate [SD:3.3]) positioned 1 cm from the UR1 and held with a retort stand (figure 5.2).
- **Local exhaust ventilation (LEV):** as for control but with an LEV system (DA-UVC1001; VODEX Ltd., UK) with the inlet positioned 10 cm inferior to the mannequin's chin and on a plane 3 cm above the UR1 (figure 5.2). The device extracts air at the inlet nozzle and passes this through a high-efficiency particulate air (HEPA) filter at 5,000 L/min. A 254-nm, 27-mW/cm^2 UV-C light source is also positioned in the airflow before filtration. Irradiated and filtered air is then returned to the room at either side of the base unit.

- **Micromotor:** as for control but using a 1:5 speed-increasing handpiece (Ti-Max Z95L; NSK, Japan) driven by an electric micromotor (NLX Nano; NSK, Japan) instead of the air turbine handpiece. Speed: 200,000 rpm, coolant flow rate: 44.8 mL/min (SD: 1.3), no chip air activated, meaning that the bur was cooled by jets of water, rather than a mist of water and air (figure 5.3).

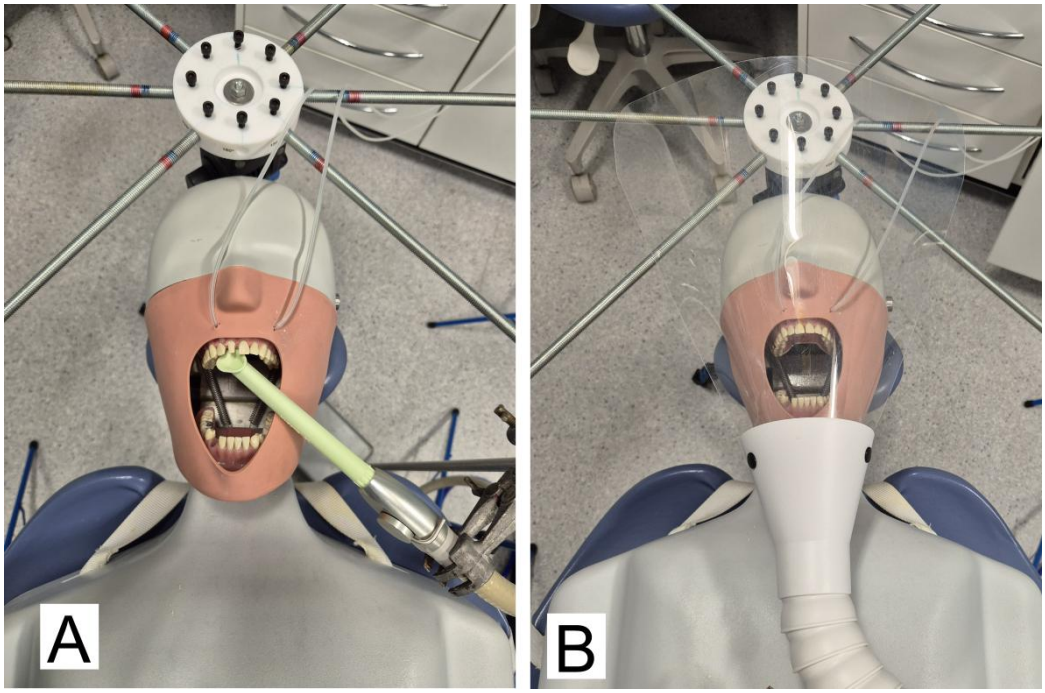

Figure 5.2. Dental bioaerosol control measures.

Positioning of (A) dental suction and (B) local exhaust ventilation used in experiments.

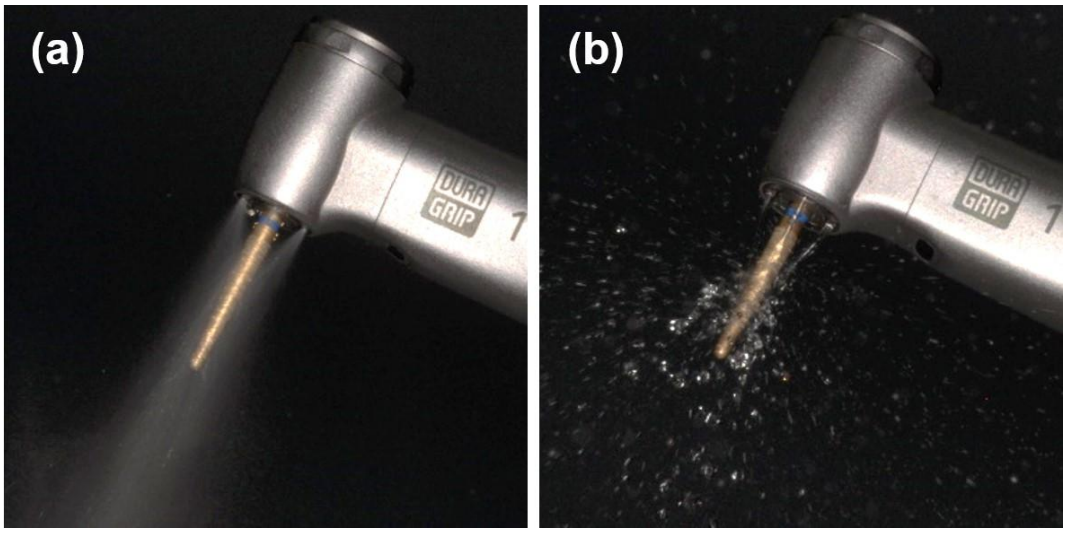

Figure 5.3. Micromotor handpiece irrigation.

Irrigation of the micromotor handpiece with chip air activated (a) showing mist of air and water, and (b) without chip air, showing jets of water only. Originally published in the *Journal of Dentistry* (Allison et al. 2021c), the author retains the rights to the image.

5.4 Effect of control measures on aerosol concentration

Mean temperature during experiments was 22.95 °C (SD: 0.43) and mean humidity was 40.39 %RH (SD: 8.43). Mean aerosol concentrations in the 3 min before the procedure (baseline), during the 10-min dental procedure, at the difference between the two are shown in table 5.1.

	Baseline aerosol concentration (0 – 3 min)		**Aerosol concentration during procedure (3 – 13 min)**		**Increase from baseline**, particles/cm^3
	Mean, particles/cm^3	SD	Mean, particles/cm^3	SD	
Control	15.72	6.65	43.51	15.22	**27.79**
Suction	12.18	4.82	22.12	2.78	**9.32**
LEV	24.60	5.44	26.06	2.14	**1.46**
Micromotor	23.42	4.67	45.60	16.79	**22.18**

Table 5.1. Mean aerosol concentration during a dental procedure with various individual aerosol control measures.

Mean and standard deviation (SD) aerosol particle number concentration in the 3 minutes preceding (baseline) and during a 10-min dental procedure with various bioaerosol control measures. Measured by optical particle counter at 0.6 m from the procedure. Difference = (procedure – baseline). *n* = 3 per condition. LEV = local exhaust ventilation.

Increases in aerosol particle number concentration were seen above baseline in the control condition from the start of the procedure, and distinct spikes in concentration were observed of up to 13-fold above baseline (figure 5.4). The increase above baseline and the presence of spikes in concentration were reduced with dental suction and practically eliminated with LEV. With the micromotor handpiece, similar increases above baseline were seen to the control condition and spikes in concentration of up to 8-fold above baseline. Aerosol concentration remained elevated above baseline for the entire period of sampling after the procedure (5 min post procedure) when the air turbine was used in the control condition. With the micromotor handpiece, the aerosol concentration reduced to baseline much more quickly after the procedure than the control condition.

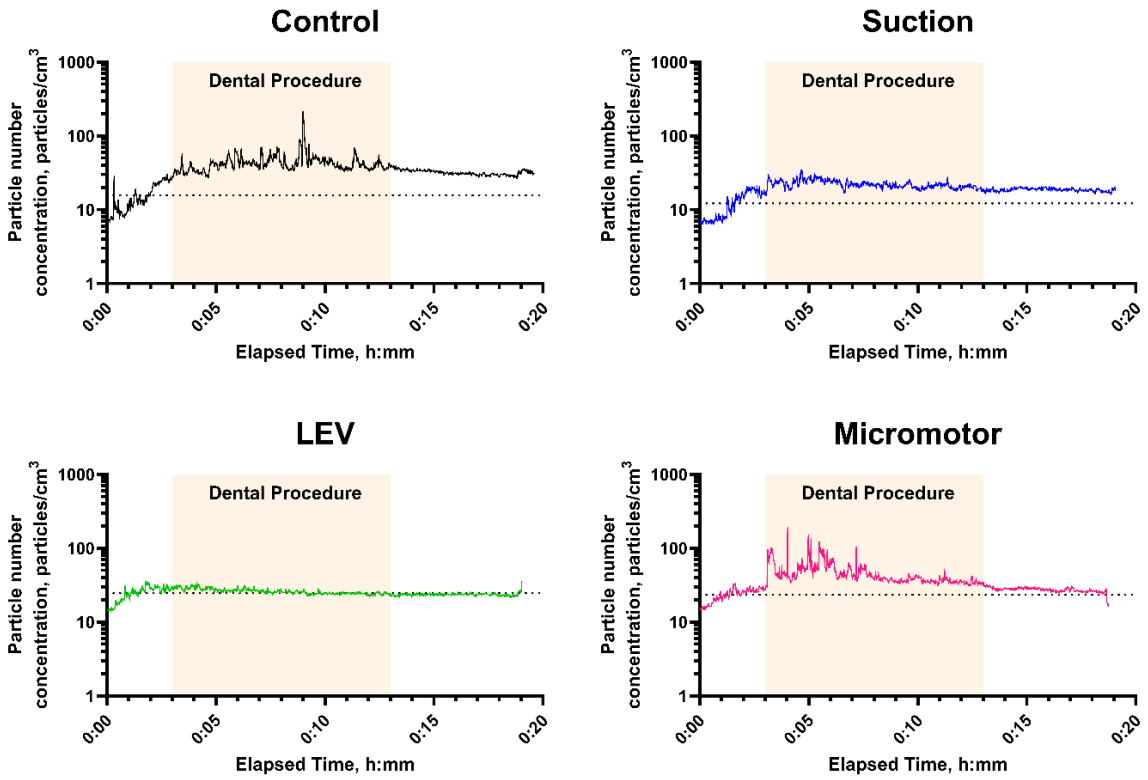

Figure 5.4. Aerosol particle concentration with various individual bioaerosol control measures.

Aerosol particle number concentration measured using an optical particle counter at 0.6 m before, during, and after a simulated dental procedure using different bioaerosol control measures. Particle concentration was summed over all particle size channels (0.3, 0.5, 1.0, 2.5, 5.0, 10.0 µm). Data shown are the average of 3 replicates with a sampling rate of 1 Hz. Individual replicate data are shown in appendix figure A.7. Shaded orange area denotes the duration of the dental procedure, and the dotted line denotes the background particle concentration in the 3 min preceding the procedure. LEV: Local Exhaust Ventilation.

OPC data was corrected for baseline by subtracting the mean of the first 3 min of data before the procedure from all data for each condition. Area under the curve (AUC) during the procedure (min 3 – 13) was then calculated (figure 5.5). Comparing AUC during the procedure, there were statistically significant differences between the different control measures (One-way ANOVA, $F(3, 8) = 10.53$, $p = 0.004$). Suction produced a 64.2% mean reduction in aerosol compared to control (*post hoc* Dunnett's test $q(8) = 4.090$, $p = 0.009$) and LEV a 76.1% reduction ($q(8) = 4.845$, $p = 0.003$). Micromotor reduced AUC by 19.9%, but this was not statistically significant ($q(8) = 1.262$, $p = 0.486$).

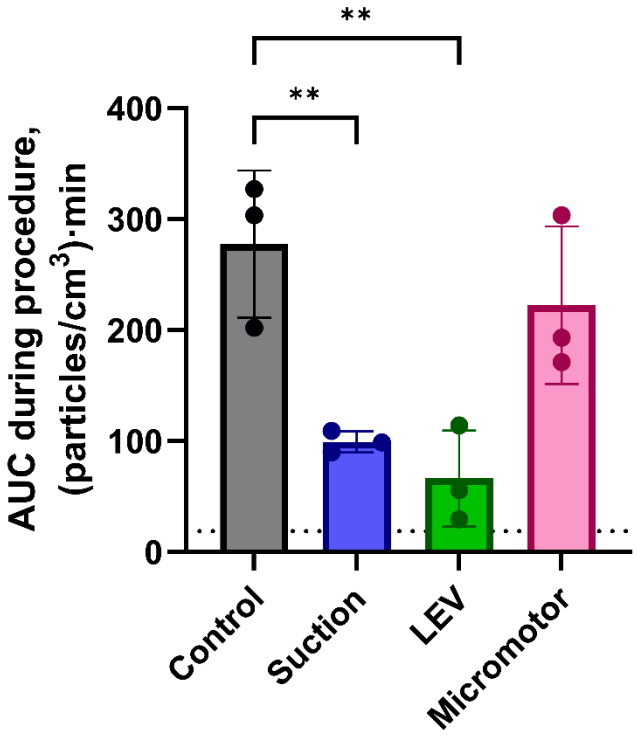

Figure 5.5. Differences in aerosol concentration during a dental procedure with various individual bioaerosol control measures.

Area under the curve (AUC) of aerosol particle number concentration (from figure 5.4) from the period during the 10-min dental procedure (3 – 13 min), corrected for baseline aerosol concentration (0 – 3 min). 3 replicates per condition, mean and standard deviation shown. LEV: Local Exhaust Ventilation. **: $p < 0.01$, one-way ANOVA with Dunnett's multiple comparisons test (comparing to control). Dotted line shows baseline aerosol concentration pooled from all conditions (mean 19.0 particles/cm^3, SD:10.8, $n = 12$).

Aerosol measured during control and suction conditions had similar particle size distributions, whereas during the LEV condition, proportionally more smaller particles were produced (84.74% ≤ 0.3 µm particles) than control (73.76% ≤ 0.3 µm particles). Micromotor produced the fewest ≤ 0.3 µm particles (67.04%) and proportionally more large particles than the other conditions (figure 5.6).

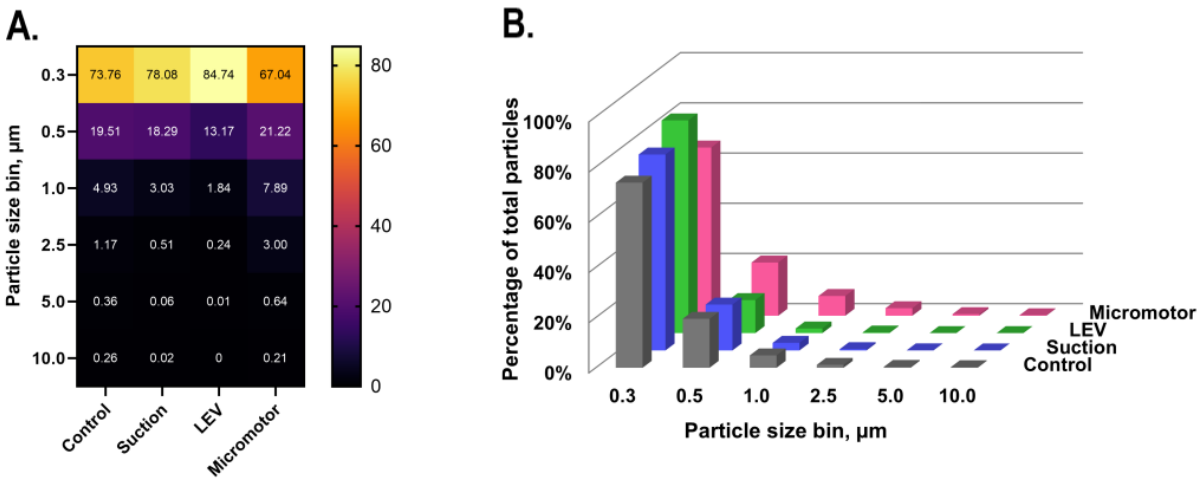

Figure 5.6. Particle size distribution with different individual bioaerosol control measures.

Percentage of total particles detected for each particle size bin with different aerosol control measures, shown as (A) heatmap and (B) grouped bar chart. OPC data from a 10-min dental procedure (*n* = 3 per condition). Numbers within cells in (A) denote the percentage of total particles contributed by that particle size. LEV = local exhaust ventilation.

5.5 Effect of control measures on infectious phage

Positive controls taken from the phage inoculum used in experiments showed a mean titre for MS2 of 1.22 x 10^{10} (SD: 1.41 x 10^{10}) PFU/mL and of 3.17 x 10^{10} (SD: 8.52 x 10^{9}) PFU/mL for phi6. Neither phage was seen in any negative control samples (figure 5.7).

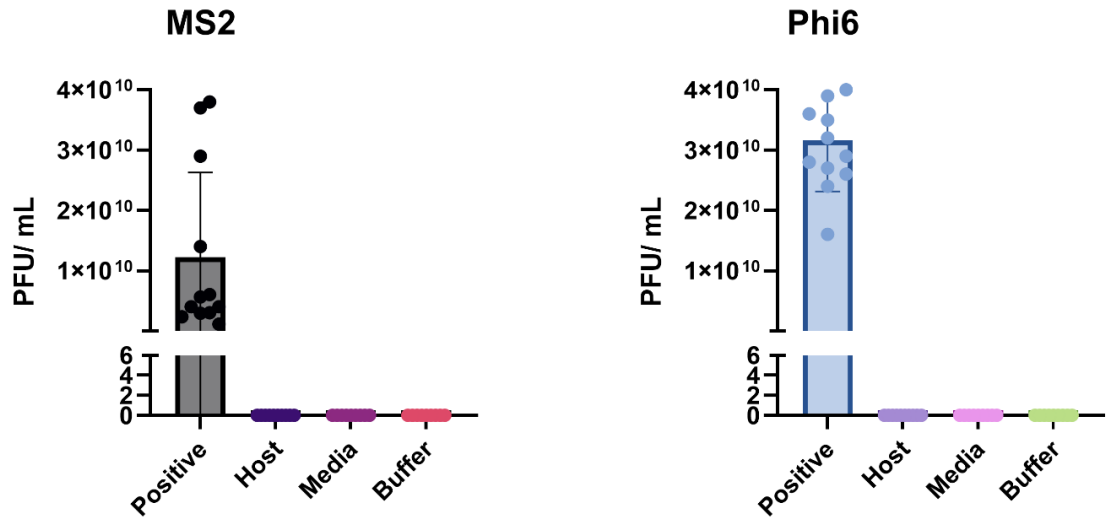

Figure 5.7. Infectious phage in positive and negative control samples.

Positive *n* = 12; host *n* = 10; others *n* = 9. PFU: Plaque-Forming Units.

For MS2, there was an overall difference in recovery of infectious virus in all surface samples between conditions (Kruskal-Wallis = 7.308, p = 0.033; figure 5.8) Recovery with suction was 99.7% lower compared to control, 99.9% lower with LEV, and 99.6% lower with micromotor, however, only LEV reached statistical significance in *post hoc* tests (Dunn's test, p = 0.038; table 5.2).

Using two-way ANOVA (main effect and interaction), both the aerosol control measure and distance from the procedure were included as factors for recovery of infectious MS2 in surface samples. Sample location accounted for 11.7% of variation in recovery ($F(2, 24) = 4.223$, p = 0.027), the aerosol control measure 21.5% of variation ($F(3, 24) = 5.103$, p = 0.007), with the interaction between the two factors (location and control measure) accounting for 34.0% ($F(6, 24) = 4.104$, p = 0.006). *Post hoc* comparison of each measure to control showed significant differences for suction (Dunnett's test, p = 0.011), LEV (p = 0.010), and micromotor (p = 0.011). Recovery by distance from the procedure is shown for each condition in figure 5.8.

In air samples, there was an overall difference in MS2 recovery between conditions (Kruskal-Wallis = 9.804, $p < 0.001$; Figure 5.8). Recovery with suction was 92.7% lower compared to control, 100% lower with LEV, and 82.1% lower with micromotor, however, only LEV reached statistical significance in *post hoc* tests (Dunn's test, p = 0.006; table 5.2).

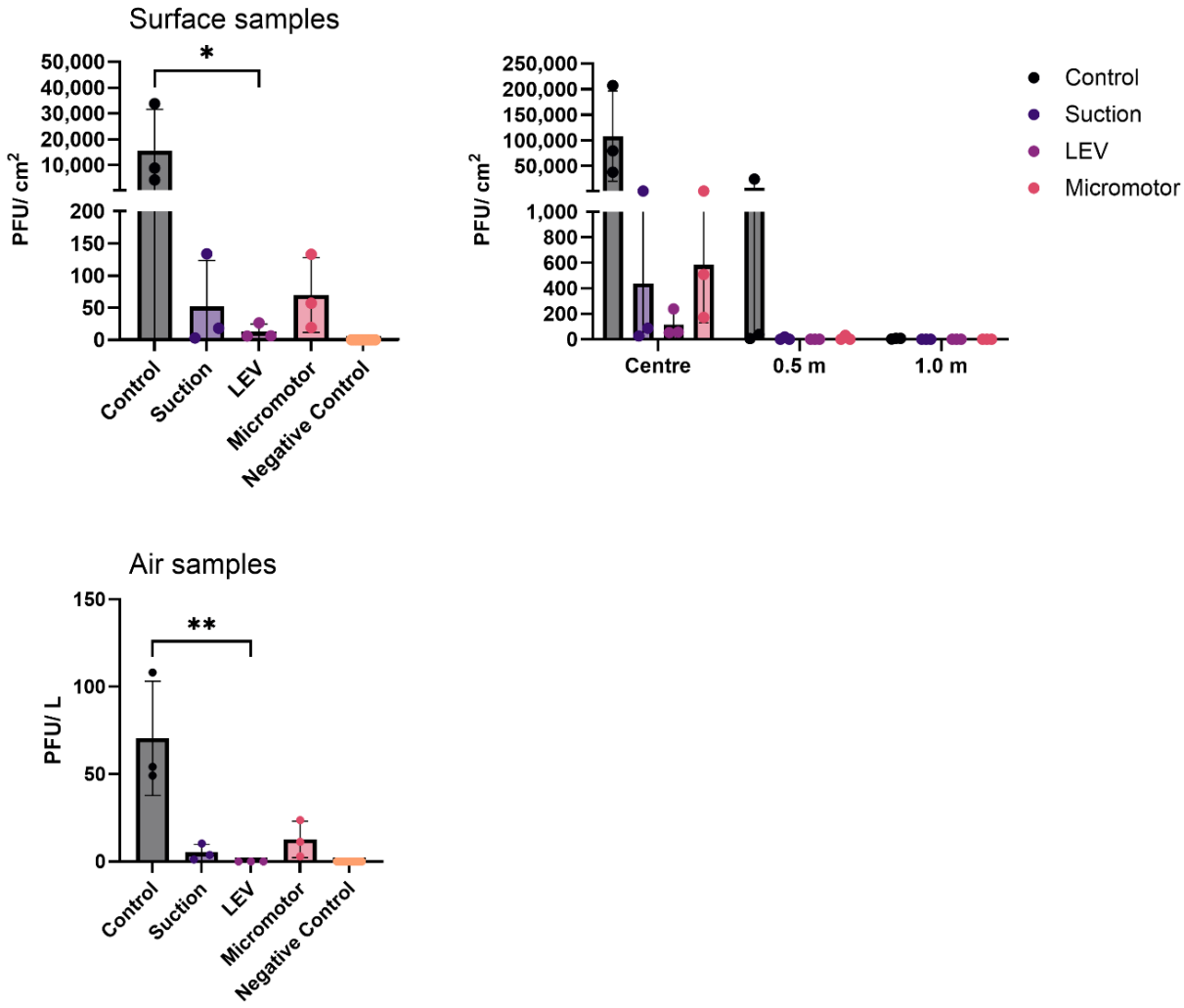

Figure 5.8. Infectious MS2 in surface and air samples during a dental procedure with various individual control measures.

MS2 recovered following a 10-min dental procedure on surfaces and air samples corrected for surface area/ air volume. For surface samples, the mean recovery in all samples for that replicate is shown (upper left panel), as well as mean recovery in samples at each distance from the procedure (upper right panel). For air samples, mean recovery in all samples within a replicate is shown. Data points show individual replicates (n = 3). Bars show mean and standard deviation. LEV: local exhaust ventilation. * = $p < 0.05$, ** = $p < 0.01$, Kruskal-Wallis test with Dunn's multiple comparisons test (comparing to control). Negative controls were not included in the statistical test.

For phi6, recovery in surface samples was 28.2% lower when suction was used compared to control, 100% lower with LEV, and 91.5% lower with micromotor, however, there was no statistically significant difference in recovery between conditions (Kruskal-Wallis = 6.310, p = 0.080; Figure 5.9; table 5.3).

Using two-way ANOVA (main effect and interaction), both the aerosol control measure and distance from the procedure were included as factors for recovery of infectious phi6 in surface samples. There was no significant effect of sample location

(F(2, 24) = 1.240, *p* = 307), aerosol control measure (F(3, 24) = 1.036, *p* = 0.394), or the interaction (F(6, 24) = 1.269, *p* = 0.308). Recovery by distance from the procedure is shown for each condition in figure 5.9.

In air samples, there was an overall difference in phi6 recovery between conditions (Kruskal-Wallis = 8.243, *p* = 0.014; figure 5.9). Recovery with suction was 39.7% higher compared to control, 100% lower with LEV, and 1,571% higher with micromotor, however, no individual condition reached statistical significance in *post hoc* tests (Dunn's test, *p* > 0.05). As the micromotor condition showed much greater recovery than control, sensitivity analysis was conducted by repeating the Kruskal-Wallis test with the micromotor data excluded. This analysis suggested no significant overall difference between conditions when micromotor data were excluded (Kruskal-Wallis = 5.609, p = 0.068; table 5.3).

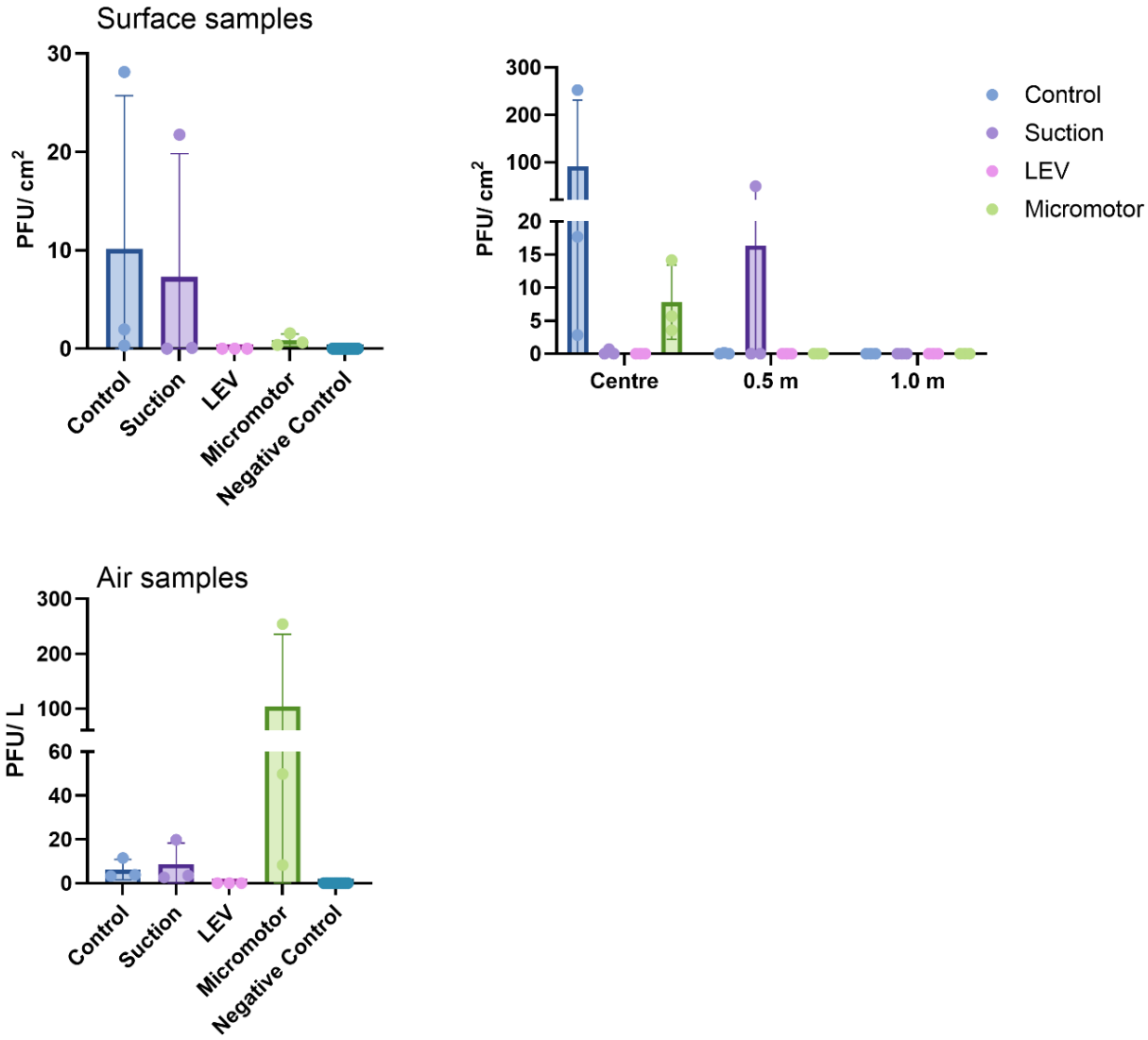

Figure 5.9. Infectious phi6 in surface and air samples during a dental procedure with various individual control measures.

Phi6 recovered following a 10-min dental procedure on surfaces and air samples corrected for surface area/ air volume. For surface samples, the mean recovery in all samples for that replicate is shown (upper left panel), as well as mean recovery in samples at each distance from the procedure (upper right panel). For air samples, mean recovery in all samples within a replicate is shown. Data points show individual replicates (*n* = 3). Bars show mean and standard deviation. LEV: local exhaust ventilation. There were no significant differences between groups (Kruskal-Wallis test with Dunn's multiple comparisons test comparing to control). Negative controls were not included in the statistical test.

	Surface samples		
	Mean, PFU/cm^2	SD	% difference compared to control
Control	15,650	15,888	-
Suction	51.8	71.6	-99.7%
LEV	12.9	11.8	-99.9%*
Micromotor	69.7	58.0	-99.6%
	Air samples		
	Mean, PFU/L	SD	% difference compared to control
Control	70.5	32.7	-
Suction	5.1	4.7	-92.7%
LEV	0	0	-100%*
Micromotor	12.6	10.4	-82.1%

Table 5.2. Recovery of infectious MS2 during a dental procedure with various individual aerosol control measures.

Mean and standard deviation (SD) recovery of infectious MS2 in surface and air samples following a 10-min dental procedure with various bioaerosol control measures, measured using plaque assays. *n* = 3 per condition. LEV = local exhaust ventilation. * = statistically significant difference (Kruskal-Wallace with *post hoc* Dunn's test, $p < 0.05$).

	Surface samples		
	Mean, PFU/cm^2	SD	% difference compared to control
Control	10.1	15.6	-
Suction	7.3	12.6	-28.2%
LEV	0.0	0.0	-100%
Micromotor	0.9	0.6	-91.5%
	Air samples		
	Mean, PFU/L	SD	% difference compared to control
Control	6.2	4.6	-
Suction	8.7	9.7	+39.7%
LEV	0.0	0.0	-100%
Micromotor	104	131	+1,571%

Table 5.3. Recovery of infectious phi6 during a dental procedure with various individual aerosol control measures.

Mean and standard deviation (SD) recovery of infectious phi6 in surface and air samples following a 10-min dental procedure with various bioaerosol control measures, measured using plaque assays. *n* = 3 per condition. LEV = local exhaust ventilation. * = statistically significant difference (Kruskal-Wallace with *post hoc* Dunn's test, $p < 0.05$).

5.6 Effect of control measures on phage RNA

Positive control samples from the phage inoculum used in experiments showed this to contain 4.48 x 10^{12} copies/mL (SD: 2.11 x 10^{12}) for MS2, and 2.10 x 10^{10} copies/mL (SD: 9.68 x 10^{9}) for phi6. Plasmid DNA standards also amplified as expected, showing 1.80 x 10^{8} copies/mL (SD: 2.84 x 10^{7}) for MS2 plasmid standards and 2.12 x 10^{10} copies/mL (SD: 1.93 x 10^{9}) for phi6 standards (figure 5.10).

One of 12 phi6 assay negative controls for the reverse transcription (RT) step amplified (2.35 x 10^{4} copies/mL; limit of detection [LoD] 1.45 x 10^{3} copies/mL), however, all other RT (*n* = 12 per phage) and no-template (*n* = 7 per phage) negative controls were negative.

Seven out of ten assay negative controls for the RNA extraction step (blank SM buffer) amplified for MS2 with mean 1.05 x 10^{6} copies/mL (SD: 2.49 x 10^{6}; LoD: 1.69 x 10^{4}). Seven out of ten RNA extraction negative controls also amplified for phi6 with mean 2.88 x 10^{4} copies/mL (SD: 7.76 x 10^{4}; LoD: 1.45 x 10^{3}).

In experiment negative controls (blank filter papers and BioSampler taken during experiments), mean recovery of MS2 in surface samples was 4.49 x 10^{4} copies/cm^{2} (SD: 7.35 x 10^{4}; LoD: 1.19 x 10^{3}) and in air samples was 2.82 x 10^{3} copies/L (SD: 7.62 x 10^{3}; LoD: 1.50 x 10^{3}; figure 5.11). For phi6, recovery in negative control surface samples was 6.43 x 10^{2} copies/cm^{2} (SD: 8.84 x 10^{2}; LoD: 1.03 x 10^{2}) and air samples was 5.39 x 10^{1} copies/L (SD: 1.48 x 10^{2}; LoD: 1.29 x 10^{2}; figure 5.12).

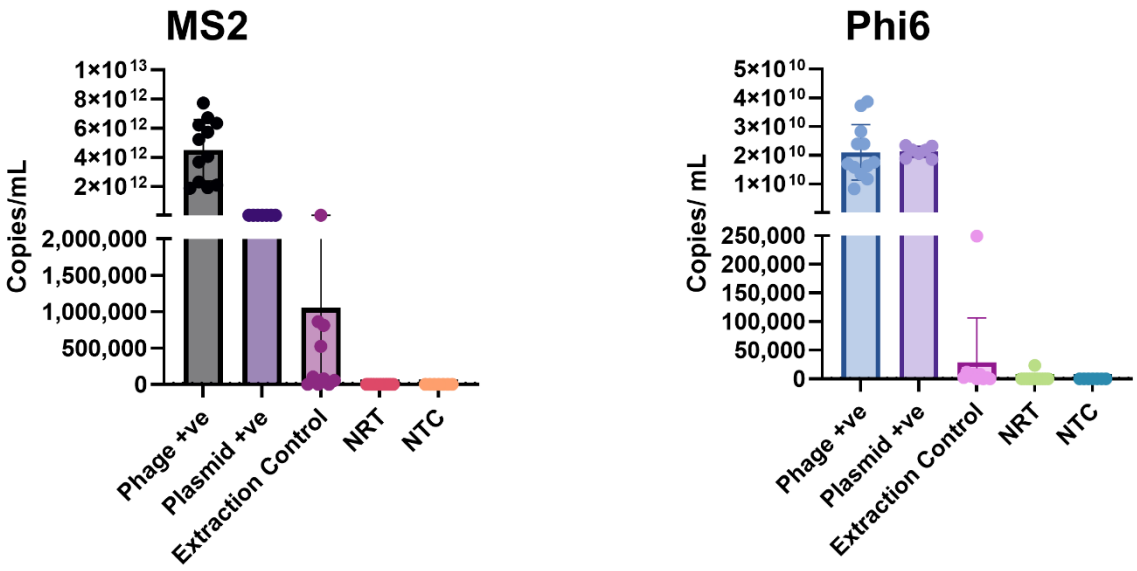

Figure 5.10. Phage RNA in positive and negative control samples.

Phage +ve (inoculum used in experiments) *n* = 12; Plasmid +ve (DNA standard used in qPCR) and no-template control (NTC) *n* = 7; extraction control (buffer used for elution) *n* = 10; no-template control (NTC, control for reverse transcription step) *n* = 7. Limit of detection, MS2: 16,891 copies/mL; phi6: 1,450 copies/mL.

For MS2, there was an overall difference in recovery of viral RNA in surface samples between conditions (Kruskal-Wallis = 8.436, $p = 0.011$; figure 5.11). Recovery with suction was 95.8% lower compared to control, 99.7% lower with LEV, and 97.4% lower with micromotor, however, only LEV reached statistical significance in *post hoc* tests (Dunn's test, $p = 0.014$; table 5.4).

Using two-way ANOVA (main effect and interaction), both the aerosol control measure and distance from the procedure were included as factors for recovery of MS2 RNA in surface samples. The control measure was the only significant factor in the ANOVA model, accounting for 17.4% of variance in recovery ($F(3, 24) = 3.202$, $p = 0.041$). Location ($F(2, 24) = 2.660$, $p = 0.091$) and the interaction ($F(6, 24) = 2.436$, $p = 0.056$) were not significant factors in the ANOVA model. *Post hoc* comparison of each measure to control showed significant differences for suction (Dunnett's test, $p = 0.048$) and LEV ($p = 0.044$), but not for micromotor ($p = 0.052$). Recovery by distance from the procedure is shown for each condition in figure 5.11.

In air samples, there was an overall difference in MS2 recovery between conditions (Kruskal-Wallis = 7.513, $p = 0.028$; figure 5.11). Recovery with suction was 73.1% lower compared to control, 71.2% lower with LEV, but 107% *higher* with micromotor.

None of the individual control measures reached statistical significance in *post hoc* tests however (Dunn's test, $p > 0.05$; Table 5.4). As the micromotor condition showed greater recovery than control, sensitivity analysis was conducted by repeating the Kruskal-Wallis test with Micromotor data excluded. The results showed little difference, with an overall significant effect (Kruskal-Wallis = 5.600, $p = 0.050$), but no individual measure reached statistical significance in *post hoc* tests (Dunn's test, $p > 0.05$).

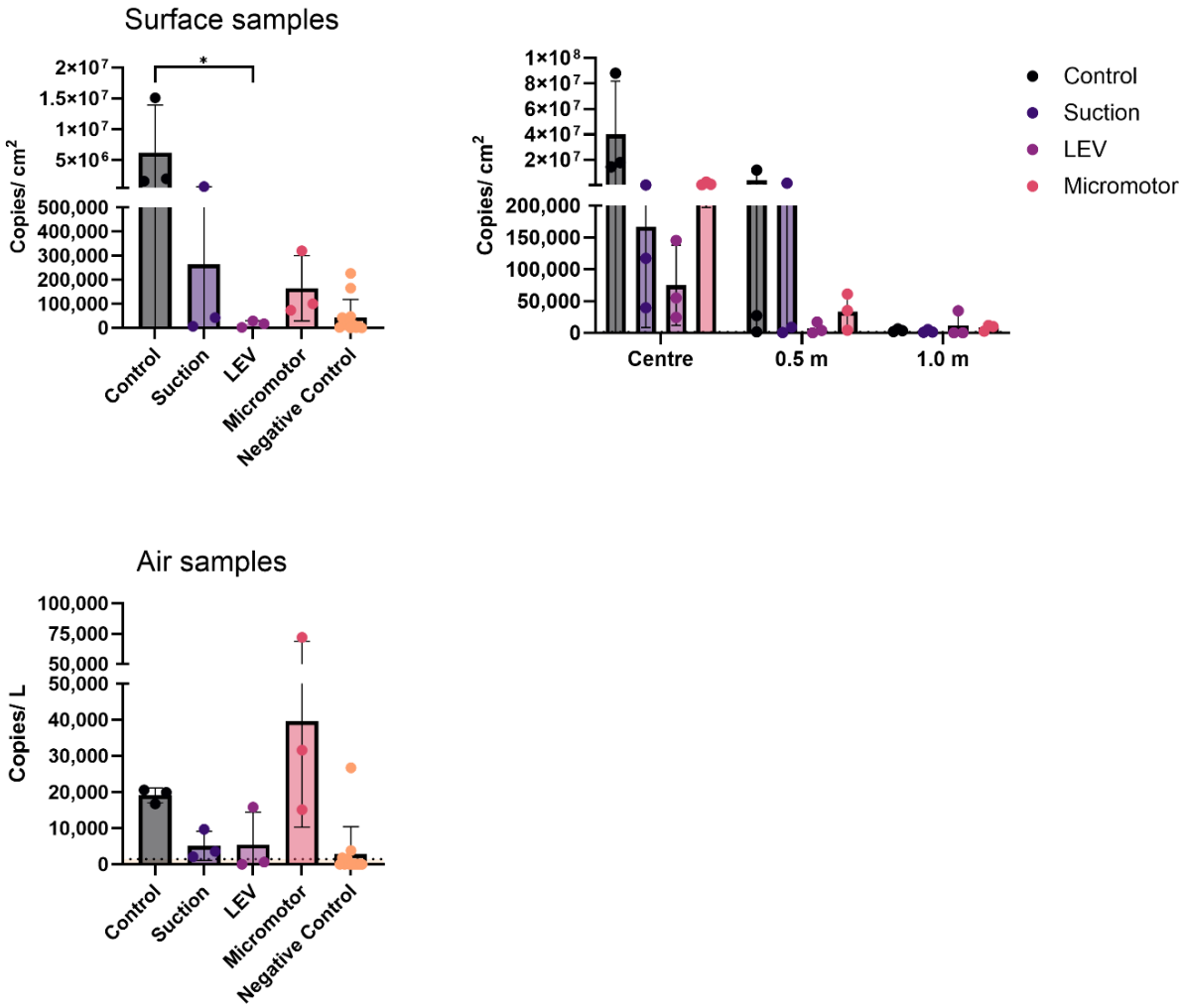

Figure 5.11. MS2 RNA in surface and air samples during a dental procedure with various individual control measures.

MS2 RNA recovered following a 10-min dental procedure on surfaces and air samples corrected for surface area/ air volume. For surface samples, the mean recovery in all samples for that replicate is shown (upper left panel), as well as mean recovery in samples at each distance from the procedure (upper right panel). For air samples, mean recovery in all samples within a replicate is shown. Data points show individual replicates ($n = 3$). Bars show mean and standard deviation. LEV: local exhaust ventilation. * = $p < 0.05$, Kruskal-Wallis test with Dunn's multiple comparisons test (comparing to control). Negative controls were not included in the statistical test. The dotted line denotes the limit of detection of the RT-qPCR assay (1,194 copies/cm^2 or 1,501 copies/L).

For phi6, there was an overall difference in recovery of viral RNA in surface samples between conditions (Kruskal-Wallis = 9.701, $p < 0.001$; figure 5.12). Recovery with suction was 94.2% lower compared to control, 99.9% lower with LEV, and 99.2% lower with micromotor, however, only LEV reached statistical significance in *post hoc* tests (Dunn's test, $p = 0.007$; table 5.5).

Using two-way ANOVA (main effect and interaction), both the aerosol control measure and distance from the procedure were included as factors for recovery of infectious MS2 in surface samples. Neither the control measure ($F(3, 24) = 2.966$, $p = 0.052$), sample location ($F(2, 24) = 2.369$, $p = 0.115$), nor the interaction ($F(6, 24) = 2.251$, $p = 0.073$) emerged as statistically significant factors in the model. No individual control measure reached statistical significance in *post hoc* comparison (Dunnett's test, $p > 0.05$). Recovery by distance from the procedure is shown for each condition in figure 5.12.

In air samples, Recovery with suction was 13.5% lower compared to control, 91.6% lower with LEV, and 18.2% lower with micromotor, however there was no statistically significant overall difference in phi6 recovery between conditions (Kruskal-Wallis = 5.069, $p = 0.170$; figure 5.12; table 5.5).

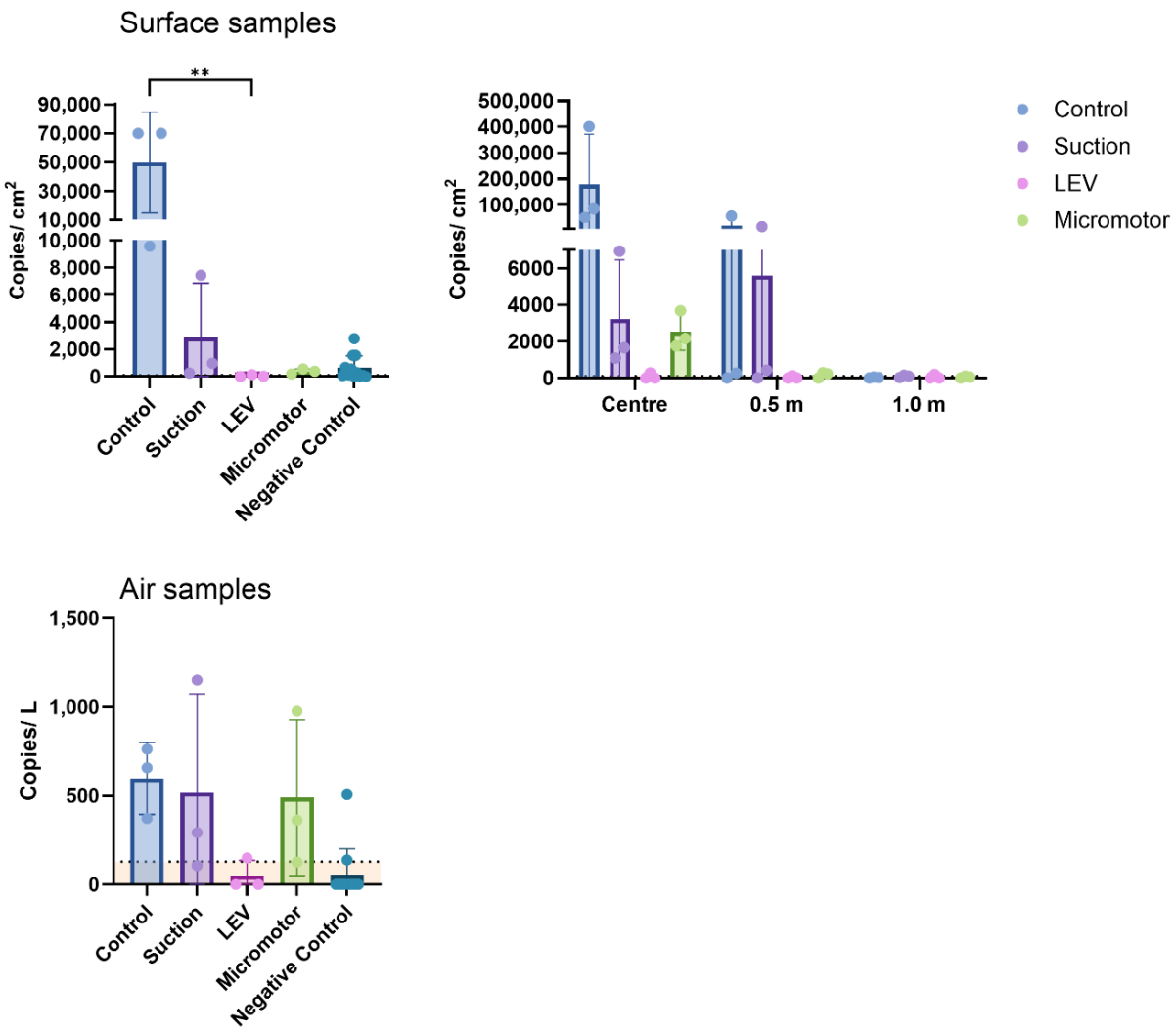

Figure 5.12. Phi6 RNA in surface and air samples during a dental procedure with various individual control measures.

Phi6 RNA recovered following a 10-min dental procedure on surfaces and air samples corrected for surface area/ air volume. For surface samples, the mean recovery in all samples for that replicate is shown (upper left panel), as well as mean recovery in samples at each distance from the procedure (upper right panel). For air samples, mean recovery in all samples within a replicate is shown. Data points show individual replicates (n = 3). Bars show mean and standard deviation. LEV: local exhaust ventilation. * = $p < 0.05$, Kruskal-Wallis test with Dunn's multiple comparisons test (comparing to control). Negative controls were not included in the statistical test. The dotted line denotes the limit of detection of the RT-qPCR assay (102 copies/cm^2 or 128 copies/L).

	Surface samples		
	Mean, copies/cm^2	SD	% difference compared to control
Control	6.25×10^6	7.68×10^6	-
Suction	2.64×10^5	4.15×10^5	-95.8%
LEV	1.66×10^4	1.33×10^4	-99.7%*
Micromotor	1.65×10^5	1.35×10^5	-97.4%
	Air samples		
	Mean, copies/L	SD	% difference compared to control
Control	1.91×10^4	2.05×10^3	-
Suction	5.13×10^3	4.03×10^3	-73.1%
LEV	5.49×10^3	8.97×10^3	-71.2%
Micromotor	3.96×10^4	2.93×10^4	+107%

Table 5.4. Recovery of MS2 RNA during a dental procedure with various individual aerosol control measures.

Mean and standard deviation (SD) recovery of MS2 RNA in surface and air samples following a 10-min dental procedure with various bioaerosol control measures, measured using RT-qPCR. *n* = 3 per condition. LEV = local exhaust ventilation. * = statistically significant difference (Kruskal-Wallace with *post hoc* Dunn's test, $p < 0.05$).

	Surface samples		
	Mean, copies/cm^2	SD	% difference compared to control
Control	4.97×10^4	3.48×10^4	-
Suction	2.89×10^3	3.96×10^3	-94.2%
LEV	5.95×10^1	7.76×10^1	-99.9%*
Micromotor	3.82×10^2	1.81×10^2	-99.2%
	Air samples		
	Mean, copies/L	SD	% difference compared to control
Control	5.98×10^2	2.02×10^2	-
Suction	5.17×10^2	5.58×10^2	-13.5%
LEV	5.00×10^1	8.66×10^1	-91.6%
Micromotor	4.89×10^2	4.39×10^2	-18.2%

Table 5.5. Recovery of phi6 RNA during a dental procedure with various individual aerosol control measures.

Mean and standard deviation (SD) recovery of phi6 RNA in surface and air samples following a 10-min dental procedure with various bioaerosol control measures, measured using RT-qPCR. *n* = 3 per condition. LEV = local exhaust ventilation. * = statistically significant difference (Kruskal-Wallace with *post hoc* Dunn's test, $p < 0.05$).

5.7 Discussion

In these experiments comparing dental bioaerosol control measures, reductions in physical aerosol concentration were seen using dental suction, LEV, and a micromotor handpiece compared to a control condition using an air turbine handpiece without any other aerosol control measure. The distribution of aerosol particle sizes produced differed between conditions, with the micromotor producing comparatively fewer small particles than the air turbine; the opposite effect was seen for suction and LEV, with smaller particles being more numerous than in the control condition. This reduction in physical aerosol corresponded with a reduction in the amount of infectious virus detected in surface and air samples around the procedure, with a particularly significant effect for LEV. The effect of the micromotor handpiece was more varied, with modest reductions in infectious MS2 compared to control in surface and air samples and in phi6 in surface samples but *increases* in phi6 recovery in air samples. Overall, comparatively greater amounts of phage RNA were recovered than infectious phage, suggesting not all dispersed phage remains infective. The pattern was similar to that seen for infective phage, with reductions in RNA recovery when bioaerosol control measures were used, especially in surface samples and for LEV. Both infectious phage and phage RNA were recovered in greater amounts closest to the procedure in samples at the centre of the sampling rig (0.2 m), consistent with the data from dispersion experiments in Chapter 4.

During the control condition, without any aerosol control measure, frequent spikes in OPC-measured aerosol concentration of up to 13-fold above baseline were observed, consistent with other studies reporting aerosol concentration over time during a dental procedure (Allerton et al. 2021; Allison et al. 2021b; Allison et al. 2021c; Shahdad et al. 2021; Tompkins et al. 2020). This is likely because the aerosol produced by the air turbine is highly directional, and fluctuations in aerosol concentration at any particular location vary as the operator moves the handpiece to conduct the dental procedure. With the micromotor handpiece, similar spikes of up to 8-fold above baseline were seen. Although such spikes have been reported for micromotor handpieces cooled by a jet of water, the amount of aerosol reported in the literature is generally less than for an air turbine (Allison et al. 2021c; Vernon et al. 2021). In the present experiments, despite similar spikes, using the micromotor reduced area under the curve by 19.9% compared to control, which would support the existing literature. The presence of distinct spikes in aerosol concentration

suggests dental professionals are exposed to transiently high concentrations of aerosol which vary over time. Studies which rely on measuring only average aerosol concentration (Dudding et al. 2022; Gheorghita et al. 2022; Rafiee et al. 2022) may therefore miss important temporal features of the aerosol produced. Spikes in aerosol concentration were substantially reduced by suction and eliminated completely by LEV. This was accompanied by reductions in area under the curve of 64.2% for suction and 76.1% for LEV, demonstrating the benefit of these control measures in reducing the total amount of aerosol that escapes the mouth.

Aerosol measured during procedures with suction and LEV had a comparatively smaller distribution of particles (78% and 84% ≤ 0.3 μm respectively) than the control condition (74% ≤ 0.3 μm), presumably because larger aerosol particles produced by the handpiece were able to escape the mouth less easily and were preferentially captured by suction or LEV. Conversely, the micromotor handpiece produced comparatively fewer small particles (65% ≤ 0.3 μm). This may be because, without high-pressure air mixing with irrigant water, the mist of small particles produced by the air turbine was not observed (figure 5.3). This is well demonstrated using imaging techniques by Sergis *et al.* (2020), who showed that two mechanisms exist to produce dental instrument aerosols: firstly the production of fine aerosol droplets by high pressure air (chip air) premixed with water irrigant, producing a plume of aerosol aligned with the direction of the bur; secondly the atomisation of irrigant water and oral fluids coming into contact with the spinning bur, producing aerosol disseminated radially from the bur. The latter is dependent on bur speed, although the authors suggest that this atomisation is minimal below 80,000 – 100,000 rpm.

Baseline aerosol concentration in the 3 min prior to the procedure (table 5.1) was higher for LEV compared to the other conditions. This is likely because while the LEV device is running, HEPA filtered air is blown out of the exhaust vents of the device back into the room, liberating particles from the surrounding surfaces and increasing overall room particle concentration. This could pose a risk in clinical practice if infectious droplets are resuspended in the air. Despite this, very little increase from baseline aerosol concentration was seen with LEV during the procedure, as any additional aerosol was captured and filtered. This demonstrates a limitation of comparing experimental measurements taken using an OPC to baseline measurements obtained under different conditions or at a different time. Doing so may give inaccurate results, as baseline aerosol concentration will vary depending on

many factors including activity in the room and environmental conditions. Correction of experimental data to the baseline values obtained immediately prior to an experiment is therefore preferable as in the present experiment (Gregson et al. 2021).

All bioaerosol control measures substantially reduced the amount of infective MS2 recovered from surfaces, with reductions of >99% seen for suction, LEV, and micromotor. Similar reductions in MS2 recovery were seen in air samples, albeit more modest for micromotor (82%), however recovery was completely eliminated by LEV. The distance from the procedure also had a significant effect on recovery, with most infectious MS2 found at the centre of the sampling rig next to the mannequin (0.2 m). Recovery of phi6 was comparatively lower in surface samples than for MS2, similar to findings in Chapter 3 and 4. In air samples, the recovery of phi6 during the control condition was considerably lower than for MS2 (6.2 PFU/L vs 70.5 PFU/L), despite this being much more similar in experiments in Chapter 4, and in both sets of experiments MS2 and phi6 starting titre was similar. The effect of bioaerosol control measures on recovery of infectious phi6 was also more mixed than for MS2, with suction showing little benefit in either surface (28% reduction) or air samples (40% increase), and micromotor showing reductions (92%) in surface samples but a substantial increase (1,571%) in air samples. Indeed, the data for phi6 demonstrate substantial noise which may limit confidence in the data for this phage. As well as this noise, the unexpected low recovery of phi6 in control air samples likely accounts for the limited benefit of control measures compared to MS2.

The increase with micromotor in air samples could potentially be due to the larger droplets produced by the micromotor handpiece being captured in the BioSamplers (located at 0.5 m), with larger droplets having the potential to hold more phage than smaller droplets produced by the air turbine in other conditions. It also may be a chance finding due to the stochastic nature of the aerosols produced and inherent variability of the dental procedure conducted. Similar to MS2, whilst not statistically significant, no infectious phi6 was recovered in surface and air samples when LEV was used, demonstrating consistent effectiveness of this measure across different viruses and sample types. Indeed, only LEV was statistically significant in *post hoc* comparisons for infectious MS2 in surface and air samples. The lack of significance in other conditions may be due to the degree of variation seen between replicates. This is an inevitable result of conducting a real dental procedure, even under

controlled conditions; for example, to complete the same procedure the same operator may not carry out the exact same sequence of movements each time. Eliminating this real-world variation would limit the clinical relevance of the model. In future studies however, a greater number of replicates should be conducted for each condition to reduce the statistical variation, making tests of significance more reliable.

For the RT-qPCR analysis, all but one assay negative control samples for the reverse transcription step (no reverse transcriptase), and all negative control samples from the qPCR step (no DNA template) did not show amplification. 70% of the assay negative controls for the RNA extraction step (blank SM buffer used for elution) did however show amplification above the assay LoD. Despite this, negative control samples taken during the experiment (blank filter papers and BioSamplers) which used the same RNA extraction process showed amplification which was closer to the LoD although amplification remained largely lower that for experimental samples. This highlights the high sensitivity of the RT-qPCR assay and the need for meticulous control of contamination. Repeating the analysis from the original samples with new reagents would have been ideal, however, insufficient original sample remained after conducting the RT-qPCR assay as all available sample (200 µL) following plaque assays, was used in the RNA extraction step. For future work, the overall volume used to elute phage from filter papers could be increased, however this would further dilute any eluted phage, lowering the sensitivity of downstream plaque assays and RT-qPCR; this approach would therefore be a trade-off.

Recovery of phage RNA was considerably higher than that of infective phage, for example, mean recovery of infectious MS2 in surface samples from the control condition was 1.56×10^4 PFU/cm^2, however recovery of MS2 RNA was 6.25×10^6 copies/cm^2, a 2.6-log difference. This suggests that the detection of viral nucleic acids does not necessarily equate to the amount of infectious virus present, and inactivation of a significant proportion of the virus dispersed is likely to occur. This will differ depending on the specific virus and its survival in air and on surfaces, but the difference in RNA recovery versus infectious virus appears to hold true for both non-enveloped MS2 and enveloped phi6.

Reductions in phage RNA recovery were broadly similar to reductions in infectious phage, with suction, LEV, and micromotor producing reductions of >95% in surface samples for MS2 and phi6, with a particularly substantial effect of LEV which showed recovery of phage RNA close to the LoD of the assay in surface samples. In air

samples, LEV again showed the most substantial effect with reductions of 71.2% in recovery of MS2 and 91.6% for phi6, with the latter being below the limit of detection. Suction showed a more mixed effect in air samples, with a 73.1% reduction in MS2 RNA, but only a 13.5 % reduction in phi6. The same was true for micromotor, with a 18.2% decrease in phi6 RNA recovery, but a 107% *increase* in MS2 recovery. This parallels the findings for infectious phage in that LEV was consistently most effective, suction more modestly effective, and micromotor having a variable effect in air samples.

Overall, the reductions observed for suction in particle concentration measured using OPC (64.2%), infectious phage in surface (up to 99.7%) and air samples (up to 92.7%), and phage RNA in surface (up to 96%) and air samples (up to 73.1%) are consistent with the findings of previously reported studies. For example, 80 – 90% reductions in the dispersion of bacteria have been reported in clinical studies when dental suction is used, particularly closest to the procedure as observed in the present data (Kumbargere Nagraj et al. 2020; Samaranayake et al. 2021; SDCEP 2021b). Other methodologies using droplet imaging (Watanabe et al. 2023), fluorescent tracers (Allison et al. 2021a), and a phage tracer (phi6) (Malmgren et al. 2023) have demonstrated reductions with dental suction of 67 – 92%. One major benefit for dental suction is that it is already widely used in routine dental practice to remove instrument irrigant and oral fluids from the mouth, and dental teams are familiar with its use. This means that some level of protection is provided from infectious aerosols when suction is used to treat patients with a known respiratory infection, or during times of high population prevalence, for example during an infectious disease outbreak as seen in the COVID-19 pandemic. There would therefore be few barriers to the implementation of this measure. More work however needs to be done to understand the risk to staff of suction devices that return unfiltered air to the treatment room given some evidence of increased infection risk (Sarapultseva et al. 2021). Systems that vent externally to the treatment room or use HEPA filtration would minimise this risk.

Similarly, the reductions observed with LEV in aerosol concentration (76.1%), infectious phage, and phage RNA in surface and air samples (up to 100%) concord with previous work. For example, reductions in bacterial dispersion in clinical studies (Takenaka et al. 2022), in aerosol concentration with particle counting instruments (Ehtezazi et al. 2021), and in recovery of fluorescent tracers in simulation studies

(Allison et al. 2021b) of 75 – 93% have been reported. One disadvantage with LEV however is that it is not widely used in dental practice and is unlikely to be readily implementable across the profession in any future outbreak. Additionally, the cost of the device could be prohibitive, with the device used in the present experiments retailing at £2,340 (~$3,150) at the time of writing, plus significant energy costs when in use. Cost is likely to be particularly prohibitive in low- and middle-income countries, potentially limiting the use of this measure. LEV devices extract air from the immediate vicinity of the dental procedure and pass the air through HEPA filters before recirculating; this design is similar to portable air cleaners, which filter and recirculate air within a room. During the COVID-19 pandemic, cheap and simple do-it-yourself designs for air cleaners consisting of panel filters and a box fan secured together with duct tape were widely circulated and implemented (The Corsi-Rosetnhal Foundation 2023). These designs have been shown to effectively reduce simulated respiratory aerosols (Derk et al. 2023), and it is conceivable that a similar approach could be used to construct a low-cost LEV device which could be more easily implemented in resource-limited settings. Another limitation of LEV is the increased noise produced by the device during use, which can be unpleasant, and adversely effects patient-reported satisfaction with treatment (Barrett et al. 2022). This is likely to limit the application of LEV in routine practice, however when treating patients with respiratory infections or during outbreaks, the benefits of LEV likely outweigh the increased noise level.

Whilst findings for suction and LEV are consistent with the existing literature, the picture for the micromotor handpiece is more mixed. With the OPC, aerosol concentration was only 19.9% lower during the procedure, compared to findings from a study using an aerodynamic particle sizer to measure aerosol concentration during treatment in patients, which found 100-fold lower aerosol concentration using an electric surgical handpiece compared to an air turbine handpiece (Dudding et al. 2022). The particle measurement instrument used in this study however was able to measure a slightly broader range of particle sizes (0.5 – 20 μm) and was positioned closer (0.22 m) to the source than the present experiments (0.3 – 10 μm; 0.6 m). Additionally, the handpiece speed used (40,000 rpm) was substantially lower than that used in the present work (200,000 rpm), and such low bur speeds for restorative work can be technically challenging (Allison et al. 2021c). Reductions in infectious phage with the micromotor were generally substantial (82.1 – 99.6%) except for phi6 air samples, where there was a 1,571% (16-fold) increase. As discussed, this may be

a result of larger droplets produced by the micromotor handpiece, as demonstrated by the OPC data, having the potential to contain more phage. This, however, conflicts with previous work using a phi6 tracer which found 360-fold reductions in surface samples, and 195-fold reductions in air samples (Vernon et al. 2021; Vernon et al. 2022). Given that simulation models using a fluorescent tracer also point to micromotor producing substantially less potentially-contaminated aerosol (Allison et al. 2021c), it is likely that the finding of increased recovery of phi6 in air samples is a spurious finding in this instance.

As Sergis *et al.* (2020) demonstrated, mixing of chip air and coolant water is the predominant mechanism of handpiece aerosol production. For any benefit from an electric micromotor handpiece over the air turbine in aerosol reduction, the micromotor must therefore use water only to cool the bur, without premixing with air. Micromotor handpieces were discussed in UK guidance on managing risk from dental bioaerosols during the COVID-19 pandemic (SDCEP 2021a). Although bur speeds of <60,000 rpm were recommended to reduce radial atomisation via contact with the spinning bur, the importance of the type of cooling (with/without chip air) was not clear in this publication. Future guidance should make this important factor clearer, and authors should consider recommending electric micromotor handpieces cooled only by water (no chip air) as a bioaerosol control measure. Some authors have suggested that irrigation only with water may reduce cooling efficiency and risk damage to the dental pulp (Allison et al. 2021c; Vernon et al. 2022), however at an irrigation rate of 30 mL/min, the use of a water-jet–cooled electric handpiece does not produced increased temperatures in the dental pulp compared to an air turbine cooled at the same rate with air and water (Lempel and Szalma 2022). Finally, despite increased torque and handpiece weight compared to an air turbine, the micromotor handpiece has favourable cutting efficiency, reported operator preference, and lower noise of operation (Eikenberg 2001; Pei et al. 2021).

In conclusion, all three bioaerosol control measures studied produced substantial reductions in the dispersion of virus within dental bioaerosols, particularly in surface samples from large droplets and settled aerosols. The mechanism of this is either by reducing the amount of physical aerosol produced, as in the case of the micromotor handpiece, or by capturing the aerosol at source in the case of suction and LEV. All measures are likely to be useful in reducing the risk of infection both when treating patients with endemic respiratory diseases and during an emerging infectious

disease outbreak, particularly when used together. Of the three measures, LEV was most effective, often eliminating detection of infectious virus in surface and air samples completely, although cost and noise may limit use in routine dental care. Suction is an effective control measure, and widespread use in dentistry makes implementation as a bioaerosol control measure straightforward. The micromotor handpiece consistently produced reductions in virus dispersion in surface samples, but this was more variable in air samples, with both increases and modest reductions observed. Combining this with the existing literature suggests this measure is likely to be beneficial, but with a greater degree of uncertainty than for LEV, for example. Incorporation of these control measures into infection prevention and control guidance will reduce risk in routine practice and help to increase preparedness and prevent the disruption to dental services seen during the COVID-19 pandemic.

Chapter 6. General Discussion

The work in this thesis built upon methods developed in Newcastle during the COVID-19 pandemic using fluorescein as a tracer to simulate microorganisms in saliva (Allison et al. 2021a; Allison et al. 2021b; Allison et al. 2021c; Holliday et al. 2021; Llandro et al. 2021). This initial work was heavily cited in national guidance and helped to support the safe reopening of dental services during the pandemic (Dental Schools Council 2020; Dental Schools Council and Association of Dental Hospitals 2020; National Services Scotland 2020; NHS England 2022b; SDCEP 2021a; UK IPC Cell 2022). Despite its impact, unanswered questions remained around the relevance of a fluorescent tracer to the behaviour of a viral pathogen; this led to the development of the bacteriophage model used in the present work, which represents a more biologically relevant surrogate.

Although viral tracers had been used before to study dental bioaerosols in laboratory settings (Fidler et al. 2021; Ionescu et al. 2021), only one group had used a bacteriophage (phi6) in clinical settings (Vernon et al. 2021) prior to the start of the present work. The data in Chapter 3 however, were the first published using MS2 to study dental bioaerosols (Allison et al. 2022). Other groups have subsequently published work in clinical settings using bacteriophages phi6, MS2, and phiX174 (Beltran et al. 2023; Liu et al. 2023; Malmgren et al. 2023; Pratt et al. 2023; Vernon et al. 2022), although none have used more than a single phage at any one time. In the present work, by using two phages together in the same experiment, the relative dispersion of each can be compared under the same conditions. The value of this approach is demonstrated by the consistent finding in the preceding chapters that enveloped phi6 is less stable on surfaces under the same conditions than non-enveloped MS2, despite similar survival in air samples. This may not be surprising given variation in survival of different viruses on inanimate surfaces including human pathogens. For example, some enveloped viruses (e.g., coronaviruses, influenza virus, RSV) have been shown to survive on surfaces from hours to days, whereas some non-enveloped viruses (e.g., adenovirus, rotavirus, rhinovirus, coxsackievirus) may retain activity for days to months (Kramer et al. 2006).

Most of the existing work using bacteriophage tracers has relied on plaque assays to quantify infectious phage; however, many clinical studies (Akin et al. 2021; Bazzazpour et al. 2022; Choudhary et al. 2022; Meethil et al. 2021; Moore et al.

2021; Thompson et al. 2013; Toroglu et al. 2003; Winslow et al. 2022) rely on molecular detection methods of human viral pathogens, such as qPCR and gene sequencing. Comparison between recovery of infectious virus in simulation experiments and viral nucleic acids in clinical studies is therefore difficult. Only one previous study, published after the beginning of the present work, has combined plaque assays with absolute quantification of viral RNA using RT-qPCR (Malmgren et al. 2023); this study however used only phi6 as a tracer, limiting ability to compare between viruses.

Several studies have sought to assess the rate of decay of aerosols after a dental procedure and determine the time after which it becomes safe to enter the room once bioaerosol has dissipated (so called “fallow time”). This fallow time was an important consideration during the COVID-19 pandemic, and specific recommendations were given at the time (SDCEP 2021a; UK Health Security Agency 2021a). Most authors have used OPCs or other particle measurement techniques to assess dental aerosol persistence (Allison et al. 2021b; Allison et al. 2021c; Ren et al. 2021; Shahdad et al. 2021). Prior to the start of the present work, no studies had looked at the persistence of viruses in air samples after a dental procedure in clinical studies or clinical simulation experiments.

The work described in this thesis therefore represents a novel approach to the study of dental bioaerosols by: 1) combining two structurally different viruses in the same experiments; 2) simultaneous quantification of infectious virus and viral nucleic acids; and 3) the use of a controlled bioaerosol chamber to measure the persistence and rate of decay of virus in air samples following a dental procedure. The overall objectives of the work are revisited below, and the progress against these objectives is reviewed in the following sections:

A. Measure the dispersion and infectivity of bacteriophage tracers in droplets and bioaerosols during simulated dental procedures (section 6.1).
B. Define the effectiveness (e.g., percentage reduction in bioaerosol dispersion) of bioaerosol control measures, such as high-volume dental suction, local exhaust ventilation, rubber dam, micromotor handpieces, and dental unit waterline disinfectants (section 6.2).
C. Demonstrate the effect of ventilation on the persistence of bioaerosols using a room-scale aerobiology chamber (section 6.3).

6.1 Infectious virus is dispersed from the mouth in dental bioaerosols

A key insight of the present work is that infectious virus is dispersed from the mouth during a dental procedure in quantities likely to be above the minimum infectious dose for several human viral pathogens (presented in Chapter 4, page 133 – 134). Dispersion of virus in droplets and large aerosols which settle onto surfaces is most significant close to the procedure (< 1m). Dental professionals are likely to be exposed to significant contamination on surfaces around the procedure, including the dental chair, instruments, clothing, and personal protective equipment. There is therefore a risk of transmission of infection via fomites in dental settings. On surfaces, there was a large difference between the amount of infectious virus recovered, with 419-fold more MS2 recovered in surface samples than phi6. In air samples, the amount of virus recovered was much more similar between MS2 and phi6, and significant amounts of infectious virus were recovered at the maximum sampling distance from the procedure (4 m). This suggests that surface contamination is most significant closest to the procedure, with high variation between the two viruses. The risk from small aerosols, which stay suspended in the air, remains high even at sites distant from the procedure with less variation between viruses.

Recovery of viral RNA was consistently higher than infective phage in the same samples. This suggests that although viral particles may be dispersed from the mouth, they may not always retain infectiveness. This is consistent with the findings of the only other study using plaque assays and RT-qPCR with a bacteriophage tracer (Malmgren et al. 2023) and of clinical studies of SARS-CoV-2 in air samples from general hospital wards (Lednicky et al. 2020; Moore et al. 2021). Studies that rely only on measuring nucleic acids to ascribe infection risk may therefore overestimate this risk and efforts should be made to also determine infectiveness.

Whist evidence from clinical studies in humans suggest that microorganisms are dispersed in dental bioaerosols in the clinic (Dudding et al. 2022; Meethil et al. 2021; Rafiee et al. 2022), evidence from epidemiological studies that this translates to infection risk is limited and mixed. For example, a study of SARS-CoV-2 seroprevalence conducted in the UK during the early COVID-19 pandemic suggests clinical members of the dental team had an increased prevalence of prior infection (~16%) compared to non-clinical members of the team and the local population at the

time (~6%) (Shields et al. 2021). However, other epidemiological studies conducted in China, Japan, and Israel at a similar time suggest the risk of transmission to dental professional following exposure to an infected individual may be low compared community transmission rates (Meng et al. 2020; Natapov et al. 2021; Tsubura et al. 2025). The reason for low transmission rates in dental settings during the COVID-19 pandemic may be because of heightened vigilance, widespread screening of patients, and empirical application of bioaerosol control measures at the time. Many of the measures found to be effective in reducing microbial dispersion in bioaerosols in the present and other work may therefore have been in place at the time of these epidemiological studies.

6.2 Viral dispersion can be controlled with simple measures

The data presented in Chapters 3 and 5 demonstrated the effectiveness of five bioaerosol control measures: dental unit waterline (DUWL) disinfectants, rubber dam, dental suction, local exhaust ventilation (LEV), and micromotor handpieces. LEV in particular appeared to be highly effective and often eliminated the dispersion of infective virus. The DUWL disinfectant ICX® reduced dispersion of MS2 in surface samples by 96.5%, whilst rubber dam reduced MS2 dispersion by 86.3% and eliminated detection of phi6. Suction and micromotor demonstrated reductions in infective virus of up to >99%, however their effects were less consistent. It is likely however, that when multiple measures are used together, dispersion of virus and therefore risk of transmission is reduced considerably. This fact may account for the low rates of transmission of SARS-CoV-2 in dental settings in the epidemiological studies discussed above in section 6.1.

As well as efficacy in bioaerosol reduction, cost and ease of implementation are also important considerations for any bioaerosol control measure. Of the measures studied, dental suction is probably the cheapest and easiest to implement as almost all dental practices will already be using this measure. In routine practice and during an infectious disease outbreak, suction would therefore be immediately implementable at minimal cost. Rubber dam is also an inexpensive and widely used approach which would be easy to implement for most dental settings. Similarly, DUWL disinfectants are almost universally used and are therefore already providing protection against transmission. Many dental practices use micromotor handpieces, or have the equipment required to do so, however the air turbine handpiece remains

the predominant high-speed dental handpiece in current use. For some settings, the implementation of micromotor handpieces, for example during an outbreak, would therefore be straightforward and for others would pose cost and logistical implications. Of all measures, LEV would be most difficult to widely implement. Despite common use during the COVID-19 pandemic, few if any dental settings use this measure routinely, and implementation would have significant financial implications. Additionally, the use of LEV is inconvenient due to the space taken up by the device, obstruction of operator access and visibility by the inlet, and the significant noise of operation (Barrett et al. 2022). Implementation of new measures during an outbreak may be further limited by difficulties in procurement. For example, national reports on the UK's response to the COVID-19 pandemic highlight significant difficulties in procurement and distribution of personal protective equipment (PPE) caused by poor preparation and ill-prepared supply chains (Baroness Hallett 2024; The British Medical Association 2024). This phenomenon was also apparent in dentistry, with lack of access to appropriate PPE being cited by multiple sources during the pandemic (Moore et al. 2022; The Royal College of Surgeons of England 2020). The impact of such financial and logistical difficulties in applying bioaerosol control measures during the COVID-19 pandemic is well explored by Vernon *et al.* (2025) in a qualitative analysis of the experiences of UK dental schools.

Aside from the measures studied in the present work, other bioaerosol control measures such as portable air cleaners (Ehtezazi et al. 2021; Liu et al. 2023), pre procedural mouthrinses (Samaranayake et al. 2021), thickening agents added to irrigants to reduce aerosolisation (Farah et al. 2022; Plog et al. 2020), and physical barriers or containment devices to prevent aerosol dispersion (Guzmán-Flores et al. 2023; Santa Rita de Assis et al. 2022) have been recommended. Many of these were considered in guidance during the COVID-19 pandemic (SDCEP 2021a), which often concluded that insufficient evidence existed to recommend use. These measures however likely play a role in reducing risk of disease transmission via dental bioaerosols, and further work should be undertaken to better understand their efficacy.

6.3 Bioaerosol persistence and the importance of ventilation

In Chapter 4, experiments in a room-scale aerobiology chamber demonstrated that at low room ventilation rates (1.5 ACH), infectious phage could remain in the air for a

significant length of time after a dental procedure. In these experiments, phi6 was still recoverable in air samples at the maximum sampling time (24 min post procedure) and regression analyses suggested it would take > 46 min for virus in the air to dissipate. Studies using particle counting methodologies have found similarly long clearance times of aerosols in dental settings (Ehtezazi et al. 2021; Shahdad et al. 2021). This long persistence time is observed for smaller aerosols which can remain airborne for prolonged periods but does not appear to be as significant with larger aerosols and droplets which fall onto surfaces. For example, a study using a fluorescent tracer found that after a dental procedure in an open plan clinic with 6.5 ACH, little additional surface contamination was observed beyond 10 min (Holliday et al. 2021).

Increasing the room ventilation rate in these experiments to 11.7 ACH dramatically reduced the amount of infectious phage detected in air samples after the procedure, with no phi6 detected from 3 min after the procedure, and regression analyses suggesting that it would take just under 9 min for phi6 to be undetectable. This finding is also consistent with studies using particle counting methodologies which demonstrate that as ventilation rate increases, aerosol clearance time reduces dramatically (Longo et al. 2023; Ren et al. 2021). The high ventilation rate (11.7 ACH) used in the present work is only slightly higher that the rate of 10 ACH recommended for all new dental facilities by current NHS guidelines (NHS England and NHS Improvement 2021). The results should therefore be directly relevant to clinical practice. It should be noted however that whilst these ventilation requirements relate to new dental facilities they do not apply to existing ones. Given that many dental clinics in primary care are in converted residential buildings without purpose-built ventilation systems, is very likely that many existing dental settings fall well short of these standards. Upgrading ventilation systems within dental practices is likely to be prohibitively expensive and logistically difficult for many providers. Outside of the commissioning of new facilities then, reliance on ventilation for the control of dental bioaerosols is unlikely to be simple where well-designed ventilation systems are not already in place, without significant investment from providers of dental services.

Whilst changes to ventilation systems are expensive and difficult to implement, many authors have assessed the effect of portable air cleaners (also referred to as air purifiers or scrubbers). These devices use a fan to draw air from the room into the device, and the air is then passed through a high efficiency particulate air (HEPA)

filter or similar, before returning the filtered air to the room. As such, they do not provide additional ventilation in the form of fresh air, however they remove particulates including microorganisms from the room. Such devices have been shown to supplement the effects of mechanical ventilation in removing physical aerosol and increasing aerosol clearance rates in dental settings (Ehtezazi et al. 2021; Ren et al. 2021). In a clinical study, a reduction of 69 – 80% in bacterial contamination in surfaces samples following dental treatment has also been demonstrated when an air cleaner is used (Capparè et al. 2022). Whilst no studies have examined the effect of air cleaners on viral dispersion in clinical studies, a simulation study using a mannequin with a PhiX174 bacteriophage tracer and a *Serratia marcescens* bacterial tracer showed substantial reduction in dispersion and residence time of both organisms (Liu et al. 2023). Whilst not directly examining air cleaning devices, an observational study of SARS-CoV-2 infection in dental professionals in three clinics in Russia during the COVID-19 pandemic provides some insight into the importance of filtration. The authors found higher infection rates in one clinic which recirculated the air extracted by the dental suction back into the clinic, compared to the two other clinics which HEPA filtered the air and exhausted this outside of the clinic (Sarapultseva et al. 2021). The authors ascribe the difference in infection rates to the suction configuration, however other confounding variables were not well reported in the paper, and it is likely that factors other than the suction also contributed to the difference in infection rates.

6.4 Limitations

The work described in this thesis has a number of important limitations which must be considered when translating findings to clinical practice or guidance. Firstly, the model aimed to simulate dispersion of virus in aerosols produced by the dental procedure, but it does not replicate respiratory aerosols produced when a patient breathes, speaks, or coughs. The benefit of this model is that the contribution of dental-procedure–derived aerosol can be ascribed in detail, however risk from other aerosols may be underestimated. For example, respiratory activities produce significant aerosol, which is proportional to respiratory effort (Wilson et al. 2021), and these aerosols contain viable virus in infected individuals (Kulkarni et al. 2016; Parhizkar et al. 2022; Santarpia et al. 2022; Yan et al. 2018). These additional

sources of infection risk should be taken into account when considering the findings of this work.

Bacteriophage tracer was infused into the mannequin's mouth via two tubes positioned adjacent to the upper right central incisor tooth and the surfaces of all teeth were covered with 1 mL of solution before starting experiments. Whilst the flow rate (1.5 mL/min) was chosen to approximate a realistic human stimulated saliva flow (Ship et al. 1991), the position of the tubes was not anatomically accurate. In reality, saliva would be produced bilaterally from parotid, submandibular, and sublingual glands, as well as numerous minor salivary glands around the oral mucosa (Drake et al. 2024). Additionally, microorganisms would also be contained within dental plaque, blood, and gingival crevicular fluid (Gupta et al. 2021) which is not replicated by the mannequin model. The arrangement used was chosen to allow simplicity and reproducibility and offer the best chance of the bacteriophage tracer being captured in the aerosol. Given that the model was established as a plausible worst-case scenario however, it is likely that the capture of oral microorganisms in dental aerosols differs in the model to *in vivo.* Despite this, similar dispersion of oral microbes has been demonstrated *in vivo*, recapitulating the present model (Akin et al. 2021; Rafiee et al. 2022).

Two structurally different bacteriophages (enveloped phi6 and non-enveloped MS2) were chosen in the present research to allow comparison between viruses. Whilst it is reasonable to assume that some aspects of these viruses' behaviour in aerosols are translatable to other viruses (particularly human viral pathogens), this may not be the case. For example, both viruses used in the present work are smaller (MS2: ~27 nm diameter; Phi6: ~85 nm) than many human respiratory viruses such as Influenza A (80-120 nm) and SARS-CoV-2 (60-140 nm) (Menter et al. 2020; Noda and Kawaoka 2010). The two phages may therefore behave differently to larger human pathogens, for instance remaining suspended in aerosols for longer due to their smaller size. Viruses, however, are not likely to be suspended in aerosols as individual viral particles but rather contained within the liquid droplets which make up the aerosol. For example, aerosols produced during dental procedures contain a mix of particles ranging from a few nanometres to 100 μm and larger (Dudding et al. 2022; Sergis et al. 2020); any virus will be carried within these droplets, many of which will be much larger than the viral particles themselves, making their size a less important factor in dispersion and persistence.

Differences were seen between survival of MS2 and phi6 in surface samples. Whilst this difference may be due to virion stability on porous surfaces and the presence of a lipid envelope as discussed earlier (see Section 3.13), other factors may account for the lower recovery of phi6. For example, in experiments looking at recovery efficiency from filter papers, no phage was recovered from non–pre-wet filter papers, suggesting desiccation is an important factor. Additionally, differences in the effects of UV exposure on each virus may contribute to differences in recovery. It is therefore vitally important to select a viral surrogate which replicates important features of any viral pathogen of interest when designing such experiments in future. Bacteriophages were chosen, as being of no risk to human health, they can be easily used in clinical settings. Additionally, plaque assays using the phages' bacterial hosts are simpler than for viruses with eukaryotic hosts, where tissue culture is necessary. The present methods would be equally applicable to non-bacteriophage viral tracers, which have been reported in laboratory settings, for example using HCoV-229E, Feline calicivirus, and Equine arteritis virus, but not in the clinic (Fidler et al. 2021; Ionescu et al. 2021; Munjaković et al. 2025).

The same dental procedure, a 10-min crown preparation on a maxillary central incisor, was conducted for all experiments. This procedure was chosen based on the observation that procedures at the front of the mouth produce more aerosol which escapes the mouth compared to those conducted on posterior teeth (Vernon et al. 2021; Watanabe et al. 2023). A procedure on an anterior tooth therefore allows the maximum amount of aerosol to be produced, giving the model greater ability to detect an effect compared to if a less aerosol-producing one were chosen. Secondly, the procedure was the same as that used in prior work conducted by the author with a fluorescent tracer (Allison et al. 2021a; Allison et al. 2021b; Allison et al. 2021c; Holliday et al. 2021; Llandro et al. 2021). This therefore allows an opportunity to compare fluorescent and bacteriophage tracers (reported elsewhere (Allison et al. 2022)). It is likely, however, that the dispersion and persistence of bioaerosols will be different for other dental procedures compared to the anterior crown preparation used in the present work.

The work was conducted in a number of settings including two enclosed single-surgery dental operatories (45.0 m^3, 4.96 ACH and 51.5 m^3, 3.30 ACH), a large open-plan clinical teaching unit (825 m^3, 6.46 ACH), and a room-scale aerobiology chamber (32.3 m^3, 1.5 – 11.7 ACH). The findings therefore relate to a range of

environments; however, the physical configuration and ventilation parameters of any particular setting will have a large influence on the behaviour of aerosols within the space. The present results should therefore be interpreted within the context of the setting where insights from these findings will be used. For example, when considering risks from dental bioaerosols in any setting, it would be sensible to understand how room volume, air exchange rate, and ventilation configuration may differ to those in the present work or other published research.

In some experiments standard deviation was large, and this may have limited the precision of the results obtained (e.g., estimates of dispersion distance, persistence time, or effect of bioaerosol control measures). This variation has also been reported in other studies using dental mannequin-based simulation models with various biological and non-biological tracers (Ahmed and Jouhar 2021; Beltran et al. 2023; Bergmann et al. 2022; Comisi et al. 2021; Emery et al. 2023; Guzmán-Flores et al. 2023; Han et al. 2021; Pratt et al. 2023; Puljich et al. 2022; Vernon et al. 2021) and also in clinical studies in humans looking at bacterial dispersion (Al-Amad et al. 2017; Bahador et al. 2021; Boccia et al. 2023; Cochran et al. 1989; Dutil et al. 2009; Dutil et al. 2007; Holloman et al. 2015; Senpuku et al. 2021; Zemouri et al. 2020c). This suggests the variation is a feature of both *in vitro* and *in vivo* studies which use a real dental procedure. This is likely due to the fact that even under controlled and reproducible conditions, there will always be variation in how the procedure is conducted by the operator between replicates, leading to variation in the data. One way to eliminate this variation would be to avoid using a real dental procedure, instead operating the handpiece in a steady state without moving it. This would not be comparable to a real clinical scenario, however, and would limit translatability of the results. An alternative would be to increase the number of replicates for each condition to allow more precise estimates.

The dental mannequin was cleaned between experiments to minimise the risk of contamination of samples with phage from previous experiments. It is possible however that despite this cleaning, some phage or phage RNA was transferred to samples, affecting the amount recovered. To reduce the risk of this, negative control samples were obtained immediately before experiments and were taken from the same locations as experimental samples. Control samples were transported to the laboratory with other samples and were processed at the same time. This provides confidence that contamination was not a significant factor.

Finally, amplification in some RT-qPCR negative control samples was observed, which may limit confidence in these results. However, where amplification was present, this was usually only slightly above the limit of detection of the assay, and always well below positive controls and samples. Whilst repeating the assays with new reagents would have been ideal, insufficient sample remained to allow this, as the protocol was optimised to elute phage from samples in the minimum eluant volume to minimise dilution. In future, accommodations should be made to allow sufficient sample for repeat assays. Importantly, the results of the RT-qPCR assays were generally in agreement with plaque assays and physical aerosol measurement with OPC, providing confidence in the data.

6.5 Implications for clinical practice

Much of the disruption to dentistry during the COVID-19 pandemic was caused by *uncertainty* over the risks from dental bioaerosols. This was because there was little high-quality evidence at the beginning of the pandemic, and policy makers and individual practitioners had little information on which to make decisions. In many countries, access to dental care was severely curtailed to limit risk in the absence of certainty around how to safely deliver care. In the UK, closure of dental services undoubtedly negatively impacted the population's oral health (Dickson-Swift et al. 2022; Stennett and Tsakos 2022) and so whilst well-intended, closing dental clinics during an outbreak clearly carries risk of harm. One important outcome of the present work would therefore be to equip dental practitioners with a better understanding of the risk from dental bioaerosols, but also of how to reduce this risk. This is generally applicable to two situations:

The first, and most immediate, would be the patient who comes into the dental practice with an active respiratory infection (e.g., influenza, COVID-19, common cold). For most patients who present in this way, elective treatment can be deferred until they have recovered, but for some this may not be possible or desirable (e.g., emergency treatment). Here, the use of measures shown in this and other work to be effective in reducing bioaerosol dispersion (suction, micromotor, LEV, rubber dam, waterline disinfectants) can be implemented for treatment of the individual patient, minimising risk to staff and other patients. Ventilation can also be maximised where possible by adjusting mechanical ventilation systems (though this is unlikely in dental practices) or by opening windows. Whilst not specifically examined in the present

work, the use of PPE appropriate for airborne transmission would obviously be appropriate based on extant IPC guidance (NHS England 2022b). In this scenario, being an endemic infection, the risk to dental professionals and patients is likely to be low, however transmission via bioaerosols risks illness, lost productivity, and in some groups (e.g., elderly, immunocompromised, pregnant), greater morbidity.

The second, and hopefully less likely, scenario would be an emerging infectious disease outbreak as was seen in early 2020 with COVID-19. Here there are likely to be high levels of community transmission and much uncertainty. In this situation, the universal application of the same measures may be appropriate, as directed by guidance from relevant bodies. Here, simple-to-implement measures such as waterline disinfectants, dental suction, rubber dam, and micromotor handpieces can be quickly put in place. Implementation of more logistically difficult measures such as ventilation, and to a lesser extent LEV, will however likely require investment on the part of the provider. In such a situation however, despite initial costs, these measures are likely to be highly effective in reducing infection risk.

Individual practitioners and service providers should consider how they might implement measures to control risk from bioaerosols in both of the above scenarios and consider implementing local policies ahead of time to allow a rapid response when needed.

6.6 Implications for policy

Specific guidance for dental settings was published during the pandemic to manage risk of COVID-19 transmission. Early in the pandemic, this related mainly to the empirical application of control measures for all patients, given high rates of community transmission, asymptomatic infection, and the absence of vaccines or effective treatments (College of General Dentistry and Faculty of General Dental Practice 2020; Dental Schools Council and Association of Dental Hospitals 2020). As the pandemic progressed, dental guidance documents stressed the importance of risk assessment to identify those patients who were unlikely to be infected and could be treated without bioaerosol control measures, and those who needed additional measures due to known or suspected infection (Office of the Chief Dental Officer England 2021; SDCEP 2021a; UK Health Security Agency 2021a). Most of these latter documents included information about PPE and post-operative fallow times, but not all included recommendations on bioaerosol control measures. Post-pandemic,

the existing NHS infection control guidance for England does not include any specific measures (other than PPE use) to reduce bioaerosol exposure when undertaking aerosol generating procedures (including dental procedures) (NHS England 2022b). Similarly, the dental framework document which supports this guidance only includes recommendations on PPE and ventilation, but not any specific bioaerosol control measures (NHS England 2022a). General and dental-specific infection control guidance needs to include better descriptions of risk during aerosol generating procedures (e.g., most frequently contaminated sites, persistence of infectious aerosols in the air) and recommendations on the use of effective control measures. Current guidance should be updated to include advice both in the context of endemic infections and during an outbreak to improve preparedness.

At the time of writing, one module of the UK COVID-19 inquiry, *Module 1 Resilience and Preparedness,* has concluded and reported (Baroness Hallett 2024). This found that the UK was poorly prepared for the pandemic, and that this led to avoidable human and financial harm. In particular, the UK prepared for the wrong pandemic, as much planning had focused on an influenza outbreak, the response to which proved largely unhelpful for the coronavirus outbreak which ultimately transpired. The report recommended, among other things, a joined-up civil emergency strategy and three-yearly UK-wide pandemic response exercises. Given the poor preparedness of the healthcare system generally (The British Medical Association 2024), and dentistry specifically (Moore et al. 2022; The Royal College of Surgeons of England 2020; Vernon et al. 2025), it is vital that the dental profession is included in this strategy and these exercises in order to prevent similar impact in any future outbreak.

As well as the provision of dental care, dental education was heavily impacted (Vernon et al. 2025), with students in some UK dental schools having to undertake an additional year of study to compensate for missed training due to the pandemic (Havergal 2021; Macluskey et al. 2022). It is therefore vital for dental education providers and relevant bodies such as Dental Schools Council to consider local contingency plans and national guidance on the delivery of dental education to allow a rapid response and bolster preparedness in an emerging infectious disease outbreak.

In 2023, the UK government published the UK Biological safety strategy which aims to create *"…a UK-wide approach to biosecurity which strengthens deterrence and resilience…"* (Cabinet Office 2023). Some specific pillars of this strategy are to:

- Develop a new strategic approach to pandemic preparedness across government.
- Develop a roadmap for UK specialist biological security science and technology infrastructure, capability, and skills.
- Deliver a coordinated package of exercises on priority biological security scenarios to improve UK preparedness.
- Increase data and intelligence capture on biological threats to the UK.

This laudable strategy aligns with the recommendations of Module 1 of the UK COVID-19 inquiry; however, the dental profession should be included in stakeholder groups to ensure any insights gained benefit oral healthcare. The strategy includes a supporting document *Priority pathogen families research and development tool*, which includes families of viral and bacterial pathogens of pandemic or epidemic potential or other biosecurity risk as priorities for research and development (UK Health Security Agency 2025). These pathogens are considered in the context of general biological security, and further work could be done to explore the potential impact of these agents specifically on healthcare provision, and dental care specifically. Interestingly, despite the finding from the UK COVID-19 inquiry that the UK prepared for the wrong (viral) pathogen, the UK Health Security Agency did not include any fungal pathogens in their priority tool. The failure to consider an entire kingdom seems like an oversight in this context.

6.7 Implications for research and future work

The present work, and similar published research in dentistry has focused on a small group of tracer organisms, particularly bacteriophages; the behaviour of these viruses in a mannequin simulation model may not translate well to the behaviour in real dental settings of many of the organisms in the priority report above (UK Health Security Agency 2025). Further work should be done to develop and characterise tracers, which include viruses, bacteria, and fungi, to maximise the relevance of the model. For example, it would be very useful to compare the behaviour in aerosols of organisms which are easy to use as tracers (e.g., MS2, phi6, phiX174, *Streptococcus mutans, Lactobacillus acidophilus, Serratia marcescens*) to priority human pathogens. This would need to be performed under appropriate biosafety conditions outside of the dental clinic but would allow translation of work in real clinical settings with tracers to human pathogens. Furthermore, it would be desirable to develop a

representative “cocktail” of tracer organisms which could be used in experiments to efficiently simulate the behaviour a wide range of human pathogens. As well as using this model for research, it may also be useful for infection prevention and control training; for example, the model could be used with clinical teams, both in dentistry, and elsewhere in healthcare (e.g., high consequence infectious disease teams) to teach and assess the effectiveness of infection control practices.

Much existing work on dental bioaerosols uses particle counting instruments such as OPCs. Whilst this is a very easy approach, and gives excellent time-resolved, location-specific data, no insight into the content of the aerosol is obtained. As such, it is vital in future work to use these methodologies in concert with biological measurements to understand not just where and how much aerosol is produced, but what it contains. This is as true within dentistry as it is in other areas of bioaerosol research. One key application of these instruments however is in the measurement of aerosol dispersion and persistence in individual settings, for example to help practitioners and healthcare providers quickly assess risk or the effect of control measures in their own settings. The ease of use of these devices and immediate data availability lends itself well to this application.

Similarly, as the present work has shown, measurements using molecular methods may not correlate well with the presence of infective virus. Future studies should therefore not only seek to detect the presence of viral (or other microbial) nucleic acids or other molecular markers, but to also demonstrate infectivity or viability. Depending on the organism studied, this may be straightforward or challenging. An alternative approach which could be employed in studies using only molecular detection, would be to would be to infer likely quantities of infectious virus using data from studies reporting molecular detection and infectious virus. Ideally, this approach would be used when studying the same or related viruses, as where viruses are dissimilar, the relationship between infectious virus and viral nucleic acids may not be the same.

Whilst the present work demonstrates the effectiveness of several bioaerosol control measures, each of these were tested in isolation. It would be desirable in future to test the cumulative benefits of using multiple measures together (e.g., suction and a DUWL disinfectant) to better understand how the control measures interact. This may help to highlight the control measures which most efficiently reduce viral dispersion in dental aerosols when used together.

Finally, whilst the mannequin model is a useful way to study risk from dental bioaerosols, further clinical work with patients is required to understand how data from this and similar models translates to what really happens in the clinic. Future work should incorporate air sampling during dental treatment to understand which microorganisms are dispersed. To this end, the author has secured funding and approvals to conduct a clinical study in patients undergoing dental treatment. Dental bioaerosol samples will be taken during treatment and compared to environmental, dental instrument irrigant, and oral rinse samples using next generation sequencing. This will allow exploration of the relative contribution of the microbiota of the oral cavity and instrument irrigant to the microbiota of dental bioaerosols. This study is expected to begin recruitment within a few months at the time of writing, and it is hoped that this work will provide new insights into the composition and origin of the dental bioaerosol microbiota.

References

Acs N, Gambino M, Brondsted L. 2020. Bacteriophage enumeration and detection methods. *Frontiers in microbiology*. 11:594868.

Adams MH. 1959. Bacteriophages. New York: Interscience Publishers.

Ahmed MA, Jouhar R. 2021. Dissemination of aerosol and splatter in clinical environment during cavity preparation: An in vitro study. *Int J Environ Res Public Health*. 18(7):3773.

Akin H, Karabay O, Toptan H, Furuncuoglu H, Kaya G, Akin EG, Koroglu M. 2021. Investigation of the presence of sars cov-2 in aerosol after dental treatment. *Int Dent J*. 72(2):211-215.

Al-Amad SH, Awad MA, Edher FM, Shahramian K, Omran TA. 2017. The effect of rubber dam on atmospheric bacterial aerosols during restorative dentistry. *J Infect Public Health*. 10(2):195-200.

Al-Sehaibany FS. 2017. Middle east respiratory syndrome in children. Dental considerations. *Saudi Med J*. 38(4):339-343.

Al-Yaseen W, Jones R, McGregor S, Wade W, Gallagher J, Harris R, Johnson I, Kc S, Robertson M, Innes N. 2022. Aerosol and splatter generation with rotary handpieces used in restorative and orthodontic dentistry: A systematic review. *BDJ Open*. 8(1):26.

Alford RH, Kasel JA, Gerone PJ, Knight V. 1966. Human influenza resulting from aerosol inhalation. *Proc Soc Exp Biol Med*. 122(3):800-804.

Allerton J, Tompkins J, Matsakas F, Butterfield D, Brown A, Buckley P. 2021. Testing of a fume and dust extraction system as mitigation for aerosol generating procedures in a dental surgery. Middlesex, UK: National Physical Laboratory. No. ISSN 2059-6030.

Allison JR, Currie CC, Edwards DC, Bowes C, Coulter J, Pickering K, Kozhevnikova E, Durham J, Nile CJ, Jakubovics N et al. 2021a. Evaluating aerosol and splatter following dental procedures: Addressing new challenges for oral healthcare and rehabilitation. *J Oral Rehabil*. 48(1):61-72.

Allison JR, Dowson C, Jakubovics NS, Nile C, Durham J, Holliday R. 2022. Waterline disinfectants reduce dental bioaerosols: A multitracer validation. *J Dent Res*. 101(10):1198-1204.

Allison JR, Dowson C, Pickering K, Červinskytė G, Durham J, Jakubovics NS, Holliday R. 2021b. Local exhaust ventilation to control dental aerosols and droplets. *J Dent Res*. 101(4):384-391.

Allison JR, Edwards DC, Bowes C, Pickering K, Dowson C, Stone SJ, Lumb J, Durham J, Jakubovics N, Holliday R. 2021c. The effect of high-speed dental handpiece coolant delivery and design on aerosol and droplet production. *J Dent*. 112:103746.

Allison JR, Tiede S, Holliday R, Durham J, Jakubovics NS. 2024. Bioaerosols and airborne transmission in the dental clinic. *Int Dent J*. 74 Suppl 2(Suppl 2):S418-S428.

Alsved M, Nygren D, Thuresson S, Medstrand P, Fraenkel CJ, Löndahl J. 2022. Sars-cov-2 in exhaled aerosol particles from covid-19 cases and its association to household transmission. *Clin Infect Dis*. 75(1):e50-e56.

Anderson B, Rashid MH, Carter C, Pasternack G, Rajanna C, Revazishvili T, Dean T, Senecal A, Sulakvelidze A. 2011. Enumeration of bacteriophage particles. *Bacteriophage*. 1(2):86-93.

Anderson CE, Wolfe MK, Boehm AB. 2023. Enveloped and non-enveloped virus survival on microfiber towels. *PeerJ*. 11:e15202.

ARHAI Scotland. Assessing the evidence base for medical procedures which create a higher than usual risk of respiratory infection transmission from patient to healthcare worker, version 1.2. 2021. Glasgow: ARHAI; [accessed 25/06/2022]. https://www.nipcm.hps.scot.nhs.uk/web-resources-container/sbar-assessing-the-evidence-base-for-medical-procedures-which-create-a-higher-risk-of-respiratory-infection-transmission-from-patient-to-healthcare-worker/.

Asadi S, Wexler AS, Cappa CD, Barreda S, Bouvier NM, Ristenpart WD. 2019. Aerosol emission and superemission during human speech increase with voice loudness. *Sci Rep*. 9(1):2348.

Ashokkumar L, Lavu V, Palraj KK, Rao SR, Balaji SK. 2023. Efficacy of chlorhexidine/herbal formulation for microbial reduction in aerosol generated

following ultrasonic scaling - a double-blinded randomized controlled trial. *Journal of Indian Society of Periodontology*. 27(1):82-86.

Author Unknown. 1867. Rubber, or coffer dam, barnums'. *Am J Dent Sci*. 1(1):49-50.

Azimi P, Keshavarz Z, Cedeno Laurent JG, Stephens B, Allen JG. 2021. Mechanistic transmission modeling of covid-19 on the diamond princess cruise ship demonstrates the importance of aerosol transmission. *Proc Natl Acad Sci U S A*. 118(8):e2015482118.

Bahador M, Alfirdous RA, Alquria TA, Griffin IL, Tordik PA, Martinho FC. 2021. Aerosols generated during endodontic treatment: A special concern during the coronavirus disease 2019 pandemic. *J Endod*. 47(5):732-739.

Baker JL, Bor B, Agnello M, Shi W, He X. 2017. Ecology of the oral microbiome: Beyond bacteria. *Trends in microbiology*. 25(5):362-374.

Baldion PA, Rodriguez HO, Guerrero CA, Cruz AC, Betancourt DE. 2021. Infection risk prediction model for covid-19 based on an analysis of the settlement of particles generated during dental procedures in dental clinics. *Int J Dent*. 2021:7832672.

Baroness Hallett. Uk covid-19 inquiry. Module 1: The resilience and preparedness of the united kingdom. 2024. [accessed 10/06/2025]. https://covid19.public-inquiry.uk/documents/module-1-full-report/.

Barrett B, McGovern J, Catanzaro W, Coble S, Redden D, Fouad AF. 2022. Clinical efficacy of an extraoral dental evacuation device in aerosol elimination during endodontic access preparation. *J Endod*. 48(12):1468-1475.

Barros MC, Pedrinha VF, Velásquez-Espedilla EG, Cuellar MRC, de Andrade FB. 2022. Aerosols generated by high-speed handpiece and ultrasonic unit during endodontic coronal access alluding to the covid-19 pandemic. *Sci Rep*. 12(1):4783-4783.

Bazzazpour S, Rahmatinia M, Mohebbi SR, Hadei M, Shahsavani A, Hopke PK, Houshmand B, Raeisi A, Jafari AJ, Yarahmadi M et al. 2022. The detection of sars-cov-2 rna in indoor air of dental clinics during the covid-19 pandemic. *Environmental science and pollution research international*. 29(57):85586-85594.

Beladiya J, Kumar A, Vasava Y, Parmar K, Patel D, Patel S, Dholakia S, Sheth D, Boddu SHS, Patel C. 2024. Safety and efficacy of covid-19 vaccines: A systematic

review and meta-analysis of controlled and randomized clinical trials. *Rev Med Virol*. 34(1):e2507.

Beltran EO, Castellanos JE, Corredor ZL, Morgado W, Zarta OL, Cortes A, Avila V, Martignon S. 2023. Tracing phix174 bacteriophage spreading during aerosol-generating procedures in a dental clinic. *Clin Oral Investig*. 27(6):3221-3231.

Bennett AM, Fulford MR, Walker JT, Bradshaw DJ, Martin MV, Marsh PD. 2000. Microbial aerosols in general dental practice. *Br Dent J*. 189(12):664-667.

Bentley CD, Burkhart NW, Crawford JJ. 1994. Evaluating spatter and aerosol contamination during dental procedures. *J Am Dent Assoc*. 125(5):579-584.

Bergmann N, Lindorfer I, Ommerborn MA. 2022. Blood and saliva contamination on protective eyewear during dental treatment. *Clin Oral Investig*. 26(5):4147-4159.

Bernard P. 1996. Positive selection of recombinant DNA by ccdb. *BioTechniques*. 21(2):320-323.

Binder RA, Alarja NA, Robie ER, Kochek KE, Xiu L, Rocha-Melogno L, Abdelgadir A, Goli SV, Farrell AS, Coleman KK et al. 2020. Environmental and aerosolized severe acute respiratory syndrome coronavirus 2 among hospitalized coronavirus disease 2019 patients. *J Infect Dis*. 222(11):1798-1806.

Bischoff WE. 2010. Transmission route of rhinovirus type 39 in a monodispersed airborne aerosol. *Infect Control Hosp Epidemiol*. 31(8):857-859.

Bischoff WE, McNall RJ, Blevins MW, Turner J, Lopareva EN, Rota PA, Stehle JR, Jr. 2016. Detection of measles virus rna in air and surface specimens in a hospital setting. *J Infect Dis*. 213(4):600-603.

Boccia G, Di Spirito F, D'Ambrosio F, De Caro F, Pecora D, Giorgio R, Fortino L, Longanella W, Franci G, Santella B et al. 2023. Microbial air contamination in a dental setting environment and ultrasonic scaling in periodontally healthy subjects: An observational study. *Int J Environ Res Public Health*. 20(3):2710.

Booth TF, Kournikakis B, Bastien N, Ho J, Kobasa D, Stadnyk L, Li Y, Spence M, Paton S, Henry B et al. 2005. Detection of airborne severe acute respiratory syndrome (sars) coronavirus and environmental contamination in sars outbreak units. *J Infect Dis*. 191(9):1472-1477.

Brown J, Gregson FKA, Shrimpton A, Cook TM, Bzdek BR, Reid JP, Pickering AE. 2021. A quantitative evaluation of aerosol generation during tracheal intubation and extubation. *Anaesthesia*. 76(2):174-181.

Cabinet Office. Uk biological security strategy. 2023. [accessed 01/08/2025]. https://www.gov.uk/government/publications/uk-biological-security-strategy/uk-biological-security-strategy-html.

Capparè P, D'Ambrosio R, De Cunto R, Darvizeh A, Nagni M, Gherlone E. 2022. The usage of an air purifier device with hepa 14 filter during dental procedures in covid-19 pandemic: A randomized clinical trial. *Int J Environ Res Public Health*. 19(9):DOI:10.3390/ijerph19095139.

Carter E, Currie CC, Asuni A, Goldsmith R, Toon G, Horridge C, Simpson S, Donnell C, Greenwood M, Walton G et al. 2020. The first six weeks - setting up a uk urgent dental care centre during the covid-19 pandemic. *Br Dent J*. 228(11):842-848.

Centres for Disease Control and Prevention. Infection prevention & control in dental settings. 2023a. CDC; [accessed 01/08/2025]. https://www.cdc.gov/dental-infection-control/hcp/?CDC_AAref_Val=https://www.cdc.gov/oralhealth/infectioncontrol/index.html.

Centres for Disease Control and Prevention. Interim infection prevention and control recommendations for healthcare personnel during the coronavirus disease 2019 (covid-19) pandemic. 2023b. CDC; [accessed 01/08/2025]. https://www.cdc.gov/covid/hcp/infection-control/?CDC_AAref_Val=https://www.cdc.gov/coronavirus/2019-ncov/hcp/infection-control-recommendations.html.

Chan VW, Ng HH, Rahman L, Tang A, Tang KP, Mok A, Liu JHP, Ho KSC, Chan SM, Wong S et al. 2021. Transmission of severe acute respiratory syndrome coronavirus 1 and severe acute respiratory syndrome coronavirus 2 during aerosol-generating procedures in critical care: A systematic review and meta-analysis of observational studies. *Crit Care Med*. 49(7):1159-1168.

Chaudhary P, Melkonyan A, Meethil A, Saraswat S, Hall DL, Cottle J, Wenzel M, Ayouty N, Bense S, Casanova F et al. 2021. Estimating salivary carriage of severe acute respiratory syndrome coronavirus 2 in nonsymptomatic people and efficacy of

mouthrinse in reducing viral load: A randomized controlled trial. *J Am Dent Assoc*. 152(11):903-908.

Chen W, Gluud C. 2005. Vaccines for preventing hepatitis b in health-care workers. *Cochrane Database Syst Rev*. CD000100:DOI:10.1002/14651858.CD14000100.pub14651853.

Chiramana S, Bindu O SH, Kadiyala K, Prakash M, Prasad T, Chaitanya S. 2013. Evaluation of minimum required safe distance between two consecutive dental chairs for optimal asepsis. *J Orofac Res*. 3:12-15.

Choudhary S, Bach T, Wallace MA, Stoeckel DC, Thornhill MH, Lockhart PB, Kwon JH, Liang SY, Burnham CD, Biswas P et al. 2022. Assessment of infectious diseases risks from dental aerosols in real-world settings. *Open Forum Infect Dis*. 9(11):ofac617.

Choukri F, Menotti J, Sarfati C, Lucet J-C, Nevez G, Garin YJF, Totet A. 2010. Quantification and spread of pneumocystis jirovecii in the surrounding air of patients with pneumocystis pneumonia. *Clin Infect Dis*. 51(3):259-265.

Clokie MRJ. 2009. Bacteriophages methods and protocols, volume 1: Isolation, characterization, and interactions. Totowa, NJ: Humana Press.

Cochran MA, Miller CH, Sheldrake MA. 1989. The efficacy of the rubber dam as a barrier to the spread of microorganisms during dental treatment. *J Am Dent Assoc*. 119(1):141-144.

Coclite D, Napoletano A, Gianola S, Del Monaco A, D'Angelo D, Fauci A, Iacorossi L, Latina R, Torre G, Mastroianni CM et al. 2020. Face mask use in the community for reducing the spread of covid-19: A systematic review. *Front Med (Lausanne)*. 7:594269.

College of General Dentistry, Faculty of General Dental Practice. 2020. Implications of covid-19 for the safe management of general dental practice: A practical guide. London: College of Genreal Dentistry, Faculty of General Dental Practice.

Comisi JC, Ravenel TD, Kelly A, Teich ST, Renne W. 2021. Aerosol and spatter mitigation in dentistry: Analysis of the effectiveness of 13 setups. *J Esthet Restor Dent*. 33(3):466-479.

Cowling BJ, Ip DK, Fang VJ, Suntarattiwong P, Olsen SJ, Levy J, Uyeki TM, Leung GM, Malik Peiris JS, Chotpitayasunondh T et al. 2013. Aerosol transmission is an important mode of influenza a virus spread. *Nat Commun*. 4:1935.

d'Herelle F. 2007. On an invisible microbe antagonistic toward dysenteric bacilli: Brief note by mr. F. D'herelle, presented by mr. Roux. 1917. *Res Microbiol*. 158(7):553-554.

Dahlke WO, Cottam MR, Herring MC, Leavitt JM, Ditmyer MM, Walker RS. 2012. Evaluation of the spatter-reduction effectiveness of two dry-field isolation techniques. *J Am Dent Assoc*. 143(11):1199-1204.

Dawson M, Soro V, Dymock D, Price R, Griffiths H, Dudding T, Sandy JR, Ireland AJ. 2016. Microbiological assessment of aerosol generated during debond of fixed orthodontic appliances. *Am J Orthod Dentofacial Orthop*. 150(5):831-838.

Day WC, Berendt RF. 1972. Experimental tularemia in macaca mulatta: Relationship of aerosol particle size to the infectivity of airborne pasteurella tularensis. *Infection and Immunity*. 5(1):77-82.

Dennehy JJ, Abedon ST. 2020. Phage infection and lysis. In: Harper DR, Abedon ST, Burrowes BH, McConville ML, editors. Bacteriophages: Biology, technology, therapy. Cham: Springer International Publishing. p. 1-43.

Dental Schools Council. Covid-19 – returning to student-led dental clinical treatments. 2020. [accessed 01/08/2025]. https://www.dentalschoolscouncil.ac.uk/wp-content/uploads/2020/07/COVID-19-report-on-returning-to-student-led-dental-clinical-treatments-v.1.1.pdf.

Dental Schools Council, Association of Dental Hospitals. Covid-19: Continuing education on open plan clinics - guiding principles to mitigate risk. 2020. [accessed 18/03/2025]. https://www.dentalschoolscouncil.ac.uk/wp-content/uploads/2021/11/Continuing-Education-on-Open-Plan-Clinics_-Guiding-Principles-to-mitigate-risk-11.21.pdf.

Department of Health. 2013. Health technical memorandum 01-05: Decontamination in primary care dental practices. London: Stationary Office.

Derk RC, Coyle JP, Lindsley WG, Blachere FM, Lemons AR, Service SK, Martin SB, Jr., Mead KR, Fotta SA, Reynolds JS et al. 2023. Efficacy of do-it-yourself air filtration

units in reducing exposure to simulated respiratory aerosols. *Build Environ*. 229:109920.

Dick EC, Jennings LC, Mink KA, Wartgow CD, Inhorn SL. 1987. Aerosol transmission of rhinovirus colds. *J Infect Dis*. 156(3):442-448.

Dickson-Swift V, Kangutkar T, Knevel R, Down S. 2022. The impact of covid-19 on individual oral health: A scoping review. *BMC Oral Health*. 22(1):422.

Drake RL, Vogl AW, Mitchell AWM. 2024. Head and neck. In: Drake RL, Vogl AW, Mitchell AWM, editors. Gray's anatomy for students. London: Elsevier. p. 817-1114.e1128.

Druett HA, Henderson DW, Packman L, Peacock S. 1953. Studies on respiratory infection: I. The influence of particle size on respiratory infection with anthrax spores. *J Hyg (London)*. 51(3):359-371.

Druett HA, Henderson DW, Peacock S. 1956a. Studies on respiratory infection. Iii. Experiments with brucella suis. *J Hyg (Lond)*. 54(1):49-57.

Druett HA, Robinson JM, Henderson DW, Packman L, Peacock S. 1956b. Studies on respiratory infection. Ii. The influence of aerosol particle size on infection of the guinea-pig with pasteurella pestis. *J Hyg (Lond)*. 54(1):37-48.

Dudding T, Sheikh S, Gregson F, Haworth J, Haworth S, Main BG, Shrimpton AJ, Hamilton FW, group A, Ireland AJ et al. 2022. A clinical observational analysis of aerosol emissions from dental procedures. *PLoS One*. 17(3):e0265076-e0265076.

Dutil S, Meriaux A, de Latremoille MC, Lazure L, Barbeau J, Duchaine C. 2009. Measurement of airborne bacteria and endotoxin generated during dental cleaning. *J Occup Environ Hyg*. 6(2):121-130.

Dutil S, Veillette M, Mériaux A, Lazure L, Barbeau J, Duchaine C. 2007. Aerosolization of mycobacteria and legionellae during dental treatment: Low exposure despite dental unit contamination. *Environ Microbiol*. 9(11):2836-2843.

Ehtezazi T, Evans DG, Jenkinson ID, Evans PA, Vadgama VJ, Vadgama J, Jarad F, Grey N, Chilcott RP. 2021. Sars-cov-2: Characterisation and mitigation of risks associated with aerosol generating procedures in dental practices. *Br Dent J*. (Online):DOI:10.1038/s41415-41020-42504-41418.

Eikenberg SL. 2001. Comparison of the cutting efficiencies of electric motor and air turbine dental handpieces. *Gen Dent*. 49(2):199-204.

Emery MA, Reed D, McCracken B. 2023. Novel use of riboflavin as a fluorescent tracer in the dissemination of aerosol and splatter in an open operatory dental clinic. *Clin Exp Dent Res*. 9(3):500-508.

Escombe AR, Moore DAJ, Gilman RH, Pan W, Navincopa M, Ticona E, Martínez C, Caviedes L, Sheen P, Gonzalez A et al. 2008. The infectiousness of tuberculosis patients coinfected with hiv. *PLoS Med*. 5(9):e188.

Farah RI, Althunayyan AA, Al-Haj Ali SN, Farah AI. 2022. Reduction of aerosols and splatter generated during ultrasonic scaling by adding food-grade thickeners to coolants: An in-vitro study. *Clin Oral Investig*. 26(3):2863-2872.

Fedorenko A, Grinberg M, Orevi T, Kashtan N. 2020. Survival of the enveloped bacteriophage phi6 (a surrogate for sars-cov-2) in evaporated saliva microdroplets deposited on glass surfaces. *Sci Rep*. 10(1):22419.

Fidler A, Steyer A, Manevski D, Gašperšič R. 2021. Virus transmission by ultrasonic scaler and its prevention by antiviral agent: An in vitro study. *J Periodontol*. 93(7):e116-e124.

Finlay WH, Stapleton KW, Chan HK, Zuberbuhler P, Gonda I. 1996. Regional deposition of inhaled hygroscopic aerosols: In vivo spect compared with mathematical modeling. *J Appl Physiol (1985)*. 81(1):374-383.

Firquet S, Beaujard S, Lobert PE, Sané F, Caloone D, Izard D, Hober D. 2015. Survival of enveloped and non-enveloped viruses on inanimate surfaces. *Microbes Environ*. 30(2):140-144.

Fisher EM, Richardson AW, Harpest SD, Hofacre KC, Shaffer RE. 2012. Reaerosolization of ms2 bacteriophage from an n95 filtering facepiece respirator by simulated coughing. *Ann Occup Hyg*. 56(3):315-325.

Fréalle E, Valade S, Guigue N, Hamane S, Chabé M, Le Gal S, Damiani C, Totet A, Aliouat EM, Nevez G et al. 2017. Diffusion of pneumocystis jirovecii in the surrounding air of patients with pneumocystis colonization: Frequency and putative risk factors. *Med Mycol*. 55(5):568-572.

Frerichs RR, Htoon MT, Eskes N, Lwin S. 1992. Comparison of saliva and serum for hiv surveillance in developing countries. *Lancet*. 340(8834-8835):1496-1499.

Gallagher JE, K.C S, Johnson IG, Al-Yaseen W, Jones R, McGregor S, Robertson M, Harris R, Innes N, Wade WG. 2020. A systematic review of contamination (aerosol, splatter and droplet generation) associated with oral surgery and its relevance to covid-19. *BDJ Open*. 6(1):25.

Gendron L, Verreault D, Veillette M, Moineau S, Duchaine C. 2010. Evaluation of filters for the sampling and quantification of rna phage aerosols. *Aerosol science and technology : the journal of the American Association for Aerosol Research*. 44(10):893-901.

Gheorghita D, Kun Szabo F, Ajtai T, Hodovany S, Bozoki Z, Braunitzer G, Antal MA. 2022. Aerosol reduction of 2 dental extraoral scavenger devices in vitro. *Int Dent J*. 72(5):691-697.

Goldlust K, Ducret A, Halte M, Dedieu-Berne A, Erhardt M, Lesterlin C. 2023. The f pilus serves as a conduit for the DNA during conjugation between physically distant bacteria. *Proceedings of the National Academy of Sciences*. 120(47):e2310842120.

Graetz C, Hülsbeck V, Düffert P, Schorr S, Straßburger M, Geiken A, Dörfer CE, Cyris M. 2022. Influence of flow rate and different size of suction cannulas on splatter contamination in dentistry: Results of an exploratory study with a high-volume evacuation system. *Clin Oral Investig*. 26(9):5687-5696.

Graziani F, Izzetti R, Lardani L, Totaro M, Baggiani A. 2021. Experimental evaluation of aerosol production after dental ultrasonic instrumentation: An analysis on fine particulate matter perturbation. *Int J Environ Res Public Health*. 18(7):3357.

Gregorova P, Heinonen M-MK, Sarin LP. 2022. An improved rt-qpcr method for direct quantification of enveloped rna viruses. *MethodsX*. 9:101737.

Gregson FKA, Sheikh S, Archer J, Symons HE, Walker JS, Haddrell AE, Orton CM, Hamilton FW, Brown JM, Bzdek BR et al. 2021. Analytical challenges when sampling and characterising exhaled aerosol. *Aerosol science and technology : the journal of the American Association for Aerosol Research*. 56(2):160-175.

Grenier D. 1995. Quantitative analysis of bacterial aerosols in two different dental clinic environments. *Applied and environmental microbiology*. 61(8):3165-3168.

Guha S, Hariharan P, Myers MR. 2014. Enhancement of icrp's lung deposition model for pathogenic bioaerosols. *Aerosol science and technology : the journal of the American Association for Aerosol Research*. 48(12):1226-1235.

Gupta S, Mohindra R, Chauhan PK, Singla V, Goyal K, Sahni V, Gaur R, Verma DK, Ghosh A, Soni RK et al. 2021. Sars-cov-2 detection in gingival crevicular fluid. *J Dent Res*. 100(2):187-193.

Gustin KM, Belser JA, Veguilla V, Zeng H, Katz JM, Tumpey TM, Maines TR. 2015. Environmental conditions affect exhalation of h3n2 seasonal and variant influenza viruses and respiratory droplet transmission in ferrets. *PLoS One*. 10(5):e0125874.

Guzmán-Flores EC, Fuentes-Ayala AR, Martínez-Martínez AC, Aguayo-Félix DE, Arellano-Osorio MV, Campuzano-Donoso M, Román-Galeano NM, Llerena-Velásquez M, Vásquez-Tenorio Y. 2023. Reduction of aerosol dissemination in a dental area generated by high-speed and scaler ultrasonic devices employing the "prime protector". *PLoS One*. 18(8):e0278791.

Han P, Li H, Walsh LJ, Ivanovski S. 2021. Splatters and aerosols contamination in dental aerosol generating procedures. *Appl Sci*. 11(4):1914.

Hao XY, Lv Q, Li FD, Xu YF, Gao H. 2019. The characteristics of hdpp4 transgenic mice subjected to aerosol mers coronavirus infection via an animal nose-only exposure device. *Animal Model Exp Med*. 2(4):269-281.

Harper DR. 2021. Introduction to bacteriophages. In: Harper DR, Abedon ST, Burrowes BH, McConville ML, editors. Bacteriophages: Biology, technology, therapy. Cham: Springer International Publishing. p. 3-16.

Hauri AM, Hofstetter I, Seibold E, Kaysser P, Eckert J, Neubauer H, Splettstoesser WD. 2010. Investigating an airborne tularemia outbreak, germany. *Emerg Infect Dis*. 16(2):238-243.

Hausler WJ, Madden RM. 1966. Microbiologic comparison of dental handpieces 2. Aerosol decay and dispersion. *J Dent Res*. 45(1):52-58.

Havergal C. Scottish dental students forced by covid to repeat a year. 2021. [accessed 01/08/2025]. https://www.timeshighereducation.com/news/scottish-dental-students-forced-covid-repeat-year.

Hermida M, Ferreiro MC, Barral S, Laredo R, Castro A, Diz Dios P. 2002. Detection of hcv rna in saliva of patients with hepatitis c virus infection by using a highly sensitive test. *J Virol Methods*. 101(1-2):29-35.

Hernandez-Vasquez A, Barrenechea-Pulache A, Comande D, Azanedo D. 2022. Mouthrinses and sars-cov-2 viral load in saliva: A living systematic review. *Evid Based Dent*. (Online):DOI:10.1038/s41432-41022-40253-z.

Hinds W. 1999. Aerosol technology: Properties, behavior, and measurement of airborne particles. New York: John Wiley & Sons, Ltd.

Hiwar W, Adamson CS, Brenner DJ, Fletcher LA, King M-F, McQuaid JB, Tidswell E, Noakes CJ, Wood K, Eadie E. 2025. Experimental analysis to quantify inactivation of microorganisms by far-uvc irradiation in indoor environments. *Building and Environment*. 274:112734.

Holliday R, Allison JR, Currie CC, Edwards DC, Bowes C, Pickering K, Reay S, Durham J, Lumb J, Rostami N et al. 2021. Evaluating contaminated dental aerosol and splatter in an open plan clinic environment: Implications for the covid-19 pandemic. *J Dent*. 105:103565.

Holloman JL, Mauriello SM, Pimenta L, Arnold RR. 2015. Comparison of suction device with saliva ejector for aerosol and spatter reduction during ultrasonic scaling. *J Am Dent Assoc*. 146(1):27-33.

Hoogenkamp MA, Brandt BW, Laheij A, de Soet JJ, Crielaard W. 2021. The microbiological load and microbiome of the dutch dental unit; 'please, hold your breath'. *Water Res*. 200:117205.

Horsophonphong S, Chestsuttayangkul Y, Surarit R, Lertsooksawat W. 2021. Efficacy of extraoral suction devices in aerosol and splatter reduction during ultrasonic scaling: A laboratory investigation. *J Dent Res Dent Clin Dent Prospects*. 15(3):197-202.

Hurley S, Neligan M. Letter to general dental practices and community dental services (ref: 001559), 25th march. 2020. [accessed 10/05/2022]. https://wokingham.moderngov.co.uk/documents/s43592/Issue%203%20Preparedness%20letter%20for%20primary%20dental%20care%20-%2025%20March%202020.pdf.

Huynh HT, Nkamga VD, Drancourt M, Aboudharam G. 2015. Genetic variants of dental plaque methanobrevibacter oralis. *Eur J Clin Microbiol Infect Dis*. 34(6):1097-1101.

Innes N, Johnson IG, Al-Yaseen W, Harris R, Jones R, Kc S, McGregor S, Robertson M, Wade WG, Gallagher JE. 2021. A systematic review of droplet and aerosol generation in dentistry. *J Dent*. 105:103556.

Ionescu AC, Brambilla E, Manzoli L, Orsini G, Gentili V, Rizzo R. 2021. Aerosols modification with h2o2 reduces airborne contamination by dental handpieces. *J Oral Microbiol*. 13(1):1881361.

Ionescu AC, Cagetti MG, Ferracane JL, Garcia-Godoy F, Brambilla E. 2020. Topographic aspects of airborne contamination caused by the use of dental handpieces in the operative environment. *J Am Dent Assoc*. 151(9):660-667.

Jackson T, Deibert D, Wyatt G, Durand-Moreau Q, Adisesh A, Khunti K, Khunti S, Smith S, Chan XHS, Ross L et al. 2020. Classification of aerosol-generating procedures: A rapid systematic review. *BMJ Open Respir Res*. 7(1):e000730.

Jimenez JL, Marr LC, Randall K, Ewing ET, Tufekci Z, Greenhalgh T, Tellier R, Tang JW, Li Y, Morawska L et al. 2022. What were the historical reasons for the resistance to recognizing airborne transmission during the covid-19 pandemic? *Indoor Air*. 32(8):e13070.

Johnson GR, Morawska L, Ristovski ZD, Hargreaves M, Mengersen K, Chao CYH, Wan MP, Li Y, Xie X, Katoshevski D et al. 2011. Modality of human expired aerosol size distributions. *J Aerosol Sci*. 42(12):839-851.

Johnson IG, Jones RJ, Gallagher JE, Wade WG, Al-Yaseen W, Robertson M, McGregor S, K. C S, Innes N, Harris R. 2021. Dental periodontal procedures: A systematic review of contamination (splatter, droplets and aerosol) in relation to covid-19. *BDJ Open*. 7(1):15 (2021).

Kamimura H, Watanabe J, Sugano T, Kohisa J, Abe H, Kamimura K, Tsuchiya A, Takamura M, Okoshi S, Tanabe Y et al. 2021. Relationship between detection of hepatitis b virus in saliva and periodontal disease in hepatitis b virus carriers in japan. *J Infect Chemother*. 27(3):492-496.

Katelaris AL, Wells J, Clark P, Norton S, Rockett R, Arnott A, Sintchenko V, Corbett S, Bag SK. 2021. Epidemiologic evidence for airborne transmission of sars-cov-2 during church singing, australia, 2020. *Emerg Infect Dis*. 27(6):1677-1680.

Kazantzis G. 1961. Air contamination from high-speed dental drills. *Proceedings of the Royal Society of Medicine*. 54(3):242-244.

Killingley B, Mann AJ, Kalinova M, Boyers A, Goonawardane N, Zhou J, Lindsell K, Hare SS, Brown J, Frise R et al. 2022. Safety, tolerability and viral kinetics during sars-cov-2 human challenge in young adults. *Nat Med*. 28(5):1031-1041.

Kim SH, Chang SY, Sung M, Park JH, Bin Kim H, Lee H, Choi JP, Choi WS, Min JY. 2016. Extensive viable middle east respiratory syndrome (mers) coronavirus contamination in air and surrounding environment in mers isolation wards. *Clin Infect Dis*. 63(3):363-369.

Kimmitt PT, Redway KF. 2016. Evaluation of the potential for virus dispersal during hand drying: A comparison of three methods. *J Appl Microbiol*. 120(2):478-486.

King MF, Noakes CJ, Sleigh PA, Camargo-Valero MA. 2013. Bioaerosol deposition in single and two-bed hospital rooms: A numerical and experimental study. *Building and Environment*. 59:436-447.

Kliner M, Keenan A, Sinclair D, Ghebrehewet S, Garner P. 2016. Influenza vaccination for healthcare workers in the uk: Appraisal of systematic reviews and policy options. *BMJ Open*. 6(9):e012149.

Klymus KE, Merkes CM, Allison MJ, Goldberg CS, Helbing CC, Hunter ME, Jackson CA, Lance RF, Mangan AM, Monroe EM et al. 2020. Reporting the limits of detection and quantification for environmental DNA assays. *Environmental DNA*. 2(3):271-282.

Koletsi D, Belibasakis GN, Eliades T. 2020. Interventions to reduce aerosolized microbes in dental practice: A systematic review with network meta-analysis of randomized controlled trials. *J Dent Res*. 99(11):1228-1238.

Kool JL, Weinstein RA. 2005. Risk of person-to-person transmission of pneumonic plague. *Clin Infect Dis*. 40(8):1166-1172.

Kramer A, Schwebke I, Kampf G. 2006. How long do nosocomial pathogens persist on inanimate surfaces? A systematic review. *BMC Infect Dis*. 6:130.

Kulkarni H, Smith CM, Lee Ddo H, Hirst RA, Easton AJ, O'Callaghan C. 2016. Evidence of respiratory syncytial virus spread by aerosol. Time to revisit infection control strategies? *Am J Respir Crit Care Med*. 194(3):308-316.

Kumbargere Nagraj S, Eachempati P, Paisi M, Nasser M, Sivaramakrishnan G, Verbeek JH. 2020. Interventions to reduce contaminated aerosols produced during dental procedures for preventing infectious diseases. *Cochrane Database Syst Rev*. 10(10):CD013686.

Kutter JS, de Meulder D, Bestebroer TM, Lexmond P, Mulders A, Richard M, Fouchier RAM, Herfst S. 2021. Sars-cov and sars-cov-2 are transmitted through the air between ferrets over more than one meter distance. *Nat Commun*. 12(1):1653.

Kwon S-B, Park J, Jang J, Cho Y, Park D-S, Kim C, Bae G-N, Jang A. 2012. Study on the initial velocity distribution of exhaled air from coughing and speaking. *Chemosphere*. 87(11):1260-1264.

Lamont RJ, Koo H, Hajishengallis G. 2018. The oral microbiota: Dynamic communities and host interactions. *Nature reviews Microbiology*. 16(12):745-759.

Lederberg EM, Lederberg J. 1953. Genetic studies of lysogenicity in escherichia coli. *Genetics*. 38(1):51-64.

Lednicky JA, Lauzard M, Fan ZH, Jutla A, Tilly TB, Gangwar M, Usmani M, Shankar SN, Mohamed K, Eiguren-Fernandez A et al. 2020. Viable sars-cov-2 in the air of a hospital room with covid-19 patients. *Int J Infect Dis*. 100:476-482.

Lempel E, Szalma J. 2022. Effect of spray air settings of speed-increasing contra-angle handpieces on intrapulpal temperatures, drilling times, and coolant spray pattern. *Clin Oral Investig*. 26(1):523-533.

Li RWK, Leung KWC, Sun FCS, Samaranayake LP. 2004. Severe acute respiratory syndrome (sars) and the gdp. Part ii: Implications for gdps. *Br Dent J*. 197(3):130-134.

Li Y, Leung GM, Tang JW, Yang X, Chao CY, Lin JZ, Lu JW, Nielsen PV, Niu J, Qian H et al. 2007. Role of ventilation in airborne transmission of infectious agents in the built environment - a multidisciplinary systematic review. *Indoor Air*. 17(1):2-18.

Li Y, Qian H, Hang J, Chen X, Cheng P, Ling H, Wang S, Liang P, Li J, Xiao S et al. 2021. Probable airborne transmission of sars-cov-2 in a poorly ventilated restaurant. *Build Environ*. 196:107788.

Lin K, Marr LC. 2017. Aerosolization of ebola virus surrogates in wastewater systems. *Environ Sci Technol*. 51(5):2669-2675.

Lin K, Schulte CR, Marr LC. 2020. Survival of ms2 and φ6 viruses in droplets as a function of relative humidity, ph, and salt, protein, and surfactant concentrations. *PLoS One*. 15(12):e0243505.

Lindsley WG, Blachere FM, Thewlis RE, Vishnu A, Davis KA, Cao G, Palmer JE, Clark KE, Fisher MA, Khakoo R et al. 2010. Measurements of airborne influenza virus in aerosol particles from human coughs. *PLoS One*. 5(11):e15100.

Liu Z, Zhang P, Liu H, He J, Li Y, Yao G, Liu J, Lv M, Yang W. 2023. Estimating the restraint of sars-cov-2 spread using a conventional medical air-cleaning device: Based on an experiment in a typical dental clinical setting. *Int J Hyg Environ Health*. 248:114120.

Llandro H, Allison J, Currie C, Edwards D, Bowes C, Durham J, Jakubovics N, Rostami N, Holliday R. 2021. Evaluating splatter and settled aerosol during orthodontic debonding: Implications for the covid-19 pandemic. *Br Dent J*. (Online)(1):DOI:10.1038/s41415-41020-42503-41419.

Lloro V, Giovannoni ML, Luaces VL, Manzanares MC. 2021. Perioral aerosol sequestration suction device effectively reduces biological cross-contamination in dental procedures. *Eur J Dent*. 15(2):340-346.

Longo AB, Rier E, Porter C, Wohl G, Fritz PC. 2023. Factors modulating fallow period of aerosol-generating dental procedures in a clinical setting. *J Can Dent Assoc*. 89:n5.

Łoś J, Zielińska S, Krajewska A, Michalina Z, Małachowska A, Kwaśnicka K, Łoś M. 2021. Temperate phages, prophages, and lysogeny. In: Harper DR, Abedon ST, Burrowes BH, McConville ML, editors. Bacteriophages: Biology, technology, therapy. Cham: Springer International Publishing. p. 119-150.

Macluskey M, Anderson AS, Shepherd SD. 2022. The impact of a 1-year covid-19 extension on undergraduate dentistry in dundee: Final year students' perspectives of their training in oral surgery. *Dent J (Basel)*. 10(12):230.

Madden RM, Hausler WJ. 1963. Microbiological comparison of dental handpieces. 1. Preliminary report. *J Dent Res*. 42(5):1146-1151.

Malmgren R, Välimaa H, Oksanen L, Sanmark E, Nikuri P, Heikkilä P, Hakala J, Ahola A, Yli-Urpo S, Palomäki V et al. 2023. High-volume evacuation mitigates viral aerosol spread in dental procedures. *Sci Rep*. 13(1):18984.

Mathews CK. 2015. Bacteriophage t4. In: John Wiley & Sons L, editor. Encyclopedia of life sciences. New York: John Wiley & Sons, Ltd. p. 1-11.

McDonnell G, Russell AD. 1999. Antiseptics and disinfectants: Activity, action, and resistance. *Clinical microbiology reviews*. 12(1):147-179.

Meethil AP, Saraswat S, Chaudhary PP, Dabdoub SM, Kumar PS. 2021. Sources of sars-cov-2 and other microorganisms in dental aerosols. *J Dent Res*. 100(8):817-823.

Meng L, Ma B, Cheng Y, Bian Z. 2020. Epidemiological investigation of ohcws with covid-19. *J Dent Res*. 99(13):1444-1452.

Meng R, Jiang M, Cui Z, Chang J-Y, Yang K, Jakana J, Yu X, Wang Z, Hu B, Zhang J. 2019. Structural basis for the adsorption of a single-stranded rna bacteriophage. *Nat Commun*. 10(1):3130.

Menter T, Haslbauer JD, Nienhold R, Savic S, Hopfer H, Deigendesch N, Frank S, Turek D, Willi N, Pargger H et al. 2020. Postmortem examination of covid-19 patients reveals diffuse alveolar damage with severe capillary congestion and variegated findings in lungs and other organs suggesting vascular dysfunction. *Histopathology*. 77(2):198-209.

Micik RE, Miller RL, Mazzarella MA, Ryge G. 1969. Studies on dental aerobiology: I. Bacterial aerosols generated during dental procedures. *J Dent Res*. 48(1):49-56.

Miller RL, Micik RE, Abel C, Ryge G. 1971. Studies on dental aerobiology: Ii. Microbial splatter discharged from the oral cavity of dental patients. *J Dent Res*. 50(3):621-625.

Miller SL, Nazaroff WW, Jimenez JL, Boerstra A, Buonanno G, Dancer SJ, Kurnitski J, Marr LC, Morawska L, Noakes C. 2021. Transmission of sars-cov-2 by inhalation of respiratory aerosol in the skagit valley chorale superspreading event. *Indoor Air*. 31(2):314-323.

Moore G, Rickard H, Stevenson D, Aranega-Bou P, Pitman J, Crook A, Davies K, Spencer A, Burton C, Easterbrook L et al. 2021. Detection of sars-cov-2 within the healthcare environment: A multi-centre study conducted during the first wave of the covid-19 outbreak in england. *J Hosp Infect*. 108:189-196.

Moore R, Keshani D, Coulthard P. 2022. Uk oral surgeons' early response to the covid-19 pandemic and impact on patient care. *Oral Surg*. 15(3):315-323.

Munjaković H, Mikuletič T, Zayed N, Kolenc M, Manevski D, Triglav T, Steyer A, Teughels W, Seme K, Fidler A et al. 2025. Electrolyzed saline prevents virus transmission in dental procedures: An in vitro study. *J Dent Res*. 104(2):211-220.

Myatt TA, Johnston SL, Zuo Z, Wand M, Kebadze T, Rudnick S, Milton DK. 2004. Detection of airborne rhinovirus and its relation to outdoor air supply in office environments. *Am J Respir Crit Care Med*. 169(11):1187-1190.

Natapov L, Schwartz D, Herman HD, Markovich DD, Yellon D, Jarallah M, Liphshiz I, Carmeli Y, Karakis I. 2021. Risk of sars-cov-2 transmission following exposure during dental treatment - a national cohort study. *J Dent*. 113:103791.

National Services Scotland. 2020. Ventilation, water and environmental cleaning in dental surgeries relating to covid-19. Edinburgh: National Services Scotland.

Nederfors T, Nauntofte B, Twetman S. 2004. Effects of furosemide and bendroflumethiazide on saliva flow rate and composition. *Arch Oral Biol*. 49(7):507-513.

NHS England. Dental framework – supporting guidance for primary and community care dental settings. 2022a. [accessed 01/08/2025]. https://www.england.nhs.uk/publication/national-infection-prevention-and-control/#heading-11.

NHS England. National infection prevention and control manual for england version 2.11. 2022b. [accessed 01/08/2025]. https://www.england.nhs.uk/publication/national-infection-prevention-and-control/.

NHS England, NHS Improvement. 2021. Health technical memorandum 03-01 specialised ventilation for healthcare premises part a: The concept, design, specification, installation and acceptance testing of healthcare ventilation systems. London: NHS Improvement.

NHS Estates. 2003. Htm 2022 - supplement 1: Dental compressed air and vacuum systems. London: The Stationary Office.

Nield H. 2020. A short history of infection control in dentistry. *BDJ Team*. 7(8):12-15.

NIHR AGP Research Group. Aerosol generating procedures research prioritisation report. 2021. NIHR; [accessed 25/06/2022]. https://www.nihr.ac.uk/news/new-research-priorities-identified-aerosol-generating-procedures-related-covid-19.

Noda T, Kawaoka Y. 2010. Structure of influenza virus ribonucleoprotein complexes and their packaging into virions. *Rev Med Virol*. 20(6):380-391.

Noordien N, Mulder-van Staden S, Mulder R. 2021. In vivo study of aerosol, droplets and splatter reduction in dentistry. *Viruses*. 13(10):1928.

Office for National Statistics. Which occupations have the highest potential exposure to the coronavirus (covid-19)? 2020. [accessed 29/08/2024]. https://www.ons.gov.uk/employmentandlabourmarket/peopleinwork/employmentandemployeetypes/articles/whichoccupationshavethehighestpotentialexposuretothecoronaviruscovid19/2020-05-11.

Office of the Chief Dental Officer England. 2021. Dental standard operating procedure: Transition to recovery, version 6. London: Office of The Chief Dental Officer England.

Ono K, Inoue H, Masuda W, Morimoto Y, Tanaka T, Yokota M, Inenaga K. 2007. Relationship of chewing-stimulated whole saliva flow rate and salivary gland size. *Arch Oral Biol*. 52(5):427-431.

Orr C, Hurd FK, Corbett WJ. 1958. Aerosol size and relative humidity. *Journal of Colloid Science*. 13(5):472-482.

Ou Q, Placucci RG, Danielson J, Anderson G, Olin P, Jardine P, Madden J, Yuan Q, Grafe TH, Shao S et al. 2021. Characterization and mitigation of aerosols and spatters from ultrasonic scalers. *J Am Dent Assoc*. 152(12):981-990.

Parhizkar H, Dietz L, Olsen-Martinez A, Horve PF, Barnatan L, Northcutt D, Van Den Wymelenberg KG. 2022. Quantifying environmental mitigation of aerosol viral load in a controlled chamber with participants diagnosed with coronavirus disease 2019. *Clin Infect Dis*. 75(1):e174-e184.

Patil R, Hindlekar A, Jadhav GR, Mittal P, Humnabad V, Di Blasio M, Cicciù M, Minervini G. 2023. Comparative evaluation of effect of sodium hypochlorite and chlorhexidine in dental unit waterline on aerosolized bacteria generated during dental treatment. *BMC Oral Health*. 23(1):865.

Pei DD, Meng YC, Fayed AS, You YF, Wu ZX, Lu Y. 2021. Comparison of crown fit and operator preferences between tooth preparation with electric and air-turbine handpieces. *J Prosthet Dent*. 125(1):111-116.

Peng X, Nguyen A, Ghosh D. 2018. Quantification of m13 and t7 bacteriophages by taqman and sybr green qpcr. *J Virol Methods*. 252:100-107.

Pérez-Brocal V, Moya A. 2018. The analysis of the oral DNA virome reveals which viruses are widespread and rare among healthy young adults in valencia (spain). *PLoS One*. 13(2):e0191867-e0191867.

Pierre-Bez AC, Agostini-Walesch GM, Smith PB, Hong Q, Hancock DS, Davis M, Marcelli-Munk G, Mitchell JC. 2021. Ultrasonic scaling in covid-era dentistry: A quantitative assessment of aerosol spread during simulated and clinical ultrasonic scaling procedures. *Int J Dent Hyg*. 19(4):474-480.

Plog J, Wu J, Dias YJ, Mashayek F, Cooper LF, Yarin AL. 2020. Reopening dentistry after covid-19: Complete suppression of aerosolization in dental procedures by viscoelastic medusa gorgo. *Phys Fluids (1994)*. 32(8):083111.

Poolkerd W, Swatasuk B, Saengpitak M, Muangsawat S, Klankeo P, Thotsaporn K, Ampornaramveth RS. 2024. Metataxonomics study of dental bioaerosols affected by waterline disinfection. *BMC Oral Health*. 24(1):1575.

Poranen MM, Daugelavicius R, Ojala PM, Hess MW, Bamford DH. 1999. A novel virus-host cell membrane interaction. Membrane voltage-dependent endocytic-like entry of bacteriophage straight phi6 nucleocapsid. *The Journal of cell biology*. 147(3):671-682.

Pratt A, Eckermann N, Venugopalan SR, Uribe LM, Barlow L, Nonnenmann M. 2023. Evaluation of aerosols in a simulated orthodontic debanding procedure. *Sci Rep*. 13(1):4826.

Puljich A, Jiao K, Lee RSB, Walsh LJ, Ivanovski S, Han P. 2022. Simulated and clinical aerosol spread in common periodontal aerosol-generating procedures. *Clin Oral Investig*. 26(9):5751-5762.

Rafiee A, Carvalho R, Lunardon D, Flores-Mir C, Major P, Quemerais B, Altabtbaei K. 2022. Particle size, mass concentration, and microbiota in dental aerosols. *J Dent Res*. 101(7):785-792.

Randall K, Ewing ET, Marr LC, Jimenez JL, Bourouiba L. 2021. How did we get here: What are droplets and aerosols and how far do they go? A historical perspective on the transmission of respiratory infectious diseases. *Interface Focus*. 11(6):20210049.

Rayyan A, Ather A, Hargreaves KM, Ruparel NB. 2022. Effect of sodium hypochlorite in dental unit waterline on aerosolized bacteria generated from endodontic procedures. *J Endod*. 48(10):1248-1256.

Ren YF, Huang Q, Marzouk T, Richard R, Pembroke K, Martone P, Venner T, Malmstrom H, Eliav E. 2021. Effects of mechanical ventilation and portable air cleaner on aerosol removal from dental treatment rooms. *J Dent*. 105:103576.

Reynolds KA, Sexton JD, Pivo T, Humphrey K, Leslie RA, Gerba CP. 2019. Microbial transmission in an outpatient clinic and impact of an intervention with an ethanol-based disinfectant. *Am J Infect Control*. 47(2):128-132.

Riley EC, Murphy G, Riley RL. 1978. Airborne spread of measles in a suburban elementary school. *Am J Epidemiol*. 107(5):421-432.

Riley RL, Mills CC, O'Grady F, Sultan LU, Wittstadt F, Shivpuri DN. 1962. Infectiousness of air from a tuberculosis ward. Ultraviolet irradiation of infected air: Comparative infectiousness of different patients. *Am Rev Respir Dis*. 85:511-525.

Roine E, Raineri DM, Romantschuk M, Wilson M, Nunn DN. 1998. Characterization of type iv pilus genes in pseudomonas syringae pv. Tomato dc3000. *Mol Plant Microbe Interact*. 11(11):1048-1056.

Samaranayake LP, Fakhruddin KS, Buranawat B, Panduwawala C. 2021. The efficacy of bio-aerosol reducing procedures used in dentistry: A systematic review. *Acta Odontol Scand*. 79(1):69-80.

Santa Rita de Assis J, Garcez AS, Suzuki H, Montalli VAM, Fujii DN, Prouvot MB, Suzuki SS. 2022. Assessment of a biosafety device to control contamination by airborne transmission during orthodontic/dental procedures. *Int J Dent*. 8302826:DOI:10.1155/2022/8302826.

Santarpia JL, Herrera VL, Rivera DN, Ratnesar-Shumate S, Reid SP, Ackerman DN, Denton PW, Martens JWS, Fang Y, Conoan N et al. 2022. The size and culturability of patient-generated sars-cov-2 aerosol. *J Expo Sci Environ Epidemiol*. 32(5):706-711.

Santarpia JL, Rivera DN, Herrera VL, Morwitzer MJ, Creager HM, Santarpia GW, Crown KK, Brett-Major DM, Schnaubelt ER, Broadhurst MJ et al. 2020. Aerosol and surface contamination of sars-cov-2 observed in quarantine and isolation care. *Sci Rep*. 10(1):12732.

Sarapultseva M, Hu D, Sarapultsev A. 2021. Sars-cov-2 seropositivity among dental staff and the role of aspirating systems. *JDR Clin Trans Res*. 6(2):132-138.

Schneider CA, Rasband WS, Eliceiri KW. 2012. Nih image to imagej: 25 years of image analysis. *Nat Methods*. 9(7):671-675.

SDCEP. 2021a. Mitigation of aerosol generating procedures in dentistry a rapid review (version 1.2). Scotland: Scottish Dental Clinical Effectiveness Programme.

SDCEP. 2021b. Ventilation information for dentistry. Scotland: Scottish Dental Clinical Effectiveness Programme.

Senpuku H, Fukumoto M, Uchiyama T, Taguchi C, Suzuki I, Arikawa K. 2021. Effects of extraoral suction on droplets and aerosols for infection control practices. *Dent J (Basel)*. 9(7):80.

Sergis A, Wade W, Gallagher J, Morrell A, Patel S, Dickinson C, Nizarali N, Whaites E, Johnson J, Addison O et al. 2020. Mechanisms of atomization from rotary dental instruments and its mitigation. *J Dent Res*. 100(3):261-267.

Sethi KS, Mamajiwala A, Mahale S, Raut CP, Karde P. 2019. Comparative evaluation of the chlorhexidine and cinnamon extract as ultrasonic coolant for reduction of bacterial load in dental aerosols. *Journal of Indian Society of Periodontology*. 23(3):226-233.

Shahdad S, Hindocha A, Patel T, Cagney N, Mueller JD, Koched A, Seoudi N, Morgan C, Fleming PS, Din AR. 2021. Fallow time determination in dentistry using aerosol measurement in mechanically and non-mechanically ventilated environments. *Br Dent J*. (Online):DOI:10.1038/s41415-41021-43369-41411.

Shahdad S, Patel T, Hindocha A, Cagney N, Mueller JD, Seoudi N, Morgan C, Din A. 2020. The efficacy of an extraoral scavenging device on reduction of splatter contamination during dental aerosol generating procedures: An exploratory study. *Br Dent J*. (Online):DOI:10.1038/s41415-41020-42112-41417.

Shields AM, Faustini SE, Kristunas CA, Cook AM, Backhouse C, Dunbar L, Ebanks D, Emmanuel B, Crouch E, Kroger A et al. 2021. Covid-19: Seroprevalence and vaccine responses in uk dental care professionals. *J Dent Res*. 100(11):1220-1227.

Ship JA, Fox PC, Baum BJ. 1991. How much saliva is enough? 'Normal' function defined. *J Am Dent Assoc*. 122(3):63-69.

Shrimpton AJ, Brown JM, Cook TM, Penfold CM, Reid JP, Pickering AE. 2022. Quantitative evaluation of aerosol generation from upper airway suctioning assessed during tracheal intubation and extubation sequences in anaesthetized patients. *J Hosp Infect*. 124:13-21.

Sia SF, Yan LM, Chin AWH, Fung K, Choy KT, Wong AYL, Kaewpreedee P, Perera R, Poon LLM, Nicholls JM et al. 2020. Pathogenesis and transmission of sars-cov-2 in golden hamsters. *Nature*. 583(7818):834-838.

Siret V, Barataud D, Prat M, Vaillant V, Ansart S, Le Coustumier A, Vaissaire J, Raffi F, Garré M, Capek I. 2006. An outbreak of airborne tularaemia in france, august 2004. *Eurosurveillance*. 11(2):598.

Sistrom M, Park D, O'Brien HE, Wang Z, Guttman DS, Townsend JP, Turner PE. 2015. Genomic and gene-expression comparisons among phage-resistant type-iv pilus mutants of pseudomonas syringae pathovar phaseolicola. *PLoS One*. 10(12):e0144514.

Stennett M, Tsakos G. 2022. The impact of the covid-19 pandemic on oral health inequalities and access to oral healthcare in england. *Br Dent J*. 232(2):109-114.

Stern EL, Johnson JW, Vesley D, Halbert MM, Lawrence BS, Williams LE, Blume P. 1974. Aerosol production associated with clinical laboratory procedures. *Am J Clin Pathol*. 62(5):591-600.

Sugai K, Kawada-Matsuo M, Nguyen-Tra Le M, Sugawara Y, Hisatsune J, Fujiki J, Iwano H, Tanimoto K, Sugai M, Komatsuzawa H. 2023. Isolation of streptococcus mutans temperate bacteriophage with broad killing activity to s. mutans clinical isolates. *iScience*. 26(12).

Suprono MS, Won J, Savignano R, Zhong Z, Ahmed A, Roque-Torres G, Zhang W, Oyoyo U, Richardson P, Caruso J et al. 2021. A clinical investigation of dental evacuation systems in reducing aerosols. *J Am Dent Assoc*. 152(6):455-462.

Svec D, Tichopad A, Novosadova V, Pfaffl MW, Kubista M. 2015. How good is a pcr efficiency estimate: Recommendations for precise and robust qpcr efficiency assessments. *Biomol Detect Quantif*. 3:9-16.

Tag El Din AM, Ghoname NAH. 1997. Efficacy of rubber dam isolation as an infection control procedure in paediatric dentistry. *La Revue de Santé de la Mediterranée Orientale*. 3:530-539.

Takenaka S, Sotozono M, Yashiro A, Saito R, Kornsombut N, Naksagoon T, Nagata R, Ida T, Edanami N, Noiri Y. 2022. Efficacy of combining an extraoral high-volume evacuator with preprocedural mouth rinsing in reducing aerosol contamination produced by ultrasonic scaling. *Int J Environ Res Public Health*. 19(10):6048.

Tang JW, Bahnfleth WP, Bluyssen PM, Buonanno G, Jimenez JL, Kurnitski J, Li Y, Miller S, Sekhar C, Morawska L et al. 2021. Dismantling myths on the airborne transmission of severe acute respiratory syndrome coronavirus-2 (sars-cov-2). *J Hosp Infect*. 110:89-96.

The British Medical Association. Covid-19: How well-protected was the medical profession? 2024. The British Medical Association,; [accessed 10/06/2024]. https://www.bma.org.uk/advice-and-support/covid-19/what-the-bma-is-doing/covid-19-how-well-protected-was-the-medical-profession.

The Corsi-Rosetnhal Foundation. The corsi-rosenthal foundation. 2023. [accessed 22/05/2025]. https://corsirosenthalfoundation.org/.

The Royal College of Surgeons of England. 40% of dental surgeons lack protective kit to keep them safe. 2020. [accessed 10/06/2025]. https://www.rcseng.ac.uk/dental-faculties/fds/faculty/news/archive/40-percent-of-dental-surgeons-lack-protective-kit-to-keep-them-safe/.

Thomas RJ. 2013. Particle size and pathogenicity in the respiratory tract. *Virulence*. 4(8):847-858.

Thomas RJ, Davies C, Nunez A, Hibbs S, Eastaugh L, Harding S, Jordan J, Barnes K, Oyston P, Eley S. 2012. Particle-size dependent effects in the balb/c murine model of inhalational melioidosis. *Front Cell Infect Microbiol*. 2:101.

Thomas RJ, Webber D, Collinge A, Stagg AJ, Bailey SC, Nunez A, Gates A, Jayasekera PN, Taylor RR, Eley S et al. 2009. Different pathologies but equal levels of responsiveness to the recombinant f1 and v antigen vaccine and ciprofloxacin in a murine model of plague caused by small- and large-particle aerosols. *Infect Immun*. 77(4):1315-1323.

Thompson K-A, Pappachan JV, Bennett AM, Mittal H, Macken S, Dove BK, Nguyen-Van-Tam JS, Copley VR, O'Brien S, Hoffman P et al. 2013. Influenza aerosols in uk hospitals during the h1n1 (2009) pandemic – the risk of aerosol generation during medical procedures. *PLoS One*. 8(2):e56278.

To KK, Lu L, Yip CC, Poon RW, Fung AM, Cheng A, Lui DH, Ho DT, Hung IF, Chan K-H et al. 2017a. Additional molecular testing of saliva specimens improves the detection of respiratory viruses. *Emerging microbes & infections*. 6(6):e49-e49.

To KK, Lu L, Yip CC, Poon RW, Fung AM, Cheng A, Lui DH, Ho DT, Hung IF, Chan KH et al. 2017b. Additional molecular testing of saliva specimens improves the detection of respiratory viruses. *Emerg Microbes Infect*. 6(6):e49.

Tompkins J, Quincey P, Allerton J, Williams K. 2020. Feasibility study on the detection of airborne particulates in a dental surgery using an optical particle counter. Middlesex, UK: National Physical Laboratory. No. ISSN 1754-6030.

Toroglu MS, Bayramoglu O, Yarkin F, Tuli A. 2003. Possibility of blood and hepatitis b contamination through aerosols generated during debonding procedures. *Angle Orthod*. 73(5):571-578.

Totura A, Livingston V, Frick O, Dyer D, Nichols D, Nalca A. 2020. Small particle aerosol exposure of african green monkeys to mers-cov as a model for highly pathogenic coronavirus infection. *Emerg Infect Dis*. 26(12):2835-2843.

Tran K, Cimon K, Severn M, Pessoa-Silva CL, Conly J. 2012. Aerosol generating procedures and risk of transmission of acute respiratory infections to healthcare workers: A systematic review. *PLoS One*. 7(4):e35797.

Tseng CC, Li CS. 2005. Collection efficiencies of aerosol samplers for virus-containing aerosols. *J Aerosol Sci*. 36(5):593-607.

TSI Inc. 2012. Application note pd-001: Getting data you need with particle measurements. Minessota, USA.

Tsubura Y, Komiyama Y, Ohtani S, Hyodo T, Shiraishi R, Yagisawa S, Yaguchi E, Tsubura-Okubo M, Houzumi H, Nemoto M et al. 2025. Sars-cov-2 did not spread through dental clinics during the covid-19 pandemic in japan. *Infect Dis Rep*. 17(3):70.

Tung-Thompson G, Libera DA, Koch KL, de Los Reyes FL, 3rd, Jaykus LA. 2015. Aerosolization of a human norovirus surrogate, bacteriophage ms2, during simulated vomiting. *PLoS One*. 10(8):e0134277.

UK Health Security Agency. Covid-19: Infection prevention and control dental appendix. 2021a. [accessed 09/07/2025]. https://www.gov.uk/government/publications/wuhan-novel-coronavirus-infection-prevention-and-control/covid-19-infection-prevention-and-control-dental-appendix.

UK Health Security Agency. Infection prevention and control for seasonal respiratory infections in health and care settings (including sars-cov-2) for winter 2021 to 2022. 2021b. London: Department of Health and Social Care; [accessed 09/07/2025]. https://www.gov.uk/government/publications/wuhan-novel-coronavirus-infection-prevention-and-control/covid-19-guidance-for-maintaining-services-within-health-and-care-settings-infection-prevention-and-control-recommendations.

UK Health Security Agency. Priority pathogen families research and development tool. 2025. [accessed 01/07/2025]. https://www.gov.uk/government/publications/priority-pathogen-families-research-and-development-tool.

UK IPC Cell. A rapid review of aerosol generating procedures (agps). 2022. [accessed 17/06/2022]. https://www.england.nhs.uk/publication/national-infection-prevention-and-control/.

Veena HR, Mahantesha S, Joseph PA, Patil SR, Patil SH. 2015. Dissemination of aerosol and splatter during ultrasonic scaling: A pilot study. *J Infect Public Health*. 8(3):260-265.

Vejerano EP, Marr LC. 2018. Physico-chemical characteristics of evaporating respiratory fluid droplets. *J R Soc Interface*. 15(139):20170939.

Verbeek JH, Rajamaki B, Ijaz S, Sauni R, Toomey E, Blackwood B, Tikka C, Ruotsalainen JH, Kilinc Balci FS. 2020. Personal protective equipment for preventing

highly infectious diseases due to exposure to contaminated body fluids in healthcare staff. *Cochrane Database Syst Rev*. 4(4):CD011621.

Vernon JJ, Black EVI, Dennis T, Devine DA, Fletcher L, Wood DJ, Nattress BR. 2021. Dental mitigation strategies to reduce aerosolization of sars-cov-2. *J Dent Res*. 100(13):1461-1467.

Vernon JJ, Lancaster PE, Black EVI, Devine DA, Fletcher L, Wood DJ, Nattress BR. 2022. Increased handpiece speeds without air coolant: Aerosols and thermal impact. *J Dent Res*. 102(1):53-60.

Vernon JJ, Vinall-Collier K, Csikar J, Emms G, Lancaster PE, Nattress BR, Wood DJ. 2025. Future-proofing dentistry: A qualitative exploration of covid-19 responses in uk dental schools. *Eur J Dent Educ*. 29(1):124-135.

Vila T, Rizk AM, Sultan AS, Jabra-Rizk MA. 2019. The power of saliva: Antimicrobial and beyond. *PLoS Pathog*. 15(11):e1008058.

Volckens J, Good KM, Goble D, Good N, Keller JP, Keisling A, L'Orange C, Morton E, Phillips R, Tanner K. 2022. Aerosol emissions from wind instruments: Effects of performer age, sex, sound pressure level, and bell covers. *Sci Rep*. 12(1):11303.

Wade WG. 2013. Detection and culture of novel bacteria. In: Jakubovics NS, Palmer Jr RJ, editors. Oral microbial ecology: Current research and new perspectives. Norfolk: Caister Academic Press.

Wang C, C., Prather Kimberly A, Sznitman J, Jimenez Jose L, Lakdawala Seema S, Tufekci Z, Marr Linsey C. 2021. Airborne transmission of respiratory viruses. *Science*. 373(6558):eabd9149.

Warfel JM, Beren J, Merkel TJ. 2012. Airborne transmission of bordetella pertussis. *J Infect Dis*. 206(6):902-906.

Watanabe J, Iwamatsu-kobayashi Y, Kikuchi K, Kajita T, Morishima H, Yamauchi K, Yashiro W, Nishimura H, Kanetaka H, Egusa H. 2023. Visualization of droplets and aerosols in simulated dental treatments to clarify the effectiveness of oral suction devices. *J Prosthodont Res*. 68(1):85-91.

WHO. Infection prevention and control of epidemic and pandemic prone acute respiratory infections in healthcare – who guidelines. 2014. [accessed 09/07/2025].

https://www.who.int/publications/i/item/infection-prevention-and-control-of-epidemic-and-pandemic-prone-acute-respiratory-infections-in-health-care.

Wilson NM, Marks GB, Eckhardt A, Clarke AM, Young FP, Garden FL, Stewart W, Cook TM, Tovey ER. 2021. The effect of respiratory activity, non-invasive respiratory support and facemasks on aerosol generation and its relevance to covid-19. *Anaesthesia*. 76(11):1465-1474.

Winslow RL, Zhou J, Windle EF, Nur I, Lall R, Ji C, Millar JE, Dark PM, Naisbitt J, Simonds A et al. 2022. Sars-cov-2 environmental contamination from hospitalised patients with covid-19 receiving aerosol-generating procedures. *Thorax*. 77(3):259-267.

Wood ME, Stockwell RE, Johnson GR, Ramsay KA, Sherrard LJ, Kidd TJ, Cheney J, Ballard EL, O'Rourke P, Jabbour N et al. 2019. Cystic fibrosis pathogens survive for extended periods within cough-generated droplet nuclei. *Thorax*. 74(1):87.

Wu WG, Shum MH, Wong IT, Lu KK, Lee LK, Leung JS, Lao HY, Lee AW, Hau PT, Chan CT et al. 2023. Probable airborne transmission of burkholderia pseudomallei causing an urban outbreak of melioidosis during typhoon season in hong kong, china. *Emerg Microbes Infect*. 12(1):2204155.

Xie X, Li Y, Chwang AT, Ho PL, Seto WH. 2007. How far droplets can move in indoor environments--revisiting the wells evaporation-falling curve. *Indoor Air*. 17(3):211-225.

Yamamoto K, Kurihara M, Matsusue Y, Imanishi M, Tsuyuki M, Kirita T. 2009. Whole saliva flow rate and body profile in healthy young adults. *Arch Oral Biol*. 54(5):464-469.

Yan J, Grantham M, Pantelic J, Bueno de Mesquita PJ, Albert B, Liu F, Ehrman S, Milton DK. 2018. Infectious virus in exhaled breath of symptomatic seasonal influenza cases from a college community. *Proc Natl Acad Sci U S A*. 115(5):1081-1086.

Yang M, Chaghtai A, Melendez M, Hasson H, Whitaker E, Badi M, Sperrazza L, Godel J, Yesilsoy C, Tellez M et al. 2021a. Mitigating saliva aerosol contamination in a dental school clinic. *BMC Oral Health*. 21(1):52.

Yang Q, Saldi TK, Gonzales PK, Lasda E, Decker CJ, Tat KL, Fink MR, Hager CR, Davis JC, Ozeroff CD et al. 2021b. Just 2% of sars-cov-2−positive individuals carry

90% of the virus circulating in communities. *Proc Natl Acad Sci U S A*. 118(21):e2104547118.

Yassi A, Moore D, Fitzgerald JM, Bigelow P, Hon C-Y, Bryce E, B. C. Interdisciplinary Respiratory Protection Study Group. 2005. Research gaps in protecting healthcare workers from sars and other respiratory pathogens: An interdisciplinary, multi-stakeholder, evidence-based approach. *J Occup Environ Hyg*. 47(1):41-50.

Yoon HY, Lee SY. 2019. Susceptibility of bacteria isolated from dental unit waterlines to disinfecting chemical agents. *J Gen Appl Microbiol*. 64(6):269-275.

Yu IT, Li Y, Wong TW, Tam W, Chan AT, Lee JH, Leung DY, Ho T. 2004. Evidence of airborne transmission of the severe acute respiratory syndrome virus. *The New England journal of medicine*. 350(17):1731-1739.

Zargar B, Sattar SA, Kibbee R, Rubino J, Khalid Ijaz M. 2022. Direct and quantitative capture of viable bacteriophages from experimentally contaminated indoor air: A model for the study of airborne vertebrate viruses including sars-cov-2. *J Appl Microbiol*. 132(2):1489-1495.

Zemouri C, de Soet JJ, Volgenant CMC, Crielaard W, Laheij A. 2020a. Heterogeneity in the efficacy of dental chemical disinfectants on water-derived biofilms in vitro. *Biofouling*. 36(5):587-596.

Zemouri C, Laheij A, Volgenant CMC, Brandt BW, Crielaard W, Buijs MJ, Zaura E, de Soet JJ. 2020b. Chlorine-based duwl disinfectant leads to a different microbial composition of water derived biofilms compared to h2o2-based chemical disinfectants in vitro. *PeerJ*. 8:e9503.

Zemouri C, Volgenant CMC, Buijs MJ, Crielaard W, Rosema NAM, Brandt BW, Laheij A, De Soet JJ. 2020c. Dental aerosols: Microbial composition and spatial distribution. *J Oral Microbiol*. 12(1):1762040.

Appendix. Supplementary Data

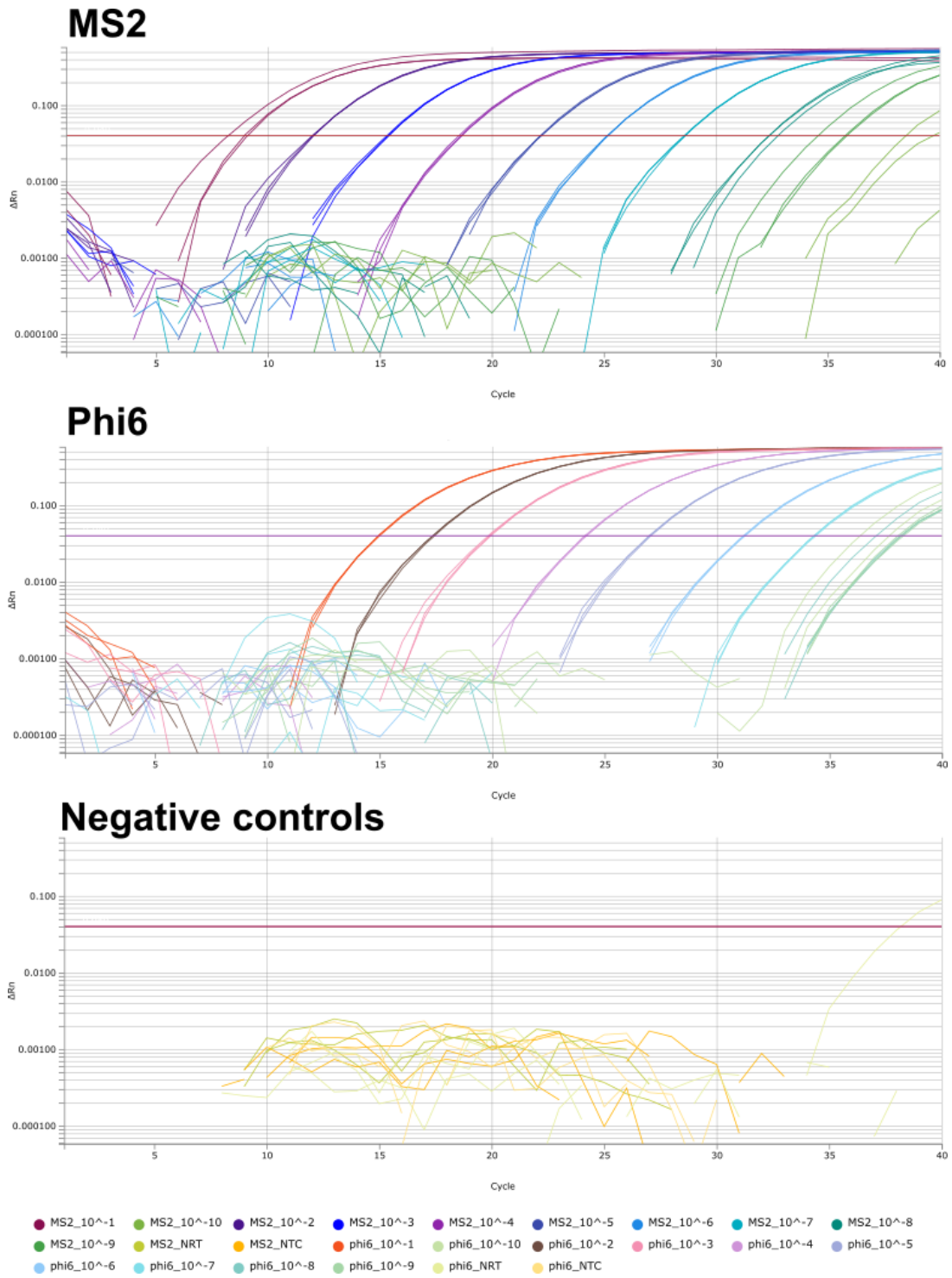

Figure A.1. Representative qPCR amplification plots.

Plots shown are from a single RT-qPCR experiment using cDNA synthesised from bacteriophage MS2 and phi6 RNA. RNA was extracted from lysates of MS2 (2.9 x 10^{10} Plaque-Forming Units [PFU]/ mL) and phi6 (9.0 x 10^{10} PFU/mL). Stock solution was 10-fold serially diluted before RNA extraction to cover the range 2.3 x 10^{-2} – 2.3 x 10^{7} PFU per qPCR reaction for MS2 and 7.2 x 10^{-2} – 7.2 x 10^{7} PFU per reaction for phi6. All samples were run in triplicate, and no-template (NTC) and no-reverse-transcriptase (NRT) controls were included. MS2, phi6, and negative control samples are shown on separate charts for clarity.

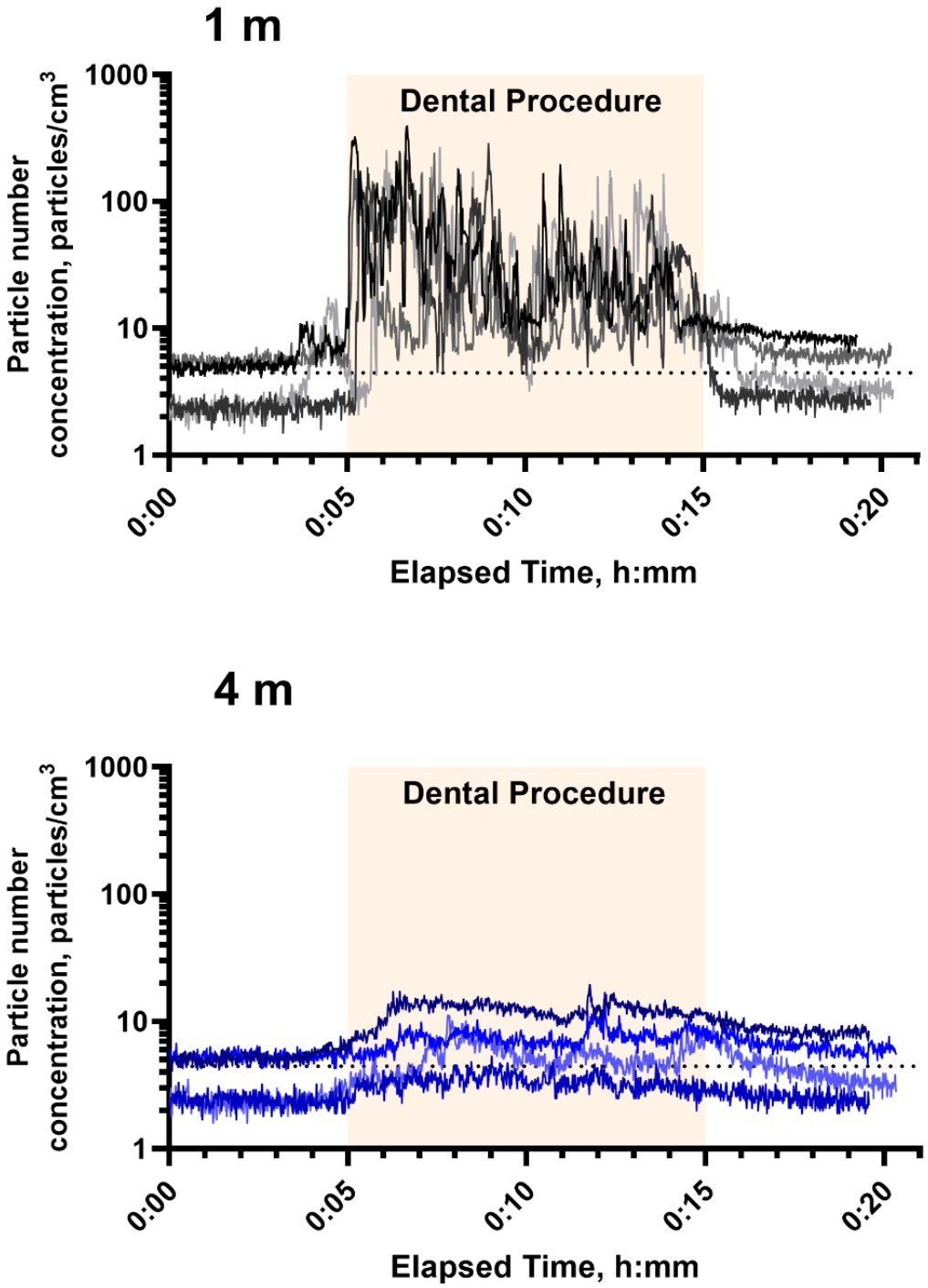

Figure A.2. Aerosol concentration measured at 1m and 4m (replicate data).

Aerosol particle number concentration in dispersion experiments measured by optical particle counter at 1m and 4m from the dental procedure. Particle concentration was summed across all particle size channels (0.3, 0.5, 1.0, 2.5, 5.0, 10.0 μm). Each trace shows an individual replicate (n = 4) with sampling rate of 1 Hz. The orange shaded area denotes the period of the dental procedure (10 min) and the dotted line denotes the mean aerosol concentration in the 5 min preceding the procedure at that location (baseline).

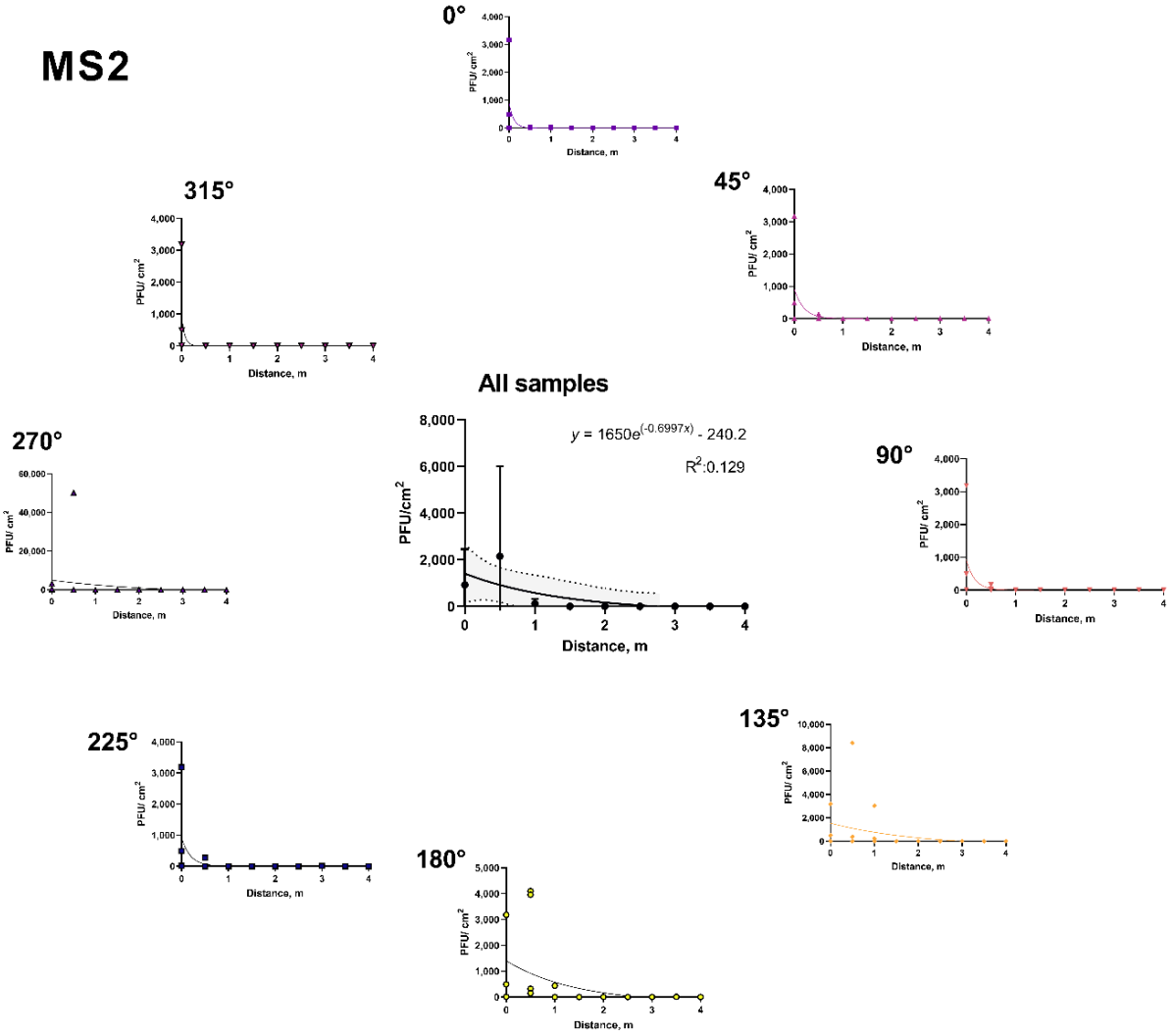

Figure A.3. Dispersion of infectious MS2 over distance by location.

Recovery of infectious MS2 from filter paper surface samples from four experiment replicates. Each data point in peripheral graphs shows the mean amount of phage recovered in plaque assays at that distance, per replicate averaged across four replicates of the experiment. In the central graph, mean recovery and standard deviation are shown. The central graph shows samples at all locations. Peripheral graphs show samples only from the corresponding sampling arm as denoted. Non-linear regressions curves (one-phase decay model), curve equations, and R^2 are shown. Surrounding shaded areas represent 95% confidence intervals of the curve where it was possible to calculate this. PFU: Plaque-Forming Units.

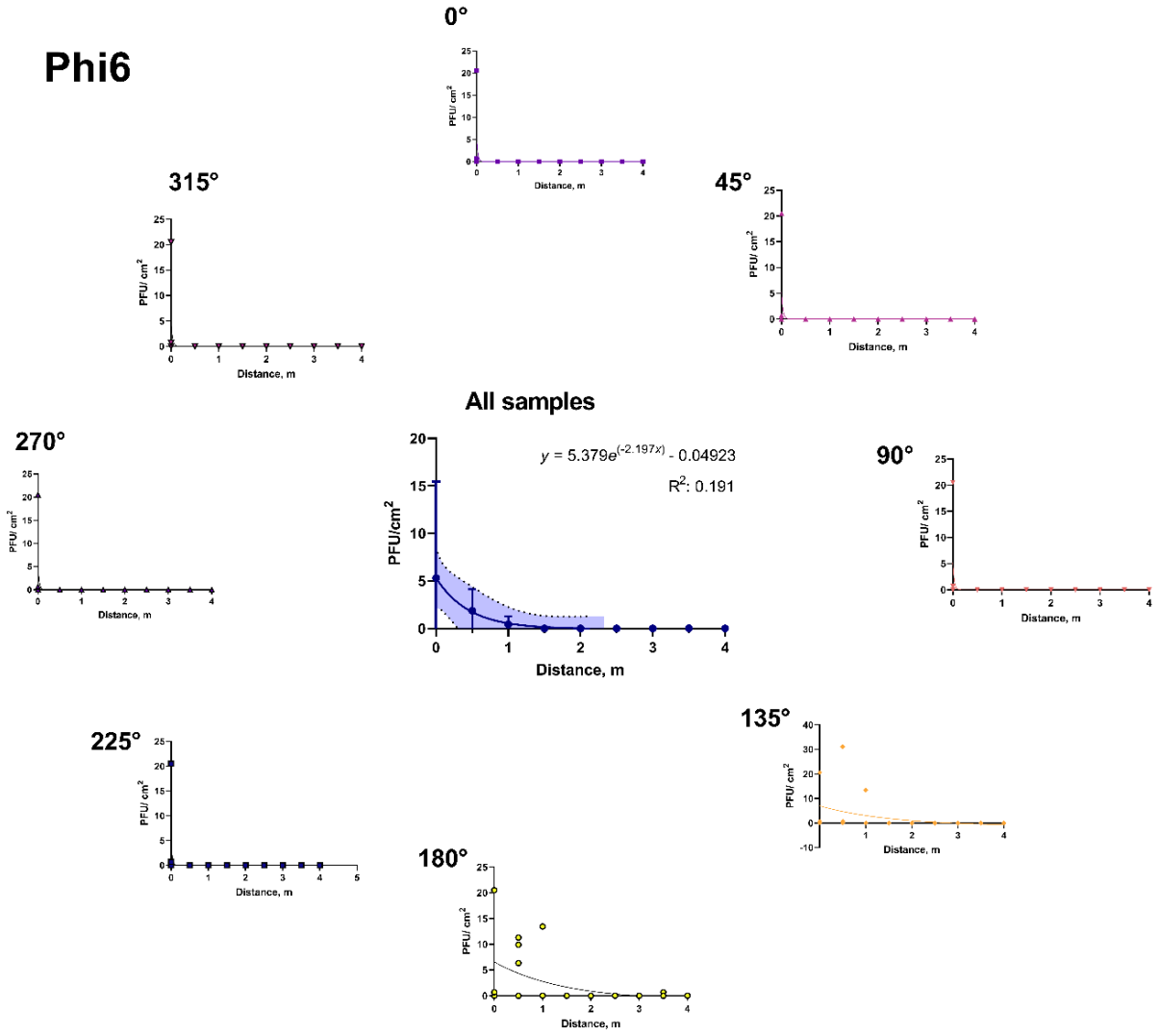

Figure A.4. Dispersion of infectious phi6 over distance by location.

Recovery of infectious phi6 from filter paper surface samples from four experiment replicates. Each data point in peripheral graphs shows the mean amount of phage recovered in plaque assays at that distance, per replicate averaged across four replicates of the experiment. In the central graph, mean recovery and standard deviation are shown. The central graph shows samples at all locations. Peripheral graphs show samples only from the corresponding sampling arm as denoted. Non-linear regressions curves (one-phase decay model), curve equations, and R^2 are shown. Surrounding shaded areas represent 95% confidence intervals of the curve where it was possible to calculate this. PFU: Plaque-Forming Units.

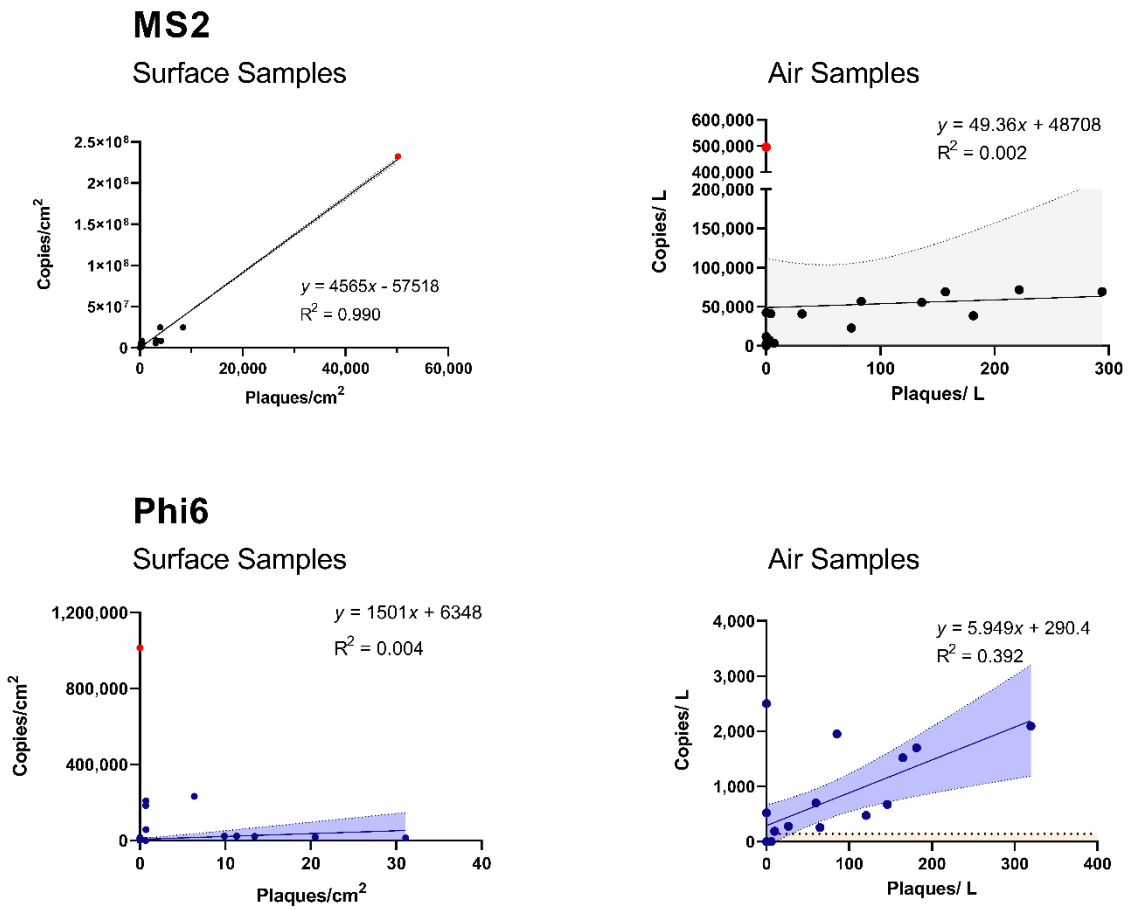

Figure A.5. Relationship between infectious phage and phage RNA.

Linear regression with all data included of infectious MS2 and phi6 phage (plaques) versus phage RNA (copies) recovered from surface samples and air samples. Linear regression curves and 95% confidence intervals (shaded areas) are shown, along with curve equations and associated R^2. The dashed line enclosing the orange shaded area denotes the limit of detection of the RT-qPCR assay. All data are included without any exclusion of outliers, however outliers identified visually are denoted as red datapoints (no outlier for phi6 air samples).

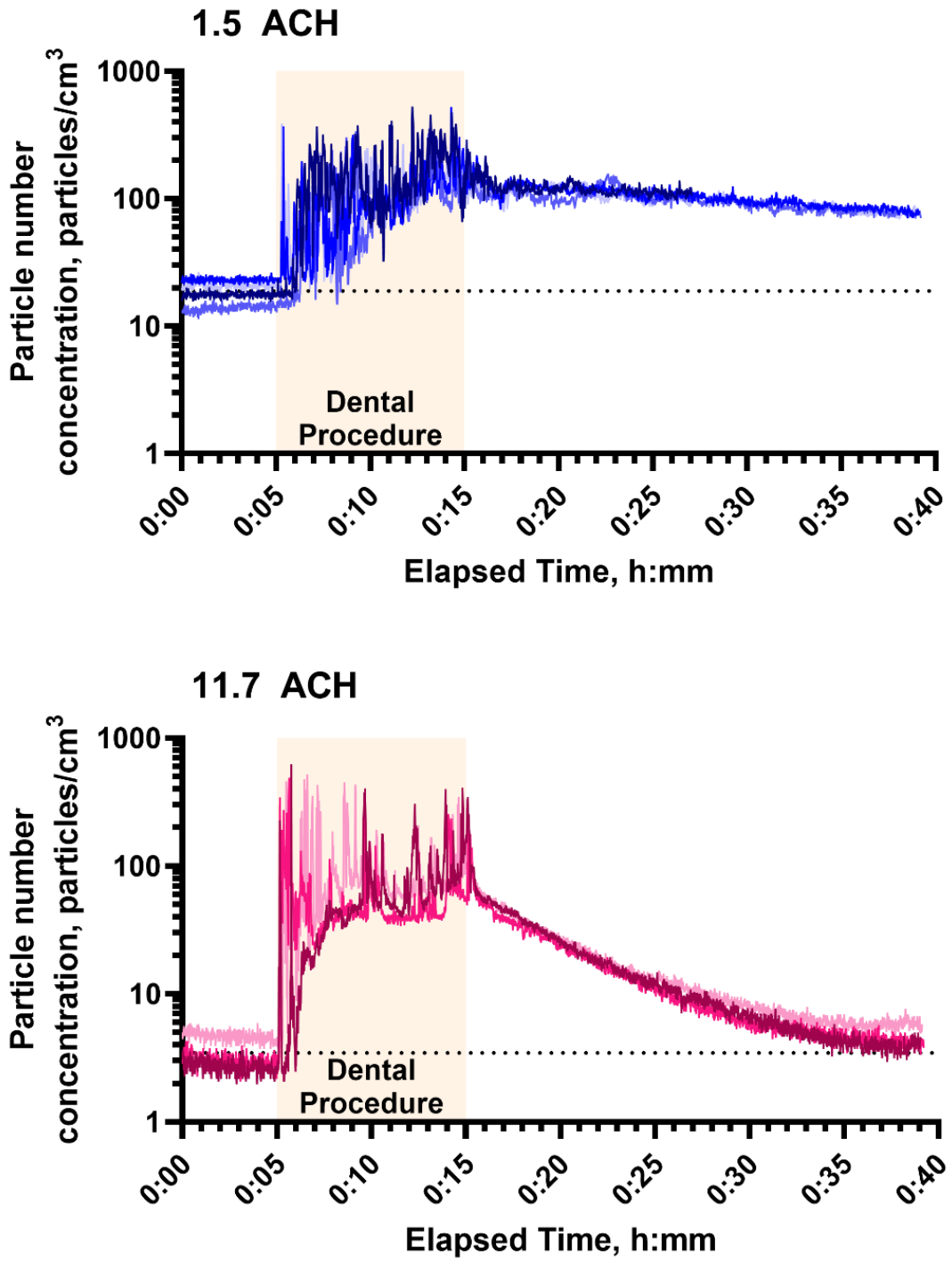

Figure A.6. Aerosol concentration over time at 1.5 ACH and 11.7 air changes per hour (ACH) (replicate data).

Aerosol particle number concentration during persistence experiments. Measured by optical particle counter during a 10-min dental procedure (denoted by orange shaded area) at 1.5 and 11.7 air changes per hour (ACH). Particle concentration was summed across all particle size channels (0.3, 0.5, 1.0, 2.5, 5.0, 10.0 µm). Data from three, 39-min replicates are shown (with one additional replicate [*n* = 4] included of 27-min duration for 1.5 ACH only). Sampling rate 1 Hz. Dotted line denotes the mean aerosol concentration in the 5 min preceding the procedure at that ventilation rate.

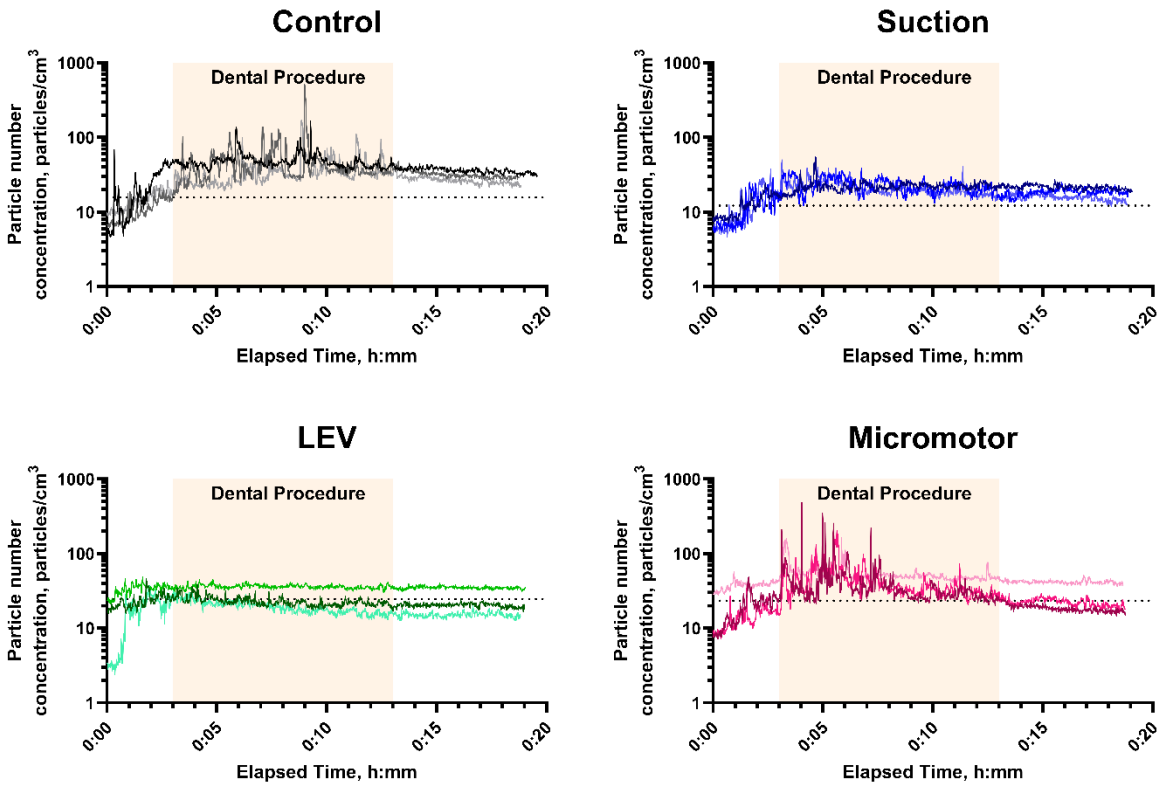

Figure A.7. Aerosol particle concentration with various individual bioaerosol control measures (replicate data).

Aerosol particle number concentration measured using optical particle counter before, during, and after a simulated dental procedure using different bioaerosol control measures. Particle concentration was summed over all particle size channels (0.3, 0.5, 1.0, 2.5, 5.0, 10.0 µm). Each data series shown is an individual replicate (n = 3) with a sampling rate of 1 Hz. Shaded orange area denotes the duration of the dental procedure, and the dotted line denotes the background particle concentration in the 3 min preceding the procedure from 3 replicates. LEV: Local Exhaust Ventilation.